Lecture 5

Solid catalysts

Catalyst components

A solid catalyst consists of mainly three components :

1. Catalytic agent
2. Support /carrier
3. Promoters and Inhibitors

Catalytic agent:

These are the catalytically active component in the catalyst. These components generate the active sites that participate in the chemical reaction. Activity of any catalyst is proportional to the concentration of these active sites. Though concentration of the active sites depends on the amount of catalytically active component, however, it is not always directly proportional. Availability of active sites depends mainly on the dispersion of catalytic agent. The dispersion is defined as ratio of total number of exposed atoms/molecules of catalytic agent available for reaction to total number of atoms/molecules of catalytic agent present in the catalyst sample.

Catalytic agents may be broadly divided in the following categories:

i. Metallic conductors (e.g Fe, Pt, Ag, etc.)
ii. Semiconductors (e.g. NiO, ZnO,etc.)
iii. Insulators (e.g. Al_2O_3, SiO_2, MgO etc.)

Metallic conductors: The metals that have strong electronic interaction with the adsorbates are included in this category. The metals are used in various catalytic reactions such as methanol synthesis, oxidation , hydrogenation and dehydrogenation processes.

Examples of metal catalysts :

Cu for water gas shift reaction and methanol synthesis ; Ag for oxidation of ethylene to ethylene oxide, Au for oxidation of methanol to formaldehyde; Fe for ammonia synthesis; Pd and Pt for hydrogenation of olefins, dienes, aniline or nitriles as well as dehydrogenation of alkanes, alcohols, cyclohexanes, cyclohexanols etc.

Semiconductors :

The oxides and sulfides of transition metals that have catalytic activity are included in this category. Similar to conducting metals, they are also capable of electronic interaction with adsorbed species and catalyze the same type of reactions. Usually the lower valence band electrons participate in bonding. The upper conduction band separated by band gap energy is empty unless electrons are promoted by heat or radiation. Semiconductor characteristics may be intrinsic or induced by addition of foreign ion, creating cationic or anionic vacancies. Common transition oxides and sulfides such as CuO, AgO, NiO CoO, Fe_2O_3 , MnO, Cr_2O_3, FeS, V_2O_5 show conductivity. These materials participate in catalytic reactions and reaction occurs through acceptation or donation of electrons between the reactant material and catalysts. Few applications of semiconductor catalysts are : CuO for oxidation of nitric oxides, NiO for dehydrogenation of alkanes, MnO_2 for oxidation of alcohols, and V_2O_5 for oxidation of hydrocarbons.

Insulators : Catalytic functions of insulators are different from that of conductor and semi conductor materials. Insulators have large values of band gap energy and very low concentration of impurity levels. The electrons remain localized in valence bonds and redox type reactions involving electronic interaction as observed for metal or semiconductor catalysts does not occur. However, insulators have sites that generate protons, thereby, promote carbonium ion based reactions such as cracking, isomerization or polymerization. Al_2O_3, SiO_2, SiO_2-Al_2O_3, zeolites, MgO, CaO, $MgAl_2O_4$, SiO-MgO are few examples of the insulators used as catalysts.

Support or carrier

Support or carrier provides large surface area for dispersion of small amount of catalytically active agent. This is particularly important when expensive metals, such as platinum, ruthenium, palladium or silver are used as the active agent. Supports give the catalysts its physical form, texture, mechanical resistance and certain activity particularly for bifunctional catalysts. Area of the support can range from 1 - 1000 m^2/gm. Common supports are alumina, silica, silica-alumina, molecular sieves etc. The surface area of α - alumina is in the range 1-10 m^2/gm whereas the surface area for γ or η - alumina can be in the range 100 – 300 m^2/gm.

Support may be inert or interact with the active component. This interaction may result in change in surface structure of the active agent and thereby affect the catalyst activity and selectivity. The support may also exhibit ability to adsorb reactant and contribute to the reaction process.

Promoters :

Promoters are generally defined as substances added during preparation of catalysts that improve the activity or selectivity or stabilize the catalytic agents. The promoter is present in a small amount and by itself has little or no activity.

Promoters are termed as physical or chemical promoter depending on the manner they improve the catalyst performance.

The additives that maintain physical integrity of the support and/or deposited catalytic agents are termed as physical promoters. For example, addition of small quantities of alumina to an iron catalyst employed in ammonia synthesis prevents sintering of the iron crystallites. Thus, for this catalyst, alumina is a physical promoter. The addition of K_2O to the same catalyst increases the intrinsic activity of the iron crystallites and therefore acts as a chemical promoter. The promoter can be added during catalyst preparation or during reaction.

Negative promoters or inhibitors: Inhibitors act opposite to promoters. When added in small amounts, these can reduce catalyst activity, selectivity or stability. Inhibitor is particularly useful for reducing the activity of a catalyst for undesirable side reactions. In oxidation of ethylene, ethylene dichloride is added to inhibit CO_2 formation thus acting as an inhibitor.

Industrial catalysts

Industrial catalysts can be broadly grouped into three categories:

1. Bulk catalysts : When the entire catalyst consists of the catalytically active substance ,then the solid catalyst is called a bulk catalyst. Examples include silica-alumina catalysts for catalytic cracking; iron- molybdate for oxidation of methanol to formaldehyde; iron doped with alumina and potassium oxide for the synthesis of ammonia.
2. Supported catalysts: In supported catalysts, the catalytically active materials are dispersed over the high surface area support material. For example, hydrodesulphurization is carried out over molybdenum oxide supported on alumina.
3. Mixed agglomerates : These catalysts are agglomerated mixture of active substance and support. These type of catalysts are used less frequently.

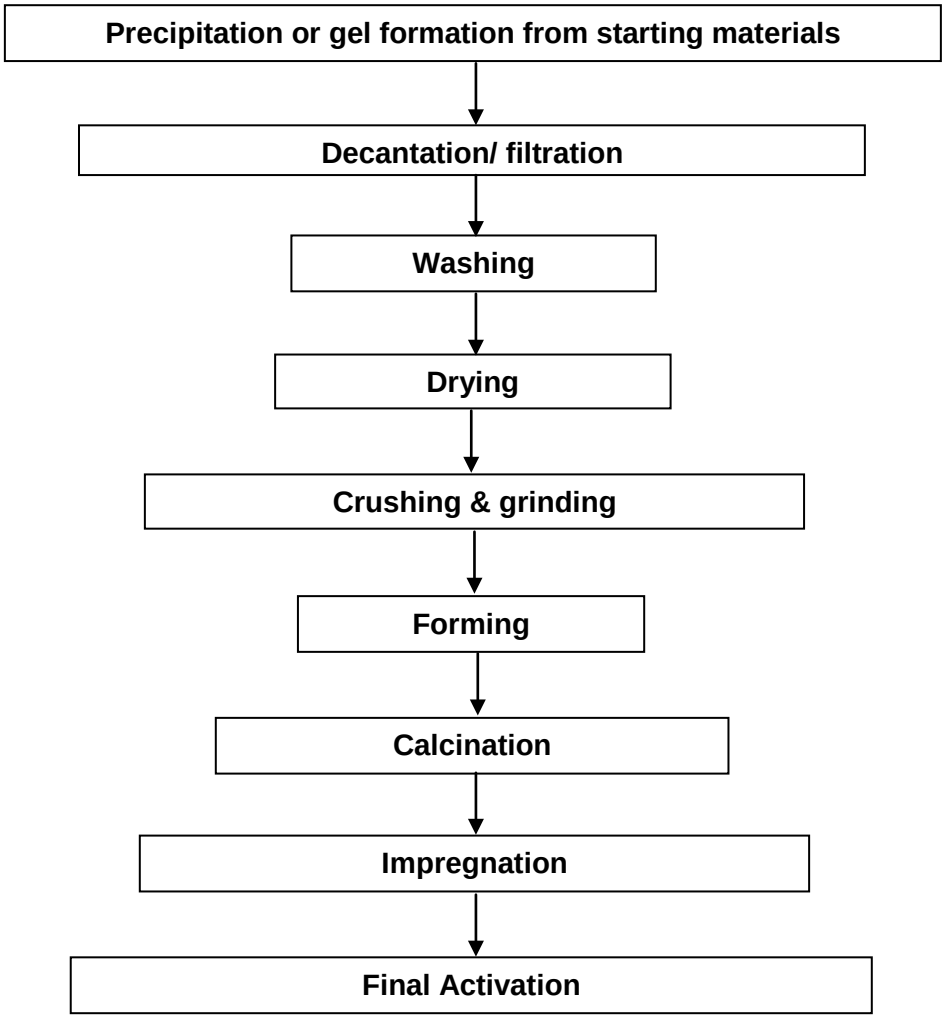

Fig. 1. Basic unit operations in solid catalyst preparation

Preparation of solid catalyst

The catalyst preparation methods can broadly categorized as follows :

1. Bulk preparation process:
   Bulk catalysts and supports are prepared by this method. Bulk preparation is mainly done by the following methods :
   a. Precipitation process
   b. Sol gel process
2. Impregnation process:
   Supports are first prepared by bulk preparation methods and then impregnated with the catalytically active material. The active materials can be deposited on the supports by various methods. Most of the methods involve aqueous solutions and liquid solid interface. In some cases, deposition is done from the gas phase and involves gas- solid interface.
3. Physical mixing :
   Mixed agglomerated catalysts are prepared by this method. These catalysts are prepared by physically mixing the active substances with a powdered support or precursors of support in ball mill. The final mixture is then agglomerated and activated.

Basic unit operations involved in preparation of solid catalyst is shown in Fig 1. Each step is discussed in detail in the following sections.

Book References :

- J.J. Carberry , Chemical and catalytic reaction engineering, Dover Publications, 2001
- G. Ertl, H. Knozinger & J. Weitkamp, Handbook of Heterogeneous Catalysis, Vol 1, Wiley – VCH, 1997
- R. J. Farrauto & C. H. Bartholomew, Fundamentals of Industrial Catalytic Processes, Blackie Academic & Professional, 1997
- J.T. Richardson, Principle of catalysts development, Plenum Press, 1989

Lecture 6

Precipitation and co-precipitation

In this process, the desired component is precipitated from the solution. Co precipitation is used for simultaneous precipitation of more than one component. Catalysts based on more than one component can be prepared easily by co-precipitation. The precipitation process is used for preparation of bulk catalysts and support material such as Al_2O_3, SiO_2, TiO_2, ZrO_2 etc.

Process

In general, the metal hydroxides are precipitated from their precursor salt solution because of their low solubility. The precipitation of hydroxides can be performed either by starting from an alkaline solution which is acidified or from acidic solution by raising the pH. However, most hydroxides for technical application are precipitated from an acidic solution by the addition of an alkaline precipitating agent. Usually, ammonia or sodium bicarbonate is used as the precipitating agent. Highly soluble inorganic salts such as nitrates, carbonates or chlorides are generally used as metal precursors. For example, preparation of alumina is done by precipitating aluminium hydroxide from aluminium nitrate solution by addition of ammonium hydroxide.

$$Al(NO_3)_3 + NH_4OH \rightarrow Al(OH)_3 \downarrow + NH_4NO_3$$

During precipitation, several processes occur and the major steps are :

1. liquid mixing / supersaturation
2. nucleation
3. crystal growth to form primary products
4. aggregation of the primary particles

Initial mixing or interdispersing of components in the solution has a significant effect on the precipitation. Good mixing result in a more homogeneous product particularly in case of co- precipitation. Rate of stirring primarily affects the nucleation whereas growth rate is much less influenced by this factor. Stirring rate also affect the aggregation. Aggregate size can be influenced by changing the stirring rate and the manner of mixing.

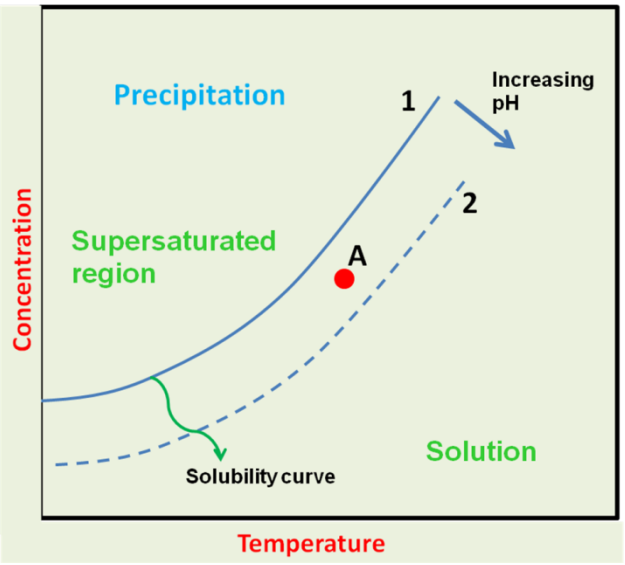

Fig 1. Parameters affecting supersaturation

For nucleation to occur the solution must be super saturated with respect to the components which is to be precipitated. Parameters affecting supersaturation is shown in Fig. 1. In supersaturated region the system is unstable and precipitation occurs with any small disturbance. The supersaturaton region is approached either by increasing the concentration through evaporation, lowering the temperature or by increasing pH. The solubility of a component increases with temperature as shown in Fig. 1. The solubility curve is also function of pH. As pH increases solubility decrease and curve shift from 1 to position 2. Then the point which was initially in solution region becomes in supersatured region. The increase in pH is the most convenient method for precipitation. The reaction during precipitation, $M^{n+} + nOH^{-} \rightleftharpoons M(OH)_n$, is controlled by increasing the pH through addition of a basic solution. Hence by raising the pH value of a solution by addition of alkaline or ammonium hydroxide the corresponding metallic hydroxide compounds can be made insoluble and precipitated from solution. Commonly used

reagents are NaOH, KOH, NH_4OH, carbonates and bicarbonates. Particles within supersaturated region develop in two steps : nucleation and growth.

Nucleation may proceed spontaneously through the formation of $M(OH)_n$ entities or be initiated with seed materials such as dust , particle fragments, roughness of vessels surface. Addition of seed material enhances rate of nucleation. The nucleus is defined as the smallest solid phase aggregate of atoms, molecule or ions which is formed during precipitation and which is capable of spontaneous growth. In super saturated solution when the concentration exceeds a critical threshold value, a nucleus will form and the precipitation will begin. As long as the concentration of the species stays above the nucleation threshold, new particles are formed. Nucleation starts with the formation of clusters which are capable of spontaneous growth by the subsequent addition of monomers until a critical size is reached. Clusters, smaller than the critical size, tend to re–dissolve, while larger clusters continue to grow. As soon as the concentration falls below the critical concentration due to consumption of the precursors by nucleation or by the growth process, only growth of existing particles continues. Growth proceed through adsorption of ions on surface of seeded particle. This growth is a function of concentration, temperature and pH. Rates of nucleation and growth can be independently controlled. If nucleation is faster than growth, the system produces a narrow distribution of small particles. Fast growth results in narrow distribution of large particles.

Several equations are proposed for nucleation rate and the most commonly used is :

$$\frac{dN}{dt} = \beta \exp\left[\frac{-16\pi\sigma^3\nu^2}{3(kT)^3 \ln^2 s}\right]$$

where β is the pre-exponential term, σ is solid –fluid interfacial energy, υ is solid molecular volume and T is the temperature. The super saturation ‘s’ is defined as the ratio of actual concentration to solubility; $s = \frac{\text{actual concentration}}{\text{solubility}}$

The equation can be simplified as $\frac{dN}{dt} = \beta \exp\left[\frac{-A}{\ln^2 s}\right]$ $\qquad A = \frac{16\pi\sigma^3\nu^2}{3(kT)^3}$

Thus, nucleation strongly depends on the concentration as well as temperature. There is a critical super saturation concentration below which nucleation is very slow and above which nucleation is very fast.

There are several mechanisms of crystal growth and most of these lead to the simple equation of growth rate, $G = k\left(c - c_{eq}\right)^n$, where 'k' is the kinetic coefficient, 'c' is the actual concentration and 'c_{eq}' is the equilibrium concentration. The value of exponent 'n' lies in the range of 1 to 2 and often close to 1.

Hence, the dependency of the crystallite growth rate on concentration is closer to a linear function while nucleation rate increases exponentially with concentration. Therefore, high super-saturation level promotes nucleation rather than crystal growth and favor the precipitation of highly dispersed materials. In contrast, precipitation from a more dilute solution tends to produce fewer but larger crystals.

Apart from nucleation and crystal growth, aggregation is also an important step. Aggregation leads to fewer and larger but yet porous particles. It is the formation of clusters of nano-scale primary particles into micrometer scale secondary particles. Physical and chemical forces can hold these particles together. Porosity is then determined by how the particles are stacked and the pores are considered as void spaces between the primary particles. Because of very high super-saturation during the precipitation of most base metal hydroxides or carbonates , nucleation is spontaneous.

Process variation

Precipitation process can be carried out in different ways. The process can be carried out either in batch mode or in continuous mode. The other process variation that affects the precipitate properties is the sequence of addition of the starting materials.

In a batch process, the salt solution from which the metal hydroxide is to be precipitated is taken in a vessel and the precipitating agent is added. The advantage of this method is its simplicity. However, variation of batch composition during precipitation process is a major limitation. This can lead to differences in the properties of the precipitate formed in the initial-and final stages. The continuous process involves

continual simultaneous addition of salt solution and precipitating agent to a vessel with simultaneous withdrawal of precipitate. This process has a higher demand on process control. All the parameters (pH, temperature, concentration, residence time) can be controlled as desired.

The order of addition of starting materials also affects the final properties of the precipitated catalysts. Different schemes of addition of starting materials in precipitation process is shown in Fig. 2.When metal solution is added to the precipitating agent, the product tends to be homogeneous since the precipitating agent is present in large excess. This process is particularly important in co-precipitation as it give more homogeneous product than the process where the precipitating agent is added to a mixed metal solution. In the latter case, the hydroxide with lower solubility tends to precipitate first, resulting in formation of non-homogeneous product. Simultaneous addition of both reagents to a buffer solution of constant pH results in better homogeneity and process control. In this process, ratio of metal salt and precipitating agent can be controlled. However, product at the start and at the end may vary due to change in concentration of other ions that are not precipitated. These counter ions tend to occlude in larger extent in final products. Aging is also longer for final products. Aging represent time of formation of coprecipitated and its separation from solution. Aging results in change in structure and properties of hydroxide network. Aging leads to more crosslinked network.

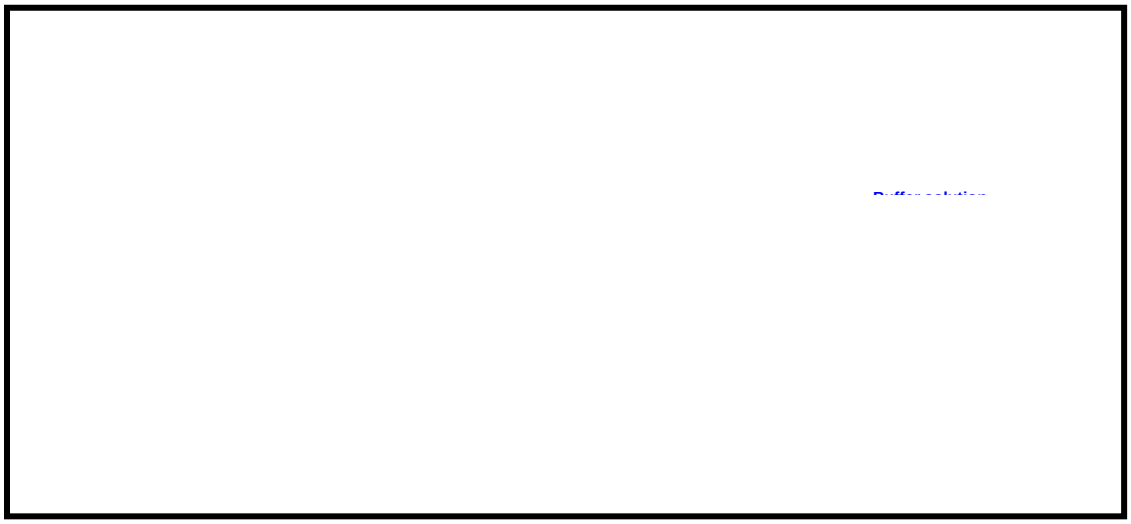

Fig. 2. Different schemes of addition of starting materials in precipitation process

Advantages and disadvantages: The main advantage of the precipitation process is the possibility of creating pure and homogenous material. However, the major disadvantages include necessity of product separation after precipitation and generation of the large volume of salt containing solutions. There is also difficulty in maintaining a constant product quality throughout the whole precipitation process if the precipitation is carried out discontinuously.

Process parameters

In addition to the process variations discussed above there are many other parameters that affect the final product properties as shown in Fig.3. The properties of the final product that are affected include phase formation, chemical composition, purity, particle size, surface area, pore size and pore volume. It is necessary to optimize the parameters to produce the desired product.

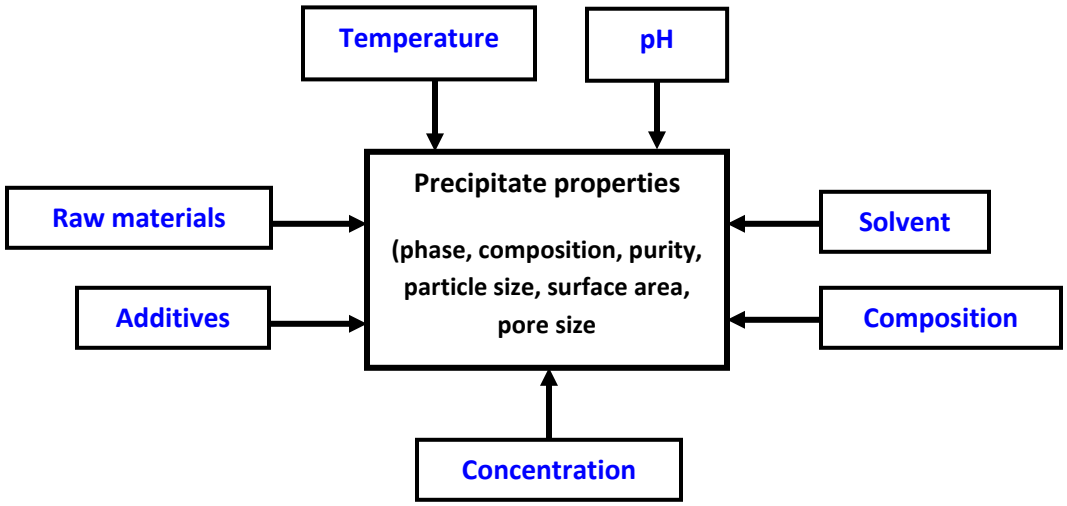

Fig. 3. Parameters affecting the properties of the precipitate

Effect of raw materials : The precursors are usually chosen with counter ions that can easily be decomposed to volatile products during heat treatment steps. Nitrates and carbonate salts are preferably used as metal precursors whereas ammonia or sodium carbonate as the precipitating agent. Chloride and sulphate ions act as poisons in many catalytic processes. Such ions should be avoided in the precipitation process. However, if the precipitation is needed to be carried out in the presence of these ions then repeated washing steps are necessary to remove these ions from the precipitate.

The nature of the counter ions present in the solution can also influence particle morphology, particle size and phase distribution. It has been observed that preparation of MoO_3 from Na_2MoO_4 precursor salt results in small particles with relatively high surface area whereas use of $(NH_4)_6Mo_7O_{24}$ as precursor salt results in larger particles.

Effect of pH : pH directly control the degree of super saturation and hence is expected to affect the final properties. But the influence of pH is not simple and has to be investigated experimentally for the specific system. In aluminium oxide system, the precipitation pH is one of the parameters that determines the phase formation. In general, it has been found that precipitation in alkaline medium (pH > 8) leads to the formation of bayerite (β-$Al(OH)_3$), while precipitation in more acidic conditions favors formation of boehmite (γ-AlO(OH)).

Effect of concentration and composition: It is desirable to precipitate at high concentration levels of metal ions. This increases the space time yields by decreasing the vessel volume for the same mass of precipitate. Moreover, higher degree of super-saturation leads to faster precipitation. Higher concentration levels also results in smaller particle size and higher surface areas due to increased nucleation rates.

If the catalysts are prepared by co-precipitation, the composition of solution determines the composition of the final product. Deviation from solution composition generally occurs if the solubilities of the different components differ significantly and the precipitation is not complete. The precipitation can be carried out simultaneously or sequentially. When the solubility of the components is not too different, then the precipitation will occur almost simultaneously. However, if the solubility of the components differs significantly then the component with lower solubility will preferentially precipitate resulting in sequential precipitation.

Effect of solvent : For preparation of bulk catalysts and supports, water is almost exclusively used as the solvent for economic reason. Organic solvents are much more expensive to use. Furthermore, solubilities of most metal salts used as the precursors are lower in organic solvents. Organic solvents are also environmentally hazardous. So use of organic solvents is very limited. These are used only in specific cases where product quality obtained is better by using organic solvent.

Effect of temperature : The precipitation temperature is a decisive factor in controlling precipitate properties such as primary crystallite size , surface area and the phase formed. Till date it is very difficult to predict the exact nature and extent of effect of the precipitation temperature on the properties and is generally determined experimentally. Nucleation rates are extremely sensitive to temperature. In general, most precipitation processes are carried out above room temperature , often close to 373 K for obvious reason that the precipitation is more rapid. A higher temperature may result in an increase in crystallite size, though this depends on the kinetics of different elementary processes. Sometimes, no effect of temperature or even lowering of size of the crystallites is observed as in the case of ZnO system. Temperature also affects the phase formation. During preparation of Ni/SiO_2 catalysts, at high temperatures nickel hydro-silicate is obtained while at lower temperatures, the main precipitate is nickel hydroxide.

When use of high temperature is detrimental, the rotary evaporator is often used to remove the solvent from slurry solution. Rotary evaporator is a vacuum evaporator in which pressure is lowered above the slurry so that boiling point of the solvent is reduced and it can be removed without using excessive heating. In the evaporator a rotating evaporating flask is connected to vapor duct to draw off the vapor and thereby, reduce the pressure within evaporator system. Sample solution is gently heated in bath, usually water bath, to enhance the solvent removal. The separated solvent vapor can be condensed back using a condenser and collected in a separate flask.

Effect of Additives : Additives are substances which are not necessary ingredients of a precipitation reaction. The properties of the precipitates can strongly be influenced by additives. The most widely used additives are organic molecules which are added to the precipitate in order to control the pore structure. Such organic molecules can later be removed from the precipitate in the calcination step.

A very promising route for the preparation of the high surface area oxides is the use of surfactants as additives. Removal of the surfactant by calcination steps leaves a well-defined pore network. The pore diameter can be adjusted in the range of 2-10 nm. These all are treated as trade secrets and details are not available in the public domain.

Preparation of dual oxides catalysts by coprecipitation

Mixed oxide support and catalyst can be prepared by coprecipitation method. As discussed earlier, for coprecipitation, the solubility of the two components should be in similar range for simultaneous precipitation resulting in homogeneous product. Otherwise the precipitation will be sequential resulting in non-homogeneous product.

Two examples are discussed below.

1. **SiO_2-Al_2O_3**

SiO_2-Al_2O_3 is used in catalytic cracking process and is also used as support for active metals in various applications. Preparation of dual oxides by coprecipitation is similar to precipitation of single oxide. At pH 6 (at 50 ^{0}C) the precipitation of both silica and alumina sols begins and gelation takes places.

2. **NiO-Al_2O_3**

NiO-Al_2O_3 is used for hydrogenation and methanation reactions. Although this catalyst can be produced by other route, coprecipitation method of preparation is also done to increase the intimate interaction between active metal and support. The sodium bicarbonate can be used as precipitating agent for formation of nickel aluminium hydroxyl carbonate with good homogeneity of final product**.**

Book References :

- K.P. de Jong. , Synthesis of solid catalysts , Wiley –VCH, 2009
- J.T. Richardson, Principle of catalysts development, Plenum Press, 1989
- G. Ertl, H. Knozinger & J. Weitkamp, Handbook of Heterogeneous Catalysis Vol 1, Wiley – VCH, 1997
- R. J. Farrauto & C. H. Bartholomew, Fundamentals of Industrial Catalytic Processes, Blackie Academic & Professional, 1997
- S. P. S. Andrew, Chemical Engineering Science 36 (1981) 1431-1445

Lecture 7

Sol gel method

In the sol gel process, initially a stable colloidal solution called sol is formed. The sol is a liquid suspension of solid particles ranging in size from 1 nm to 1 micron. It can be obtained by hydrolysis and partial condensation of precursors such as an inorganic salt or a metal alkoxide. The further condensation of sol particles into a three dimensional network produces a gel material. The gel is a diphasic material in which the solids encapsulate the solvent. The molecular weight of the oxide species produced continuously increases. The materials are referred to as aqua sol or aqua gels when water is used as a solvent and aquosol or alcogel when alcohol is used. The general scheme of preparation by sol gel method is shown in Fig. 1

The encapsulated liquid can be removed from a gel by either evaporative drying or with supercritical drying /extraction. The resulting solid products are known as xerogel and aerogel, respectively. When gels are dried by evaporation, the dried product is called xerogel. When the gels are dried by supercritical drying, the dried gel is called aerogels. The aerogel retains high porosity and has very high pore volume.

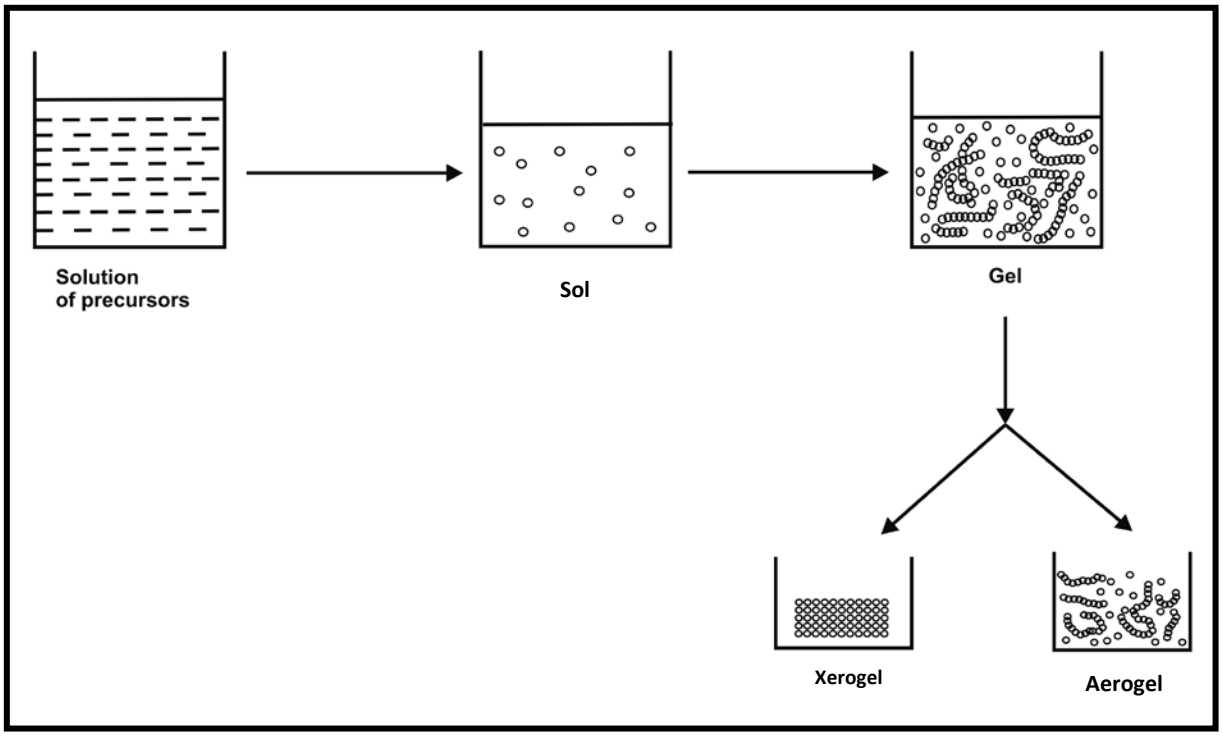

Fig. 1. General scheme of preparation by sol gel method

The sol gel method is distinguished from other routes of material preparation from solutions or melts such as precipitation and crystallization by two main characteristics:

1. Formation of clear colloidal solution due to primary condensation of dissolved molecular precursors.
2. These colloidal particles merge during subsequent gelation stage into polymeric chains by chemical bonding between local reactive groups at their surface.

Both stages are controlled by condensation chemistry that can include as a first step, hydrolysis of hydrated metal ions or metal alkoxides molecules. The condensation chemistry in this case is based on olation/oxolation reactions between hydroxylated species. Olation is a condensation process in which a hydroxyl bridge "–OH--" bridge is formed between two metal centers.

The oxolation is a condensation reaction in which an oxo bridge "-O-" is formed between two metal centers. The steps in sol gel processing are shown in Fig. 2 and discussed below.

Activation and polycondensation : Metal alkoxides are used as precursors in sol-gel operation. Metal alkoxides are most extensively used as these are commercially available in high purity and their solution chemistry is well documented. For preparation of alumina and zirconia, aluminium propoxide and zirconium propoxide are used respectively as precursors.

The metal alkoxides are hydrolysed in alcohol solution containing a controlled amount of water. The sol gel chemistry can be represented by following two reactions :

Hydrolysis: $\text{-M-OR} + H_2O \longrightarrow \text{-MOH} + \text{ROH}$

Condensation: $\text{-M-OH} + \text{XO-M-} \longrightarrow \text{-M-O-M-} + \text{XOH}$

Where M= metal ; X = H or R (alkyl group)

This is a very simplified representation without giving details of the intermediate or end products. However, this gives an idea of the formation of three dimensional gel network coming from the condensation of partially hydrolyzed species.

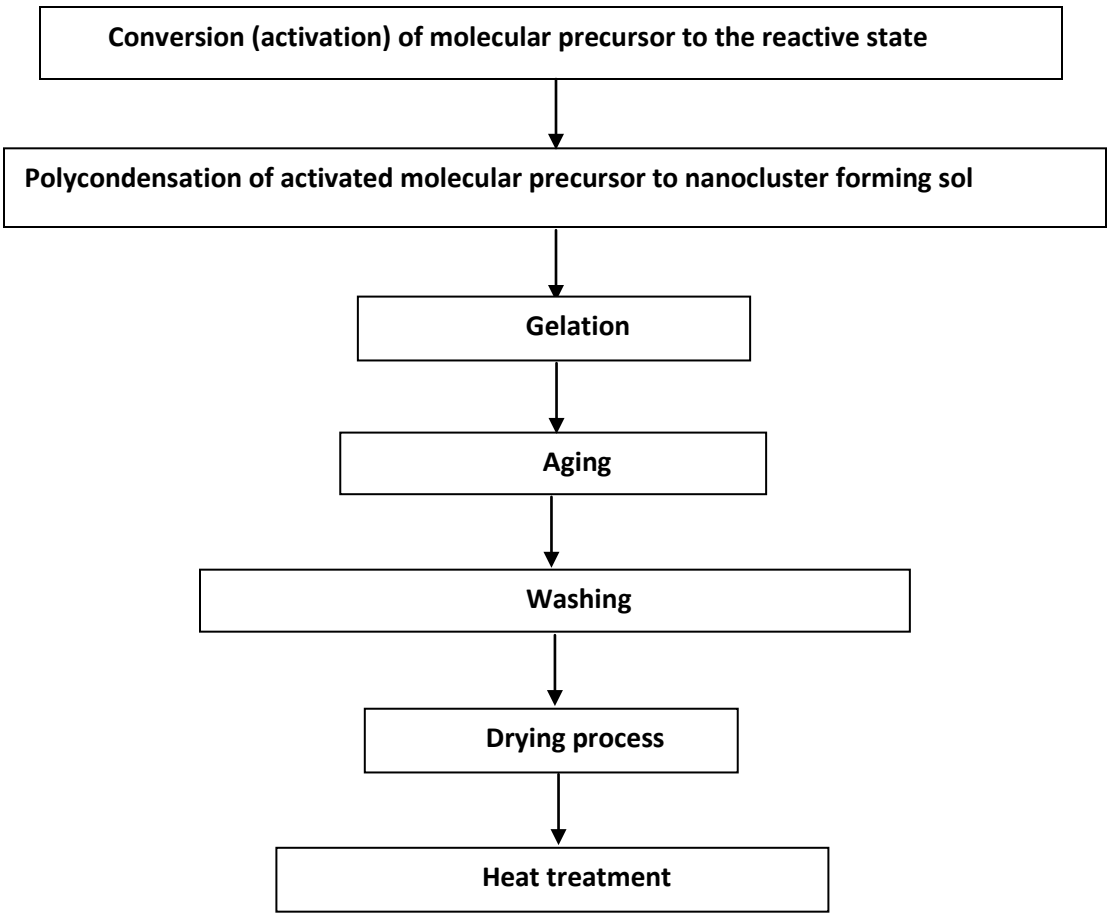

Fig. 2. Basic steps in sol gel processing

Parameters affecting any of the two reactions will affect the properties of the final product. Two of the main parameters that affect are (1) amount and rate of water addition and (2) pH of the solution. The amount of water added is expressed in terms of hydrolysis ratio 'h' and defined as

$$h = \frac{\text{moles of water}}{\text{moles of metal alkoxide M(OR)}_m}$$

When h < 1, there is less possibility of forming infinite network because of the presence of few M-OH groups for cross linking and gelation. If excess amount of water is present, that is h>m, extensively cross linked gel can be formed. For a given amount of water, another way to control the process is to control the rate of addition of water.

The pH of the system affects the relative rate of hydrolysis and condensation. Fig. 3 compares the rates of hydrolysis and condensation of tetra ethyl ortho silicate (TEOS), a very widely used precursors , as a function of pH. Under acidic conditions, hydrolysis occurs at a faster rate than condensation and the resulting gel is weakly branched. Under basic conditions, the reverse occurs and the resulting gel is highly branched and contains colloidal aggregates. Subsequently, dried and heat treated samples have different surface functions and pore structures.

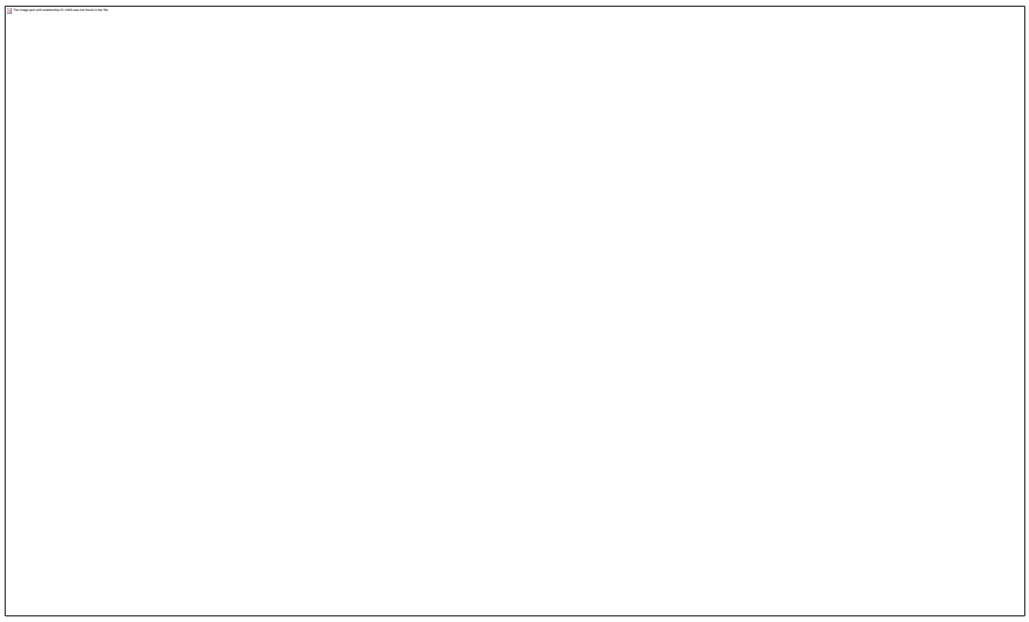

Fig. 3. Effect of relative rates of hydrolysis and condensation reactions on gel structure.

Gelation : After a period of time the sol experiences a transition from liquid solution to a cross-linked gel state where it can support an elastic stress. This period of time is known as gel time or gelation time, and during this time the viscosity of the solution undergoes a rapid increase corresponding to the transition from a viscous fluid to an elastic gel. At the end of gelation there is a continuous phase containing a structure that reflects formation and branching of particles under specific growth conditions. The formation of a network results in entrapping of the solution. The gel structure is determined by the ionic character of the M-O bond and the relationship between the hydrolysis and condensation rate.

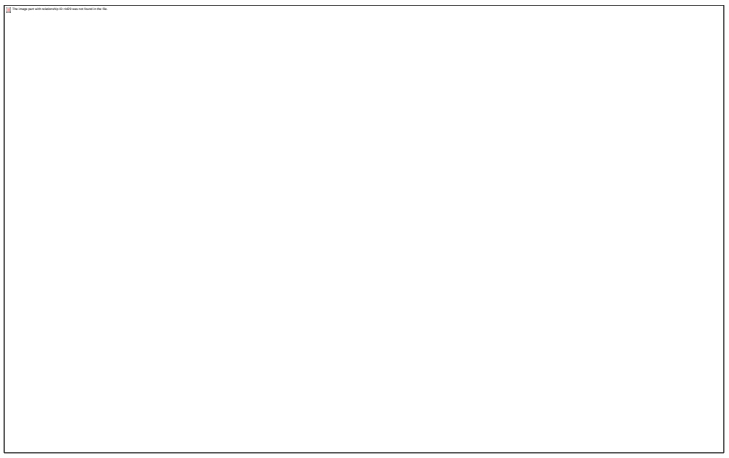

Fig. 4. Double layer structure for particles

Effect of zeta potential on gelation: The particle surface may be positively or negatively charged depending on the pH. With an acidic solution, that is low pH, the equilibrium is driven towards positive surfaces. As pH increases, the surfaces become less positively charged and finally negatively charged. However, the effective charge on the surface is partially neutralized by the counter- ions in the solution that may originate from the bases used during precipitation or electrolytes added during aging. Theses counter- ions form a space charge, part of which is held sufficiently strongly to be carried along as the particles move with Brownian motion (Fig. 4). The result is an effective charge called Zeta potential. Both the original charge and the neutralizing counter- ions respond to pH changes. This zeta potential determines the rate of gelation. If the charge is high, particles effectively repel one another and avoid contact. If it is low, then thermal motion leads to collision and coalescence. These rates are highest at the isoelectric point where the zeta potential is zero. The variation of zetapotential with pH for alumina is shown in Fig. 5.

Fig. 5. Effect of pH on zeta potential of alumina

Two other important parameters are temperature and solvent. Varying temperature is most effective when it can alter the relative rate of the competing reactions. Solvent can change the nature of an alkoxide through solvent exchange or affect the condensation reaction directly.

Aging : After visible formation of gel, processing proceeds to the aging step where the structure and the properties of the formed network continue to change up to the point that yields the target density. It represents the time between the formation of the gel and the removal of solvent. As long as the pore liquid remains in the matrix, a gel is not static and can undergo many transformations. This step includes four processes : polycondensation , syneresis, coarsening , and phase transformation.

Polycondensation between surface functional groups continues to occur after the gel point. This process is actually desirable as it leads to a more cross-linked network that is mechanically stronger and consequently easier to handle. However, extensive condensation can lead to shrinking of the gel to such an extent that the solvent is actually expelled in a phenomenon called syneresis. Parameters that affect this process include temperature, time, and pH of the pore liquid. However, studies off theses effects are still very qualitative.

A typical preparation of zirconia aerogel is shown in Fig. 6. Zirconium propoxide is used as precursor for zirconium. The sol prepared from precursor solution is aged for 2h and then supercritically dried. In this example calcination is done in two steps.

Fig. 6. Sol gel parameters in preparation of zirconia aerogels

Book References :

- K.P. de Jong. , Synthesis of solid catalysts , Wiley –VCH, 2009
- J.T. Richardson, Principle of catalysts development, Plenum Press, 1989
- G. Ertl, H. Knozinger & J. Weitkamp, Handbook of Heterogeneous Catalysis Vol 1, Wiley – VCH, 1997
- R. J. Farrauto & C. H. Bartholomew, Fundamentals of Industrial Catalytic Processes, Blackie Academic & Professional, 1997

Lecture 8

Supported catalysts

Supported catalysts are prepared by deposition of the active metal on the support materials. The main purpose of using a support is to achieve an optimal dispersion of the catalytically active component and to stabilize it against sintering. But in many reactions the support is not inert and the overall process consists of two catalytic functions both for active components and support.

Supported catalysts are prepared in two main steps:

1. Deposition of the precursor of the active component on the support.
2. Transformation of this deposited precursor to catalytically active site.

The final active component can be in metallic state, oxide form or reduced from depending on the requirements.

There are various deposition methods. Most of these involve aqueous solutions and liquid solid interface. In some cases, deposition is also done from the gas phase and involves gas- solid interface. The methods most frequently used are:

a. impregnation
b. ion exchange

Impregnation

Impregnation can be classified in two categories according to the volume of solution used.

Dry or incipient impregnation

In this method, a previously dried support is contacted with volume of solution equal to its pore volume. The solution contains the required amount of the precursors of the active phase. As soon as the support is placed in contact with the solution, the solution is drawn into the pores by capillary suction. In case of proper wetting, no excess solution remains outside the pore space. Part of the air present in the pores is imprisoned and compressed under the effect of capillary forces. The pressure developed inside the imprisoned gas

bubbles depends on the radius, r, of the curve of the liquid -gas meniscus and may reach several MPa when r < 100 nm as a result of Young - Laplace law, $\triangle P = P - P' = \frac{2\gamma}{r}$, where γ is the liquid- gas interfacial tension. Considerable forces will thus be exerted on the portions of the pore walls in contact with these bubbles. The walls that are not strong enough may break down causing a degradation of the mechanical properties. Occasionally, even bursting of the catalyst grains occurs. However, the development of the high pressure is a transitory phenomenon. Under highly compressed conditions, air dissolves and progressively escapes from the solid.

Wet / diffusional impregnation

In this method, the pore space of the support is first filled with the same solvent as used in the impregnating precursor solution. The wetted support is then treated with the impregnating precursor solution. Here the actual impregnation takes place in diffusional condition when solvent filled support is dipped in the precursor solution.

The first phase of saturation of the support by solvent involves the characteristics of dry impregnation. But in the second phase, when solvent saturated support is added to the impregnating solution, high pressure is not developed within the pores. The precursor salt migrates progressively from the solution into the pores of the support. The driving force at all times is the concentration gradient between the bulk solution and the solution within the pores. The impregnation time is much longer than for dry impregnation.

Wet impregnation should be avoided when the interaction between the precursors and the support is too weak to guarantee the deposition of the former.

Mechanism of impregnation: The mechanism of wet impregnation is simpler compared to dry impregnation. In wet impregnation, the distribution of the solute inside the pores is assumed to be governed by two phenomena (Fig 1):

1. Diffusion of the solutes within the pores. It is described by Fick's law
2. Adsorption of the solute onto the support. This depends on the adsorption capacity of the surface and on the adsorption equilibrium constant.

The distribution of the precursors within the pellets depends on the balance between these diffusion and adsorption phenomena.

(a) Wet impregnation **(b) Dry impregnation**

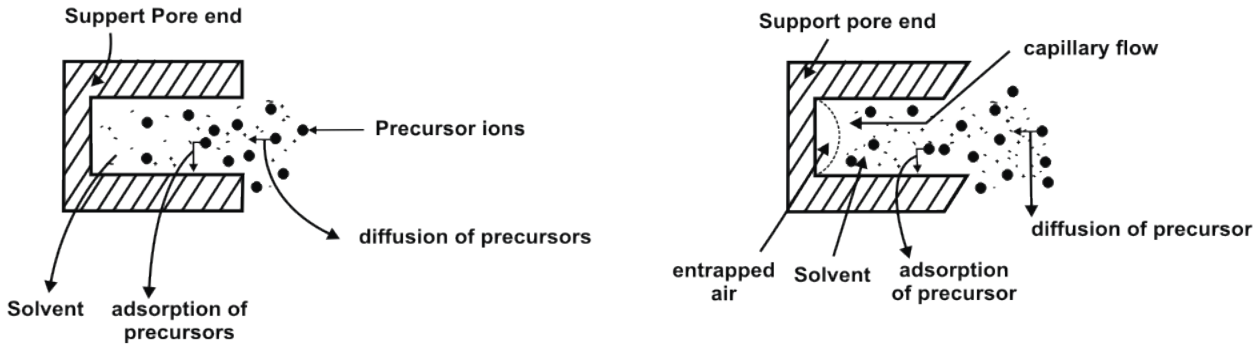

Fig. 1. Schematic representation of basic processes involved during impregnation of precursors on porous support.

In case of dry impregnation, in addition to diffusion and adsorption processes, another phenomenon occurs, which is the pressure driven capillary flow of the solution inside the empty pores. This can be represented by Darcy's law. An important parameter from introduction of Darcy law is the solution viscosity 'μ'. In case of aqueous solution and in the common range of concentration used for impregnation, viscosity increases almost proportionally with concentration. It also increases with the presence of organic ligands attached to the metal ions. Viscosity and concentration have opposite effects on precursor diffusion; a high concentration tends to favor the diffusion of the solute towards the centre of the pellet, while a high viscosity tends to hinder the diffusion.

Drying

Impregnation is followed by elimination of the solvent. The impregnated sample is heated in an oven in a flow of gas, as discussed earlier. The gas may be air, oxygen, nitrogen or any other gas depending on the requirement. The temperature is generally maintained slightly higher than the boiling point of the solvent e.g 110-120 ^{0}C for water. The elimination of water from the pores leads to the increase of precursor concentration

up to saturation and consequent crystallization, preferably on the seeds resulting from the interaction with the support. Apart from temperature, heating rate affects the drying process.

(a) Constant rate period of drying **(b) Falling rate period of drying**

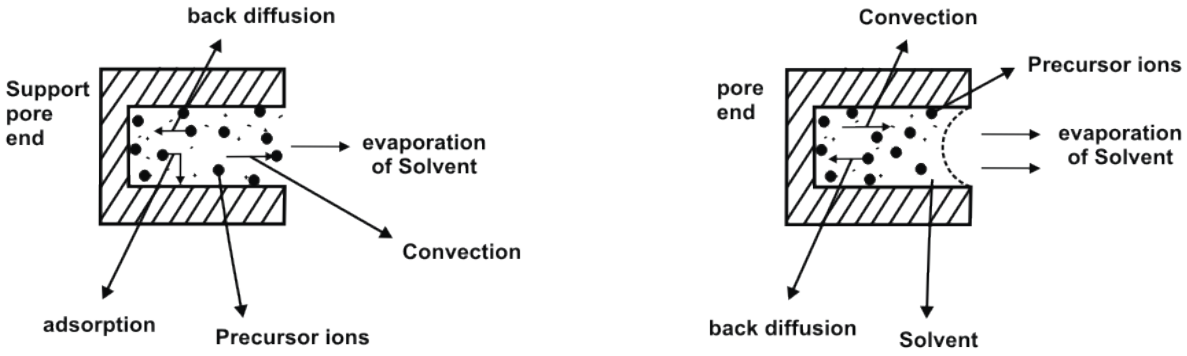

Fig. 2. Schematic representation of drying process during impregnation method

Drying Mechanism: The drying process can be modeled considering the outward convective flow of liquid towards the pore mouth at pellet surface where the solvent evaporation occurs. This convective flow can be described by Darcy's law and is associated with the outward flow of the precursors that is favored by a low viscosity of the solution. As the precursor concentration increases near the outer surface of the pellet due to this outward flow, an inward back diffusion of precursors, which can be modeled by Ficks law, takes place. Apart from these two flows in opposite directions, another factor that needs to be considered is the interaction between the precursor and support surface. Schematic representation of drying process during impregnation method is shown in Fig. 2.

The distribution of the precursor phase in the pellet or its segregation at the outer surface depends on the relative contribution of adsorption, convection and back-diffusion as long as the flow of solvent is high. This corresponds to constant rate period of drying.

As the solvents recedes inside the pores, evaporation occurs within the pores corresponding to the falling rate period. The drying regime is defined as slow if the constant rate period predominates and as fast if it is falling- rate period controlled.

Precursor distribution: The distribution of precursors within the pores of support depends on various factors. The different conditions of impregnation and drying can result in broadly three types of precursor distribution as described in Table 1. In Egg shell type distribution the precursors are preferentially accumulated near the pore wall. This type of distribution is obtained if during impregnation precursors are strongly adsorbed on the pore wall. High viscosity of the solution also tends to result in egg shell distribution. For slow drying, egg shell distribution can result even in low viscosity and weak adsorption conditions. In egg yolk type distribution the precursors are accumulated in the interior core of the pores. Egg yolk distribution is obtained if during impregnation, the competing ions are present that have stronger interaction with the pore wall of supports. Fast drying regime with predominant back diffusion also results in egg yolk distribution. In uniform precursor distribution, precursors are uniformly distributed across the pores. If the adsorption of the solutes is weak and the time is long enough, distribution tends to be uniform. Uniform distribution also results when precursors and competitors interact equally with the surface or the impregnating solution is concentrated and viscous. Room temperature drying with weakly adsorbing precursors also tends to give uniform precursor distribution. For powders, the equilibrium is reached within few minutes. However, in case of pellets it may take up to several hours to reach a uniform distribution of the precursors.

Table 1. Distribution of precursor at different conditions of impregnation and drying.

Precursor distribution	Conditions of Impregnation and drying
Egg shell distribution 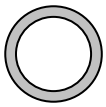	1. Strong adsorption of precursors during impregnation 2. High viscosity of impregnating solution 3. Slow drying regime for low concentration, low viscosity and weak adsorption conditions
Egg yolk distribution 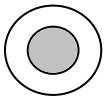	1. In presence of competitor ions that have stronger interaction with the supports 2. Fast drying regime with predominant back diffusion
Uniform distribution 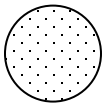	1. Precursors and competitors interact equally with the surface. 2. Impregnating solution is concentrated and viscous 3. Room temperature drying with weakly adsorbing precursors

Parameters affecting the impregnation process

The pH of the solution is an important parameter in the impregnation process. On liquid side, pH determines the most abundant species in solution to be deposited on to the support. HNO_3, carboxylic acids, ammonia are usually used for adjusting the pH because these can decompose during thermal treatment. On solid side, pH controls the nature of surface charge and the number of charged sites, in other words, the zeta potential. During impregnation, the extent of interaction between the metal complex and the support is controlled by parameters such as isoelectric point of oxide support, temperature and nature of support and dopants.

Ion exchange

Ion exchange consists of replacing an ionic species by another ionic species in electrostatic interaction of the precursors with the surface of a support. The support containing the ion A is dipped into an excess volume (compared to the pore volume) of a solution containing ion B that is to be introduced. Ion B gradually penetrates into the pore space of the support and takes the place of ion A, which passes into the solution. This continues until equilibrium is established corresponding to a given distribution of the two ions between the solid and solution.

Natural ion exchangers: Natural exchangers are composed of a frame work having charge that is neutralized by ions of opposite charge. For example, zeolite has negatively charged framework due to the particular environment of aluminium. Aluminium, just like silicon, is effectively situated in the centre of a tetrahedron of four oxygen atoms which have four negative charges, where as aluminium has only three positive charges. The tetrahedron (AlO_4) thus have an overall one negative charge distributed over the oxygen atoms and this charge is neutralized by the presence of various cations such as Na^+, K^+ etc. These cations are not definitively bonded to the framework but may be replaced by other cations during an ion exchange operation. Zeolite has a constant number of these exchange sites which are equal to the number of aluminium atoms in their framework. Clays, silicates are also cation exchangers.

Mechanism of single ion exchange: Single ion exchange takes place when in the solid-solution system only two ions interact. If ion A^+ on the solid Z is to be replaced by ion B^+ present in the solution then in the simple case of two monovalent cations, the exchange equilibrium can be written as $A_z^+ + B_s^+ \rightleftharpoons B_z^+ + A_s^+$

The subscripts ‘s’ and ‘z’ represent solution and solid, respectively. In case of ideal exchange, that is both the exchanger and solution are ideal with single type of adsorption sites, the equilibrium constant K_a can be written as

$$K_a \rightleftharpoons \frac{C_{BZ} C_{AS}}{C_{BS} C_{AZ}}$$

C_{AZ} = concentration of ion A^+ in the solid

C_{AS} = concentration of ion A^+ in the solution

C_{BZ} = concentration of ion B^+ in the solid

C_{BS} = concentration of ion B^+ in the solution

$C_{AZ} + C_{BZ} = C_Z$ = total concentration of cations in the solid

$C_{AS} + C_{BS} = C_S$ = total concentration of cations in the solution

Therefore it follows that

$$C_{BZ} = \frac{K_a C_Z C_{BS}}{C_S\left(K_a - 1\right)C_{BS}}$$

If it is not an ideal system, the above equation must be expressed in terms of concentration and activity coefficients.

Example: Na^+ ions in NaY zeolites can be replaced by NH_4^+ ions. NaY zeolite [$Na_2O.Al_2O_3$. 5 SiO_2] contains 9.9 wt% Na and 73% Na can be exchanged.

Book References :

- K.P. de Jong. , Synthesis of solid catalysts , Wiley –VCH, 2009
- J.T. Richardson, Principle of catalysts development, Plenum Press, 1989
- G. Ertl, H. Knozinger & J. Weitkamp, Handbook of Heterogeneous Catalysis Vol 1, Wiley – VCH, 1997
- R. J. Farrauto & C. H. Bartholomew, Fundamentals of Industrial Catalytic Processes, Blackie Academic & Professional, 1997

Lecture 9

Washing and filtering

Washing can be done by decantation. This method is time consuming. In this method the precipitate or gel is added to a large volume of distilled water and the suspension is thoroughly stirred. Then, the suspension is allowed to settle. The foreign undesirable ions are desorbed from particles as they settle down slowly at the bottom. When a clear interface is visible, the water is removed by decantation and the process is repeated. The number of washings required is determined by checking the impurity level of the decanted water. After washing, the precipitate or gel is filtered. The process can be reversed. That is the filtration is done first and the precipitate or gel is washed with distilled water in the subsequent step. This method takes less time. Impurity level in the wash water is checked to determine the required number of washings.

Drying

Drying is described as the elimination of water or solvent from the pores of the precipitate or gel. It can be done in two ways:

- Solvent evaporation
- Super critical drying

Solvent evaporation : This type of drying is done in a conventional oven at 100-200 ^{0}C and is generally accompanied by a contraction of the structure. In case of gel, the product obtained from ordinary drying is known as dry gel or xerogel. Initially, drying occurs through evaporation of moisture from the outside surface of the materials. The rate of water loss is constant and the mass transfer is controlled by temperature, relative humidity and flow rate of air over the surface and the size of the filtrate. The process continues until the moisture content drops to about 50%. Continued moisture loss occurs with a declining rate in which evaporation is controlled by capillary forces. The saturation point decreases as the pore become smaller and the evaporation slows until water is forced into larger pores by concentration gradient. At the moment of drying, as the pore liquid is evaporated from a gel network, the capillary pressure associated with the liquid vapor interface within a pore can become very large for small pores. The capillary pressure that can develop in a pore of

radius r is $P = \frac{2\gamma \cos\alpha}{r}$, where P is capillary pressure, γ is surface tension, r the pore radius and α is the contact angle between liquid and solid. The capillary pressure with water evaporating from a pore with a radius of 1 nm is in the order of 1480 atm. Large capillary tension can lead to collapse of internal structure resulting in loss of pore volume and surface area. This phenomenon is more significant for a gel having more intricate porous structure compared to ordinary precipitated material. For a given pore size, the capillary pressure can be reduced by

1. Using a solvent with a lower surface tension or with a contact angle close to 90^0.
2. Eliminating the liquid -vapor interface altogether with either supercritical or freeze drying.

If temperature gradient is high so that evaporation rate is much faster compared to removal of moisture that is slowed by smaller pores, then large internal pressure of steam develops and also leads to collapse of structure. Therefore, high temperature gradient in the sample must be avoided. Drying at a lower temperature gives less surface area loss since evaporation rates are lower.

Supercritical drying is aimed at eliminating the liquid vapor interface and the accompanying capillary pressure responsible for structure collapse during conventional drying particularly for gels. It is used where retention of original microstructure of the product is important. This process typically involves displacement of water using an alcohol followed by removal of this alcohol/water mixture using supercritical carbon dioxide. In this process, the gels are placed in an autoclave filled with ethanol. The system is pressurized to at least 750-850 psi with CO_2 and cooled to 5-10 ^{0}C. Liquid CO_2 is then flushed through the vessel until all the ethanol has been removed from the vessel and gels. When the gels are ethanol-free, the vessel is heated to a temperature above the critical temperature of CO_2 (31 ^{0}C). As the vessel is heated, the pressure of the system rises. CO_2 is carefully released to maintain a pressure slightly above the critical pressure of CO_2 (1050 psi). The system is held at these conditions for a short time, followed by a slow, controlled release of CO_2 to ambient pressure. As with previous steps, the length of

time required for this process is dependent on the thickness of the gels. The process may last anywhere from 12 hours to 6 days.

Calcination or sintering

After the removal of pore liquid, further heat treatment is necessary to convert the precipitate or dry gel to catalytically useful form. After drying, the next step of heat treatment is known as calcination. Often the heating is done in the presence of flowing air or oxygen to burn any residual organics or to oxidize the sample. Multiple changes occur during this process including:

1. Active phase generation: The hydroxide form is converted to oxide form.

2. Stabilization of mechanical properties: The catalysts sample is subjected to a more severe heat treatment than that is likely to be encountered in a reactor. This ensures the stability of its textural and structural properties during reaction.

3. Loss of chemically bound water: The chemically bound water is removed at higher temperature.

4. Changes in pore size distribution and surface area due to sintering: Exposing the sample to high temperature over an extended period of time leads to sintering and consequently decreases the surface area.

5. Change in phase distribution: Higher temperature cause material to crystallize into different structural forms. Fig. 1 shows the formation of various phases of alumina when calcined at different temperatures.

The extent of change in the physical characteristics of the final sample depends on following parameters: temperature, heating rate, heating time and gaseous environment.

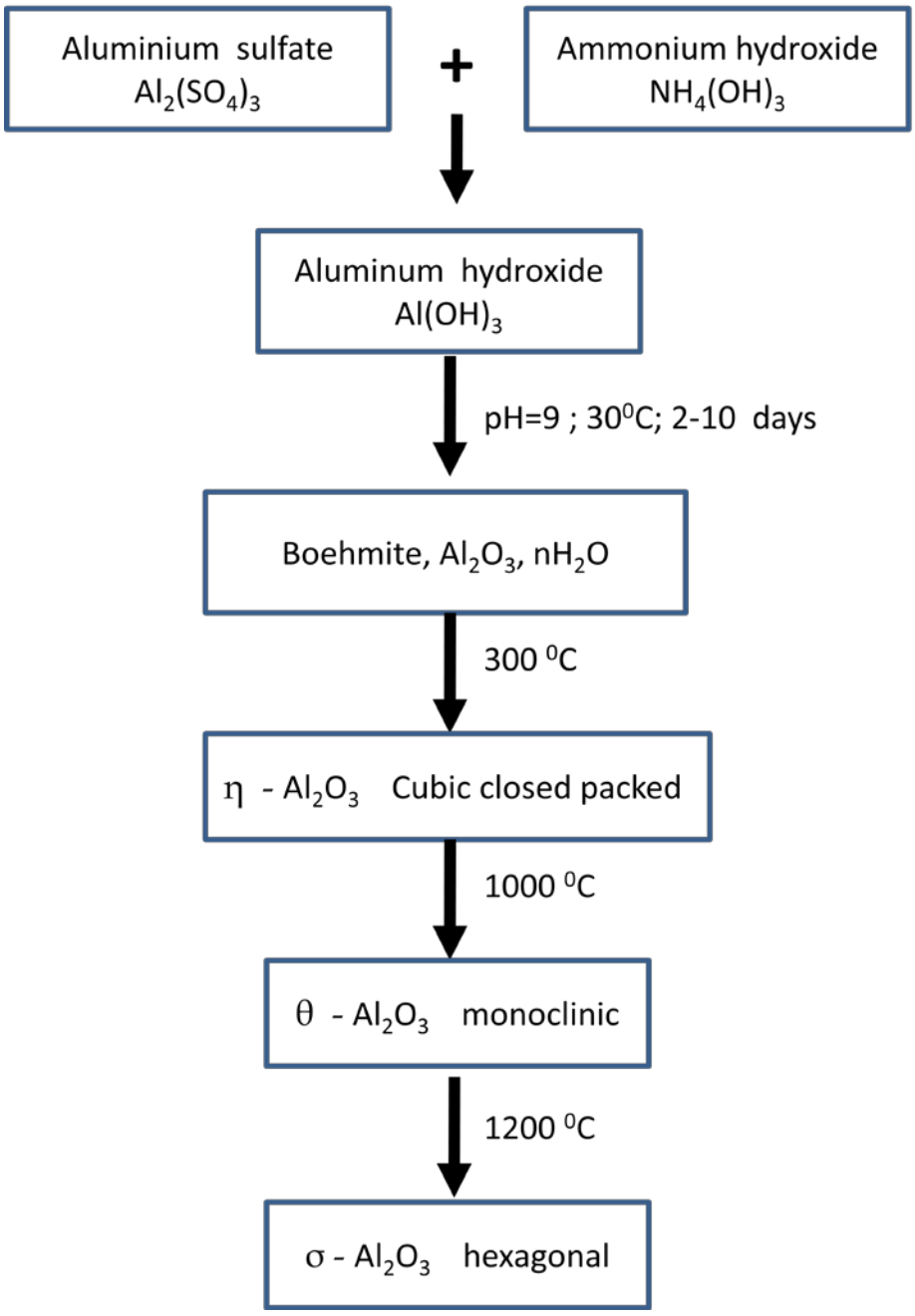

Fig. 1. Formation of various phases of alumina on calcination at different temperatures

Catalyst shaping and formulation

Mainly, solid catalysts are used in industrial catalytic processes and these are formulated in different forms such as pellets, extrudates, granules or sphere form.

Formulation and shaping of solid catalysts is done to :

(a) avoid high pressure drop in fixed and moving beds
(b) increase thermal resistance against sintering fracture or phase transition
(c) increase mechanical resistance against crushing and attrition
(d) ensuring high effective heat conductivity in fixed and moving bed for strongly exothermic and endothermic reactions

Aiming at highest catalyst efficiency is the primary objective in catalyst design because conversion, selectivity and thermal resistance are strongly affected by the above-mentioned parameters. Some of the common catalysts formulation techniques are :

a. pellet formation
b. granulation
c. extrusion
d. spray drying

Pellet formation :

It is a high pressure agglomeration technique producing particles of uniform shape and dimensions. Typically, the dry catalyst powders are compressed in a dye by applying forces between 50-80 kN with a pending tool. Factors such as ultimate tensile strength of the materials, moisture content, porosity, stickiness are important. Some materials, such as kieselguhr, undergo easy pellet formation whereas other materials such as alumina require addition of small amount of plasticizers or lubricants such as graphite, talc etc. Important processing parameters are the maximum applied pressure and the rate of pressure rise. Both influence the hardness of the pellets as well as the integrity of compacted particles.

Granulation :

This is a size enlargement process by wet tumbling. In this method, the particles are tumbled in a cylinder. A cohesive liquid is sprayed onto the catalyst powder such that the wetted particles stick together. The granules grow by contacting further particles. Product with wide size distribution can be produced by controlling parameters such as binders type and concentration, rpm of pan, granulation time and angle of inclination of pan. Typically, pan granulation yields spherical particles of diameters in the range of 2-20 mm.

Extrusion :

It is a widely used technique. In this method, a suspension or paste of the catalyst powder is passed through a profiled die that determines the shape of the body. Screw extruders are very common in use. Slurry of the catalyst is fed to the extrudate at one end and the screw forces the slurry through the holes at the other end. As the ribbon of slurry emerges from the holes, a knife is arranged at the end to cut it to the required size. Particles of narrow size distribution can be obtained by this method.

Spray drying :

This process involves atomization of slurry feedstock into a spray of droplets and contacting the droplets with hot air in a drying chamber. Particle sizes are determined by the size of droplets, which is controlled by design of spray nozzles, slurry flow rate, slurry viscosities. Products in a spray dryer are spheres of diameters in the range of 0.05 to 0.5 mm.

The schematic diagram of catalyst formulation techniques are shown in Fig. 2.

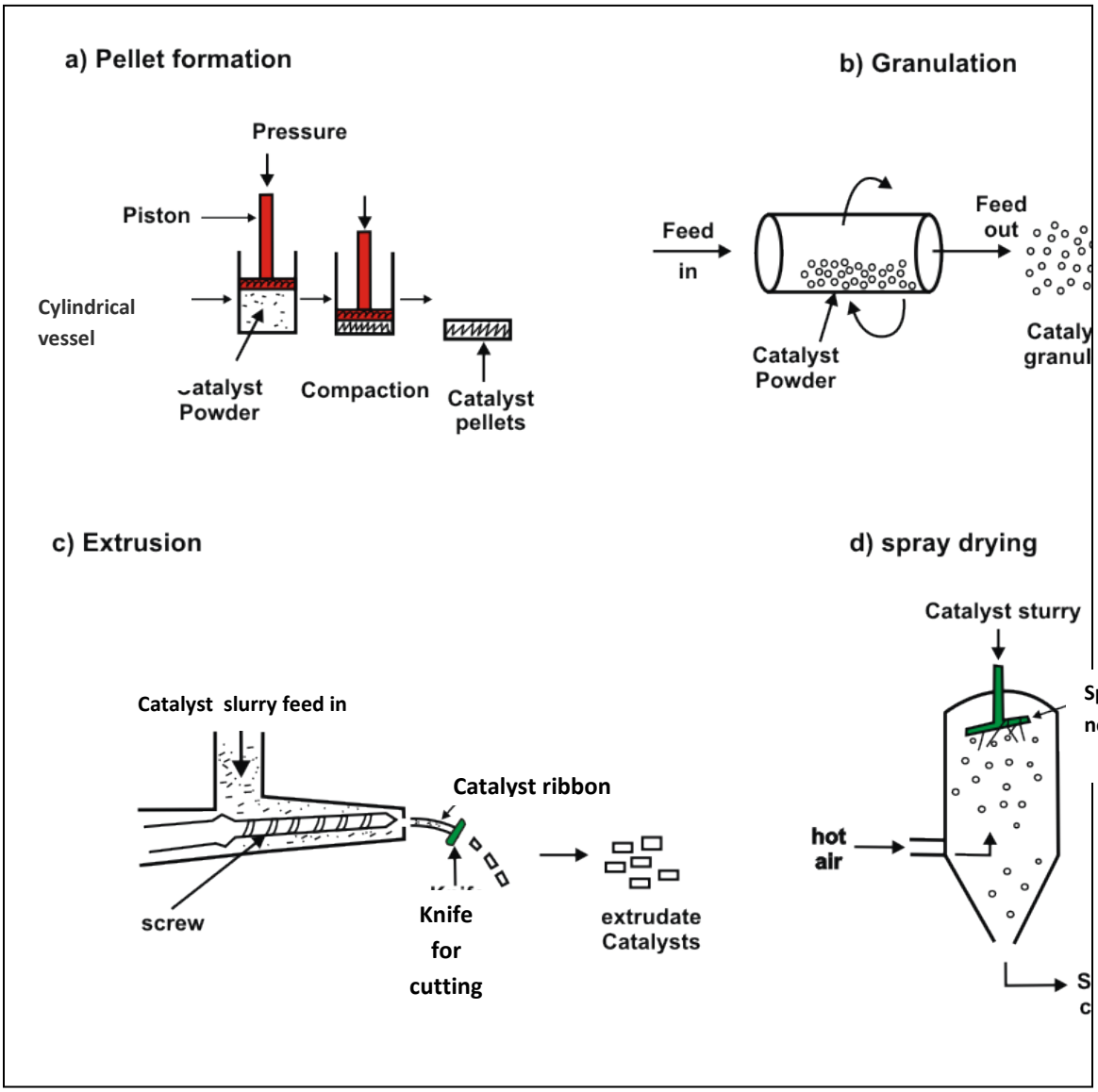

Fig. 2. Schematic diagram of different catalysts formulation techniques

Book References :

- K.P. de Jong. , Synthesis of solid catalysts , Wiley –VCH, 2009
- J.T. Richardson, Principle of catalysts development, Plenum Press, 1989
- G. Ertl, H. Knozinger & J. Weitkamp, Handbook of Heterogeneous Catalysis, Vol 1, Wiley – VCH, 1997
- R. J. Farrauto & C. H. Bartholomew, Fundamentals of Industrial Catalytic Processes, Blackie Academic & Professional, 1997
- J.J. Carberry , Chemical and catalytic reaction Engineering, Dover Publications, 2001

Lecture 10

Catalyst characterization

Characterization of heterogeneous catalyst refers to the determination of its physical and chemical characteristics, which are responsible for its performance in a reaction. Characteristics of catalysts include:

- Chemical composition of the bulk and surface of the solids
- Surface area and porosity (micro, meso and macro)
- Bulk solid structure, phase composition, crystallite size
- Surface morphology
- Surface chemical properties such as:
    - location and oxidation state of active metals
    - acid-base property
    - reducible – oxidizable property
- Aggregate properties such as aggregate or particle size, density, mechanical strength and attrition resistance
- Catalytic properties : activity , selectivity, stability

Objectives of characterization

The primary objective of catalyst characterization is to understand the relationship among physical, chemical and catalytic properties. For this purpose, the physical and chemical properties are determined by various characterization techniques and related to its activity and selectivity. This is essential for design and process optimization. The characterization is also done to monitor the changes in physical and chemical properties of the catalyst during preparation, activation and reaction stages for better understanding and quality control. Determination of the extent of deactivation of catalysts during the reaction process is also important. Characterization of used catalysts can help to determine the causes of deactivation and minimize it. It also helps to design procedures for catalysts regeneration.

Characterization Techniques

In this section some of the characterization techniques that are most commonly used will be discussed. These techniques are summarized below.

1. **Structural analysis**

(a) Surface area

- widely accepted BET (Brunauer, Emmet and Teller) method used for analyzing multilayer physisorption isotherms of inert gases to determine the surface area

(b) pore analysis by

- BJH method
- mercury intrusion method

(c) X-Ray Diffraction (XRD) :

- can detect crystalline materials having crystal domains greater than 3-5 nm.
- characterization of bulk crystal structure and chemical phase composition.

2. **Chemisorption technique**

- determines dispersion of metal in catalysts
- determination of surface metal area

3. **Thermal analysis**

(a) temperature programmed reduction (TPR) :

- measures the rate of reduction of active metals as function of temperature.
- can be correlated with activity of catalysts

(b) temperature programmed desorption (TPD) :

- measurement of rate of desorption of adsorbed molecules as function of temperature
- mainly used to of study acid –base property of catalysts

(c) Thermo Gravimetric Analysis (TGA) :

- measurement of weight loss (or gain) as a function of temperature in a controlled gaseous atmosphere;

- process associated with mass change can be detected and analyzed

(d) Differential Thermal Analysis (DTA)

- monitoring the temperature difference between sample and reference
- process associated with latent heat of transition can be detected and analyzed

4. Spectroscopic techniques

(a) Infra red spectroscopy

- identify compounds and investigate sample composition
- Study of structure and bonds

(b) Raman spectroscopy :

- study of oxidation state and interaction of metal oxides

5. Microscopic technique

(a) Scanning electron microscopy (SEM):

- image the topography of solid surface
- resolution better than 5 nm.

(b) transmission electron microscopy (TEM) :

- determines the micro –texture and micro structure
- resolution better than 0.2 nm

Surface area, pore size, pore volume determination

Determination of surface area and pore distribution of catalysts is important to understand the extent of dispersion possible for the active metals. Higher surface area of support results in higher dispersion of the active metals. Hence supports of higher surface area are desirable.

Pores are usually formed during drying or calcination of hydroxides precipitates or gel. The size and number of pores determines the internal surface area. Pore size also determines the accessibility of reactants to the active sites and the ability of diffusion of products back to the bulk fluid. Hence pore structure and surface area must be optimized to provide maximum utilization of active sites for a given feed stock.

Working principle and instrumentation

The basic components of volumetric physical adsorption analyzer as shown in Fig. 1 are:

1) Analysis manifold of accurately known volume and temperature

2) Vacuum system with valve to manifold

3) Source of adsorptive gas (typically, N_2) with valve to manifold

4) Pressure transducer and temperature sensor

5) Sample tube connected to analysis manifold

6) Liquid nitrogen bath

Determination of internal surface area is based on adsorption and condensation of N_2 at liquid N_2 temperature, 77K. Initially, the sample is evacuated at 293-523 K (120-250 ^oC) followed by cooling to 77 K by liquid N_2. Then gradually the partial pressure of nitrogen above the sample is increased. Some quantity of gas will be adsorbed by the sample and removed from the gas phase. After stabilization the equilibrated pressure is recorded and amount of nitrogen adsorbed at each equilibrated pressure is noted. The isotherm, volume adsorbed as function of relative pressure p/p_o, is plotted from the data. The pressure over the sample is gradually increased until pressure reaches near saturation pressure, by when

the complete adsorption isotherm is developed. The desorption isotherm is measured by a step-wise reduction in pressure until a low pressure over the sample is achieved. Although the volumes are adsorbed at different conditions, the values are reported at STP conditions. Fig. 2 shows a typical N_2 adsorption and desorption isotherm at 77 K for alumina.

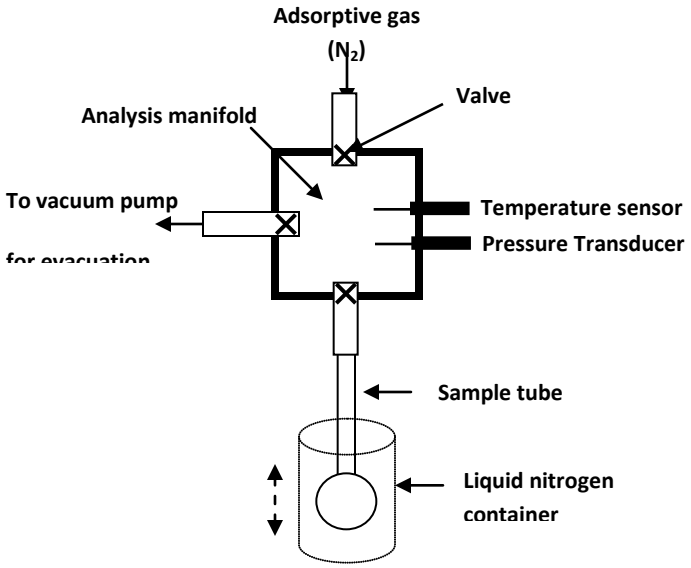

Fig. 1. Basic components of volumetric physical adsorption analyzer

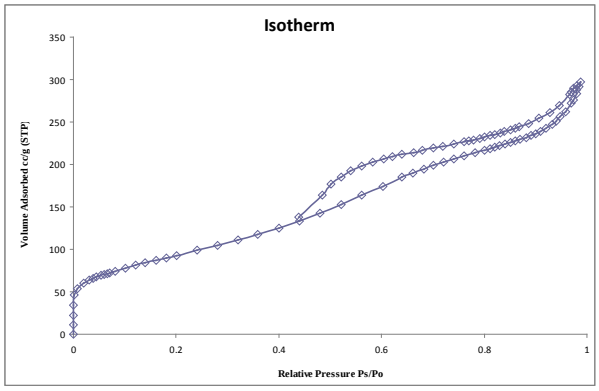

Fig. 2. A typical N_2 adsorption and desorption isotherm at 77 K for alumina

Adsorption using Argon and Krypton

Krypton is used as adsorbate at 77 K for low surface area analysis while, Argon adsorption at 77 K and liquid argon temperature (87K) is often used for micro and mesopores analysis.

To measure very low surface area the number of molecules trapped in the void volume of sample cell needs to be reduced. The number of molecules left in void volume can be reduced by using adsorbate such as Krypton with low vapor pressure at liquid nitrogen temperature. The saturation pressure of Krypton at liquid nitrogen temperature is 0.35 kPa which is much lower compared to that of N_2 (101.3 kPa). Consequently the number of Krypton molecules in free space of sample cell, at any given relative pressure, is significantly reduced compared to that of nitrogen at liquid nitrogen temperature, though amount of adsorption will be only slightly less. Hence, Krypton adsorption at 77 K is much more sensitive and can be applied to measure surface areas down to 0.05 m^2. The cross sectional area used for Krypton is 0.202 nm^2.

For analysis of ultramicropores less 0.7 nm, the nitrogen adsorption at 77 K is not satisfactory. The pore width of 0.7 nm corresponds to bilayer thickness of nitrogen molecule. For ultramicropores, pore filling occurs at relative pressure of 10^{-7} to 10^{-5}, where the rate of diffusion and attainment of adsorption equilibration is very slow. Consequently measurement becomes time consuming and may also cause non-equilibrated adsorption isotherms with erroneous results. On the other hand argon fills the micropores of dimension 0.4-0.8 nm in most cases at much higher relative pressure as compared to nitrogen. This leads to accelerated diffusion and equilibration process and result in reduction of analysis time as well as increase in accuracy. Argon adsorption is advantageous for pore size analysis of zeolites and other microporous materials.

The typical surface area values of different supports and catalysts are summarized in Table 1.

Table 1. Typical surface area values of different support and catalyst.

Support/catalyst	BET surface area m^2/g	Application
Activated carbon	500-2000	Used as support for various process
Zeolites	500-1200	Used as catalyst and support
Al_2O_3-SiO_2-Zeolites	100-600	Fluid catalytic cracking catalysts
Ni/Al_2O_3	100-150	Methanation catalyst
$Cu/Zn/Al_2O_3$		Methanol synthesis catalyst
MnO_x/Al_2O_3	140-180	Catalyst for total oxidation of volatile organic carbon
$Fe/K/Al_2O_3$	20	Ammonia synthesis catalyst

Determination of surface area using BET Equation

As discussed earlier (lecture 4), the BET equation describes the relationship between volume adsorbed at a given partial pressure and the volume adsorbed at monolayer coverage. BET equation can be written in the form :

$$\frac{p}{v(p_0 - p)} = \frac{1}{v_m c} + \frac{c-1}{v_m c}\frac{p}{p_0} \quad \text{---------- (1)}$$

p = partial pressure ; p_o =saturation pressure at the experimental temperature ;

v = volume adsorbed at p; v_m = volume adsorbed at monolayer coverage ; c = constant

Monolayer coverage is determined using BET equation. The $\frac{p}{v(p_0 - p)}$ is plotted as a function of $\frac{p}{p_0}$. The plot is linear in the range of relative pressures $\frac{p}{p_0}$ = 0.05 - 0.3. At higher relative pressure p/po, the BET plot deviates from linearity as non-ideality or pore condensation was not accounted for the derivation of BET equation.

Slope and intercept of this linear plot is used for determination of monolayer capacity v_m.

The intercept and slope from the plot is given as

$$\textbf{Intercept} = \frac{1}{cv_m} \qquad \textbf{Slope} = \frac{(c-1)}{cv_m}$$

Then the monolayer volume v_m is given as , $v_m = \frac{1}{\text{slope + intercept}}(STP)$

The total number of N_2 molecules adsorbed corresponding to monolayer volume v_m can be calculated as

$$No.\ of\ N_2\ molecules = \frac{v_m\ (m^3) \times\ 6.02 \times 10^{23} (molecules / mol)}{0.0224\ (m^3 / mol)}$$

Now , each adsorbed N_2 molecule occupies an area of surface comparable to its cross section area of 0.162 nm^2.

$$SA(m^2) = \left[\frac{v_m\ (m^3) \times\ 6.02 \times 10^{23} (molecules / mol)}{(0.0224\ m^3 / mol)} \right] \times 16.2 \times 10^{-20}\ \ (m^2 / N_2 molecule)$$

Or $$SA(m^2) = v_m\ (m^3) \times 4.36 \times 10^6\ (m^{-1}) = 4.36 \times 10^6 v_m$$

Solved problem :

1.Nitrogen was employed to determine the surface area of 1.0 g sample of silica gel and results obtained shown in table below. The sample of silica gel was maintained at the normal boiling point of liquid nitrogen (77K). One molecule of nitrogen occupies 16.2 × 10^{-20} m^2 area of plane surface. Calculate the specific surface area of silica gel by the BET method. The saturated vapor pressure $\mathbf{p_0}$ of nitrogen at 77K is 101.3 kPa.

Equilibrium Pressure, p [kPa]	5.0	6.3	7.5	9.0	11.2
Volume adsorbed, (STP), V × 10^6 [m^3]	6.7	7.0	7.2	7.4	7.7

Solution :

The BET equation in following form is used. $\frac{p}{V\left(p_0 - p\right)} = \frac{1}{V_m C} + \frac{C-1}{V_m C}\frac{p}{p_0}$

The $\frac{p}{V\left(p_0 - p\right)}$ is plotted as function of $\frac{\boldsymbol{p}}{\boldsymbol{p_0}}$. The plot is shown in Fig. 3.

Table 1. Calculation for plot of BET equation

v m^3	p *kPa*	p_o *kPa*	p/p_o	$p/[v(p_o-p)]$ m^{-3}
6.7E-06	5	101.3	0.049	7.75E+03
7.0E-06	6.3	101.3	0.062	9.47E+03
7.2E-06	7.5	101.3	0.074	1.11E+04
7.4E-06	9	101.3	0.089	1.32E+04
7.7E-06	11.2	101.3	0.111	1.61E+04

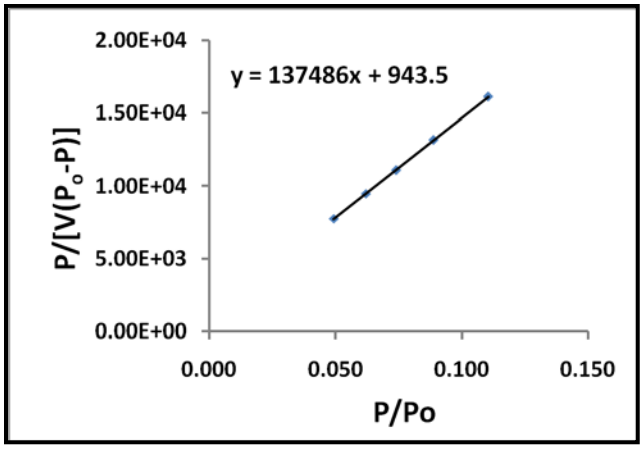

Fig. 3. Linear plot of BET equation

Intercept = 943.5 m^{-3} ; Slope = 137486 m^{-3}

Monolayer volume $V_m = \frac{1}{\text{slope + intercept}} = \frac{1}{137486 + 943.5} = 7.22 \times 10^{-6} m^3 \text{(STP)}$

Then surface area for 1 gm sample can be determined as :

$$SA = \left[\frac{7.22 \times 10^{-6}\ m^3 \times\ 6.02 \times 10^{23} molecules / mol}{22400\ \times 10^{-6} m^3 / mol} \right] \times 16.2 \times 10^{-20}\ \ m^2 / N_2 molecule$$

= 31.4 m^2

As initially 1 gm sample was used, specific surface area of sample = 31.4 m^2/g

Book reference

- S. Lowell, Joan E. Shields, Martin A. Thomas ,Characterization Of Porous Solids And Powders: Surface Area, Pore Size And Density - Springer, 2006
- J.J. Carberry , Chemical and catalytic reaction Engineering, Dover Publications, 2001
- J. M. Thomas & W. J. Thomas, Principles and Practice of Heterogeneous Catalysi, VCH, 1997
- Sam Zhang, Lin Li, Ashok Kumar, Materials Characterization Techniques, CRC Press, 2009
- Y. Leng, Materials Characterization: Introduction to microscopic and spectroscopic methods, John Wiley & Sons, 2008

Lecture 11

Pore analysis

In general, catalyst consists of pore in the range of, micropore, mesopore or macropore depending on the preparation conditions and compositions. To determine the pore size distribution within the catalyst, pore analysis is essential. Knowing the pore size distribution gives an idea about accessibility of the reactants to the active sites. The pore analysis consist of determining the average pore size, average pore volume and pore size or pore volume distribution.

Total pore volume and average pore size

Total pore volume is defined as the liquid nitrogen volume at a certain p/p_o (=0.95).Total gas adsorbed at certain p/p_o (=0.95) is converted to liquid volume assuming pores are filled with liquid adsorbate

$$V_p = V_{liq} = \frac{V_{gas}(STP)}{22.4\times10^3}\times 34.6 = V_{gas}\times 1.54\times10^{-3}\ \text{cm}^3$$

***where*, 34.6 cm^3/mol = molar volume of liquid nitrogen**

Average pore size can be estimated from the pore volume. Assuming cylindrical pore geometry average pore radius (**r**) can be expressed as: $r = \frac{2V_p}{S}$

Pore size

(a) By gas adsorption

Pore size and pore size distribution can be determined using Kelvin equation. Kelvin equation relates equilibrium vapor pressure (**p**) of a liquid contained in a capillary to equilibrium pressure of the same liquid over a free surface (**p_o**) :

$$\ln\frac{p}{p_o} = \frac{-2\gamma V_{liq}\cos\theta}{rRT} \text{ ---------- (1)}$$

γ = surface tension of liquid nitrogen
θ = contact angle (usually zero for liquid N_2)
V_{liq} = the molar volume of liquid nitrogen
r = radius of pore
R = gas constant

At any equilibrium pressure, **p**, the pore of radius less than '**r'** will be filled with the condensed vapor. Application of Kelvin equation to all points of an isotherm at relative pressure greater than that corresponding to monolayer volume where capillary condensation begins to occur, will yield information concerning the volume of gas adsorbed in pores of different radii. For nitrogen as adsorbate and substituting values of various constants, the Kelvin equation can be written as

$$\ln \frac{P}{P_o} = \frac{-2\gamma V_{liq} \cos\theta}{rRT}$$

$$\text{Or } r_k\,(nm) = 0.41 \log \frac{p}{p_0} \qquad (2)$$

$\gamma = 8.72$ mN/m

$\theta = 0$

$V_{liq} = 34.68 \times 10^{-6}$ m^3 / mol

$T = 77\ K$

R=8.314 $J / K\ mol$

The '$\mathbf{r_k}$' is the radius into which condensation occurs at the required relative pressure. This radius is called Kelvin radius. However, Kelvin radius is not the actual pore radius since some adsorption has already occurred on the pore wall prior to condensation leaving a central core of radius $\mathbf{r_k}$. Conversely, an adsorbed film remains on the wall when evaporation of the centre core takes place.

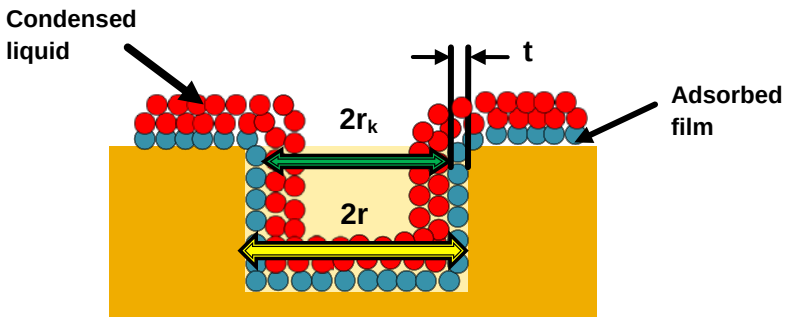

Fig. 3. Schematic showing Kelvin radius and actual pore radius during pore condensation

Then if '**r'** is the actual pore radius and the thickness of the adsorbed film is t (Fig. 3) then

$$r\ (nm) = r_k + t = \frac{2\gamma V_{liq}}{RT \ln \frac{p}{p_o}} + t = 0.41\ \log \frac{p}{p_0} + t \qquad (3)$$

Pore size distribution can be obtained by the analysis of either adsorption or desorption isotherm branches. Kelvin equation as described is applied to the desorption branch of hysteresis loop as it is more appropriate to assign wetting angle to a pore filled with liquid that possess a well defined meniscus. If '**h**' is the effective height of a monolayer, then the thickness of adsorbed layer '**t**' is given as $t = \left(\frac{V}{V_m}\right) h$. Here 'V' is the volume of gas adsorbed and 'V_m'is the volume of adsorbed monolayer. When the packing of adsorbate is hexagonal, then for nitrogen h = 3.6 A^0 and for cubic packing h= 4.3 A^0 = 0.43 nm. The '**t'** at a given relative pressure can also be calculated using Halsey equation

$$t = 3.54 \times \left[\frac{5}{2.303 \times \log \frac{p_0}{p}}\right]^{\frac{1}{3}} (\overset{o}{A}) = 0.354 \times \left[\frac{5}{2.303 \times \log \frac{p_0}{p}}\right]^{\frac{1}{3}} nm \qquad (4)$$

Pore size distribution

Most common method for determination of pore size distribution is BJH (Barrett-Joyner-Halenda) method. Assumptions are:

(i) Condensation occurs in pores when a critical relative pressure is reached corresponding to the Kelvin radius '$\mathbf{r_k}$'

(ii) When evaporation or condensation occurs, a multilayer of adsorbed film exist on the pore wall and this film has same depth/thickness as the adsorbed film on a non porous surface

(iii) Actual pore volume evaporation is composed of the volume evaporated out of the central core plus the volume desorbed from the film left on the pore walls

Steps for determination of pore size distribution are as follows:

1. $\mathbf{p/p_0}$ and $\mathbf{V_{gas}}$ (STP, cm^3/g) data obtained directly from isotherm.
2. Then Kelvin radius '$\mathbf{r_k}$'is calculated from Kelvin equation using zero wetting angle for N_2 from equation(2).
3. Then, the film thickness **t** calculated from Halsey equation (4) at each p/p_0.
4. Then the pore radius **r** calculated from equation (3).
5. Mean values of $\mathbf{r_k}$ and **r** in each decrement are calculated from successive entries.
6. Change in film thickness $\mathbf{\Delta t}$ is calculated from difference of successive values of **t .**
7. Then $\mathbf{\Delta V_{gas}}$, that is the change in adsorbed volume between successive p/p_o values, is determined by subtracting successive values .
8. Thereafter, $\mathbf{\Delta V_{liq}}$ that is the volume of liquid corresponding to $\mathbf{\Delta V_{gas}}$ is calculated as follows

$$\Delta V_{liq} = \frac{\Delta V_{gas}}{22.4\times10^3}\times 34.6 = \Delta V_{gas}\times 1.54\times10^{-3}\ \ \mathbf{cm^3}/g$$

9. Then $\mathbf{\Delta t\Sigma S}$ is determined. This represents the volume change of the adsorbed film remaining on the walls of the pores from which the central core has previously evaporated . This volume is the product of the film area $\sum\mathbf{S}$ and the decrease in film depth $\mathbf{\Delta t}$
10. Actual pore volume evaporated, V_p. is then determined. Actual pore volume evaporated is composed of the volume evaporated out of the centre core plus the volume desorbed from the film left on the pore walls, For a pore of length L,

$$\Delta V_{liq} = \pi r_k^2 L + \Delta t \Sigma S$$

Now , $V_p = \pi r^2 L$. By combining $V_p = \left[\frac{\bar{r}}{\bar{r}_k}\right]^2 \left[\Delta V_{liq} - \left(\Delta t \Sigma S \times 10^{-4}\right)\right]\ \ \mathbf{cm^3}/g$

11. The surface area of the pores walls can be calculated from pore volume by :

$$S = \frac{2V_p}{\bar{r}} \times 10^4 \quad m^2, \ V_p \text{ in } cm^3/g \text{ and r in } A^0$$

An elaborate example of pore size distribution work table can be seen in Lowell et al. for more understanding.

(a) **(b)**

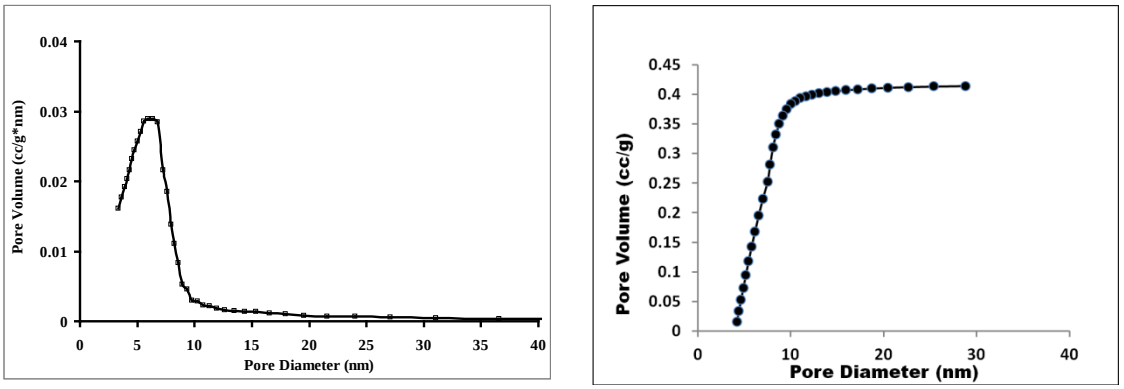

Fig. 4. Pore volume distribution of titania samples calcined at 400 ^{0}C

(a) differential (b) cumulative

Pore size distribution can be represented both in differential and cumulative ways. The Fig. 4(a) shows the differential BJH pore distribution of titania sample calcined at 400 ^{0}C. The figure shows that for the given sample pores were in the range of 2-10 nm. The corresponding cumulative pore distribution is shown in Fig. 4(b).

(b) By mercury intrusion

For macropores materials with pore diameter greater than 50 nm, the mercury intrusion method is preferred. Due to non-wetting nature of mercury on oxide supports, intrusion is met with resistance and mercury is forced to enter the pores of material under pressure. The pore radius 'r' is related to the applied pressure P as

$$P = \frac{(-2\gamma \cos \theta)}{r} \text{----------(5)}$$

The wetting or contact θ angle between mercury and solid is on average lies in the range 130-140^0 and surface tension of mercury is 0.48 N/m^2. **p** is in atm and **r** in nanometers.

As can be observed from equation (5) smaller the pore radius higher is the pressure needed for mercury to intrude in the pore. At low pressure of 0-2 atm, mercury penetrates voids between particles. At moderate pressure range of 3-500 atm large macro pores are filled. At further higher pressure range of 500-2000 atm, smaller macro pores and large mesopores are progressively filled. This technique is satisfactory for pores down to 3-5 nm dia . Maximum diameter that can be measured is usually 10^5 nm. Mercury intrusion method is carried out in the instrument known as mercury porosimeter. In a typical mercury porosimeter data, volume of mercury penetrating into pores is plotted as a function of applied pressures.

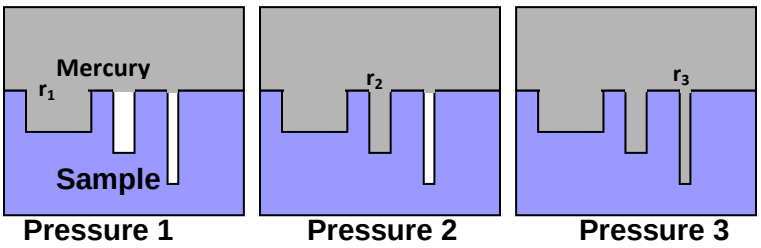

Pressure 1< Pressure 2 < Pressure 3 as $\mathbf{r_1 > r_2 > r_3}$

Fig. 5. Intrusion of mercury into pores of various sizes. Here 'r' represents the radius of pores.

The pressure required for filling up the pores as a function of pore size is schematically shown in Fig.5. As pore radius decreases in the order $r_1 > r_2 > r_3$, requried pressure for filling the pores increases in order of Pressure 1< Pressure 2 < Pressure 3.The available instruments can measure pore size up to 2 nm using a maximum operating pressure of about 400 MPa.

Table 1. Typical pore volume values of different support and catalyst.

Support/catalyst	Pore volume cm^3/g	Application
Activated carbon	0.6-0.8	Used as support for various process
Zeolites	0.5-0.8	Used as catalyst and support
Al_2O_3-SiO_2-Zeolites	0.1-0.9	Fluid catalytic cracking catalysts

Book reference

- S. Lowell, Joan E. Shields, Martin A. Thomas ,Characterization Of Porous Solids And Powders: Surface Area, Pore Size And Density - Springer, 2006
- J.J. Carberry , Chemical and catalytic reaction Engineering, Dover Publications, 2001
- J. M. Thomas & W. J. Thomas, Principles and Practice of Heterogeneous Catalysis, VCH, 1997
- Sam Zhang, Lin Li, Ashok Kumar, Materials Characterization Techniques, CRC Press, 2009

Lecture 12

X-Ray Diffraction

X-ray diffraction (XRD) is an effective method for determining the crystal structure of materials. It detects crystalline materials having crystal domains greater than 3-5 nm. It is used to characterize bulk crystal structure and chemical phase composition.

Crystalline & Amorphous materials

Materials can be classified as

- Crystalline material : Crystalline material can be single crystal or polycrystalline
- Amorphous material

Crystalline material

Crystalline materials are composed of atoms arranged in a regular ordered pattern in three dimensions. This periodic arrangement is known as crystal structure. It extends over distance much larger than the interatomic separations. In a single crystal, this order extends through the entire volume of the material. There are seven crystal systems: cubic, tetragonal, orthorhombic, rhombohedral, hexagonal, monoclinic and triclinic. Different crystal structures are based on framework of one of the 14 Bravais lattice.

Parallel planes of atoms intersecting the unit cell are used to define directions and distances in the crystal. The ‘d spacing’ is defined as the distance between adjacent planes .The orientation and interplaner spacing (d) of these lattice planes are defined by three integers h,k,l called Miller Indices. The (hkl) designate a crystal face or family of planes throughout a crystal lattice.

Polycrystalline materials consist of many small single crystal regions called grains. Grains are separated by grain boundaries. The grains can have different shapes and sizes and are disoriented with respect to each other.

Amorphous materials: When the atoms are not arranged in a regular periodic manner, the material is called amorphous. Such materials posses only short range order (distance less than a nanometer).

X-Ray Diffraction :

X-ray is a form of electromagnetic radiation having range of wavelength from 0.01-0.7 nm which is comparable with the spacings between lattice planes in the crystal. Spacing between atoms in metals ranges from 0.2-0.3 nm. When an incident beam of X-rays interacts with the target atom, X-ray photons are scattered in different directions. Scattering is elastic when there is no change in energy between the incident photon and the scattered photon. In inelastic scattering, the scattered photon loses energy. These scattered waves may superimpose and when the waves are in phase then the interference is constructive and, if out of phase, then destructive interference occurs. Atoms in crystal planes form a periodic array of coherent scatterers. Diffraction from different planes of atoms produces a diffraction pattern, which contains information about the atomic arrangement within the crystal.

Bragg's law

The X-ray beams incident on a crystalline solid will be diffracted by the crystallographic planes. Bragg's law is a simple model explaining the conditions required for diffraction. It is given as $n\lambda = 2d_{hkl}\sin\theta$, where d_{hkl} is the spacing between two planes hkl, n is an integer and λ is the wavelength. For parallel planes of atoms, with a spacing d_{hkl} between the planes, constructive interference occurs only when Bragg's law is satisfied. In diffractometers, the X-ray wavelength is fixed. Consequently, a family of planes produces a diffraction peak only at a specific angle θ. The spacing between diffracting planes of the atoms determines the peak positions. The peak intensity is determined by the atoms in the diffracting plane. Fig. 1 explains the Bragg's law. Two in-phase incident waves, beam 1 and beam 2, are deflected by two crystal planes (Z and Z_1). The diffracted waves will be in phase when the Bragg's Law, $n\lambda = 2d \sin\theta$, is satisfied. In order to keep these beams in phase, their path difference (SQ + QT) has to equal one or multiple X-ray wavelengths ($n\lambda$) i.e $SQ + QT = n\lambda$ or $SQ + QT = 2PQ \sin\theta = 2d \sin\theta = n\lambda$. Hence the

path difference depends on the incident angle (θ) and spacing between the parallel crystal planes (d).

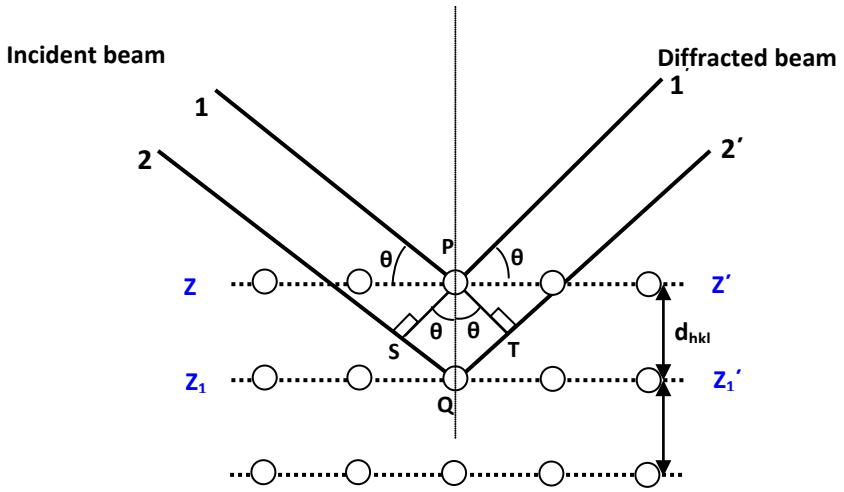

Fig. 1. Braggs analysis for X-ray diffraction by crystal planes

Working principle and Instrumentation

The instrument is called an X-ray diffractometer. In the diffractometer, an X-ray beam of a single wavelength is used to examine the specimens. By continuously changing the incident angle of the X-ray beam, a spectrum of diffraction intensity versus the angle between incident and diffraction beam is recorded.

The main components of diffractometer are

- X-ray Tube: the source of X Rays.
- Incident-beam optics: to condition the X-ray beam before it hits the sample
- Goniometer: the platform that holds and moves the sample, optics, detector, and/or tube
- Sample holder
- Receiving-side optics: to condition the X-ray beam after it has encountered the sample
- Detector: to count the number of X Rays scattered by the sample

The basic components of the diffractometer are shown in Fig 2. The 'θ' is the angle between the X-ray source and the sample, whereas 2θ is the angle between the incident beam and the detector. The incident angle θ is always half of the detector angle 2θ. The basic function of a diffractometer is to detect X-ray diffraction from materials and to record the diffraction intensity as a function of the diffraction angle (2*θ)*. The X-ray radiation generated by an X-ray tube passes through Soller slits which collimate the X-ray beam. The X-ray beam passing through the slits strikes the specimen. X-rays are diffracted by the specimen and form a convergent beam at the receiving slits before they enter a detector.

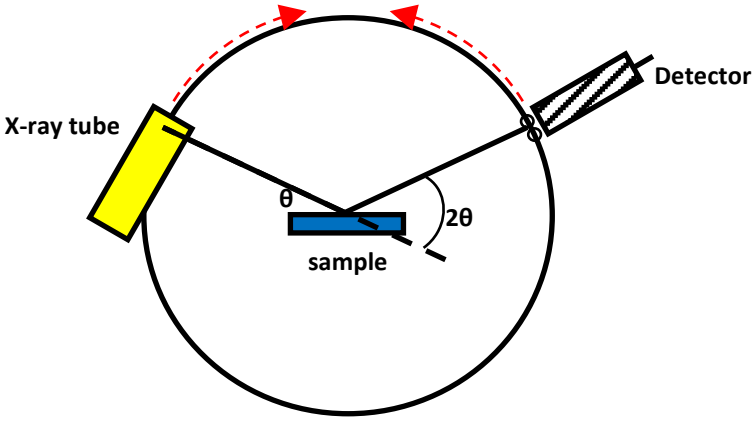

Fig. 2. Basic components of X-ray diffractometers

The diffracted X-ray beam passes through a monochromatic filter to suppress wavelengths other than K_α radiation and decrease any background radiation, before being received by the detector. The K_α radiation is generated by bombarding of target surface (Cu, Fe, Cr) by accelerated electrons. Most commonly a copper target is used generating K_α wave length of 0.154 nm.

Relative movements among the X-ray tube, specimen and the detector ensure the recording of diffraction intensity in a range of 2*θ*.

An instrument can be operated in two ways:

- tube is fixed, the sample and the detector rotates (THETA : 2-THETA arrangement)
- sample is fixed and the tube and the detector rotates (THETA:THETA arrangement)

Powder diffraction

A single crystal produces only one family of peaks in the diffraction pattern. A polycrystalline sample contains thousands of crystallites. Therefore, all possible diffraction peaks are observed. Powder diffraction is used for characterization of polycrystalline materials. The basic assumption of powder diffraction is that for every set of planes, there are statistically relevant number of crystallites that are properly oriented to diffract the incident beam. The diffraction pattern is the fingerprint of any crystalline phase. The position, intensity, shape and width of the diffraction lines gives information on the samples. Powder diffraction data consists of a record of photon intensity versus detector angle 2Θ. Diffraction data can be reduced to a list of peak positions and intensities. Each d_{hkl} corresponds to a family of atomic planes (hkl). However, individual planes cannot be resolved ~~in~~ by this method; this is a limitation of powder diffraction versus single crystal diffraction

Applications

Catalysts are extensively characterized by XRD technique.The major applications of XRD are discussed below.

1. **Phase Identification**

The catalysts are generally composed of mixture of several phases. The diffraction pattern for each phase is as unique as a fingerprint. Phases with the same chemical composition can have drastically different diffraction patterns. Phase identification is based on the comparison of the diffraction pattern of the specimen with that of pure reference phases or with a database. Databases such as the Powder Diffraction File (PDF) contain lists for thousands of crystalline phases. The PDF contains over 200,000 diffraction patterns. Modern computer programs can determine the phases present in a

sample by quickly comparing the diffraction data to all of the patterns in the database. Various crystalline phases can be quantified based on the fact that each phase of the mixture gives its characteristic diffractogram independently of the others and the intensity depends on the amount present in the mixture. The intensity of the diffraction line (hkl) from a phase α is given by

$$I_\alpha(hkl) = \frac{K_\alpha(hkl) \times X_\alpha}{\rho_\alpha \times (\mu/\rho)_m}$$

X_α = *weight* fraction of phase α
ρ_α = mass fraction of phase α
$(\mu/\rho)_m$ = mass absorption coefficient of the mixture
$K_\alpha(hkl)$ = constant for a given phase structure α, diffraction line (hkl)and set of exprimental conditions

Peak intensities are generally measured from peak heights on the assumption that peak height is proportional to peak area

2. Determination of average crystallite size

Ideally, a Bragg diffraction peak is a line without width. In reality, diffraction from a crystal specimen produces a peak with a certain width. This is known as peak broadening. The peak width depends on the size of the crystals. Peak width is inversely related to crystal size; that is, peak width increases with decreasing crystal particle size.

The average crystallite size can be determined by Scherrer formula using elementary line broadening analysis. The Scherrer formula assumes that the breadth of the diffraction peak of crystallites (small single crystals) mainly depends on the characteristics of crystallites (size and the defect in the lattice). Elementary analysis of the broadening assumes that lattice deformation is negligible. According to Scherrer, the thickness of crystallite, L, can be determined by

$$L = \frac{k\lambda}{\beta \cos\theta}$$

k = constant ; λ = wavelength of X-ray source ;
β = breadth of diffraction profile = Full width at half maxima
θ= half of the diffraction angle/Bragg angle

The diffraction corresponding to the most intense peak is selected to calculate the average crystallite size using Scherrer relation. The Scherrer formula assumes that crystallite size is the major source leading to line broadening effect of the diffractions peaks, but ~~there is always a~~ line broadening can also be due to instrumental factors such as slit width, sample size, imperfect focusing or misalignment of diffractometers.

3. Spacing between atomic planes of a crystal

Based on Bragg's Law, information on spacing between atomic planes can be obtained when constructive interference occurs. Knowing the spacing of crystallographic planes by diffraction methods, the crystal structure of materials can be determined. The plane spacing of cubic crystal is related to the lattice parameter *(a)* by the following equation.

$$d_{hkl} = \frac{a}{\sqrt{h^2 + k^2 + l^2}}$$

From Braggs Law, $n\lambda = 2d \sin\theta$.

Combining ,

$$\sin^2\theta = \frac{n^2\lambda^2}{4a^2}\left(h^2 + k^2 + l^2\right)$$

Examples

1. XRD pattern of oxide supports

Titania and zirconia are used as catalyst support or as active catalyst itself. They can be identified from their XRD pattern by comparison with the standard files. For any unknown sample the peaks are identified by comparison with the standard data. For oxides calcined at 400-500 ^{0}C, the typical XRD profiles of titania and tetragonal zirconia are shown in Fig 3.

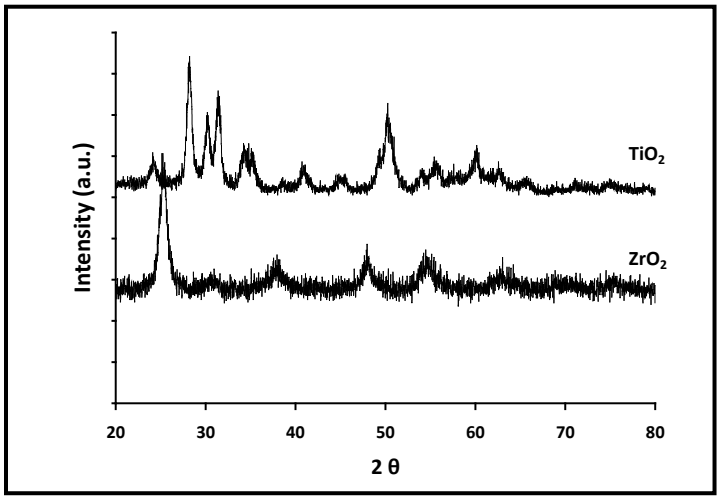

Fig. 3. XRD profiles for titania and zirconia prepared by precipitation method

Solved problem

1. A cubic crystal was placed in an x-ray diffractometer using incoming x-rays with a wavelength $\lambda = 0.154$ nm. The various peak intensities recorded at different 2θ values are given in following table.

2θ (deg)	40.3	58.3	73.2	154.2	131.2
h k l	110	200	211	400	321
Relative intensity	100	15	23	2	18

Determine the followings

i. Calculate the crystal size (Given, k=0.9; $\beta = 0.0098$)

ii. Calculate the value for the lattice constant (Assume first order diffraction with n = 1.)

Solution

i. The crystal size can be calculated using the peak corresponding to $2\theta = 40.3$ having highest peak intensity.

Hence, k = 0.9 ; $\beta = 0.0098$; λ=0.154 nm; θ=20.15, the crystal size L can determined using the Scherrer equation as follows

$$\mathbf{L = \frac{k\lambda}{\beta \cos\theta} = \frac{0.9 \times 0.154}{\beta \times \cos(20.15)} = \frac{0.1386}{0.0098 \times 0.9387} = 15.1\ nm}$$

ii. The plane spacing of cubic crystal is related to the lattice parameter (*a)* by the following equation.

$$d_{hkl}^2 = \frac{a^2}{h^2 + k^2 + l^2} \qquad [1]$$

From Braggs Law,

$n\lambda = 2d \sin\theta$ [2]

or, $n^2 \lambda^2 = 4d^2 \sin^2\theta$

or, $d^2 = \frac{n^2\lambda^2}{4\sin^2\theta}$ [3]

From [1] and [3] Combining ,

$$a^2 = \frac{n^2\lambda^2}{4\sin^2\theta}\left(h^2 + k^2 + l^2\right)$$

Using the peak corresponding to 2θ = 40.3 having highest peak intensity with [hkl] value of [110] the lattice constant '*a*' for cubic crystal can be calculated as follows.

Or

$$a^2 = \frac{1^2 \times 0.154^2}{4\left(\sin 20.15\right)^2}\left(1^2 + 1^2 + 0\right) = 0.1 \text{ nm} \qquad [\because \sin 20.15 = 0.3436]$$

Or, $a = 0.342$ nm

Book reference

- Sam Zhang, Lin Li, Ashok Kumar, Materials Characterization Techniques, CRC Press, 2009
- Y. Leng, Materials Characterization: Introduction to microscopic and spectroscopic methods, John Wiley & Sons, 2008
- Edited by R.E. Dinnerbier and S. L. J. Billinge, Powder Diffraction :Theory and Practice , RSC Publishing, 2008
- J. M. Thomas & W. J. Thomas, Principles and Practice of Heterogeneous Catalysi, VCH, 1997

Lecture 13

Chemisorption

In many catalysts, active metals are deposited on the surface of the support such as in Pt/Al_2O_3, Pt/C, Ni/Al_2O_3 etc. These metals act as active sites in various oxidation states including in zero valence state. The location and state of the active metal on the support largely depends on the preparation method of the catalyst. When prepared by impregnation method, more active metals are expected to concentrate on the surface of support, whereas in bulk preparation method active metals are trapped more within the bulk matrix. Further, these metals usually exist as clusters on the support surface and thereby, only a fraction of the total deposited metal is actually exposed to the incoming reactant molecules for participation in a reaction.

The dispersion (D) of metal is defined as $D = \left(\frac{N_S}{N_T} \right)$

where ,

N_s = total no. of exposed surface atoms

N_T = total no. of metal atoms present in the sample

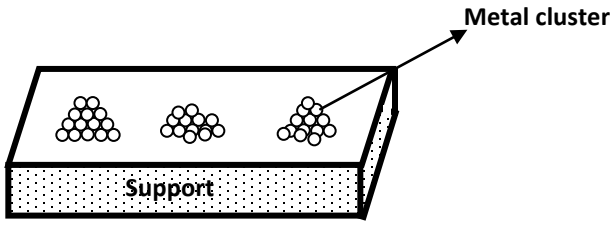

Fig. 1. Metal cluster on support surface

Chemisorption technique gives direct measurement of the number of exposed surface atoms. This method measures quantity of gas adsorbed selectively on the metal at monolayer coverage.

This technique is mainly used to study :

(1) metal dispersion and

(2) active metal area.

In this method, the sample is exposed to a gas that can chemisorb on the active metal. At monolayer coverage, the average number of surface metal atoms associated with adsorption of each gas molecule is determined. Accurate determination of metal dispersion and the active metal area is possible if stoichiometry of the chemisorption reaction is known. Pulse method is frequently used to determine the number of gas molecules adsorbed on the catalyst surface.

For a given catalyst, the adsorbate gas is chosen to minimize adsorption on the support and to have an irreversible (or weakly reversible) chemisorptions on the metal. H_2 and CO are the most commonly used adsorbate gases.

Hydrogen Chemisorption

H_2 adsorbs dissociatively on metals according to the equation :

$$H_2 + 2M_s \rightarrow 2\ M_s - H$$

M_s represents a surface metal atom.

The chemisorption stoichiometry **n** is defined as the number of metal atoms to which one adsorbate gas molecule can attach. In case of hydrogen chemisorption, one hydrogen molecule attaches with two metal atoms; hence **n** = 2 .

CO chemisorption

The CO adsorption is considerably more complex. The CO can chemisorb in various forms on metals such as Fe, Ni, Ru, Pt , Pd. The chemisorption stoichiometry varies with temperature, metal dispersion, metal loading and preparation. CO can be chemisorbed :

1. Dissociatively (CO: **n** = 2) or
2. Associatively
   - Linear (**n** =1)
   - Bridged (**n** = 2)

- Multi-bonded species (**n** = 3)

The relative proportion of the various forms depends on temperature, pressure and metal particle size.

Adsorbate gas choice

For a given catalyst, the adsorbate gas should be chosen such that it interacts irreversibly with metal or have very weak reversible interaction. The adsorbate should have minimum adsorption on the support. Most commonly used adsorbate for metal characterization is hydrogen and CO. Other gases such as O_2, N_2O, NO, N_2 etc. are also used depending on the specific application. The CO can chemisorb in different forms on metals such as iron, nickel, ruthenium, palladium, rhodium and platinum. Not knowing the exact stoichiometric relation can introduce error. The main difficulty is the formation of metal carbonyl, which are volatile as in case of nickel and rhodium. However, CO chemisorption is better suited when hydrogen can be absorbed into the metal (palladium hydride formation) or significantly adsorbed on support (such as carbon support). Oxygen chemisorption is also used. However, possibility of formation of metal oxides with variable stoichiometry may cause errors. Main application of oxygen adsorption measurement is hydrogen-oxygen titration. For cases, when interaction of metals with H_2 or CO is very low and interaction with oxygen is excessively strong resulting in bulk oxidation, such as for Cu or Ag, the adsorptive decomposition of nitrous oxide can be used.

Working principle and instruments

In pulse chemisorption technique, initially the sample is reduced with hydrogen at elevated temperature to convert the oxide to metallic form (such as NiO to Ni) .Then, the sample is flushed with an inert gas at elevated temperature, such as helium, to remove traces of any adsorbed gases. Then, sample is cooled to the analysis temperature, with inert gas flowing. Successive small pulses of adsorbate gas (of known volume) are injected in the flow of inert gas by a syringe or loop at the desired temperature. Pulses of adsorbate gas are continued to be injected until the catalyst surface is saturated. The Fig 2 shows a typical plot of peak area of adsorbate gas as function of number of pulse injected. As the figure shows, the first pulse corresponds to negligible peak area

suggesting that most of the injected gas is adsorbed. For second pulse the peak area increased compared to the first suggesting lesser amount of gas adsorbed compared to first injection. As the number of pulse increases peak area gradually increases corresponding to decreased amount of gas being adsorbed. Finally the peak area becomes constant corresponding to the area of pulse volume. The constant areas are shown by pulse number 6 and 7 in the Fig 2. The amount of gas adsorbed is obtained by calculating the difference between the volume of each pulse and the fraction of H_2 not adsorbed. The total amount of gas chemisorbed can be obtained from the number of consumed pulses. The schematic diagram of equipment for pulse chemisorption is given in Fig. 3.

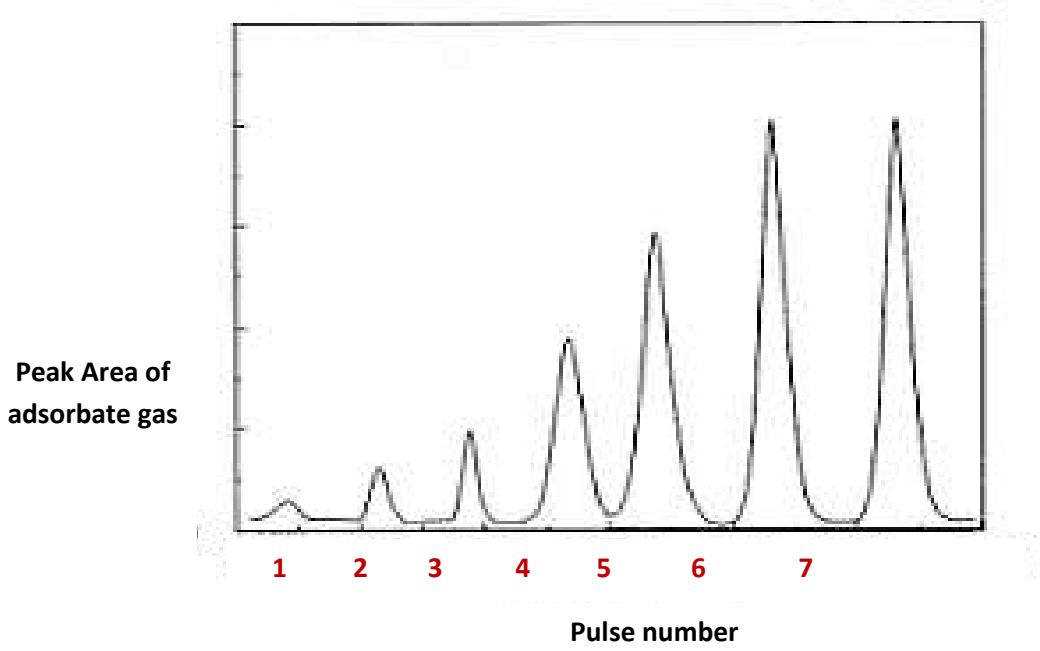

Fig. 2. A typical plot of peak area vs pulse number of adsorbate gas

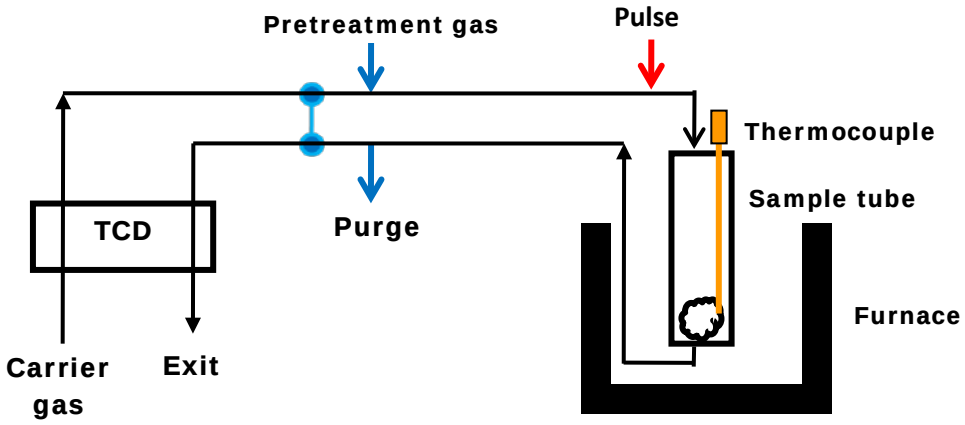

Fig. 3. Schematic diagram of equipment for pulse chemisorption

Calculations for determination of metal dispersion and active metal area :

1. The volume of active gas (CO or H_2) injected, V_{inj}, can be calculated at STP conditions using the equation below. Generally, the active gas is used as a gas mixture, such as 10% CO in helium or 10 % H_2 in argon.

$$V_{inj}\,(STP) = V_{syr} \times \frac{T_{std}}{T_{amb}} \times \frac{P_{amb}}{P_{std}} \times \frac{A}{100}$$

V_{syr} = syringe volume injected , cm^3
T_{amb} = ambient temperature, ^oC
T_{std} = standard temperature = 273K
P_{amb} = ambient pressure, mmHg
P_{std} = standard pressure = 760mmHg
A = % active gas in gas-mixture

2. The volume of active gas chemisorbed is calculated using volume injected V_{inj} and from area under the peaks as follows.

$$V_{ads}\,(STP, cm^3/gm) = \frac{V_{inj}}{m} \times \sum_{i=1}^{n}\left(1 - \frac{A_i}{A_f}\right)$$

V_{inj} = volume injected, cm^3
m = mass of the sample, gm
A_i = area of peak i
A_f = area of last peak

3. Calculation of % Metal Dispersion

Moles of metal on surface of sample = $n \times \frac{V_{ads}}{V_g}$ moles/gm

Moles of total metal present in sample = $\frac{M}{m.w \times 100}$ moles/gm

$$D = \frac{\text{Moles of metal on surface of sample}}{\text{Moles of total metal present in sample}}$$

$$D = n \times \frac{V_{ads}}{V_g} \times \frac{m.w}{M} \times 100$$

n = stoichiometry factor
V_{ads} = volume adsorbed, cm^3/gm
V_g = molar volume gas at STP = 22414 cm^3/mol
m.w. = molecular weight of the metal
M = % metal loading

$$\text{Or } \%D = \left[n \times \frac{V_{ads}}{V_g} \times \frac{m.w}{M} \times 100 \right] \times 100$$

4. Active metal surface area per gram of sample

$$A_m \left(m^2/gm\right) = \left[\text{total number of surface metal atoms}\right] \times \left[\text{cross section area of active metal}\right]$$

$$\mathbf{A_m \ \left(m^2/gm \ sample\right) = \left[\left(n \times \frac{V_{ads}}{V_g} \right) \times N_A \right] \times a}$$

n = stoichiometry factor
V_{ads} = volume adsorbed , cm^3/gm
V_g = molar volume of the gas at STP = 22414 cm^3/mol
N_A = Avogadro's number = 6.023×10^{23} molecules / mol
a = cross – sectional area of active metal atom, m^2

Solved examples :

1. ***Calculate the metal dispersion and active metal area for 0.5 wt % Platinum on Alumina catalysts by CO pulse chemisorption. The areas of the pulses are given in the table. Additional given data are :***

Sample amount: 1gm ; Analysis gas: 10%CO/He; Carrier gas: He ; Temperature: 25 ^oC ; Pulse volume: 0.5cm^3 ; stoichiometry factor of CO on Pt = 1.

Peak No.	1	2	3	4	5	6	7
Peak area	0.0	0.0	0.0003	0.001	0.005	0.007	0.007

Solution :

i. Calculation of volume of Active Gas Injected From a Syringe 10 %CO /He

$$V_{inj}\ (STP) = V_{syr} \times \frac{T_{std}}{T_{amb}} \times \frac{P_{amb}}{P_{std}} \times \frac{A}{100}$$

V_{syr} = syringe volume injected =0.5 cm^3

T_{std} = ambient temperature =22^oC

T_{amb} = standard temperature 273K

P_{amb} = ambient pressure =743mmHg

P_{std} = standard pressure=760mmHg

A = % active gas =10

$$V_{inj}\ (STP) = 0.5 \times \frac{273}{(25+273)} \times \frac{743}{760} \times \frac{10}{100} = 0.0448\ cm^3$$

ii. Calculating Volume Chemisorbed:

$$V_{ads} = \frac{V_{inj}}{m} \times \sum_{i=1}^{n} \left(1 - \frac{A_i}{A_f}\right)$$

V_{inj} = volume injected= 0.0448 cm^3 ; m = mass of the sample = 1 gm

Table 1. Calculation for volume of CO adsorbed on Pt supported on Alumina

Peak no.	A_i	$\left(1-\frac{A_i}{A_f}\right)$	$(V_i)_{ads}$ $=\frac{V_{inj}}{m}\times\left[1-\frac{A_i}{A_f}\right]$	$\Sigma(V_i)_{ads}$ $=\sum_{i=1}^{n}\frac{V_{inj}}{m}\times\left(1-\frac{A_i}{A_f}\right)$
1	0	1.0000	0.0448	0.0448
2	0	1.0000	0.0448	0.0896
3	0.0003	0.9571	0.04288	0.1325
4	0.001	0.8571	0.0384	0.1709
5	0.005	0.2857	0.0128	0.1837
6	0.007	0.0000	0	0.1837
7	0.007	0.0000	0	0.1837

From Table 1, A_f = area of last peak = 0.007

Volume of CO adsorbed on Pt supported on alumina = V_{ads} = 0.1837 cm^3/gm

iii. % Metal Dispersion:

n = stoichiometry factor, CO on Pt =1

V_{ads} = volume adsorbed=0.l837 cm^3/gm

V_g = molar volume of the gas at STP= 22414 cm^3/mol

m.w. = molecular weight of the metal Pt = 195

M = % metal = 0.5

Moles of metal on surface of sample = $n\times\frac{V_{ads}}{V_g}=1\times\frac{0.1837}{22414}=8.196\times10^{-6}$ moles / gm

Moles of total metal present in sample =

$$\frac{M}{m.w\times100}=\frac{0.5}{195\times100}=2.564\times10^{-5}\,moles/gm$$

$$\%D = \frac{8.196 \times 10^{-6}}{2.564 \times 10^{-5}} \times 100 = 31.96\ \%$$

iv. Active Metal Surface Area (per gram of sample)

$$A_m = \left[n \times \frac{V_{ads}}{V_g} \right] \times N_A \times a \quad m^2/\text{gm sample}$$

n = stoichiometry factor, CO on Pt=1

V_{ads}= volume adsorbed= 0.1837 cm^3/gm

V_g = molar volume of the gas at STP= 22414 cm^3/mol

N_A = Avogadro's number = 6.023 x 10^{23} molecules/mol

a = cross-sectional area of active metal atom =0.08 nm^2= 0.08 × 10^{-18} m^2

$$A_m = \left[1 \times \frac{0.1837}{22414} \right] \times 6.023 \times 10^{23} \times 0.08 \times 10^{-18} = 0.395 \quad m^2/\text{gm sample}$$

Book References

- G. Ertl, H. Knozinger and J. Weitkamp, Handbook of Heterogeneous Catalysis, Vol. 2,WileyVCH, 1997.
- S. Lowell, Joan E. Shields, Martin A. Thomas ,Characterization Of Porous Solids And Powders: Surface Area, Pore Size And Density - Springer, 2006

Lecture 14

Thermo analytical techniques

For heterogeneous solid catalysis, understanding the interaction between fluids and active sites on the solid surface is very important as it determine the surface reactivity. These kinds of interactions are studied by many thermo analytical techniques, carried out dynamically by application of linear temperature programme. These techniques involve recording the surface or bulk interaction of solid catalysts with gaseous environment as the temperature is increased, by continuously analyzing the gas phase composition. The temperature programmed reduction (TPR) , temperature programmed oxidation (TPO), temperature programmed desorption (TPD), thermo gravimetric analysis (TGA) and differential thermal analysis (DTA) are among the techniques used extensively for characterization of catalysts.

Temperature programmed reduction (TPR)

Temperature programmed reduction is used to determine the reducibility of the catalysts. In this method, reducible catalysts are exposed to flow of reducing gas mixture typically H_2 in Ar. The sample is initially pretreated in an oxidative atmosphere (5% O_2 in He) at predetermined temperature for 30 min and cooled to 250 ^{0}C in the same mixture. The sample is then purged with helium and cooled to room temperature. Then the preoxidized sample is reduced in a flow of H_2 in argon from room temperature to 900 ^{0}C. The carrier gas flow is maintained at a specified value (usually 30 ml /min). Temperature is linearly increased at the desired heating rate (usually 10 K/ min). The extent of reduction is continuously followed by measuring the composition (H_2 content) of the reducing gas mixture at the outlet of the reactor. The total amount of H_2 consumed is determined from the area under the peak and is used to calculate the degree of reduction and average oxidation state of the solid material after reduction.

Fig.1. shows the arrangement used for TPR/TPO analysis. The same instrument as that used for chemisorption can be used for this study.

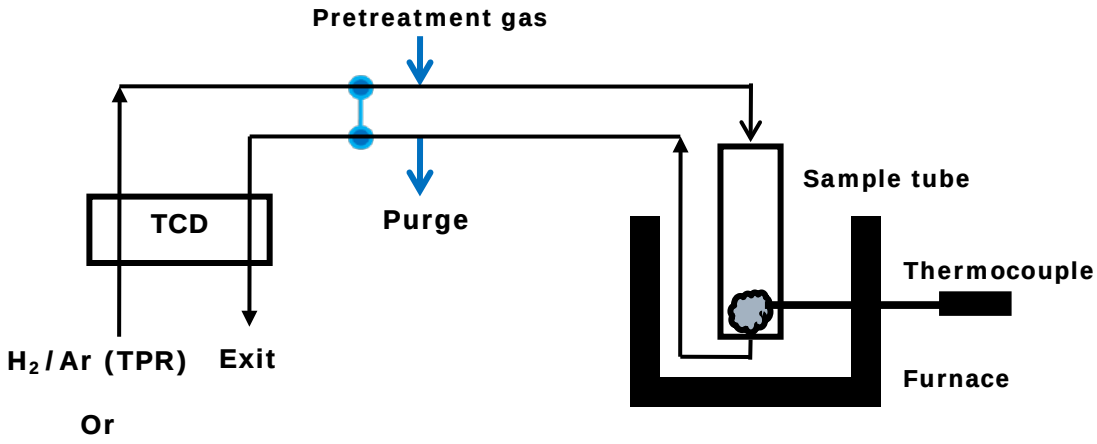

Fig. 1. Schematic diagram for TPR/TPO analysis

Parameters that affects TPR profiles are :

- Heating rate, K/s
- Initial amount of reducible species, μmol
- Flow rate of reducing gas mixture, cm^3 /sec
- Concentration of H_2 in carrier gas, ($\mu mol/cm^3$)

A higher heating rate increases the temperature of the sample faster compared to a slower heating rate, consequently reduction peaks for the sample appear at comparatively higher temperature than that at lower heating rate. On the other hand if the concentration of the hydrogen in the reducing gas mixture is increased the samples are reduced more easily resulting in sharper peaks at lower temperature compared to that at lower hydrogen concentration. Change in gas flow rate has small effect. As the initial amount of reducible species in samples increases, the area under the peak increases.

Hence the parameters have significant influence on shape of TPR profiles so that comparison between experimental results obtain under different conditions is difficult to make. Hence, for comparison, all TPR should be carried out at the same process conditions.

Application :

Solid catalysts containing reducible metals are characterized using TPR. Following infomation can be gained from TPR curves :

1. Reduction peak temperature indicates the ease of reduction and degree of interaction between different species present in the catalyst sample. A higher reduction temperature indicates higher difficulty in reduction which can be attributed to the greater degree of interaction between the active metal and support.
2. Multiple peaks indicate the presence of metal in different forms on the support having different level of interaction between species and support.
3. The extent of reduction can be calculated as follows :

$$\text{Extent of reduction} = \frac{\text{actual amount of hydrogen consumed}}{\text{theoretical amount of hydrogen consumed assuming complete reduction}}$$

The actual amount of hydrogen consumed is calculated from the area under the curve and the theoretical amount is calculated from stoichiometry of reduction equation. The average oxidation state of the solid material after reduction can be calculated thereafter.

4. Usually, reducibility of the catalysts can be correlated to its activity if the mechanism involves redox reactions.

Examples

1. **TPR of V_2O_5 catalysts**

Amount of reducible species can be quantified by amount of H_2 used by considering reduction stoichiometry as $V_2O_5 + 2H_2 \rightarrow V_2O_3 + 2H_2O$

The TPR profile of pure bulk vanadia is given in Fig. 2 . The presence of multiple peaks is attributed to the multistep reduction sequence $V_2O_5 \rightarrow V_6O_{13} \rightarrow V_2O_4 \rightarrow V_2O_3$

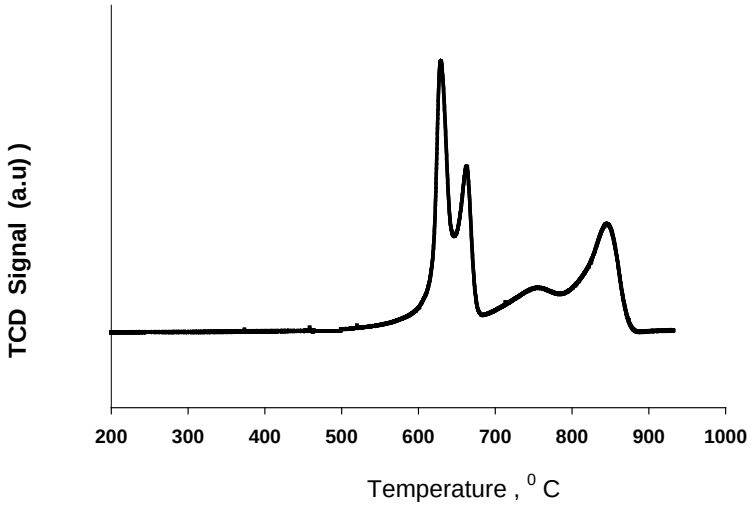

Fig. 2. Typical TPR profile of bulk vanadium oxide

2. TPR of supported nickel oxide catalysts

NiO is reduced in one step to metallic nickel according to the following equation :

$$NiO + H_2 \rightarrow Ni + H_2O$$

(A) TPR of NiO/C catalysts is shown in Fig. 3. NiO is reduced in one step. Presence of single peak suggests NiO is present in one form.

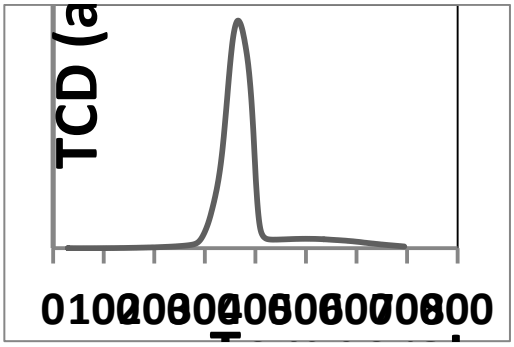

Fig. 3. Typical TPR profile of nickel oxide supported on carbon

(B) TPR of NiO supported on TiO_2 catalysts is shown in Fig. 4. On titania, the multiple reduction peaks are obtained for nickel oxide. The multiple peaks suggest the presence of Ni species in various forms. The peak at the highest temperature corresponds to the Ni species most difficult to reduce which can be attributed to the higher interaction with support.

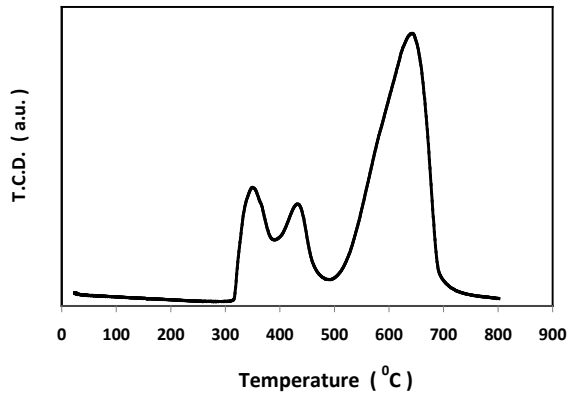

Fig. 4. Typical TPR profile of nickel oxide supported on titania

Temperature programmed oxidation (TPO)

Temperature programmed oxidation is used for investigation of the redox behavior of catalysts particularly when applied in cyclic TPR-TPO experiments. The equipment and experimental procedure are the same as for the TPR study. The only difference is that the sample should be in reduced form so that it is oxidized in the carrier gas containing oxygen. The carrier gas generally used is O_2/Ar mixture gas. Usually, it is carried out after TPR and together gives a TPR-TPO cycle.

Temperature programmed desorption (TPD)

Temperature programmed desorption technique measures the desorbed molecules from the sample surface. In TPD experiments, catalysts are pretreated in situ in oxidative atmosphere at 100-200 ^{0}C to remove any adsorbed species on the surface. Then, the sample is equilibrated with an adsorbing gas or vapor saturated with the probe molecule under well- defined conditions. After the excess gas is flushed out of the reactor, the sample is heated in a flowing inert gas stream. The concentration of the desorbing gas in

the effluent gas is continuously monitored by a thermal conductivity detector. The total area under the curve gives the total amount of desorbed probe molecules. The same instrument used for TPR can be used for TPD study. For TPD, a mass spectrometer detector can also be used to detect the evolution of species from the surface back into gas phase. TPD spectra are affected by inert gas flow rate, particle size, catalysts pore size and catalysts bed depth.

Application

TPD studies gives :

- Type and amount of different forms of adsorbed species which correspond to the presence of various peaks
- Relative bond strength between the adsorbate and surface which corresponds to various peaks at different temperatures. Higher the desorption temperature stronger the bonds and site strength.

TPD is extensively used for

- Study of acidic and basic sites on the surface
- Study of gas adsorbed on surface
- Study of organic compounds adsorbed on surface

For study of acidic and basic sites, mainly two types of probe adsorbate molecules are used for TPD studies:

1. NH_3 desorption for determining acidic sites
2. CO_2 desorption for determining basic sites

Since NH_3 is basic in nature it adsorbs on the acidic sites on the surface. The acidic sites are quantified in terms of total ammonia molecules adsorbing on the surface in μmol/gm of catalysts. However, ammonia adsorption cannot distinguish between Bronsted or Lewis acid sites and only determines the total acidic sites. CO_2 is an acidic gas and can absorb on basic sites on the catalyst-surface. This technique gives the total basic sites quantified by total CO_2 molecules adsorbed on the surface in μmol/g of catalyst.

Adsorption study of any gases such as CO, H_2, O_2, CH_4 on catalysts as required can easily be done using TPD. Total area under the curve gives capacity of adsorptions and multiple peak positions gives the bond strength.

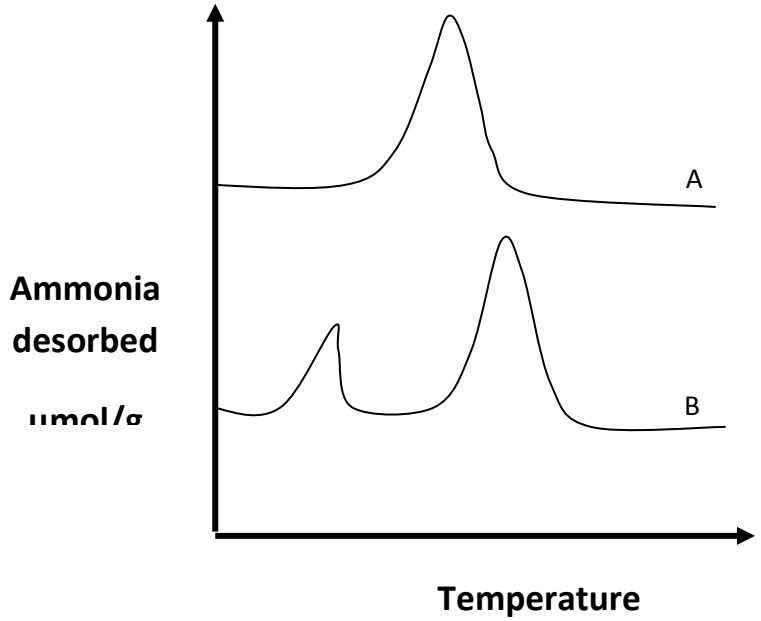

Fig. 5. Typical TPD spectra observed

Fig. 5 shows a typical NH_3-TPD spectrum observed for different samples. Curve A only has one peak suggesting existence of one type of acidic sites on the sample to which ammonia is attached, while curve B has two peaks and suggests two types of acidic sites. The lower temperature peak suggests weaker bond strength and hence weaker acidic sites, while the peak at the higher temperature means stronger bonds and hence stronger acidic sites. The area under the curve gives the amount of weaker and stronger sites. For curve B, concentration of the stronger sites is more. Similar kind of conclusions can be drawn from CO_2-TPD profiles corresponding to basic sites.

Thermogravimetric Analysis (TGA)

In thermogravimetric analysis, the change in mass of samples is monitored with an increase in temperature at specified gas environment and heating rate.

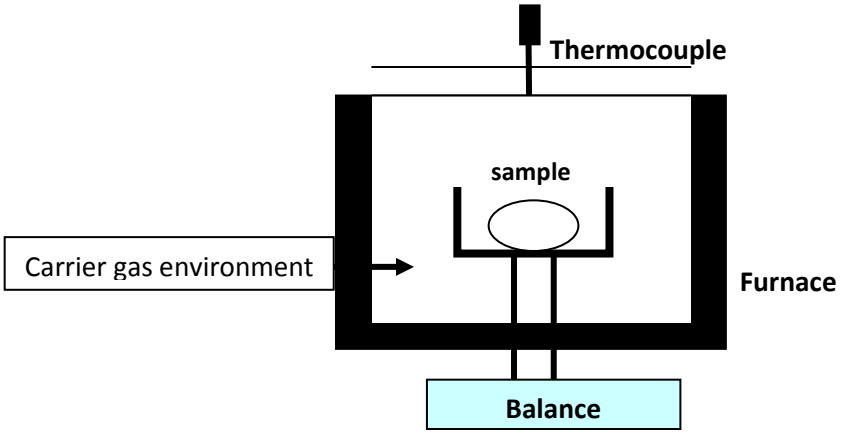

Fig. 6. Schematic diagram for thermogravimetric analysis technique

In this analysis, the sample is loaded in a small platinum crucible suspended from the arm of a microbalance. The entire arrangement is placed within a small oven, temperature of which is controlled and monitored. Analysis is carried out by raising the temperature of the sample gradually in a flow of air or inert gas such as N_2, Ar or He and the sample weight (or percentage) is plotted against temperature. The parameters affecting the TGA are : heating rate, amount of sample, carrier gas flow, nature of carrier gas etc.

Applications

TGA characterization is used to determine the thermal stability, content of moisture and volatile material, if any, or decomposition of inorganic and organic material in the catalysts. This method can also be used to study reaction kinetics with reactive gases (e.g., oxidation, hydrogenation, chlorination, adsorption/desorption) as well as pyrolysis kinetics (e.g., carbonization, sintering).

Only thermal processes that are associated with change in mass can be detected by TGA process which makes its use rather limited. However for desorption, decomposition or oxidation reaction, TGA can be used to gain useful information. The thermal stability of

materials in both inert and oxidizing atmosphere can be determined by this technique. For catalysts, information regarding moisture content , decomposition or any reactions involving mass change that may happen during calcination / reactions conditions can be determined using a similar gaseous environment. Any catalytic reaction that is accompanied by mass change such as combustion or pyrolysis can be studied using TGA. TGA can be also used to determine the extent of deactivation by deposition of coke. TGA of deactivated sample in oxidizing atmosphere will remove the deposited coke of the used catalyst and thereby the amount of deposited coke can be quantified.

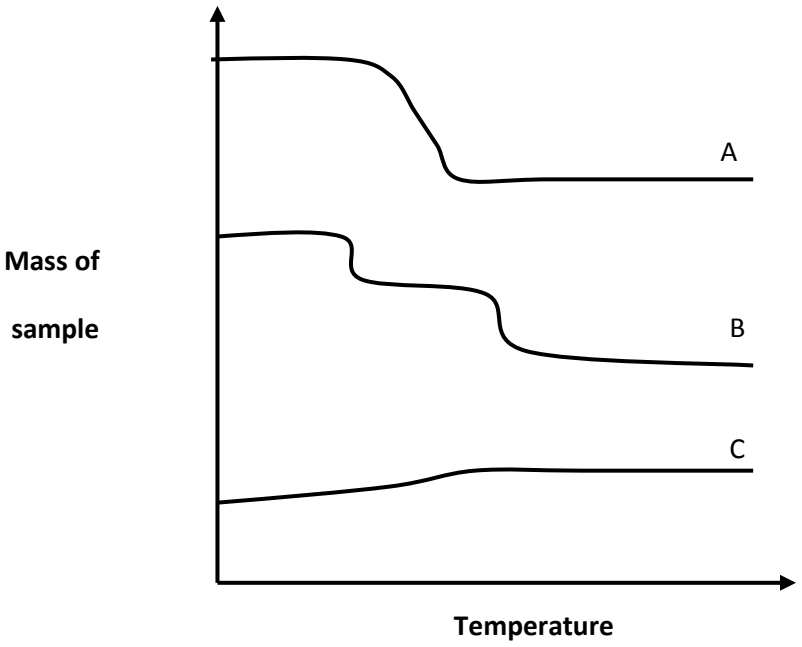

Fig.7. Different TGA curves (A) single step change (B) multistep change (C) increasing mass

Fig. 7 shows some typical curves observed during TGA analysis. Curve A represents change in a single step. This can be moisture removal or decomposition or reaction of the material. For example, TGA of carbon in air is an example of this type of curve, where carbon after reaching the specific temperature in air burn down oxidizes, producing CO_2 and CO gases.

The curve B corresponds to any change in multiple steps. The curve C on the other hand, shows an increase in the mass of the sample. This is observed for oxidation of metals such as oxidation of silver in air which results in gain in weight by formation of AgO_2. TGA does not give any information on processes which are not associated with mass change such as phase change, melting or crystallization etc.

Examples

1. **TGA of alumininium hydroxide**

The Fig. 8A shows a typical TGA profile for aluminium hydroxide prepared by precipitation method in nitrogen flow at heating rate of 10 K/min . The weight loss corresponds to conversion of aluminium hydroxide to aluminium oxide by removal of water.

2. **TGA of activated carbon**

The Fig. 8B shows a typical TGA profile for activated carbon in nitrogen flow at a heating rate of 10 K/min. The initial weight loss at 100 ^{0}C is due to removal of moisture. Since the carrier gas is inert, there is no further significant change in the weight of the sample.

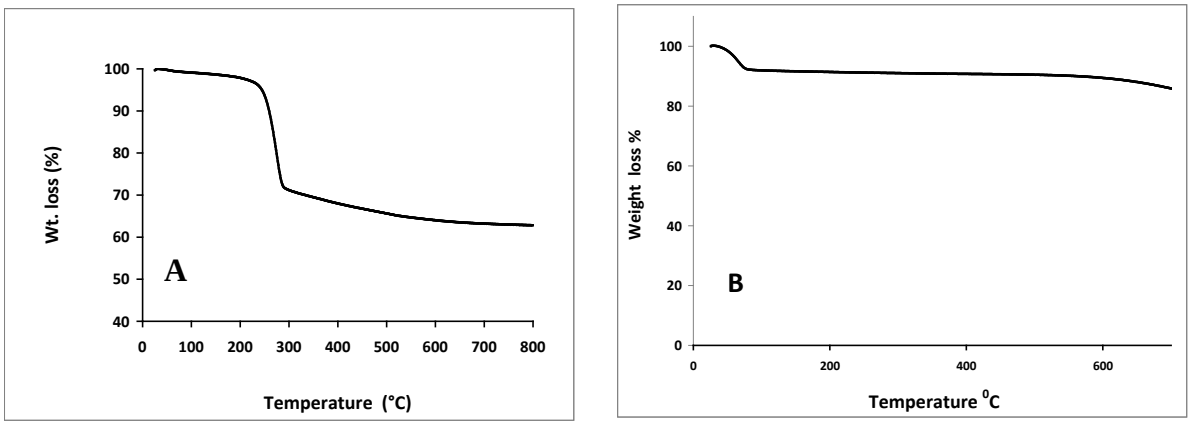

Fig. 8. Typical TGA profile for (A) aluminum hydroxide (B) activated carbon

Differential Thermal Analysis (DTA)

DTA consists of heating a sample and reference material at the same rate and monitoring the temperature difference between the sample and reference. In this method, the sample is heated along with a reference standard under identical thermal conditions in the same oven. The temperature difference between the sample and reference substance is monitored during the period of heating. As the samples undergo any changes in state, the latent heat of transition will be absorbed/evolved and the temperature of the sample will differ from that of the reference material. This difference in temperature is recorded. Hence, any change in state can be detected along with the temperature at which it occurs.

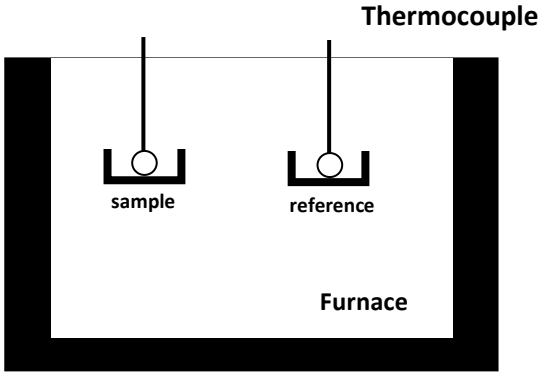

Fig. 9. Schematic diagram for differential thermal analysis technique.

When an endothermic process occurs (ΔH positive) in the sample, the temperature of sample (T_s) lags behind the temperature of reference (T_r). The temperature difference $\Delta T = (T_s - T_r)$ is recorded against reference temperature T_r and the corresponding plot is shown in Fig 10. In DTA, by convention, endothermic response is represented as negative that is by downward peaks. When an exothermic process (ΔH negative) occurs in the sample, the response will be in the reverse direction and the peaks are upward. Since the definition of $\Delta T = T_s - T_r$ is rather arbitrary, the DTA curves are usually marked with endo or exo direction.

It is essential that reference sample must not undergo any change in state over the temperature range used and both the thermal conductivity and heat capacity of reference must be similar to those of samples. Both sample and reference materials should be also inert towards sample holder or thermocouples. Alumina and silicon carbide are most

commonly used standard reference samples. DTA profiles are affected by heating rate, sample size and thermocouple position within the sample.

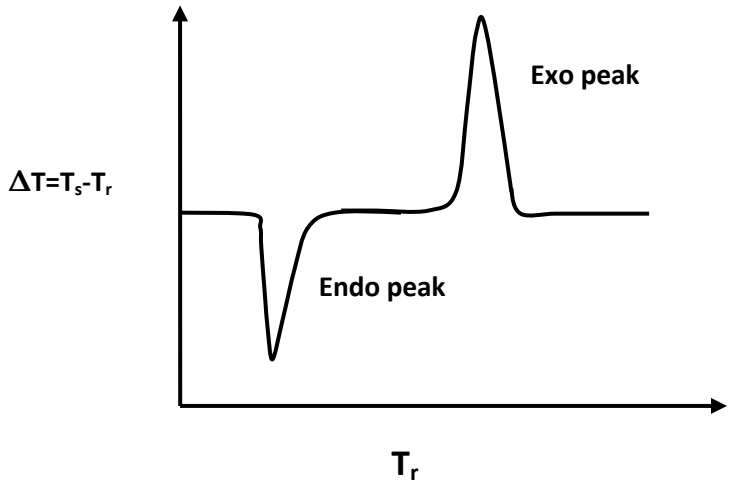

Fig. 10. Typical exo and endo peak in a DTA profile.

Application

Any change associated with enthalpy change can be studied by DTA. In general, DTA curves are used to get information about temperature and enthalpy changes for decomposition, crystallization, melting, glass transition etc. In solid catalysis, it is particularly useful to detect phase changes associated with calcination process. For example, change of aluminum hydroxide to alumina can be easily detected by DTA.

Book References

- G. Ertl, H. Knozinger and J. Weitkamp, Handbook of Heterogeneous Catalysis, Vol. 2,WileyVCH, 1997.
- M.E.Brown , Introduction to thermal analysis : Techniques and application , second edition, Springer, 2007
- E.N. Kaufmann (Ed), Characterization of Materials, Wiley –Inter Science ,2003

Lecture 15

Spectroscopy

Spectroscopy is defined as the study of the interaction of electromagnetic waves with materials. Spectroscopy is used to gain knowledge about the structure of the material.

A molecule in space can have energies in various forms; rotational energy, vibrational energy or electronic energy . These energies of molecules are quantized and a particular molecule can exist in different rotational and vibrational energy levels. The molecules can move from one level to another level only by a sudden jump involving a finite amount of energy.

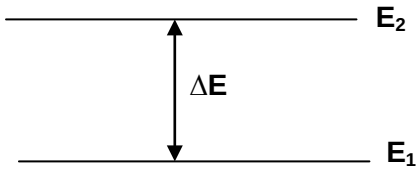

Generation of absorption spectrum

Consider two possible vibrational energy state of a molecule, E_1 and E_2. Transition can take place between the levels E_1 and E_2 provided the appropriate amount of energy $\Delta E = E_2 - E_1$ ***can be either absorbed or emitted by the system. If a molecule in state 1 is subjected to electromagnetic radiation of a single frequency*** $\nu_1 = \frac{\Delta E}{h}$ ***(monochromatic radiation, where h is Plank constant),then the energy will be absorbed from the incident radiation and the molecule will jump to state E_2 . A detector placed to collect the radiation after its interaction with the molecule will show a decrease in the intensity of frequency ν_1. If a radiation beam of wide range of frequencies is used, the detector will show that energy has been absorbed only from the ν_1 frequency and intensity of all other frequencies are unaffected. This results in an absorption spectrum.***

Molecular Vibrations

Vibration motion is described as stretching or bending depending on the nature of the change in molecular shape. Further, vibration motion can be symmetric / antisymmetric. Wave mechanics implies that any molecule can never have zero vibrational energy, *ie.*, atoms can never be completely at rest relative to each other. The harmonically oscillating molecules can undergo vibrational changes determined by simple selection rules obtained from Schrödinger equation.

The vibrations of nuclei in a molecule can be characterized with properties of the normal mode vibration. Nuclei vibrate at the same frequency and in the same phase. Nuclear motion does not cause rigid body movement (translation) or rotation of molecules. A molecule vibrates at its equilibrium position without shifting its center of gravity. Each type of molecule has a defined number of vibration modes and each mode has its own frequency. Vibration frequency varies with vibration type. The number of normal vibration modes in a molecule is related to the degrees of freedom in molecular motion. For N atomic nuclei in a molecule, there are 3N degrees of freedom as each nucleus can move in x, y or z directions. Among these, three are related to translation of a molecule along x, y or z direction as a rigid body and three related to rotation of a molecule around the x, y or z axes as a rigid body. Hence, the total vibration modes of an N-atomic molecule is $3N - 6$ .For a linear molecule , the rotation around the bond axis is meaningless, considering the nuclei as points in space. Thus, there are only two rotational degrees of freedom for the molecule and the total vibration modes are $3N - 5$.

Types of vibrations in a molecule:

- Stretching vibration
- In-planar bending vibration
- Out-of-planar bending vibration

For polyatomic molecules, the vibrations are complicated. For example, water which is a non-linear tri-atomic molecule has three allowed vibration as shown in Fig 1 [3N-6 = 3 ; N is the number of atoms in the molecule. For carbondioxide, a linear tri-atomic molecule, the number of allowed vibration is 3N-5 = 4. In Fig. 1, these vibrations are

shown. For CO_2 , there are two bending vibrations; one as shown in the figure in which the atoms moves in plane of the paper and the other in which oxygen atoms moves simultaneously into and out of the plane is not shown here. These two vibrations are identical except in directions.

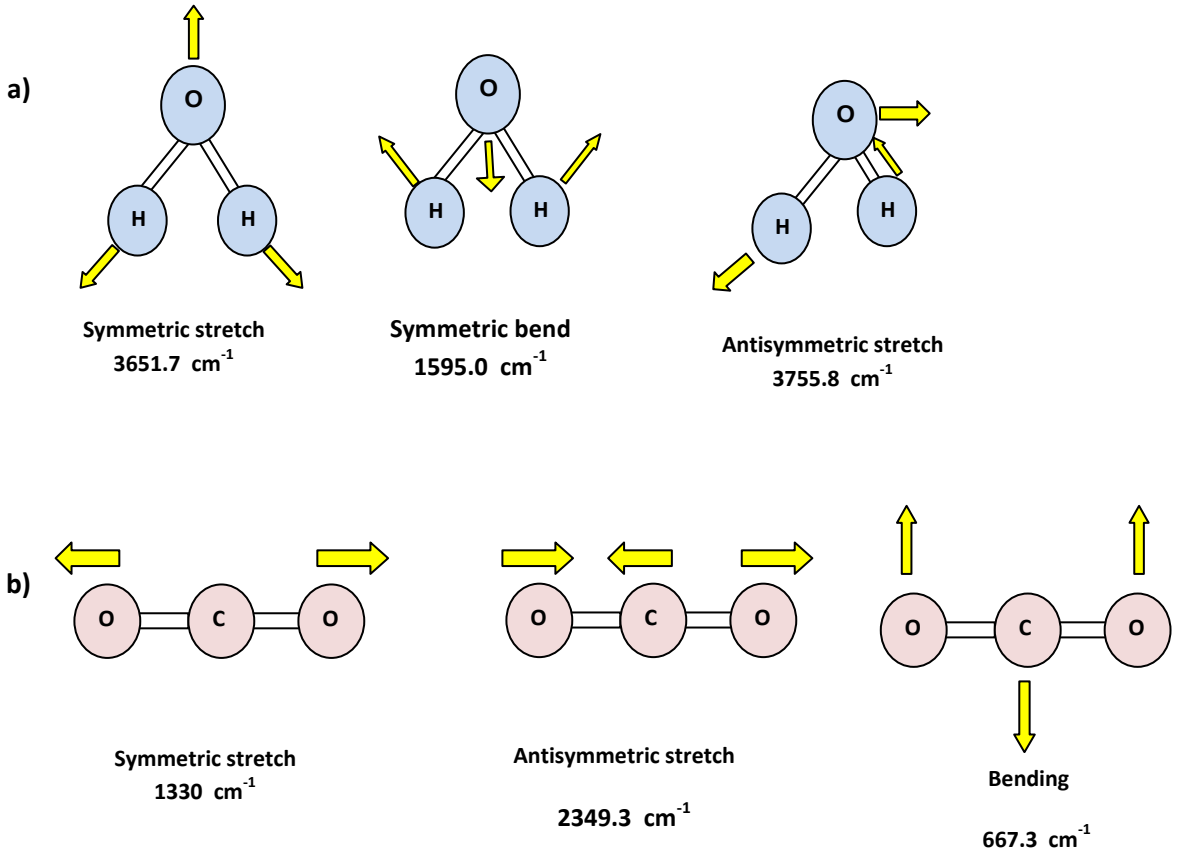

Fig. 1 : Fundamental vibrations of (a) water molecule (b) carbon-dioxide molecule

Infra red spectroscopy

Energies of infrared radiation correspond to vibrational energies of molecules. IR spectroscopy is a vibrational spectroscopy as it is based on the phenomenon of absorption of infrared radiation by molecular vibrations. IR spectroscopy gives information about the molecular structure of the materials. Both inorganic and organic materials can be analyzed. Commonly, the vibrational spectroscopy covers a wave-number range from 200 to 4000 cm^{-1}.

Infrared Activity

Among the total number of normal vibration modes in a molecule, only some can be detected by infrared spectroscopy. Such vibration modes are referred to as infrared active. To be infrared active, a vibration mode must cause a change of dipole moment in a molecule.

When a molecule has a center of positive charge and a center of negative charge and if these two centers are separated by a distance (l), the dipole moment (μ) is defined as

$\mu = el$ where, e is amount of electrical charge. Mathematically, the requirement of infrared activity is that the derivative of dipole moment with respective to the vibration is not zero.

$\left(\frac{\partial \mu}{\partial q}\right)_{q=0} \neq 0$ where , q = magnitude of normal vibration

Species with polar bonds, such as CO, NO or OH exhibits strong IR bands. Covalent bond or non-polar bonds such as C-C, – C≡C, C=C, N=N, H_2 or N_2 absorb IR weakly or not at all.

Further for polar bonds, in case of symmetric stretching if there is no change in dipole moment, the corresponding vibration will be IR-inactive. But asymmetric stretchings which are associated with change in dipole moment are always IR-active. As a guideline following can be used

- Symmetric stretch: No change in dipole moment so not IR-active
- Asymmetric stretch : Change in dipole moment so IR-active

Analysis by infrared techniques

IR radiation in the range 4000-400 cm^{-1} is used to excite stretching and bending molecular vibrations. Stretching vibrations are of highest frequency and most relevant to catalyst studies. A complex molecule is likely to have large a number of vibrations. Normal vibrations are classified in two groups :

1. ***Skeletal vibrations : In these vibrations all atoms undergo approximately the same displacement.***

   Vibration of the carbon chain in organic molecules, which falls in 1400-1700 cm^{-1} range, is an example.

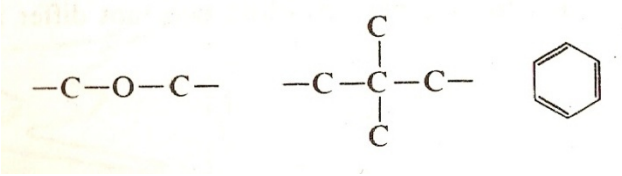

Fig. 2 : Examples of skeletal vibrations in hydrocarbons

2. Group vibrations: In some vibration modes, displacement of a small group of atoms may be much more vigorous than those of the remainder. These are called group vibrations. Group vibration frequencies are almost independent of the structure of the molecule as a whole and generally fall in the region well above or well below the skeletal mode.

Vibrations of light atoms in terminal groups, such as $-CH_3$,-OH, -C≡N, >C=O, are of high frequencies, while vibrations of heavy atoms such as -C-Cl, -C-Br, metal-metal etc. are of low frequencies. These vibrations fall in this category. Table 1 shows the stretching frequencies of some molecular groups.

Overall IR spectrum can be broadly divided in five regions :

- X-H stretch regions (4000-2500 cm^{-1}) e.g – CH, NH, OH vibrations
- Triple bond regions 2500-2000 cm^{-1} ; e.g C≡C (2100-2200) C≡N (2240-2280)
- Double bond region 2000-1500 cm^{-1} ; e.g C=O (1680-1750) C=C (1620-1680)
- fingerprint regions 1500-500 cm^{-1} ; Single bonds C-N, C-O,C-S, C-Cl etc.
- Metal adsorbate region 450-200 cm^{-1} e.g M-X ; X= C,O,N

Table 1. Stretching frequencies of some molecular group

Group	Approximate stretching frequency cm^{-1}	Group	Approximate stretching frequency cm^{-1}	Group	Approximate stretching frequency cm^{-1}
O-H	3600	C=O	1750-1600	-SH	2580
$-NH_2$	3400	C=C	1650	C-F	1050
≡CH	3300	C=N	1600	C-Cl	725
$=CH_2$	3030	C=S	1100	C-Br	650
-C≡C-	2220	-C≡CN	2250	C-I	550

Working principle and instrumentation

An FT-IR instrument uses a system called an interferometer to collect a spectrum. The interferometer consists of a source, beam-splitter, moving mirror, fixed mirror and detector.

The energy goes from the source to the beam-splitter which splits the beam into two parts.

While one half is transmitted to a moving mirror, the other half is reflected to a fixed mirror.

The moving mirror moves back and forth at a constant velocity. The two beams are reflected back from the mirrors and recombined at the beam-splitter. The beam from the moving mirror travels a different distance than the beam from the fixed mirror.

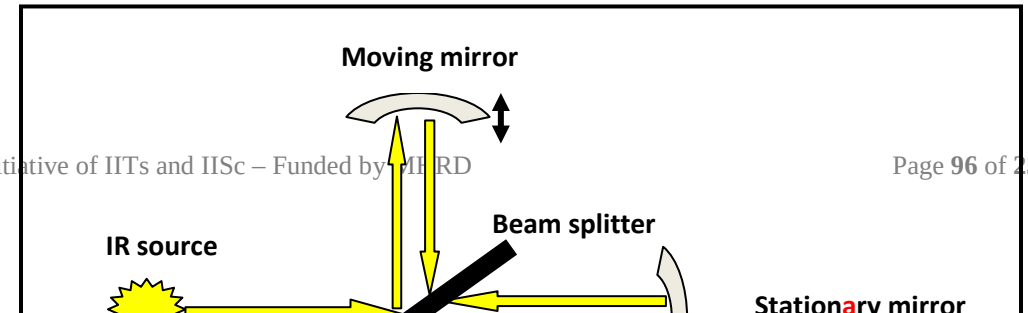

Fig. 3. Schematic diagram of FT-IR interferometer

Consequently, an optical path difference (δ) is introduced by the change in the position of moving mirror. When the reflected beams are combined, few of the wavelengths recombine constructively while others destructively creating an interference pattern. Two split beams will show constructive and destructive interference periodically, with continuous change of δ value. Completely constructive interference occurs when $\delta = n\lambda$, but completely destructive interference occurs when $\delta = (1/2 + n)\lambda$. A plot of light interference intensity as function of optical path difference is called an interferogram. This interferogram then goes from the beam-splitter to the sample, where some energy is absorbed and some is transmitted. The transmitted portion reaches the detector. The interferogram received is converted into a spectrum by using an algorithm called a Fourier transform using a computer. *Fourier transform* algorithm transfers information between a function in the time (t) domain and its corresponding one in the frequency (ω) domain.

$$F(\omega) = \frac{1}{\sqrt{2\pi}} \int_{minus\infty}^{\infty} f(t) e^{-i\omega t} \mathrm{d}t$$

Optical path difference can be considered to be in the time domain because it is obtained by multiplying time with the speed of a moving mirror. Wave-number can be considered in the frequency domain because it is equal to frequency divided by the light speed.

Thus, Fourier transformation converts an interferogram (intensity vs optical path difference) into an infrared spectrum (intensity versus wavenumber)

FT-IR plot

A reference or "background" single beam is also collected without a sample and the ratio of sample single beam to the background single beam is expressed as a transmittance spectrum. This transmittance spectrum can be converted to absorbance by using the relation $\mathbf{A = -\log T}$. The x-axis of the FT-IR spectrum is typically displayed in "wave-numbers" or cm^{-1}.

Application

In heterogeneous catalysis, IR spectroscopy is used to :

- Study the molecular structure of catalysts
- Identify adsorbed species or adsorbed reaction intermediates and their structures on catalysts
- Provide information on the nature of acid – basic sites present on catalysts surface during preparation and reaction

Examples

1. **Identification of bonds :**

Fig 4 shows the IR spectrum of alumina. In alumina, the vibrations of OH, Al-OH, and Al-O bonds generate the observed bands in the infrared region. The stretching vibration of the OH gives a very intense broadband at 3448 cm^{-1} whereas their bending vibration generate band at 1624 cm^{-1}. The band at 1523 cm^{-1} may be attributed to stretching vibrations of Al-OH bond. The low-energy region of alumina spectrum shows a broad band at 500-1000 cm^{-1}, probably produced by vibrations of Al-O bonds.

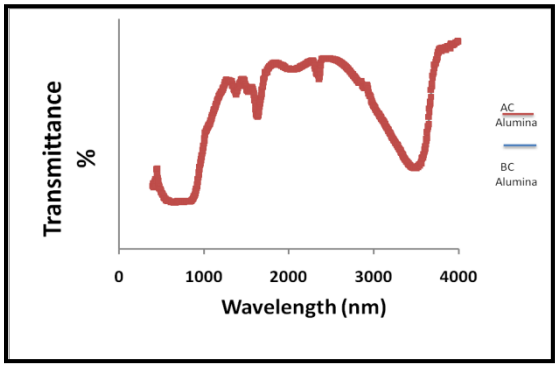

Fig. 4. IR spectrum of alumina

2. **Identification of acid sites**

Acid sites can be Lewis acids sites that accept electrons or Bronsted acids sites that donate proton. In this method, basic molecular probes are adsorbed on the surface acid sites for identification. Generally, pyridine (C_5H_5N) which can adsorb on both Lewis and Bronsted acid sites is used as the probe molecule. Pyridine hydrogen bonded at Bronsted acid sites gives IR bands at 1485-1490 and 1580-1600 cm^{-1} over zeolite catalysts whereas IR bands for pyridine coordinated to Lewis sites gives peaks at 1450 and 1620 cm^{-1}.

Book reference

- Colin N. Banwell & Elaine M. McCash ,Fundamentals of molecular spectroscopy, Tata McGraw-Hill Pub. Co. Ltd., 2000.
- Y. Leng, Materials Characterization: Introduction to microscopic and spectroscopic methods, John Wiley & Sons, 2008
- Sam Zhang, Lin Li, Ashok Kumar , Materials Characterization Techniqes, CRC Press, 2009

Lecture 16

Raman spectroscopy

Raman spectroscopy is used to analyze the internal structure of molecules and crystals. It is based on scattering phenomenon of electromagnetic radiation by molecules. Scattering by molecules can be elastic or inelastic.

- Elastic scattering : the scattered light has the same frequency as that of the source radiation. Elastic scattering is called Rayleigh scattering.
- Inelastic scattering: the scattered light has a different frequency from that of the source radiation. Inelastic scattering is called Raman scattering.

Basic process

At room temperature, most molecules are present in the lowest energy vibrational level. When a material is irradiated with intense electromagnetic radiation of single frequency it interacts with the molecule and distorts (polarize) the electron cloud around the nuclei to form a short-lived high energy state, called 'virtual state'. Energies of these virtual states are determined by the frequency of the light source used. These high energy virtual states are very unstable.

Raman Stokes scattering : During inelastic (Raman) scattering ,the molecule returns from the virtual state to a higher energy level compared to the initial stage (Fig. 1c). A fraction of photon energy is absorbed by the molecules to remain in the higher energy vibrational state, V=1 where $E_{V=1} > E_{V=0}$ and $E_{V=0}$ is the ground vibrational state. Consequently, energy of the reradiated photon is less than that of incident photon. This type of inelastic scattering is called Stokes scattering.

Raman anti-Stokes scattering : Due to thermal energy, some molecules may be present initially in the excited state, V=1. If after interaction with the incident light, the molecules from virtual state return to ground state, V=0, then the energy of the reradiated photon will increase by the amount of $\Delta E = E_{V=1} - E_{V=0}$ as shown in Fig. 1a. This type of Raman scattering is called anti-Stokes scattering and involves transfer of energy to the scattered photon.

When the electrons excited from ground energy level returns back to ground state V=0 then it corresponds to Rayleigh scattering (Fig. 1b)

Relative intensities of Stokes & anti-Stokes scattering

Relative intensities of these two processes depend on the population of the various states of the molecule. At room temperature, majority of molecules are expected to be initially in the ground energy state and excited vibrational state will be small. Consequently, anti-Stokes scattering will be weak compared to Stokes scattering. Usually in Raman scattering, Stokes scattering is recorded. As temperature rises, anti-Stokes scattering will increase relative to Stokes scattering.

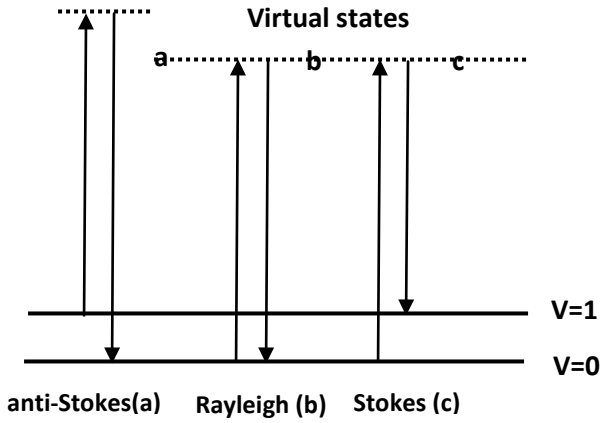

Fig. 1. Different transitions observed in Raman process

Raman Activity

To be Raman active, a vibration mode must cause polarizability changes in a molecule. Mathematically, Raman activity requires that the first derivative of polarizability (α) with respect to vibration at the equilibrium position is not zero.

$$\left(\frac{\partial \alpha}{\partial q}\right)_{q=0} \neq 0$$

The ‘q’ is the displacement of the atoms form equilibrium position. Polarization of molecules varies with directions in a three-dimensional space. For example, in a linear molecule such as CO_2, the electron cloud has the shape of an elongated ellipsoid that is more deformable along its long axis than the directions perpendicular to the long axis.

Generally, if the ellipsoid changes its size, shape and orientation with vibration, that vibration is Raman active. For example, in case of H_2O molecule, all normal mode vibrations, as shown in Fig.1a , are Raman active because the ellipsoid changes size, shape or orientation in all cases.

Table 1. Comparison of Infrared absorption and Raman scattering

Infrared spectroscopy	Raman spectroscopy
Range of IR frequencies interacts with sample	Intense radiation of single frequency interacts with sample
From incident radiation ,certain frequencies are absorbed and loss of these frequencies from incident radiation is detected.	Radiation interacts forming unstable high energy 'virtual state' and the photons are quickly re-emitted. Re-emitted photons of different energies are detected
Occurs when incident radiation energy match with the energy difference between the ground and excited states.	Do not require matching of the incident radiation to the energy difference between the ground and excited states.
To be IR active, a vibration mode must cause dipole moment changes in a molecule.	To be Raman active, a vibration mode must cause polarizability changes in a molecule.
Uses radiation energy comparable to the fundamental vibrations of most chemical bonds or systems of bonds	Uses much higher energy radiation compared to the fundamental vibrations of most chemical bonds or systems of bonds
Measure frequency of absorbed light	Measure the change of frequencies of the scattered light. Intensity of the Raman scattered component is much lower ; hence highly intense light source and a very sensitive detector are required

Selection rule

Intense Raman scattering occurs from vibrations which cause a change in the polarizability of the electron cloud around the molecule. Usually, symmetric vibrations cause the largest changes in polarizability and give the greatest scattering. In contrast for infrared absorption, the most intense absorption is caused by a change in dipole and hence asymmetric vibrations which cause this are the most intense. The two techniques usually give quite different intensity patterns. As a result, the two are often complementary and used together to give a better view of the structure of a molecule. In

some cases, vibrations of a molecule can be both infrared and Raman active. Selection rules related to symmetry is :

- Rule of thumb: symmetric=Raman active, asymmetric=IR active

Table 2. Raman and IR active band of CO_2 and H_2O molecule

CO_2		H_2O	
Symmetric stretch	**Raman active: 1335 cm^{-1}**	**Symmetric stretch**	**Both Raman and IR active : 3652 cm^{-1}**
Antisymmetric stretch	**IR active: 2349 cm^{-1}**	**Antisymmetric stretch**	**Both Raman and IR active : 3756 cm^{-1}**
Symmetric bend	**IR active : 667 cm^{-1}**	**Symmetric bend**	**Both Raman and IR active : 1596 cm^{-1}**

Working principle and instrumentation

A typical Raman system consists of the following basic components:

1) An excitation source, usually a laser

2) Sample illumination system and light collection optics

(3) Double or triple monochromator /Wavelength selector

(4) Signal processing system consisting of a detector, an amplifier, and an output device.

Sample is mounted in the sample chamber and laser light is focused on it with the help of a lens. The scattered light is collected using another lens and is focused at the entrance slit of the monochromator. The width of the monochromator slit is set for the desired spectral resolution. Monochromator effectively rejects stray light and serves as a dispersing element for the incoming radiation. Light leaving the exit slit of the monochromator is collected and focused on the surface of a detector. This optical signal is converted to an electrical signal within the detector. Signal is processed in a computer to develop the final spectrum. Schematic diagram of Raman spectrophotometer is shown in Fig. 2.

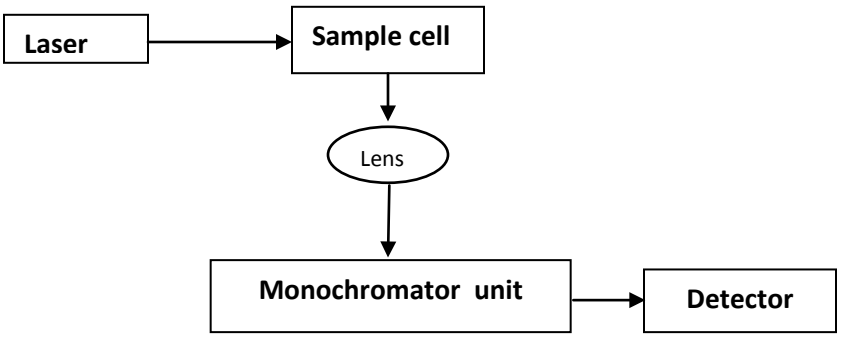

Fig. 2. Schematic diagram of Raman spectrophotometer

The major problem associated with Raman spectroscopy is the very weak intensity of the scattered light. Consequently, it requires an extremely monochromatic high-energy light source, very effective filtering of Stokes scattering and very high sensitivity of the detecting device. Excitation source must be strong enough to generate sufficient Raman signals and monochromatic to provide clean and uncomplicated spectra. A laser typically is used as the excitation source because it can provide a coherent beam of monochromatic light with high intensity. Different laser beams in ultraviolet (UV), visible (Vis) or near infrared (NIR) range are used. Argon and krypton ion laser sources, being more intense, give better spectra and are the most commonly used. Light scattered from a laser excited sample is collected with a lens and is sent through filters to a monochromator. Raman scattering is effectively separated from Rayleigh scattering by multiple monochromators . At present, various arrangements such as notch filters, tunable filters, laser stop apertures, double and triple spectrometric systems are used to reduce Rayleigh scattering

and obtain high-quality Raman spectra. Types of detectors mainly used are photomultiplier tube, photo diode array or charge coupled device.

Sample preparation

Raman analysis require no special sample preparation. All kind of samples in the form of liquid, solid or gas can be analyzed. Short measuring time, normally a few seconds, is required to obtain a Raman spectrum.

Applications

Raman shift provides information about vibrational, rotational and other low frequency transitions in molecules. It is used for the qualitative study of molecular structures. It is generally not used for quantitative studies, since due to weak Raman scattering, sensitivity is low.

Raman spectroscopy is complementary to IR spectroscopy. IR and Raman both are useful for Fingerprinting.

Examples

1. Raman spectra of titania and zirconia

The Raman spectra of titania and zirconia samples are shown in Fig. 3.

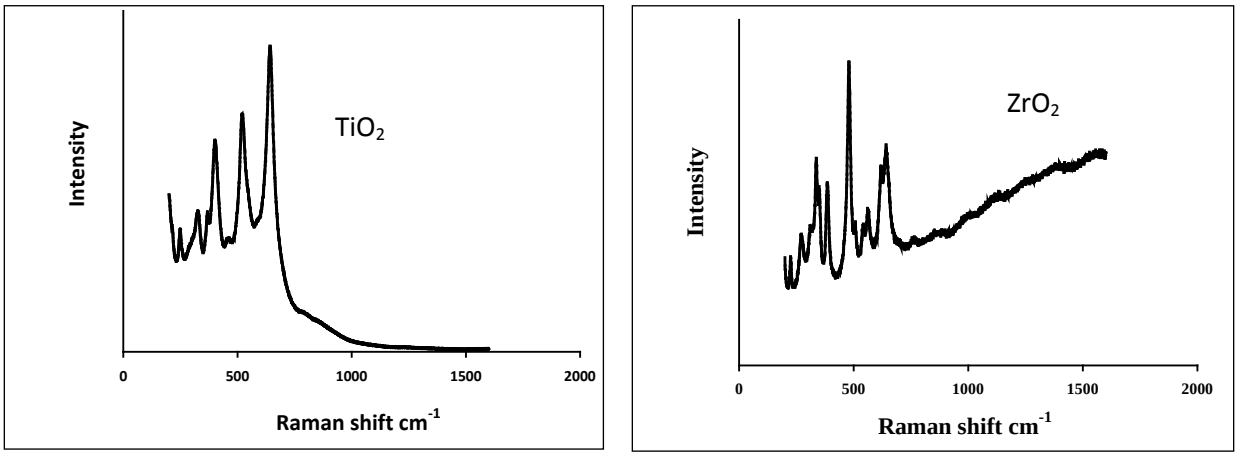

Fig. 3. Raman spectra for titania and zirconia

2. **Study of surface vanadia species**

The surface structure of supported vanadium oxide species can be studied using Raman spectroscopy. Different types of surface vanadium species are observed as shown in Fig 4. Isolated V = O and polymeric V = O gives Raman band at 1026 cm^{-1} and 1009 cm^{-1}, respectively.

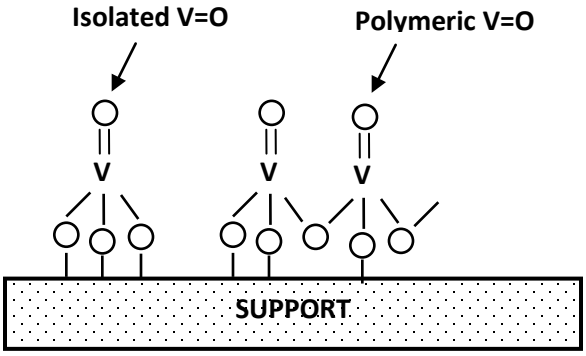

Fig. 4. Various surface vanadia species observed on supported vanadia catalysts

Book reference

- Colin N. Banwell & Elaine M. McCash ,Fundamentals of molecular spectroscopy, Tata McGraw-Hill Pub. Co. Ltd., 2000.
- Ewen Smith & Geoffrey Dent, Modern Raman Spectroscopy – A Practical Approach, John Wiley & Sons Ltd. 2005
- Y. Leng, Materials Characterization: Introduction to microscopic and spectroscopic methods, John Wiley & Sons, 2008

Lecture 17

Electron Microscopy

Microscope forms an enlarged image of the original object in order to convey its internal or external structure. The magnification and resolution of microscope is given as

(a) Magnification = objective lens × eyepiece lens

(b) Resolution (r_d) is defined as closest spacing of two points which can be clearly seen through the microscope as separate entities. Resolution can be determined as :

$$r_d = \frac{0.61\,\lambda}{\mu\,\sin\alpha} = \frac{0.61\,\lambda}{NA}$$

λ = wavelength of light
μ = refractive index of the medium between the object and objective lens
α = the half angle made by aperture at the specimen
$NA = \mu\,\sin\alpha$ = numerical aperture

By increasing the dimension or by employing large number of lenses, the magnification can be increased, while shorter wavelength yields higher resolution.

Electrons are considered as radiation with wavelength in the range 0.001 - 0.01 nm compared to 400- 700 nm wavelength of visible light used in an optical microscope. In an electron microscope, a focused electron beam is used instead of light to examine objects, and the image of the specimen is obtained on a very fine scale. Because of the use of large number of lenses and electrons of very low wavelength, magnification and resolution for electron microscopes is much higher. High magnification and resolution makes electron microscopes extremely useful for revealing ultrafine details of material microstructure. Optical microscopes have a maximum magnification power of 1000, and resolution of 0.2 μm compared to resolving power of the electron microscope that can reach 1,000,000 times and resolution of 0.2 nm. Hence, electron microscopes deliver a more detailed and clear image compared to optical microscopes.

- Two main types of electron microscopes
    - Transmission electron microscopes (TEM)
    - Scanning electron microscopes (SEM)

Transmission Electron Microscopes (TEM)

The optics of the TEM is similar to conventional transmission light microscope. It was developed in the 1930s. It is capable of displaying magnified image of thin specimen with magnification in range of 10^3 to 10^6. Information that can be obtained using TEM include :

- Topography : surface features , texture
- Morphology : shape and size of the particles
- Crystallographic arrangement of atoms
- Composition : elements and the their relative amounts

Interaction of electron beam with sample

Interaction of electron beam with the sample results in three types of electrons :

i. Unscattered electrons: These are electrons that are transmitted through the thin specimen without any interaction with the sample. Transmission of unscattered electrons is inversely proportional to the specimen thickness. The areas of specimen that are thicker will have fewer transmitted unscattered electrons and will appear darker. Conversely, thinner areas will have more transmitted electrons and will appear lighter.

ii. Elastic scattered electrons: These are incident electrons that are scattered by the atoms of the specimen in an elastic fashion; that is without any loss of energy of electrons. The elastically scattered electrons form a pattern that yields information about the orientation, atomic arrangements and phases present in the area being examined.

iii. Inelastic scattered electrons : Incident electrons that interact with the specimen atoms in an inelastic fashion and lose energy during the interaction, fall in this catagory. The extent of loss of energy by incident electrons depends on the characteristic of interacting elements and is used to study the compositional and bonding (i.e. oxidation state) information of specimen region being examined.

Working Principle and Instrumentation

The Fig. 1 shows the arrangement of components for transmission electron microscope. An electron gun at the top of the microscope emits electrons that travel through vacuum in the microscope column. Vacuum is essential to prevent strong scattering of electrons by gases. Electromagnetic condenser lenses focus the electrons into a very thin beam. Electron beam then travels through the specimen and then through the electromagnetic objective lenses. At the bottom of the microscope, unscattered electrons hit the fluorescent screen giving image of specimen with its different parts displayed in varied darkness, according to their density. The image can be studied directly, photographed or digitally recorded.

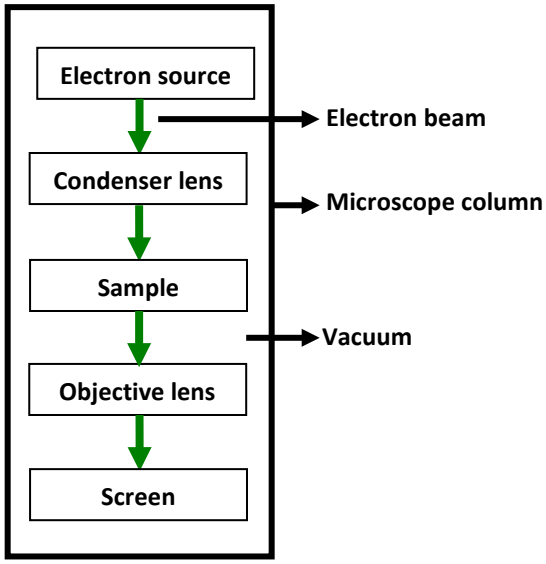

Fig. 1. Schematic diagram illustrating transmission electron microscope

A transmission electron microscope has the following components along its optical path:

1. Electron source
2. Condenser lens
3. Specimen stage
4. Objective lens and projector lens
5. Screen/photographic film/CCD camera

In the electron gun, electrons are emitted from the surface of the cathode and accelerated towards the anode by a high voltage (V_o) to form a high energy electron beam. All lenses in the electron microscope are electromagnetic. Charged electrons interact with the magnetic fields and magnetic force deflects or focuses an electron beam. The condenser lens system controls the beam diameter and convergence angles of the beam incident on a specimen.

Sample preparation

Preparation of specimens is the most tedious step in TEM. To make the material electronically transparent, material thickness is limited. Specimens have to be prepared with thickness of ~ 100 nm. For higher atomic weight material, the specimen has to be thinner. TEM sample preparation depends on type of materials used.

For bulk material, TEM specimen preparation is done in two steps :

- Pre-thinning : thinning to 0.1 mm thickness
- Final-thinning: thinning to 100 nm thickness

Pre-thinning :In pre-thinning stage, specimen less than 1mm thick is prepared by mechanical cutting (with a diamond saw). Then, a 3-mm-diameter disc is cut using punch before further reduction of thickness. Grinding is most commonly used to reduce the thickness of metal and ceramic specimens.

Final thinning :Final thinning is mainly done by electrolytic thinning & ion milling, which create a dimpled area on pre-thinned specimens that have regions of electron transparency as shown in Fig.2. In electrolytic thinning, metal specimen is made the anode in an electrolytic cell. On passing current, the metal is gradually dissolved and

deposited on the cathode. Finally tiny holes appear, the edge of which are suitable for electron transparency. In ion milling method, samples are bombarded with a beam of energetic ions to reduce the thickness by knocking atoms out of the specimen. This method can also be used for ceramics and other non-conducting materials. For polymeric and biological specimens, ultramicrotomy method is used where specimen is cut into thin sections by a cutting tool such as glass knife or diamond knife.

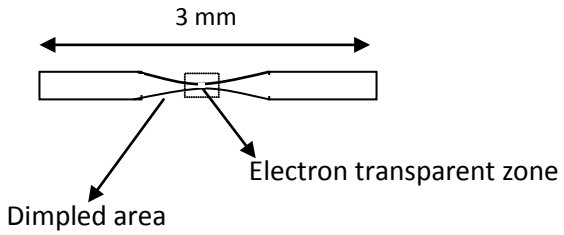

Fig.2 . Thinning of bulk specimen for TEM analysis

For powder samples, such as catalysts, the powder size is reduced by grinding, to a very fine size till the particle thickness is small enough to allow electron transmission. These fine particles are then suspended in a volatile solvent such as isopropanol. A drop of this particle suspension is placed on a thin carbon foil supported by a conventional microscope grid. On evaporation of solvents, the powder particles are ready for observation. Alternatively, the powders can be embedded in some suitable matrix such as epoxy resin or metals, from which a flat sheet of 3 mm diameter is cut out to study by conventional methods.

Magnification and resolution

Magnification and resolution is defined in the same way as for transmission light microscope.

- Magnification of any convergent lens *M* is given by

$$M = \frac{v - f}{f}$$

f = focal length of lens ;v = distance between image and lens

- Resolution of electron microscope can be written as

$$r = \frac{0.61\,\lambda}{\alpha}$$

α = Angle through which beams are deflected ; λ= wave length of electrons
For λ=0.0037 nm (wave length of 100 kV electrons) and α = 0.1 radians (~5 degrees) resolution of ~0.02 nm is obtained

Scanning electron microscope

SEM is most widely used type of electron microscope for study of microscopic structure. In SEM, image is formed by focused electron beam that scans over the surface area of specimen. The incident beam in SEM is also called electron probe. The incident beam is of typically 10 nm diameter in contrast to beam of TEM which is about 1 μm. In SEM, image is not formed by instantaneous illumination of the whole field as for TEM. SEM is relatively easy to operate and maintain, compared to a TEM. In TEM, unless specimen is made very thin, electrons are strongly scattered within the specimen or even adsorbed rather than transmitted. SEM overcomes this limitation.

Electron sample interactions

The interaction of electron beam with samples results in secondary electrons andbackscattered electrons that are detected by standard SEM equipment.

Secondary Electrons : As incoming electrons pass through the specimen, they impart some of their energies to electrons of nearby specimen atom. This causes ionization of the electrons of the specimen atom and slight energy loss and path change of the incident electrons. These ionized electrons then leave the atom with a very small kinetic energy (5eV) and are termed as secondary electrons. The secondary electrons escape from a volume near the specimen surface, at a depth of 5–50 nm and hence are useful to gain topography related information.

Backscattered Electrons: Some of the electrons of the incident beam collide with the specimen atoms that fall in the path and are reflected or back scattered. The production of backscattered electrons varies directly with the atomic number of the specimen. When backscattered electrons are detected, higher atomic number elements appear brighter than

lower atomic number elements. This interaction is utilized to differentiate parts of the specimen that have different average atomic number.

Working principle and instrumentation

In SEM, there are several electromagnetic lenses, including condenser lenses and one objective lens. Electromagnetic lenses are for electron probe formation, not for image formation directly, as in TEM. Two condenser lenses reduce the crossover diameter of the electron beam. The objective lens further reduces the cross-section of the electron beam and focuses the electron beam as probe on the specimen surface. Objective lens thus functions like a condenser. This is in contrast to TEM where objective lens does the magnification.

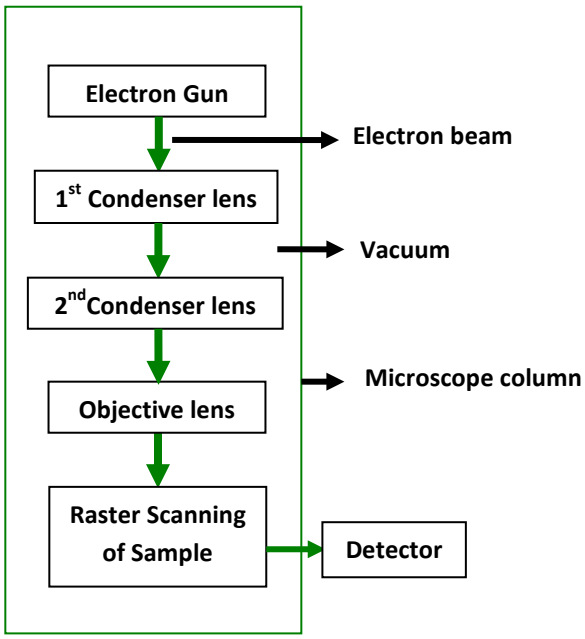

Fig. 3. Schematic diagram illustrating scanning electron microscope

Electron probe or beam is scanned across the specimen and the procedure is known as Raster scanning. Raster scanning causes the beam to sequentially cover a rectangular area on the specimen. The signal electrons emitted from the specimen are collected by the detector, amplified and used to reconstruct the image according to one-to-one correlation

between scanning points on the specimen and picture points on the screen of cathode ray tube (CRT). CRT converts the electronic signals to a visual display.

Everhart–Thornley is commonly used detector in SEM. It consists of a scintillated photo multiplier system. As electrons strike the scintillator, photons are emitted. The photon is transmitted a light pipe into a photomultiplier tube, which converts the photon into pulses of electrons, which are amplified and used to modulate the intensity of CRT.

Magnification and Resolutions

Magnification

In SEM, image is not magnified by any lens as opposed to TEM where magnification is determined by power of the objective lens. Magnification of SEM is determined by the ratio of the linear size of the display screen to the linear size of the specimen area being scanned. Raster displayed on the CRT is larger than the corresponding Raster scanned by the electron beam on the specimen (Fig 4). The linear magnification is given by

$$Linear\ magnification = \frac{side\ length\ of\ \ CRT\ [L]}{side\ length\ of\ \ raster\ [l]}$$

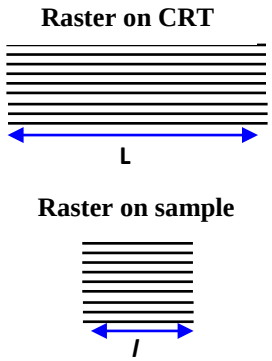

Fig. 4 . Raster on sample and corresponding raster on CRT

For example, if electron beam is made to scan 10 μm×10 μm raster on the specimen and the corresponding image raster is displayed on CRT screen as 100mm × 100 mm, then linear magnification will be

$$Linear\ magnification = \frac{side\ length\ of\ CRT\ [L]}{side\ length\ of\ raster\ [l]} = \frac{100\times10^{-3}m}{10\times10^{-6}m} = 10000$$

SEM is able to provide image magnification from about 20× to greater than 100,000× .

Resolutions (Pixels)

Image performance in SEM can be explained on the basis of the picture element or pixel. The amplified signal from the detector makes a minimum spot size of ~ 0.1 mm or 100 micrometer in the CRT. The spot on the CRT mimics the movement of the electron beam on the specimen. Therefore for each of the pixels on the CRT, there is a corresponding pixel on the specimen. The size of specimen pixel (p) is given by $p = \frac{100}{M}\mu m$ where M = magnification

Resolution is defined as the smallest separation of two points that a microscope can detect as separate entities. In order to resolve two features A and B in Fig 5 they must occupy separate pixels. Therefore, working resolution of SEM can be no better than the specimen pixel size 'p' as given by above equation.

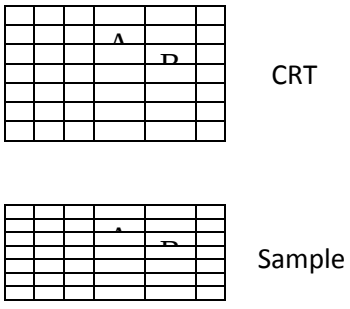

Fig. 5. Raster as array of picture points or pixel on CRT and sample

Resolution of SEM is also controlled by the size of the electron probe scanning the specimen. If the electron probe is larger than the specimen pixel, then the signal from adjacent pixels are merged and the resolution is degraded (Fig 6a).If electron probe is smaller than specimen pixel, then signal will be weaker and noisy (Fig 6b).For optimum performance, probe diameter or sampling volume is made equal to the specimen pixel diameter (Fig 6c).This means that for optimum performance, the probe size should be adjusted as the magnification of the microscope is altered. However, ultimate resolution depends on the smallest probe which can provide adequate signal from the specimen.

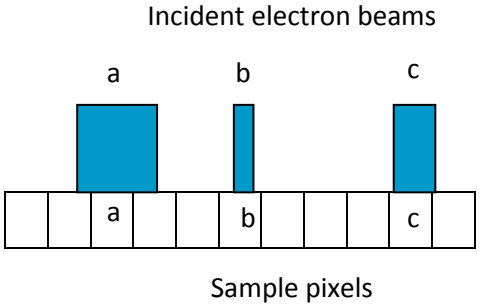

Fig. 6.Size of the electron probe scanning the specimen with respect to specimen pixel.

Sample preparation

Sample preparation for SEM is minimal. This has made SEM more widely used than TEM which requires a very thin specimen and tedious sample preparation procedure. Sample preparation for SEM involves only sizing the specimens to fit SEM specimen holder and removing surface contaminants. This also helps to preserve the surface characteristics for topographic study.

Examples

Fig 7 shows SEM image of titania samples prepared by precipitation using $TiCl_2$ as precursor. The image shows that the prepared titania sample consisted of particles with wide size distribution and irregular shape. The size of the particles can be measured manually by using the scale given in the figure or by any image analysis software.

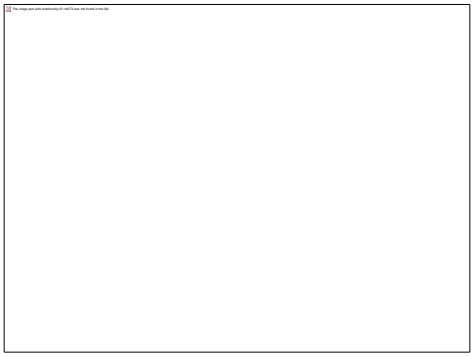

Fig. 7. SEM image of titania samples prepared by precipitation method

Energy dispersive spectrometer (EDS)

In this method, the X-ray generated from interaction of electron beam with sample, is used for chemical analysis of the sample. As high energy electrons strike the sample surface, along with secondary and backscattered electrons, characteristic X-rays are emitted whose wave length depends on nature of atoms in sample. These X-rays can be used to characterize all type of solid materials. The characteristics X-ray is generated when an inner shell electron is knocked out of the atom and the vacant site is filled with electron from outer shell. The excess energy is released and the amount of released energy, corresponding to X-ray range, is characteristics of the particular atom.

For example, if a K shell electron has been knocked out of a molybdenum atom, and vacancy is filled by L electron, then ΔE= 17400 eV, is emitted as K_α X-ray of Mo. The wave length of the corresponding X-ray is $\lambda = \frac{hc}{\Delta E} = 0.071$ nm. On the other hand if vacancy is filled by M shell electron, the difference in energy is $\Delta E \sim 19600$ eV. Then the corresponding X-ray emitted is Mo K_β , λ = 0.063 nm. The K-series lines are more

frequently used for analysis. For heavier atoms, the energy required to knockout the K-shell electron increases and consequently exciting the K series line become difficult. In these cases L series and M series of lines can be used which are generated by knocking of L or M shell electrons.

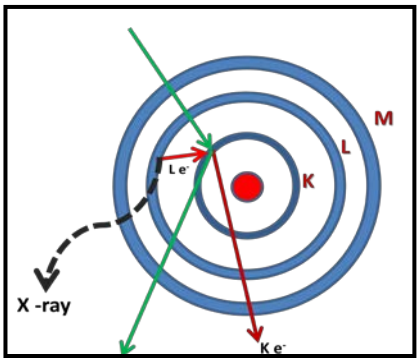

Fig. 8. Emission of X-ray when outer L shell electron fills the K shell electron vacancy

The energy and wavelength of X-rays are different for each atomic species and by measuring them, the elements present in sample can be detected and quantified. From X-ray spectrum following analysis can be done:

1. Measurement of wavelength/energy of each characteristics X-ray emitted. It can be used to determine the elements present in sample. This is a qualitative analysis.
2. Measurement of X-ray of any type emitted per unit time. This corresponds to amount of the element present in sample. This is quantitative analysis.

SEMs are equipped with an energy dispersive spectrometer or EDS detection system which is able to detect and display most of the X-ray spectrum. The detector normally consists of semiconducting silicon or germanium. Since, the X-rays can not be deflected, the detector has to be placed in line of sight of the specimen. In order to collect as many X-rays as possible, the detector is placed near the specimen (20 mm or less from the specimen). It normally occupies a similar position to the secondary electron detector. Each incoming X-rays to the detector excites a number of electrons into the conduction band of the silicon leaving an identical number of positively charged holes in the outer electron shells. The energy required for each of these excitations is only 3.8 eV,

consequently the number of electron-hole pairs generated is proportional to the energy of the X-ray photon being detected. For example, an Al K_{α} X-ray having energy of 1.49 keV, will give rise to approximately [(1.49 × 1000) eV/3.8 eV] = 392 electron hole-pairs. If voltage is applied across the semiconductor, a current will flow as each X-ray is absorbed in the detector and the magnitude of the current will be exactly proportional to the energy of the X-ray. The current which flows between the electrode when an X-ray enters the detector lasts for an extremely short time, less than 1 μs and is normally referred as pulse. Each pulse is amplified and stored in a computer. The EDS spectrum of alumina is shown in Fig 9. It shows the peak due to Al and O.

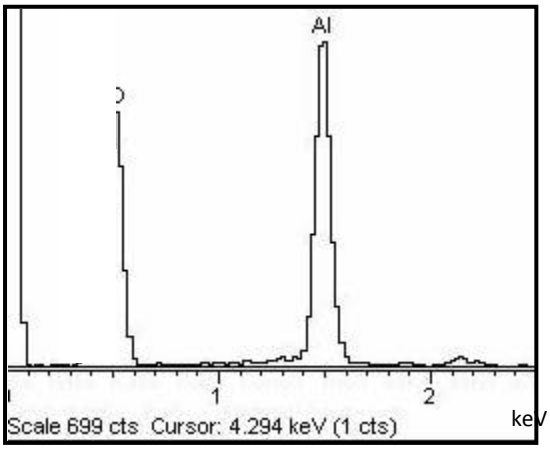

Fig. 9 EDS spectra of alumina

Book reference

- P.J. Goodhew, J. Humphreys ,R. Beanland, Electron microscopy and analysis , 3rd ed.,Taylor & Francis, 2001
- Y. Leng, Materials Characterization: Introduction to microscopic and spectroscopic methods, John Wiley & Sons, 2008

Lecture 18

Reactor types and catalysts test

Reactor types

Reactors can be classified based on different criterion such as size, reactor material, methods of charging and discharging or type of fluid flow. For fluid – solid heterogeneous system reaction rate is based on mass of solid catalyst rather than on reactor volume. In laboratory scale, the reactions are carried out in micro reactors with diameters ranging from 1 – 5 mm for testing up to 0.1 – 1gm of catalysts. In industry, diameter and height of reactors can vary from 1 to 10 m and 2 to30 m respectively. The reactor materials also vary depending on usage. Laboratory reactors are usually made of glass, quartz or stainless steel with few mm wall thicknesses. The large industrial reactors depending on usage are usually made of mild steel or stainless steel or other alloys. The wall thickness can range from of 6-15 mm depending on process pressure. Depending on the operation, reactor can be batch, mixed flow or packed bed type. The choice of reactor depends on the type of reaction. For examples, many hydrogenation reactions are carried out in CSTR while many of the solid catalysts are tested in packed bed reactor. Reactor selection also depends on the type of catalyst and its activity, selectivity and deactivation behavior. The schematic diagram of different type of reactors is shown in Fig 1.

For study of catalytic reactions in laboratory different reactors are used. For example fluid-solid **c**atalytic reactions are studied in (1) packed bed reactors heated in furnace, (2) Carberry reactors equipped with rotating catalyst basket and cooling or heating jacket or (3) Berty reactor with internal circulation and cooling or heating jacket. For reactions involving gas-liquid-solid, slurry CSTR with cooling or heating jacket or packed bed reactor with downflow, upflow or countercurrent flow of gas and liquids are used. Laboratory reactors are mainly used for measuring reaction kinetics and catalyst activity at different conditions of temperature and pressure.

Fixed bed reactor

The fixed bed or packed bed reactors are most commonly used for study of solid catalyst. A fixed bed reactor usually consists of a cylindrical vessel packed with catalyst pellets and easy to design and operate. The metal support grid and screen is placed near the bottom to support the catalyst. Inert ceramic balls are placed above the catalyst bed to distribute the feed evenly.

Advantages of packed bed or fixed bed reactor include ideal plug flow behavior, lower maintenance cost and reduced loss due to attrition and wear. Heat management is very important aspect for design of fixed bed reactor. Poor heat distribution may result in non uniform reaction rates and consequently low reactant conversion. Poor heat transfer may also result in generation of hot spots and thermal degradation of catalyst. However, the situations are observed more in large fixed bed and for highly exothermic or endothermic reactions when temperature control is difficult. The regeneration or replacement of catalyst is also difficult in fixed bed reactors and process needs to be shutdown. Another major disadvantage of packed bed reactor is plugging of bed due to coke deposition which results in high pressure drop. High pressure drop is also observed for small beads or pellets of catalysts. However, increase in pellet size increases the pore diffusion limitation.

Catalyst pellet sizes are usually in the range of 1 to 10 mm. Non-uniform packing of catalysts can cause channeling of fluids leading to poor heat and mass transfer. The column to particle diameter is maintained in between 10 to 20 to minimize channeling. The bed voidage is usually 70 to 90 %. Plug flow behavior is ensured by maintaining ratio of reactor length to catalyst particle diameter greater than 50. The allowed pressure drop is less than 0.5 inch water per foot of bed depth. Usually the ratio of bed height to diameter is maintained greater than 0.5.

For better heat management for very highly exothermic (or endothermic) reaction the multitubular reactor is used with catalyst packed inside the tubes. The cooling (or heating) fluid flows through the shell side. The length is limited by allowable pressure drop. The multitubular reactor has high surface area for heat transfer per unit volume. For

determination of heat transfer and mass transfer properties several correlations are available in literature.

Fluidized bed reactors

In fluidized bed reactor catalyst pellets of average size less than 0.1 mm are fluidized by the reactant fluid. The linear velocity is maintained above the minimum fluidization velocity required to obtain the fluidized bed. As the superficial velocity increases, the bed expands and become increasingly dilute. At high enough linear velocity, the smallest catalyst particles escape from the bed and have to be separated from exhaust gases and recycled.

In fluidized bed, heat transfer is much better resulting in more uniform temperature compared to packed bed reactor. Frequent regeneration of catalyst can be done without any shutdown of the process. However, fluidized bed is a complicated system to operate and requires extensive investments and high operating and maintenance cost. Other major disadvantages are attrition and loss of catalysts due to fluidized condition. Modeling of fluidized bed flow is complex. The fluidized bed is assumed to consist of bubble and emulsion phases which can be modeled respectively by plug flow and CSTR, as the emulsion phase is assumed to be well mixed. Correlation for heat and mass transports are available in literature. The reactor is extensively used for catalytic cracking process.

Carberry reactor or Berty reactor

For catalytic investigations, reactors equipped with rotating basket or fixed basket with internal circulation can be used. These CSTR type reactors are used to minimize the inherent mass and heat transfer limitations observed in fixed-bed reactors. These reactors are frequently used in industry to evaluate reaction mechanism and reaction kinetics. The most common type of reactors used are Carberry and the Berty reactors.

The main feature of the Carberry reactor is that the catalyst particles are contained in a spinning basket or embedded in the blades of a spinning agitator. The mounted catalyst is rapidly rotated resulting in good mixing between reactants in fluid phase and

the solid catalyst. This minimizes the mass transfer and heat transfer resistances. The basket or impellers can spin up to 2,500 rpm.

The Berty reactor uses an internal recycling to achieve perfectly mixed behavior. The catalyst is contained in a fixed bed basket through which the reacting gases circulate. The catalyst basket is equipped with large diameter impellers rotated in order to circulate gases & liquids past solid catalysts. An internal recirculation rate of 10 to 15 times of the feed rate effectively eliminates external diffusion resistance and temperature gradient. Retaining the solid catalyst in a spinning woven wire mesh basket allows gas / liquid circulation with low pressure drop. Circulating the reactants past the catalyst minimize wearing & breakage.

Multiphase reactors

Slurry reactors

The catalytic reaction can also be carried out in two–phase or three –phase stirred tank reactors also known as slurry reactors. In three –phase reactor, gas and liquid reactants are brought into contact with solid catalyst particles. In two–phase reactor, fluid phase is usually liquid reactant in contact with the solid catalyst. The reaction of gaseous reactant with catalyst is usually carried out in fixed bed reactor. In three –phase slurry reactor the gaseous reactant and solid catalysts are dispersed in continuous liquid phase by mechanical agitation using stirrer. The efficient stirring ensures nearly uniform composition throughout the reactor. This kind of reactor is used in hydrogenation, oxidation, halogenations and fermentation process. The advantages include nearly isothermal operation and good heat and mass transfers. The use of powder catalysts having high activity minimizes the intraparticle diffusion limitation. The reactors can be operated in batch, semi batch or continuous mode. In three – phase system bubbles of gas rise through agitated slurry. Solid particles are in size range of 0.01to 1.0 mm. The solid concentration can be up to 30 vol. %. Lower concentration is also used. In hydrogenation of oil with nickel catalyst, the solid content is 0.5 vol. %. The external transport effects are important in slurry reactors and details are discussed in lecture no. 30. Hydrogenation of oils is carried out in slurry of nickel catalyst particles. Industrial hydrogenation

reactors are usually of the size in the range of 500-200 L. The reactors are operated up to pressure of 200 atm and temperature of 350 ^{0}C. The reactors are equipped with internal agitator, gas inlet, facility for insitu sampling and heater or cooler for temperature control.

Trickled bed reactors

In trickled bed reactor gaseous and liquid reactants flow co-currently downward over a packed bed of solid catalyst particles. The liquid is distributed across the reactor cross section by a distributor plate. The gas enters at the top and distributed along with the liquid. The liquid flows downward by gravity and drag of the gas. For low liquid flow rates and low to moderate gas flow rates, the gas phase is continuous with liquid trickling down forming film over the solid catalyst. The thickness of the liquid film has been estimated to vary between 0.01 and 0.2 mm. This flow regime is known as a trickle flow regime. The fluid approaches plug flow leading to higher conversion than slurry reactors for the same reactor volume. Other advantages include ease of installation, minimal catalyst handling and low catalyst attrition as in packed bed reactor. Disadvantages include maldistribution of flow resulting in channeling or bypassing, possibility of non uniformity in packing, incomplete contacting or wetting and intraparticle diffusion resistance. Catalyst bed depth is limited by pressure drop, catalyst crush strength and maximum adiabatic temperature increase for stable operation. The reactor length to diameter ratio can vary between 1 and 10 depending on the allowable pressure drop. Other parameters important for trickled bed include void fraction of bed, holdup for phases, wetting efficiency (fraction of catalyst wetted by liquid), gas – liquid mass transfer coefficient, liquid–solid mass transfer coefficient, liquid and gas mixing, pressure drop and heat transfer coefficients. The wetting efficiency of the catalyst is important for reaction rate and increases with increasing liquid rate. The trickle bed reactor is most commonly used for hydrogenation and hydrodesulfurization reactions.

Bioreactors

In bioreactor live cells or enzymes are used as catalyst to perform the biochemical reactions. Bioreactor operations are limited by the conditions favorable for the biological systems. Most living cells can tolerate only mild conditions of temperature and pH. Hence in bioreactors stringent control of temperature, pH or any contamination is needed. Bioreactor may have two phases, liquid-solid as in anaerobic process or three phases, gas, liquid and solid as in aerobic process. The solid phase typically contains the cells (bacteria, fungi, algae etc.) that serve as biocatalyst. The density of biocatalytic phase is close to water. The biocatalyst can also be used in immobilized form in which cells are trapped within solid or semi solid structure such as porous particles or gel. Liquid is primarily water with dissolves the feed and products. In aerobic bioreactor the gas phase consists of primarily air and product gas CO_2. Bioreactors are mainly operated in batch or semi batch mode allowing better control of process parameters. Increasing number of bioreactor is operated in continuous mode such as in wastewater treatment, lactic acid production, production of human insulin etc.

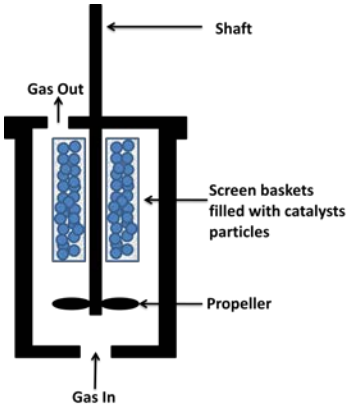

a) Carberry reactor

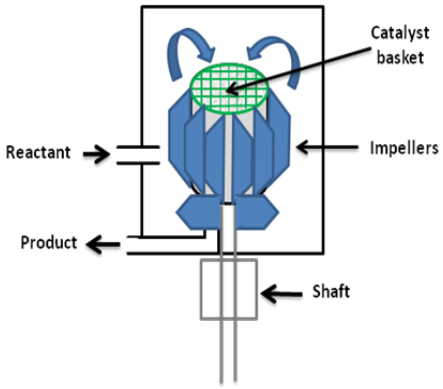

b) Berty reactor

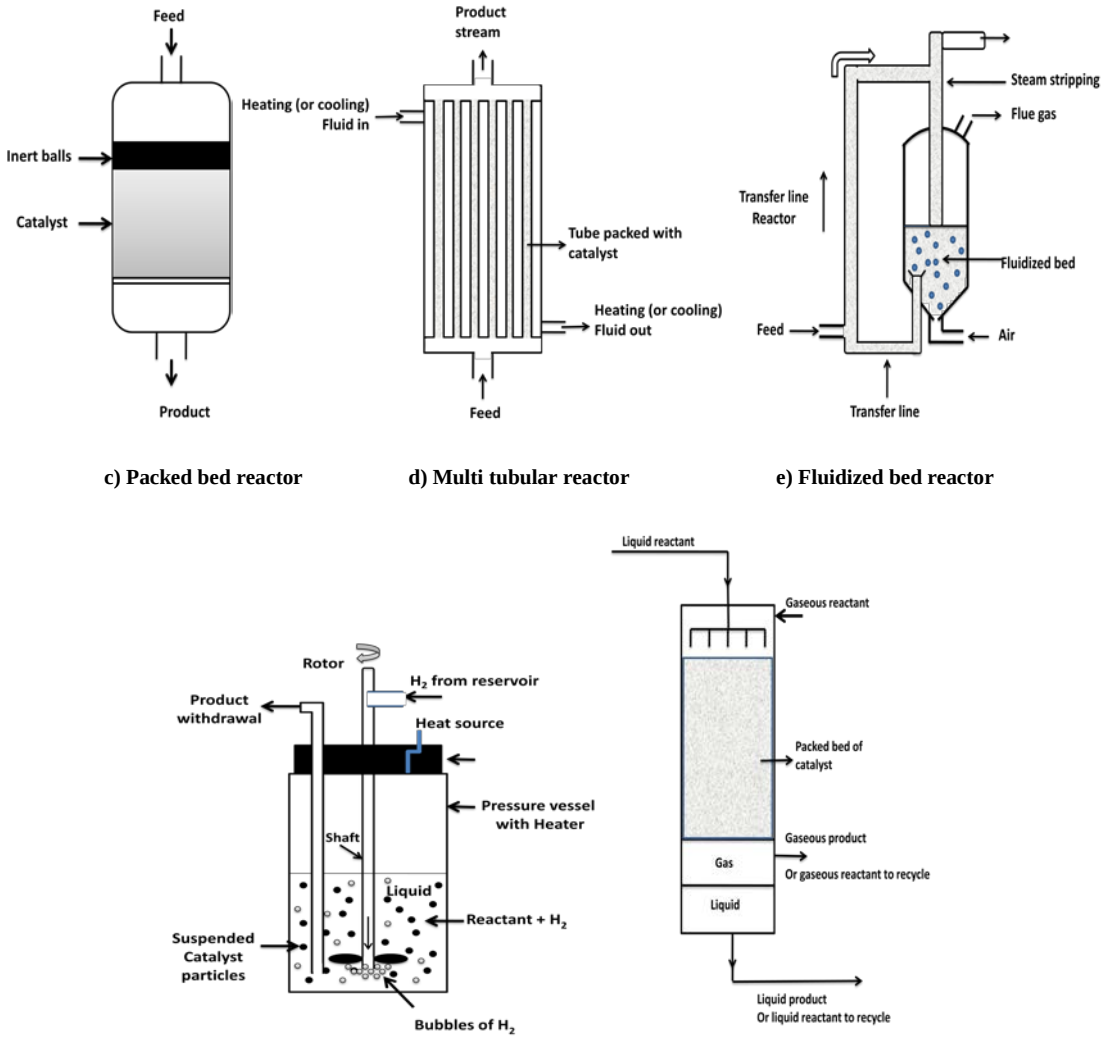

c) Packed bed reactor **d) Multi tubular reactor** **e) Fluidized bed reactor**

g) Agitated slurry reactor **f) Trickled bed reactor**

Fig. 1. Schematic diagram of different type of reactors

Catalyst tests

Activity and selectivity

The performance of catalyst is characterized by its activity for reaction and selectivity for a product. The activity of a catalyst for a reaction at specified conditions is generally expressed in terms of rate of reaction at that condition over the catalyst. The catalyst that shows higher rate of reaction at the given conditions is said to have higher activity. For solid catalyzed reaction, rate can be defined as, r = g mol of reacted /s. g of catalyst. Here mass of solid is used because amount of catalyst is important. The reactor volume

that contains the catalysts is of secondary importance. Activity is also expressed in terms of conversion of a reactant achieved. Higher the conversion at given conditions, higher is the activity of the catalyst for that reaction. The conversion can be defined as follows

$$\text{Conversion } (\%) = \frac{\text{Moles of reactant in inlet stream- Moles of reactant in outlet stream}}{\text{Moles of reactant in inlet stream}} \times 100$$

For supported metal catalysts, defining activity in terms of metal sites is more useful as the metal sites actually act as the active sites for chemical reactions. Hence, activity is often expressed in terms of turnover frequency or TOF. TOF is defined as the number of molecules reacting per active site per second (s^{-1}). Though the TOF value is expected to be constant for a particular metal catalyst for a given reaction at specified conditions, however, in reality significant difference may be observed due to differences in catalyst preparation, metal support interaction, crystallite size, surface structure and morphology etc.

$$\text{TOF} = \frac{\text{Total no. of molecules reacting}}{\text{total no. of metal sites} \times \text{seconds}} \quad s^{-1}$$

The next important parameter determining the performance of catalyst is selectivity for a particular product. The selectivity of a product X can be defined in several ways. One of the definitions is shown below:

$$\text{Selectivity of X } (\%) = \frac{\text{Moles of product X}}{\text{Total moles of all products}} \times 100$$

The performance of catalyst is tested in a suitable experimental setup. Fig. 2 shows a schematic diagram of a simple experimental setup for studying gas phase reaction over solid catalysts. Typically, solid catalysts are tested in a tubular down-flow reactor. A simple manometer or any pressure gauge can be included before the reactor to ensure that the pressure drop is within acceptable limits**.** All the reactants are combined in a mixer and sent to the reactor where it comes in contact with the catalyst bed. The product gases or liquids are usually analyzed using a gas chromatograph equipped with suitable

columns. The columns are selected so that the product compounds are separated efficiently giving distinct peaks that can be easily identified and quantified. Further detector type and temperature as well as carrier gas type and flow rates are also important parameters determining the retention time and peak area in a chromatograph. Catalytic tests are carried out at predetermined range of temperature, pressure, feed composition and total flow rates depending on reactions. The catalysts amount range to be used is also fixed according to the requirement.

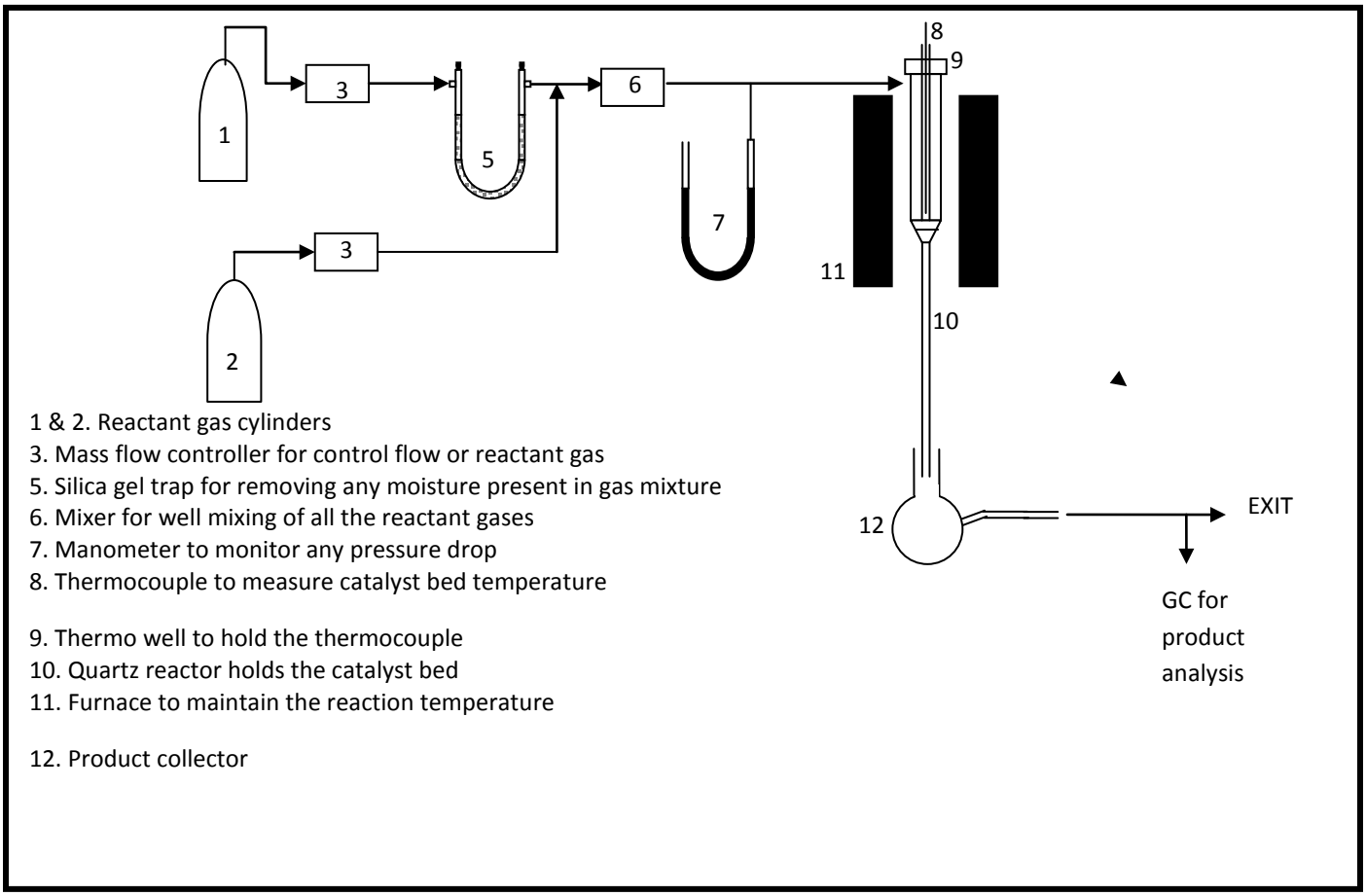

Fig. 2. Schematic diagram of a typical experimental setup

2.3.2.1 Collecting data from laboratory reactors

Kinetic data are collected for the following purposes:

– Determination of activity-selectivity and deactivation data for catalyst selection

– Determination of reaction mechanism and kinetic parameters for understanding the reaction at the fundamental level so the reaction process can be modeled which can be used for design of reactors.

Investigation of the reaction kinetics is done at steady state conditions for most active and selective catalyst. The effect of temperature and partial pressures of reactants on the activity and selectivity is investigated in the desired temperature range. The process of data collection typically involve three major steps :

1. Selection of a reaction and catalyst
2. Selection of reactor type
3. Analysis of data

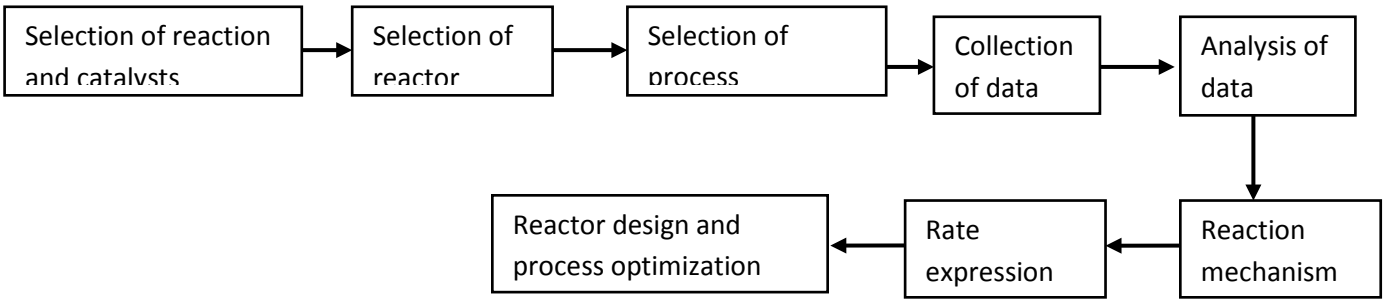

Fig. 2. Steps for obtaining and analyzing kinetic data

To measure the specific catalytic activity or intrinsic reaction kinetics, the data must be collected in absence of any pore diffusion limitations, mass transfer limitations or heat transfer limitations. For analysis of data collected in the presence of mass transfer or heat transfer limitations, suitable criterion should be included during analysis. Deactivation of catalysts should be also avoided during data collection. These will be discussed in detail in later sections. Further data should be collected over a wide range of temperature and reactant concentrations to provide adequate reaction model that can be applicable at wide temperature and concentration range.

Mode of reactor operations

Reactors can be operated in two ways:

1. Integral mode
2. Differential mode

Integral reactors

When a reactor is operated at high conversion, the reactor is said to be an integral reactor. When reaction takes place in a packed bed reactor at high conversion there is possibility of wide variation of conversion and reaction rate within the reactor even under isothermal conditions. Hence, the integral form of design equation is to be used. This is the basis for design for an ideal packed bed reactor.

$$\frac{W}{F_{A_o}} = \int_0^{x_{Af}} \frac{dX_A}{-r_A} \tag{1}$$

Differential reactors

When the reaction in a tubular reactor is carried out at very low conversions, the changes in conversion and reaction rate across the reactor are small enough to be neglected and the rate can be considered constant across the reactor. Then the rate in above equation [1] can be considered constant and taken out of the integral and the equation can be simplified to

$$\frac{W}{F_{Ao}} = \frac{X_A}{-r_A}$$

This above equation is same as for mixed flow reactor or CSTR. In this case analysis of data is simplified.

Book Reference

- J. M. Smith, Chemical Engineering Kinetics, McGrawHill Book Company, 1981
- J.J. Carberry , Chemical and catalytic reaction Engineering, Dover Publications,2001
- D.W.Green, R.H. Perry, Perry´s chemical engineer´s handbook, 8th Edition, McGrawHill Company,2007
- H. S. Fogler, Elements of Chemical reaction engineering, Prentice Hall of India, 1999
- R. J. Farrauto, C. H. Bartholomew, Fundamentals of Industrial catalytic Processes, Blackie Academic & Professional, 1997

Lecture 19

Reaction mechanism and kinetic study

Reaction mechanism and rate equations

For irreversible gas phase reaction $A(g) \rightarrow B(g)$, global rate for catalyst particles is expressed in terms of temperature and concentration of A in bulk gas stream which can be measured or specified directly. Global rates of catalytic reactions are usually expressed per unit mass of catalyst.

Power law model

For homogeneous reaction, power law form of rate equation is used where rate is function of concentration and rate is determined by fitting data to the equation. The exponents on the concentration is the apparent order of the reaction and 'k' is the kinetic constant or reaction rate constant which is independent of concentration and depends on temperature.

For reactions A+B $\rightarrow$ C+D

$$\gamma_a = -\frac{dC_a}{dt} = kC_A^{\alpha}C_B^{\beta}$$

Here α is the order with respect to A and β is the order with respect to B

This power law approach can also be used for solid catalytic reactions. This analysis is simple. The major disadvantage of this method is that it ignores all the factors associated with adsorption and reaction mechanism on surface of solid catalyst. Hence, power law kinetics fails to adequately describe any solid catalytic process and the rate equation derived from mechanistic model is more preferred. Power law kinetics is preferred as a mode of obtaining preliminary value of rate parameters for solid catalyzed reactions.

Langmuir-Hinshelwood –Hougen-Watson(LHHW) model

The rate equation derived from mechanistic model that simulates the actual surface phenomenon during the process is preferred for reactions involving solid catalysts. The Langmuir-Hinshelwood–Hougen-Watson(LHHW) approach is one of the most commonly used way of deriving rate expressions for fluid solid catalytic reactions. The advantages of this method are that :

(1) Rate derived by this method takes into account the adsorption-desorption process occurring over the surface along with the surface reaction.
(2) Rate equation derived can be extrapolated more accurately to concentrations lying beyond the experimentally measured values.

During this method of derivation of rate expression, all the physical transport steps like mass transfer from bulk phase to catalyst surface or diffusion of reactants from pore mouth to interior pore (intraparticle diffusion) are excluded. Thus, it is assumed that the external and internal mass transport processes are very rapid relative to the chemical rate process occurring on or within the catalyst particle. The chemical rate depends on :

(1) chemisorption steps
(2) surface reaction steps
(3) desorption steps

This simple kinetic model assumes isothermal condition about and within catalyst that is temperature gradient is zero.

In LHHW model development, the rate equation is first derived in terms of surface concentration of adsorbed species and vacant sites. Then, these surface concentrations are related to the fluid or bulk concentration that is directly measurable.

For the reaction $A + B \rightleftharpoons C + D$

Let r_a = rates of adsorption (g mol/s.gm of catalyst)

r_s = rates of surface reaction (g mol/s.gm of catalyst)

r_d =rates of desorption (g mol/s.gm of catalyst)

C_{AS} = concentration of adsorbed A on surface (g mol/gm of catalyst)

C_{BS} = concentration of adsorbed B on surface (gmol/gm of catalyst)

C_{cs} = concentration of adsorbed C on surface (g mol/gm of catalyst)

C_{DS} = concentration of adsorbed D on surface (g moles/gm of catalyst)

C_O = total concentration of active sites on surface (g mol/gm of catalyst)

C_V = concentration of vacant sites on surface (g mol/gm of catalyst)

C_A = concentration of A in bulk gas phase (g mol/cm^3)

Similarly C_B, C_C, C_D are the concentrations of B,C,D in the bulk gas phase, respectively.

Let the reaction follows the mechanism given below ;

(1) $A + S \rightleftharpoons A.S$ --- Adsorption of reactant A on surface vacant site S

(2) $B + S \rightleftharpoons B.S$ --- Adsorption reactant B on surface vacant site S

(3) $A.S + B.S \rightleftharpoons C.S + D.S$ --- Surface reaction between adsorbed A and B

(4) $C.S \rightleftharpoons C + S$ --- Desorption of product C from surface creating a vacant site

(5) $D.S \rightleftharpoons D + S$ ---Desorption of product D from surface creating a vacant site

Among the various steps described, the slowest step controls the overall rate of reaction and the other remaining steps are assumed to be at near equilibrium conditions. This approach greatly simplifies the overall rate expression, reducing the number of rate constants and equilibrium constants to be determined from experimental data. Further

each step in this method is assumed to be elementary and the number of sites is conserved in each step.

Therefore, the controlling step can be either of the following:

(1) Surface reaction
(2) Adsorption
(3) Desorption

Now total concentration of active sites on surface, C_O , will be the summation concentrations of all sites on which either reactants or products are adsorbed and the concentration of vacant sites.

$$\therefore C_O = C_V + C_{AS} + C_{BS} + C_{CS} + C_{DS}$$

Where, C_V is the concentration of vacant sites.

Case 1 : Rate is surface reaction controlling

The surface reaction is the slowest step and is the rate controlling. According to the mechanism, surface reaction occurs between adsorbed A and adsorbed B producing adsorbed C & adsorbed D.

$$AS + BS \rightleftharpoons CS + DS$$

The rate of surface reaction is given as

$r_S = k_S C_{AS} C_{BS} - k_S' C_{CS} C_{DS}$ k_s = rate constant for forward surface reaction

k_S' = rate constant for reverse surface reaction

$$= k_S \left[C_{AS} C_{BS} - \frac{k_S'}{k_S} C_{CS} C_{DS} \right]$$

$$= k_S \left[C_{AS} C_{BS} - \frac{1}{K_S} C_{CS} C_{DS} \right] \qquad \because K_S = \frac{k_S}{k_S'} \qquad (1)$$

Now, since all the other steps are considered to be in equilibrium, therefore concentration of adsorbed species can be obtained as follows.

For adsorption steps and desorption steps :

From step (1) $K_A = \frac{C_{AS}}{C_{A.}C_V}$ From step (4) $K_C = \frac{C_{CS}}{C_{C.}C_V}$

From step (2) $K_B = \frac{C_{BS}}{C_{B.}C_V}$ From step (5) $K_D = \frac{C_{DS}}{C_{D.}C_V}$

K_A, K_B, K_C, K_D are adsorption equilibrium constants.

Then, the adsorbed phase concentrations can be written as

$$C_{AS} = K_A C_A C_V \; C_{CS} = K_C C_C C_V$$

$$C_{BS} = K_B C_B C_V \; C_{DS} = K_D C_D C_V$$

Substituting all these value in equation (1)

$$r_S = k_S \left[C_{AS} C_{BS} - \frac{1}{K_S} C_{CS} C_{DS} \right] = k_S \left[K_A C_A C_V . K_B C_B C_V - \frac{K_C}{K_S} C_C C_V . K_D C_D C_V \right]$$

or, $$r_s = k_S \left[K_A K_B C_A C_B C_V^2 - \frac{K_C K_D}{K_S} C_C C_D C_V^2 \right]$$

or $$r_S = k_S K_A K_B \left[C_A C_B - \frac{K_C K_D}{K_S K_A K_B} C_C C_D \right] C_V^2 \qquad (2)$$

Now , $C_O = C_{AS} + C_{BS} + C_{CS} + C_{DS} + C_V$

$$C_O = K_A C_A C_V + K_B C_B C_V + K_C C_C C_V + K_D C_D C_V + C_V$$

$$= C_V \left[1 + K_A C_A + K_B C_B + K_C C_C + K_D C_D \right]$$

$$C_V = \frac{C_O}{1 + K_A C_A + K_B C_B + K_C C_C + K_D C_D} \quad (3)$$

For the reaction A+B $\rightleftharpoons$ C+D , at equilibrium , the overall equilibrium constant is $K = \frac{C_C C_D}{C_A C_B}$.

All concentrations correspond to the equilibrium conditions in gas phase.

$$K = \frac{\left(C_{CS} / K_C C_V\right)\left(C_{DS} / K_D C_V\right)}{\left(C_{AS} / K_A C_V\right)\left(C_{BS} / K_B C_V\right)} = \frac{C_{CS} C_{DS}}{C_{AS} C_{BS}} \cdot \frac{K_A K_B C_V^2}{K_C K_D C_V^2}$$

Or , $K = \frac{K_A K_B}{K_C K_D} . K_S$ $\quad\quad$ $\because K_S = \frac{C_{CS} C_{DS}}{C_{AS} C_{BS}}$ $\quad (4)$

Substituting (3) &(4) in equation (2),

$$r_S = k_S K_A K_B \left[C_A C_B - \frac{1}{K} C_C C_D \right] \frac{C_O^2}{\left(1 + K_A C_A + K_B C_B + K_C C_C + K_D C_D\right)^2}$$

$$r_S = k_S K_A K_B C_O^2 \frac{C_A C_B - \frac{1}{K} C_C C_D}{\left(1 + K_A C_A + K_B C_B + K_C C_C + K_D C_D\right)^2} \quad (5)$$

The above rate expression can also be derived in terms of bulk partial pressure.

Case 2: Rate is adsorption control

(a) Adsorption of A controlling

Let adsorption of A be the slowest step so that adsorption of B, surface reaction and desorption of C are at equilibrium.

Adsorption of A is given as

$A + S \rightleftharpoons AS$

Rate of adsorption $r_a = k_a C_A C_V - k_d C_{AS}$

$$r_a = k_a\left[C_A C_V - \frac{k_d}{k_a} C_{AS}\right]$$

Or, $r_a = k_a\left[C_A C_V - \frac{1}{K_A} C_{AS}\right]$ $\quad K_A = \frac{k_a}{k_d}$ (adsorption equilibrium constant for A)

$$r_a = k_a C_V\left[C_A - \frac{1}{K_A}\frac{C_{AS}}{C_V}\right] \qquad (6)$$

Now as other steps are in equilibrium :

$$K_S = \frac{C_{CS} C_{DS}}{C_{AS} C_{BS}}$$

$$K_B = \frac{C_{BS}}{C_B C_V} \; K_C = \frac{C_{CS}}{C_C C_V} \; K_D = \frac{C_{DS}}{C_D C_V}$$

$$C_{BS} = K_B C_B C_V \qquad C_{CS} = K_C C_C C_V \; C_{DS} = K_D C_D C_V$$

Then ,

$$C_{AS} = \frac{C_{CS} C_{DS}}{K_S C_{BS}} = \frac{K_C C_C C_V . K_D C_D C_V}{K_S K_B C_B C_V} = \frac{K_C K_D}{K_S K_B}\frac{C_C C_D C_V}{C_B}$$

Substituting value in equation (6)

$$r_a = k_a C_V\left[C_A - \frac{1}{K_A C_V}\frac{K_C K_D}{K_S K_B}\frac{C_C C_D C_V}{C_B}\right]$$

$$r_a = k_a C_V\left[C_A - \frac{K_C K_D}{K_S K_A K_B}\frac{C_C C_D}{C_B}\right]$$

$$r_a = k_a C_V\left[C_A - \frac{1}{K}\frac{C_C C_D}{C_B}\right] \qquad (7)$$

$K = \frac{K_S K_A K_B}{K_C K_D}$ = Overall equilibrium constant.

Now $C_0 = C_V + C_{AS} + C_{BS} + C_{CS} + C_{DS}$

$$= C_V + \frac{K_C K_D}{K_S K_B} \cdot \frac{C_C C_D C_V}{C_B} + K_B C_B C_V + K_C C_C C_V + K_D C_D C_V$$

$$= C_V \left[1 + \frac{K_C K_D}{K_S K_A} \frac{K_A}{K_B} \left(\frac{C_C C_D}{C_B} \right) + K_B C_B + K_C C_C + K_D C_D \right]$$

$$= C_V \left[1 + \frac{K_A}{K} \frac{C_C C_D}{C_B} + K_B C_B + K_C C_C + K_D C_D \right]$$

$$C_V = \frac{C_O}{1 + \frac{K_A}{K} \frac{C_C C_D}{C_B} + K_B C_B + K_C C_C + K_D C_D} \quad \because K = \frac{K_S K_A K_B}{K_C K_D}$$

Substituting value of C_V in equation (7)

$$r_a = k_a C_0 \frac{C_A - \left[\frac{C_C C_D}{K C_B} \right]}{1 + \frac{K_A C_C C_D}{K C_B} + K_B C_B + K_C C_C + K_D C_D} \tag{8}$$

For a given catalyst C_0 is constant.

Similarly expression when desorption of product is the rate controlling step can be derived. For desorption of C controlling the whole reaction, the rate expression can be derived as

$$r_d = k_d C_0 K \frac{C_A C_B - \left[\frac{C_C C_D}{K} \right]}{1 + K_A C_A + K_B C_B + K_C K C_A C_B + K_D C_D}$$

Eley Rideal model

Apart from power law and Langmuir-Hinshelwood models, other kinetic models are also used to fit the data. EleyRideal model depicts the reaction mechanism in which one reactant species (say A) is adsorbed while the second reactant species (say B) is not adsorbed on the catalyst surface. The reaction then occurs when the passing gas molecules of B in gas phase directly reacts with the adsorbed species A. The schematic representation is shown in Fig. 1.

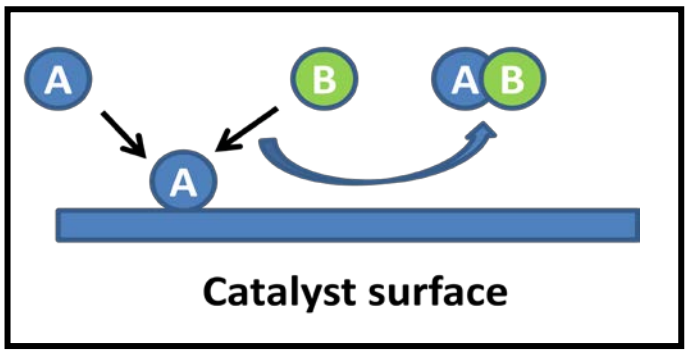

Fig. 1. Eley Rideal mechanism for reaction of adsorbed A with gas phase B producing product AB

(1) $A + S \rightleftharpoons AS$

(2) $AS + B\ (g) \rightarrow P$

Assuming that step 2, the reaction between adsorbed A and gas phase B is irreversible and the rate determining step, then the rate of reaction can be written as

$$r = k\ C_{As}\ C_B \qquad (9)$$

The concentration of adsorbed A can be given as $C_{AS} = K_A C_A C_V$

$$\text{Now}, C_O = C_{AS} + C_V = K_A C_A C_V + C_V = C_V(1 + K_A C_A)$$

$$C_V = \frac{C_O}{1 + K_A C_A}$$

$$C_{AS} = \frac{K_A C_A C_O}{1 + K_A C_A}$$

Substituting value of C_{AS} in equation (9)

$$r = k\ C_{AS}\ C_B = \frac{kC_O K_A C_A C_B}{1 + K_A C_A}$$

If the products are chemisorbed then the reaction may become reversible as shown below.

$$AS + B(g) \underset{k_b}{\overset{k}{\rightleftharpoons}} PS$$

$$PS \rightarrow P + S$$

Then the rate expression can be written as

$$r = k\ C_{As}\ C_B - k_b C_{Ps}$$

The concentration of adsorbed product is $C_{PS} = K_P C_P C_V$

$$C_O = C_{AS} + C_{Ps} + C_V = K_A C_A C_V + K_p C_P C_V + C_V = C_V(1 + K_A C_A + K_P C_P)$$

$$C_V = \frac{C_O}{1 + K_A C_A + K_P C_P}$$

$$C_{AS} = K_A C_A C_V = \frac{K_A C_A C_O}{1 + K_A C_A + K_P C_P}$$

$$C_{PS} = K_P C_P C_V = \frac{K_P C_P C_O}{1 + K_A C_A + K_P C_P}$$

Substituting C_{AS} and C_{PS} in rate expression,

$$r = k\ C_{As}\ C_B - k_b C_{Ps} = k\left(C_{AS} C_B - \frac{1}{K} C_{PS}\right) \qquad \because K = \frac{k}{k_b}$$

$$r = k\left(\frac{K_A C_A C_O}{(1 + K_A C_A + K_P C_P)} C_B - \frac{1}{K} \frac{K_P C_P C_O}{(1 + K_A C_A + K_P C_P)}\right)$$

$$r = kC_O \frac{\left(K_A C_A C_B - \frac{K_P}{K} C_P \right)}{1 + K_A C_A + K_P C_P}$$

Estimation of model parameters

The various parameters in the kinetic models such as rate constants, reaction orders, and equilibrium constants are derived by fitting the experimental data. The optimal values of the parameters in the rate equation of a heterogeneous reaction are determined traditionally by using gradient or direct search methods. For success of this method, a very good initial estimate of the parameters is required. This proves to be difficult in most cases. If the initial estimates are far from the global optima, then it is likely that the gradient or direct search method will not converge at all or will converge to local optima. Recently genetic algorithm (GA) is increasingly applied in estimation of kinetic parameters. The major advantage of this method is that it is not dependent on the initial estimate of the parameters. GA performs a multi-directional search.

Book Reference

- J. M. Smith, Chemical Engineering Kinetics, McGrawHill Book Company, 1981
- J.J. Carberry, Chemical and catalytic reaction Engineering, Dover Publications, 2001
- H. S. Fogler, Elements of Chemical reaction engineering, Prentice Hall of India,1999
- R. J. Farrauto and C. H. Bartholomew, Fundamentals of Industrial catalytic Processes, Blackie Academic & Professional, 1997

Lecture 20

Analyzing data from laboratory reactors

The objectives of analyzing data include

- Determining catalyst activity, selectivity and stability
- Determining the effect of important process variables such as temperature, pressure, reactant concentrations
- Finding a rate equation

Elimination of mass transfer and pore diffusion limitations

In a solid catalyzed reaction, the presence of mass transfer and pore diffusional resistances can significantly affect the rate of the reaction. The details will be discussed in lecture no. 22 to 24. To ensure that no internal or external mass transfer resistances are present under the operating conditions, preliminary experiments are carried out.

Elimination of mass transfer limitations

For checking if external mass transfer is affecting the rate of reaction, conversion data is obtained by increasing the flow rate of the feed but keeping the W/F_{AO} constant. Fig. 5 shows the plot of conversion as a function of linear velocity of fluid at constant W/F_{AO} at a given temperature, usually the highest temperature is used during reaction.

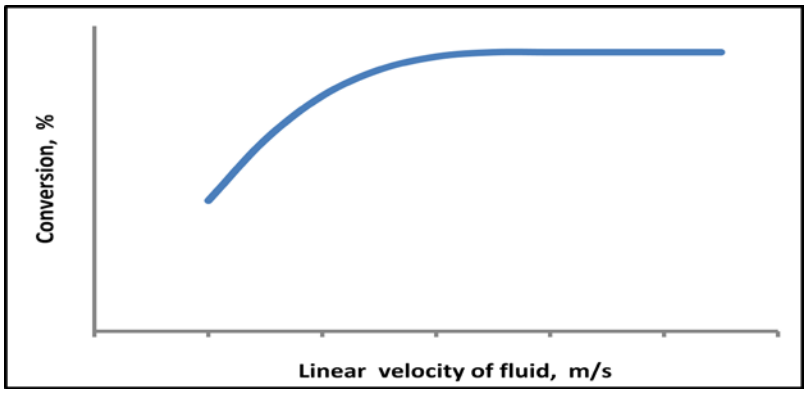

Fig. 5. Typical plot of conversion as a function of linear velocity of fluid at constant W/F_{AO} and temperature

It can be observed that at low fluid velocity, conversion increases with increasing fluid velocity and subsequently becomes constant at higher flow rates, implying that external mass transfer does not affect the rate of reaction at this fluid velocity. Due to external mass transfer limitation the concentration of reactant near catalyst surface is lower than the bulk phase concentration. The effect is maximum at lower fluid velocity when the resistance to transport is considerable. With increase in fluid velocity, the turbulence effectively enhances the mixing in fluid phase and the concentration of reactant near the catalyst surface approaches the bulk phase concentration. Consequently reaction rate increases increasing the conversion. At high velocity due to high turbulence the mass transfer limitation is totally removed and the reactant concentration near the catalyst surface becomes equal to that of bulk phase concentration and the conversion reaches the maximum limiting values. Thereafter any change in fluid velocity does not affect the conversion as shown in the figure. Kinetic study should always be carried out at conditions where the effect of external mass transfer on conversion is negligible.

Elimination of pore diffusion limitations

Weisz criterion $R_s^2 \frac{r_p \rho_p}{C_s D_e} \leq 1$ can be used to determine the significance of intraparticle diffusion. Here R_s=pellet radius; r_p=observed rate; ρ_p = pellet density, C_s = surface concentration; D_e effective diffusivity. Reactions should be carried out at the conditions when Weisz criterion is satisfied so that the intraparticle diffusion could be neglected for these operating conditions. This is discussed in details in lecture no. 24. The effectiveness of porous catalyst can also be determined experimentally by measuring conversion with successively smaller catalyst pellets until no further change in conversion occurs. The pore diffusion resistance decreases the concentration within the pellets thereby decreasing the conversion. The pore diffusion resistance is considered to be negligible for the catalyst size range for which the conversion does not change with size. For study of intrinsic reaction kinetics, catalyst pellet size is chosen where the intraparticle diffusion could be neglected.

Elimination of homogeneous phase reaction and deactivation

When reaction is carried out over a fixed bed of solid catalyst there may be possibility of non-catalytic homogeneous reactions occurring in gas phase. If any non-catalytic homogeneous reactions occur along with heterogeneous catalytic reactions, then data collected will give erroneous kinetics for the heterogeneous reaction. Hence, reaction should be carried out in an empty reactor without using any catalyst to determine the contribution of homogeneous phase reactions, if any, at the desired operating conditions. Kinetic study should be carried out at operating conditions for which contribution of homogeneous phase reactions is negligible.

In addition, deactivation studies should be carried out by operating the reactor for long run lengths. If any significant deactivation occurs, than it should be taken into account for further analysis.

Integral analysis of rate data

In this method a series of run are made in a packed bed at a fixed initial concentrations C_{A0} and a fixed temperature while varying the catalyst mass W and/or initial molar flow rate F_{A0} to generate a range of W/F_{A0} values at different conversions $X_{A.}$ A rate equation is then selected for testing using the design equation for packed bed reactor.

$$\frac{W}{F_{A_o}} = \int_0^{x_{Af}} \frac{dX_A}{-r_A} \qquad (1)$$

First simpler rate equations such as zero order, first order, second order irreversible are tried. Mechanistic reaction models can also be tested. The W/F_{A0} and the right hand integral in equation (1) are evaluated numerically and plotted to test for linearity (Fig 1). Linearity of the plot is used as criterion for judging if the selected rate equation is a useful model for the data i.e consistent with the data. If not then another rate equation may be tried.

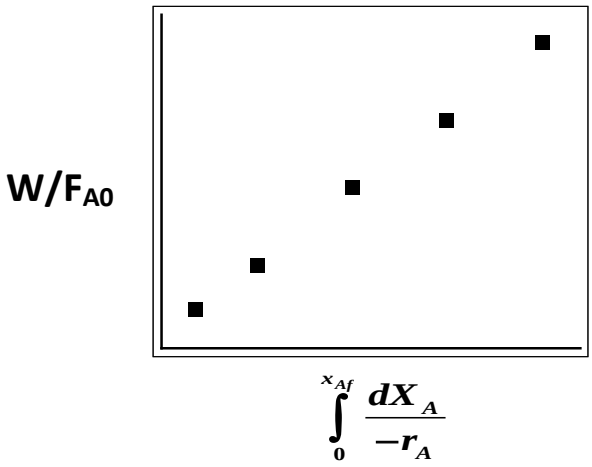

Fig. 1. Typical plot of W/F_{A0} vs integral value for linearity test in integral analysis of rate data

Differential analysis of rate data

In this method, the data are collected as in the previous case. A plot of conversions X_A versus W/F_{Ao} is made for each set of runs at a fixed temperature (Fig 2) . A best fit of data is made.Tangent to the fitted curve are drawn at regular interval along the curve corresponding to the best fit. The slopes of this tangent are evaluated which correspond to the reaction rate $-r_A = \frac{dX_A}{d(W/F_{Ao})}$

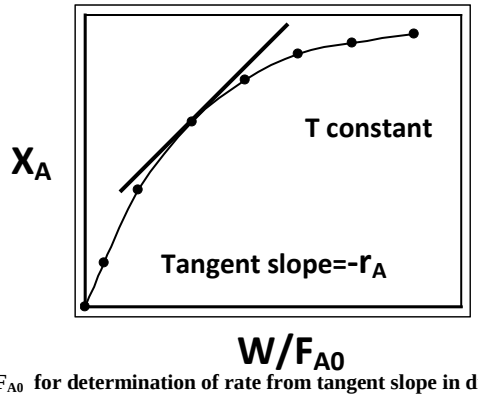

Fig. 2. Typical plot of X_A vs W/F_{A0} for determination of rate from tangent slope in differential analysis of data

Tangents can be evaluated more accurately by differentiating the equation for best fit of data and evaluating the derivative at various intervals over the data set. Values of $-r_A$ versus C_A are plotted to determine the reaction orders. For example for an irreversible reactions in which data are fitted by a simple power rate law $-r_A = kC_A^n$, a plot of $\ln(-r_A)$ vs $\ln C_A$ is linear with a slope of order n. The rate constant value can be determined from

the intercept. If rate vs temperature data available then it is possible to determine the apparent activation energy from Arrhenius equation k = A exp(-E/RT). The slope of the plot of ln k vs 1/T gives the activation energy E of the reaction.

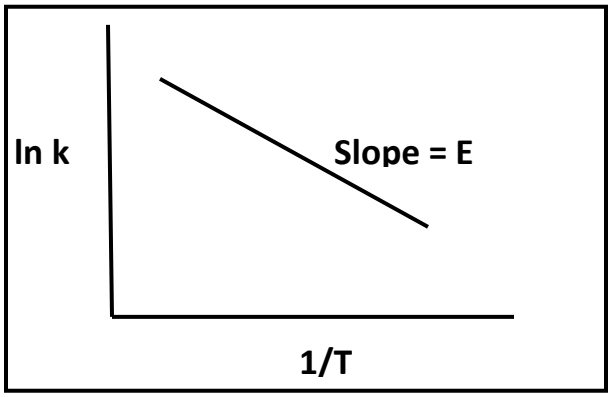

Fig. 3. A typical Arrhenius plot for determination of activation energies

Linear and nonlinear regression of rate data

For a Langmuir –Hinshelwood type rate equation $-\mathbf{r_A} = \dfrac{\mathbf{k\ p_A\ p_B}}{\mathbf{1+K_A p_A + K_B p_B}}$, the value of rate law parameters k, K_A, K_B cannot be analyzed as simply as in power law kinetics. The rate law parameters can be determined by linear least square or nonlinear least square method. In linear least square method, the above LH rate equation can be linearized by dividing throughout by p_A and p_B and inverting it as shown below:

$$-\frac{\mathbf{p_A p_B}}{\mathbf{r_A}} = \frac{\mathbf{1}}{\mathbf{k}} + \frac{\mathbf{K_A}}{\mathbf{k}}\mathbf{p_A} + \frac{\mathbf{K_B}}{\mathbf{k}}\mathbf{p_B}$$

The parameters can be estimated by multiple regression technique using the following equation for N experimental runs. For the i^{th} run :

$$\mathbf{Y_i = a_o + a_1 X_{1i} + a_2 X_{2i}}$$

The best values of the parameters a_0, a_1 and a_2 are found by solving following three equations

$$\sum_{i=1}^{N} Y_i = Na_o + a_1\sum_{i=1}^{N} X_{1i} + a_2\sum_{i=1}^{N} X_{2i}$$

$$\sum_{i=1}^{N} X_{1i}Y_i = a_o\sum_{i=1}^{N} X_{1i} + a_1\sum_{i=1}^{N} X_{1i}^2 + a_2\sum_{i=1}^{N} X_{1i}X_{2i}$$

$$\sum_{i=1}^{N} X_{2i}Y_i = a_o\sum_{i=1}^{N} X_{2i} + a_1\sum_{i=1}^{N} X_{1i}X_{2i} + a_2\sum_{i=1}^{N} X_{2i}^2$$

The above LH rate equation can also be solved by non-linear regression analysis. Usually linearized least square analysis is used to obtain the initial estimates of the rate parameters and used in non-linear regression. In non linear analysis the rate law parameters are first estimated to calculate the rate of reaction 'r_c'. Then the values of rate law parameters that will minimize the sum of the squares of difference of the measured reaction rate r_m and the calculated reaction rate r_c , that is the sum of $(r_m-r_c)^2$ for all data points, are searched. If there are N experiments with K number of parameter values to be determined then the function to be minimized is given by $\sigma^2 = \sum_{i=1}^{N} \frac{(r_{im} - r_{ic})^2}{N-K}$

Here r_{im} and r_{ic} are the measured and calculated reaction rate for 'i'th run respectively. The parameter values giving the minimum of the sum of squares, σ^2, can be searched by various optimization techniques using software packages.

Initial rate analysis

Initial rate analysis for a reaction may be done to understand the mechanism of a reaction. Initial rate is defined as the rate at zero conversion. It is obtained by extrapolation of the rate vs conversion data to zero conversion. For higher accuracy, the conversion data are collected at very low conversion region. In this method, the dependence of initial rate data on partial pressure or total pressure of the reactant is studied.

Consider the reaction $A + B \rightleftharpoons C + D$

The rate expression derived from Langmuir Hinshelwood model when surface reaction is controlling is

$$r_S = k_S K_A K_B C_O^2 \frac{C_A C_B - \frac{1}{K} C_C C_D}{\left(1 + K_A C_A + K_B C_B + K_C C_C + K_D C_D\right)^2} \qquad (2)$$

Now at zero conversion all the product concentration will tend to zero, hence putting C_C =0 & C_D =0, the rate expression [2] simplifies to

$$r_i = k_S K_A K_B C_O^2 \frac{C_A C_B}{\left(1 + K_A C_A + K_B C_B\right)^2} \qquad (3)$$

where $\mathbf{r_i}$ is the initial rate. Now, if a equimolal initial concentration of C_A and C_B is used then C_A=C_B . Then assuming ideal gas mixture, $C_A = \frac{p_A}{RT}$, where p_A is the partial pressure of A.

Similarly $C_B = \frac{p_B}{RT}$ where p_B is the partial pressure of B .

Now since it is an equimolal mixture, then at initial condition. $p_A = p_B = \frac{p_t}{2}$ where p_t is the total pressure.

Or $C_A = C_B = \frac{p_t}{2RT}$

Then substituting C_A and C_B in equation [3] becomes

$$r_i = k_S K_A K_B C_O^2 \frac{\left(\frac{p_t}{2RT}\right)^2}{\left(1 + K_A \frac{p_t}{2RT} + K_B \frac{p_t}{2RT}\right)^2}$$

Or $$r_i = \frac{p_t^2\left(\frac{k_S K_A K_B C_O^2}{4R^2T^2}\right)}{\left[1+\left(\frac{K_A+K_B}{2RT}\right)p_t\right]^2}$$

Or $$r_i = \frac{Ap_t^2}{\left[1+Bp_t\right]^2}$$

Where $A = \frac{k_S K_A K_B C_O^2}{4R^2T^2}$ and $B = \frac{K_A + K_B}{2RT}$

On plotting initial rate $\mathbf{r_i}$ as a function of total pressure $\mathbf{p_t}$, a typical curve as shown in Fig 4A is obtained. Hence if kinetic data for a reaction give similar plot then it can be deduced that the reaction is surface reaction controlled.

When adsorption of A is controlling the dependence of initial rate on total pressure can be derived in similar way as $$r_i = \frac{Ap_t}{1+Bp_t}$$

Where $A = \frac{k_a C_O}{2RT}$ and $B = \frac{K_B}{2RT}$

For this mechanism a typical plot of initial rate r_i as a function of total pressure p_t is shown in Fig 4B. When reaction data satisfy this plot then the reaction is said to be adsorption A controlling. In similar way other models can be tested for fitting.

However, it should be noted that though the initial rate analysis is simple and can reduce the number of rate expressions to be tested against the experimental but cannot substitute a differential or integral analysis. It should be used as only as preliminary kinetic analysis method.

Fig. 4.Typical plot for initial rate vs total pressure for reactions $A + B \rightleftharpoons C + D$ when equimolal mixture of A and B is used.A) surface reaction controlling B) adsorption of A controlling

Book Reference

- J. M. Smith, Chemical Engineering Kinetics, McGrawHill Book Company, 1981
- H. S. Fogler, Elements of Chemical reaction engineering, Prentice Hall of India., 1999
- R. J. Farrauto& C. H. Bartholomew, Fundamentals of Industrial catalytic Processes, Blackie Academic & Professional, 1997
- O. Levenspiel , Chemical reaction engineering, John Wiley & sons. 1995
- J.J. Carberry ,Chemical and catalytic reaction Engineering, Dover Publications, 2001.

Lecture 21

Solved example

1. A catalytic reaction, $A \rightarrow 4B$ is studied in a packed bed reactor using various amount of catalysts. The out let concentration and corresponding conversion is given in following Table 1. Given $F_{A0} = 2$ mol / h and $C_{A0} = 0.1$ mol / litre

   The rate equations for this reaction can be calculated using
   i. Integral method of analysis
   ii. Differential method of analysis

Table 1:

Runs	1	2	3	4	5
Catalysts used, kg	0.02	0.04	0.08	0.12	0.16
$C_{A,out}$, mol/litre	0.075	0.061	0.045	0.035	0.028
X_A	0.07	0.15	0.25	0.33	0.36

(i) For integral analysis

The design equations for packed bed reactor is given as

$$\frac{W}{F_{A_o}} = \int_0^{X_{Af}} \frac{dX_A}{-r_A}$$

Assuming a first order kinetics $-r_A = kC_A$ and substituting

Then $\frac{W}{F_{A_o}} = \int_0^{X_{Af}} \frac{dX_A}{kC_A}$

Now $C_A = \frac{C_{AO}(1-X_A)}{1+\varepsilon_A X_A}$ Where $\varepsilon_A = \frac{4-1}{1} = 3$

ε_A is the fractional change in volume of the system between no conversion and complete conversion of reactant A.

Or $$\frac{W}{F_{A_o}} = \int_0^{x_{Af}} \frac{dX_A}{kC_A} = \frac{1}{kC_{AO}} \int_0^{x_{Af}} \frac{1+\varepsilon_A X_A}{(1-X_A)} dX_A$$

For first order irreversible reaction for plug flow, integrated from of RHS for any constant of $\boldsymbol{\varepsilon_A}$ is as follows.

Or $$\frac{W}{F_{AO}} kC_{AO} = (1+\varepsilon_A) \ln \frac{1}{(1-X_A)} - \varepsilon_A X_A \qquad (1)$$

Substituting values of $\boldsymbol{C_{AO}}$, $\boldsymbol{F_{AO}}$, $\boldsymbol{\varepsilon_A}$ in equation (1)

$$\left(\frac{W}{20}\right) k = 4 \ln \frac{1}{(1-X_A)} - 3X_A$$

Hence plotting $\left[\left(\frac{W}{20}\right) k\right]$ vs $\left[4 \ln \frac{1}{(1-X_A)} - 3X_A\right]$ a straight line is obtained.

It suggests that assumption of first order kinetics is correct. The rate constant can be obtained from slope of the plot which is 95.8 litres/hr.kg catalyst

The rate equation can be written as $-r_A = kC_A$ =[95.8 litres/hr.kg catalysts] C_A

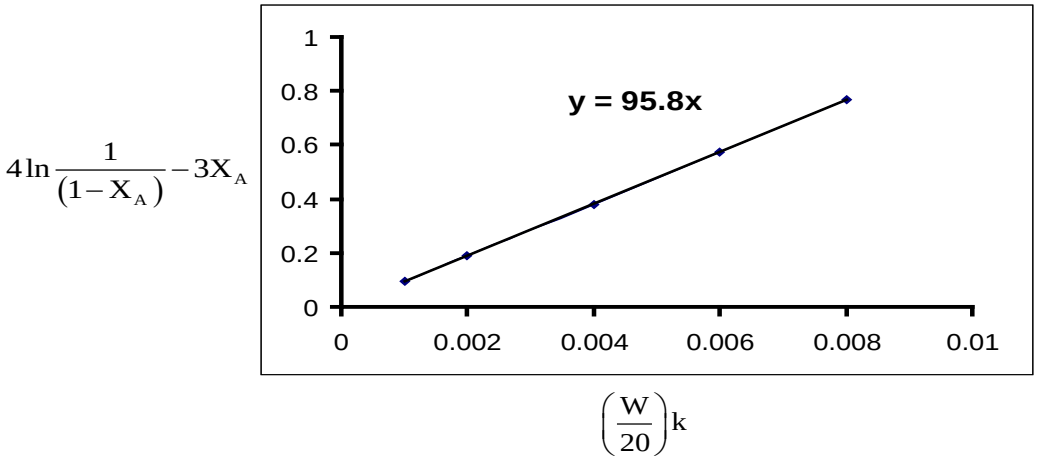

Fig. 6. Plot of $\left(\frac{W}{20}\right) k$ vs $\left[4 \ln \frac{1}{(1-X_A)} - 3X_A\right]$ in integral analysis of data

(ii) For differential analysis

$$-r_A = \frac{dX_A}{d(W/F_{Ao})}$$

W	W/F_{Ao}	X_A	$-r_A$ (Calculated from slope Fig 7A)
0.02	0.01	0.07	7.2
0.04	0.02	0.15	6.1
0.08	0.04	0.25	4.3
0.12	0.06	0.33	3.1
0.16	0.08	0.36	2.3

The X_A vs W/F_{AO} plot is shown in Fig 7(A) and used to calculate rate.

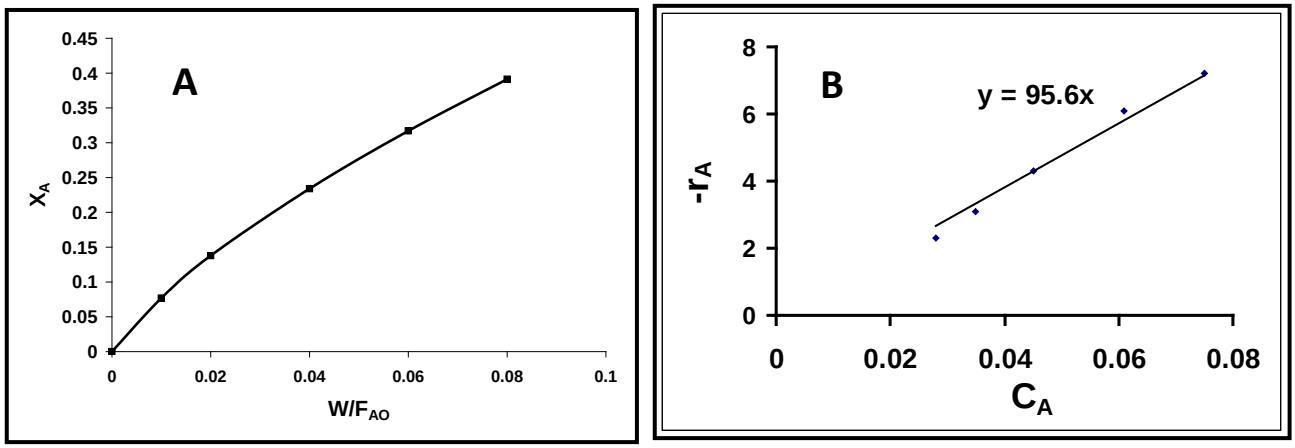

Fig. 7. Plots for differential analysis of data (A) X_A vs W/F_{AO} (B) r_A vs C_A plot

If $-r_A$ is plotted against C_A a straight line is obtained of slope k (Fig 7B). Since the line is straight line passing through origin, the order of the reaction is one as also obtained from integral analysis.

Hence the rate is $-r_A = kC_A$ =[95.6 litres/hr.kg catalysts] C_A

Book Reference

- J. M. Smith, Chemical Engineering Kinetics, McGrawHill Book Company, 1981
- H. S. Fogler, Elements of Chemical reaction engineering, Prentice Hall of India., 1999
- O. Levenspiel , Chemical reaction engineering, John Wiley & sons. 1995

Lecture 22

Effect of transport processes

Effect of external transport on catalytic reaction rate

Transfer of reactants from bulk fluid to surface of catalyst particles depends on the concentration difference which is affected by the velocity pattern of fluid near the catalyst surface, physical properties of fluid and intrinsic rate of chemical reactions. While the fluid properties affect the mass transfer between fluid and catalyst surface, the intrinsic rate is determined by the condition and properties of catalyst. The external concentration profiles for reactant for solid catalytic reaction in absence and presence of mass transfer limitation is shown in Fig. 1. In absence of mass transfer there is no difference in concentration of reactant at bulk and near the catalyst surface. However, presence of significant mass transfer resistance results in a decrease in the concentration of reactants at the catalyst surface compared to that in the bulk fluid. Consequently, the observed rate is less than the intrinsic rate evaluated at bulk fluid reactant concentration.

In addition to mass transfer limitation, there may be a temperature difference between the bulk fluid and catalyst surface. The magnitude depends on the heat transfer coefficient between the fluid and catalytic surface, reaction rate constant and heat of reaction. If the reaction is endothermic, the temperature at the catalyst surface will be less than the bulk fluid temperature and the observed rate will be less than that determined at the bulk fluid temperature. If the reaction is exothermic, the temperature of catalyst surface will be more than the bulk fluid temperature. Therefore, the observed rate will be higher or lower than corresponding bulk fluid conditions, depending on both heat transfer and mass transfer effects. Rate at the surface will be higher due to heat transfer limitations and lower due to mass transfer limitations. Depending on the relative magnitude, the overall rate will be increased or decreased. Discussion in subsequent sections is limited to isothermal conditions.

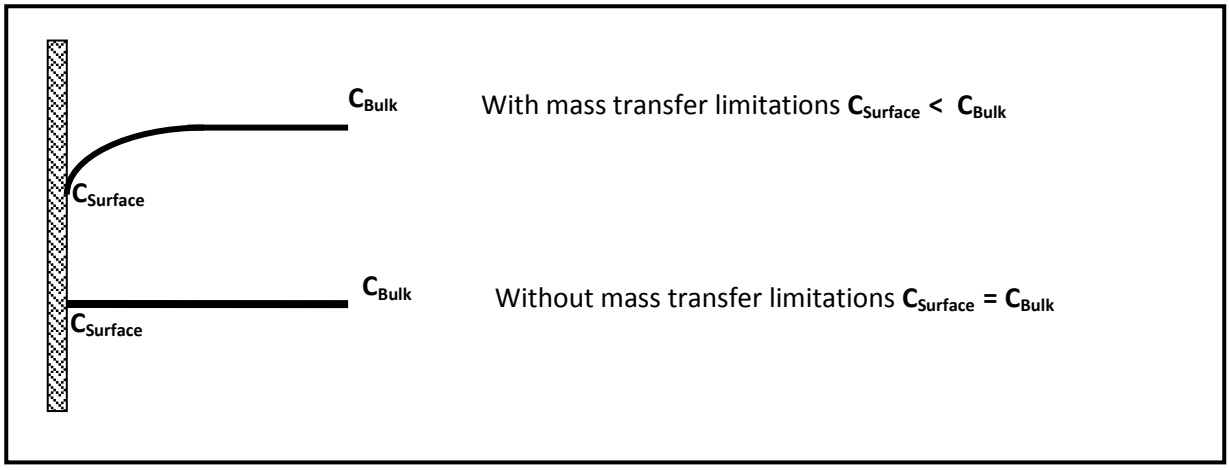

Fig. 1. External concentration profiles for reactant for solid catalytic reactions in absence and presence of mass transfer limitations

Reaction rate in presence of significant external mass transfer limitation

Consider a gaseous irreversible reaction A ➔ B that is occurring on a solid catalyst. Assume the reaction to be of first order with respect to **A**. Since the reaction is irreversible, the concentration of B at the catalyst surface does not influence the rate. Also assume desorption of B to be very fast (path -3).

Hence the reaction is controlled by the following two steps

1. transportation of A from bulk to catalyst surface (path -1)
2. reaction of A to B at catalyst surface (path -2)

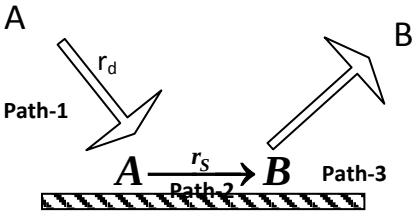

Diffusion rate of A from bulk gas to surface is $r_d = k_m a_m \left(C_b - C_s\right)$ (1)

Surface reaction rate is $r_s = kC_s$ (2)

Here, rate is mol /s. g catalyst.

Where,

C_b = bulk gas concentration of A, mol/cm^3

C_s = catalyst surface concentration of A, mol/cm^3

k_m = mass transfer coefficient between bulk gas and solid surface , cm/s

a_m = external surface area, cm^2/g

k = reaction rate constant, cm^3/s.g catalyst for first order recation

At steady state, rate of diffusion and surface reaction rate will be equal. Hence $r_d = r_s$

And overall reaction rate can be expressed by either of two

$$r_d = r_s = r_p \qquad (3)$$

Here, r_p is the steady state rate per unit mass of catalyst pellets.

From (1) , (2) and (3)

Or, $r_p = k_m a_m \left(C_b - C_s\right) = kC_s$ (4)

Or , $C_s = \dfrac{k_m a_m}{k + k_m a_m} C_b$

Substituting the value of C_s in $r_p = kC_s$

$$r_p = kC_s = \frac{k\ k_m a_m}{k + k_m a_m} C_b \qquad (5)$$

Or $r_p = k_o C_b$

Where $k_o = \dfrac{k\ k_m a_m}{k + k_m a_m}$. The k_o is called the overall rate constant.

Equation (5) is the rate expression at steady state for a first order reaction in terms of bulk concentration when significant mass transfer limitation is present.

Now , $k_o = \dfrac{k\ k_m a_m}{k + k_m a_m}$

Or. $\dfrac{1}{k_o} = \dfrac{1}{k} + \dfrac{1}{k_m a_m}$

Case 1 : When diffusion controls the process, that is reaction is very fast then $k >> k_m a_m$. Hence from equation (5) it can be written as

$$r_p = \frac{k\ k_m a_m}{k + k_m a_m} C_b = \frac{k\ k_m a_m}{k} C_b$$

Or $r_p = k_m a_m C_b$ (6)

Case 2 : When surface reaction controls the overall process ,that is diffusion is very fast then $k << k_m a_m$

Hence from equation (5) it can be written as

$$r_p = \frac{k\ k_m a_m}{k + k_m a_m} C_b = \frac{k\ k_m a_m}{k_m a_m} C_b$$

Or $r_p = k\ C_b$. (7)

Mass transfer coefficient in packed bed for solid-fluid system

Average transport coefficient between bulk stream and particle surface can be determined from following correlation in terms of dimension less groups characterizing the flow conditions.

$$\mathbf{j_D = \frac{K_m \rho}{G}\left(\frac{a_m}{a_t}\right)\left(\frac{\mu}{\rho D}\right)^{2/3}}$$

Where a_m is the effective mass transfer area and a_t is the total external area of the particles. For Reynolds number greater than 10, the following relationship can be used.

$$\mathbf{j = \frac{0.458}{\varepsilon_B}\left(\frac{dG}{\mu}\right)^{-0.407}}$$

Where,

G = superficial mass velocity based upon cross sectional area of empty reactor = uρ

d_p = diameter of spherical catalyst particles

μ = viscosity of fluid

ρ = density of fluid

D= molecular diffusivity of component being transferred

ε_B = void fraction of the bed

Other correlations are also available in the literature.

Effect of external mass transfer resistance on order of reaction

Consider a irreversible and gas phase reaction $\boldsymbol{A \rightarrow B}$. Assume true order of the reaction to be n = 2 . Hence actual reaction rate can be written as,

$$\boldsymbol{r_p = k\ C_s^2}$$

Now if the rate is mass transfer controlled, then from (6) rate is given as $r_p = k_m a_m C_b$

Experimental data plotted as rate vs C_b will give a straight line (passing through origin).

Now if the external diffusion is not taken into account then based on the experimental data it will be assumed that reaction is first order with respect to concentration because for first order reaction, $r_p = kC_b$, the plot of rate versus concentration gives a straight line with slope k passing through the origin. Hence in this case, the rate will be interpreted as $r_p = kC_b$ and the order will be interpreted as one. However, this interpretation will be a false conclusion as actual order of the reaction is two and it is appearing one only because external diffusion is controlling the process. Regardless of the intrinsic kinetics, if external mass transfer is controlling, the experimentally determined order will always appear as unity.

Effect of external mass transfer resistance on activation energy of reaction

Consider an irreversible and gas phase reaction $\boldsymbol{A \rightarrow B}$. Assume the reaction to be first order with respect to A.

Then, $\boldsymbol{r_p = k_0 C_b}$ where $\boldsymbol{k_0 =}$ overall rate constant

Rates are measured over a nonporous catalyst at different temperature and observed rates are used to calculate the overall rate constant $\boldsymbol{k_0}$. The corresponding activation energy can be obtained from Arrhenius equation as follows

$$\boldsymbol{k_0 = A' e^{\frac{-E'}{RT}}}$$

Here the activation energy E' is known as apparent activation energy and A' as apparent frequency factor. This E' is not the true activation energy corresponding to surface reaction as we will see in the following section.

Now $\boldsymbol{k_0}$ overall rate constant is given as

$$\text{Or}, \quad k_0 = \frac{k\ k_m a_m}{k + k_m a_m} \qquad (8)$$

If E is the true activation energy of the surface reaction then by substituting $\boldsymbol{k = Ae^{\frac{-E}{RT}}}$ in equation (8)

$$k_0 = \frac{Ae^{\frac{-E}{RT}} k_m a_m}{Ae^{\frac{-E}{RT}} + k_m a_m} \qquad (9)$$

1. At high temperature , $Ae^{\frac{-E}{RT}} >> k_m a_m$
   Then from equation (9) , $k_0 \cong k_m a_m$ which is nearly a constant value as k_m is relatively insensitive to temperature

(2) At low temperature, $Ae^{\frac{-E}{RT}} << k_m a_m$, then $k_0 \cong Ae^{\frac{-E}{RT}}$ and a straight line is obtained on Arrhenius plot.

If the Arrhenius equation is plotted over the entire range of temperature, then at low temperatures, the slope corresponds to the correct (or true) activation energy **E** of the surface reaction. As temperature increases, a curve is obtained, which flattens to a horizontal line corresponding to constant value of '$k_m a_m$'. Hence when experimental rate data for fluid solid catalytic reaction shows a curved Arrhenius plot then it is possible that mass transfer resistance is significant and external diffusion plays an important role in kinetics. This situation is for isothermal conditions.

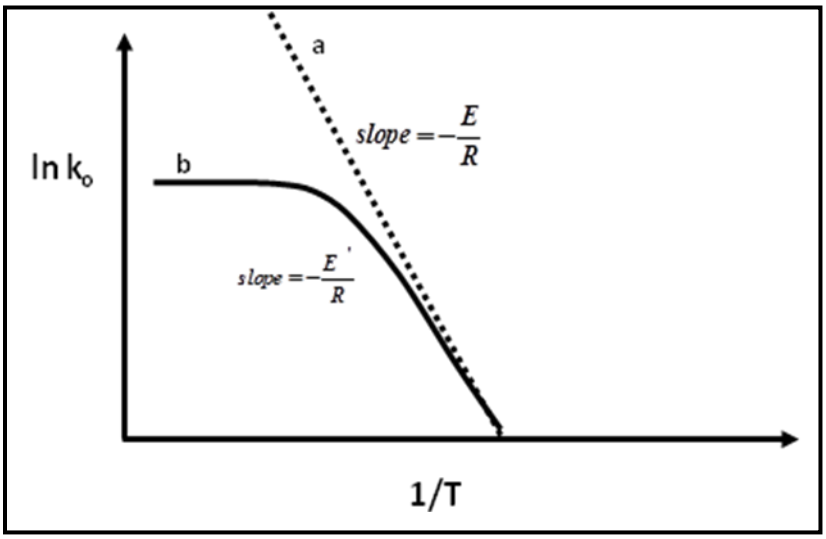

Fig. 2. Arrhenius plot for reaction (a) without external mass transfer resistance and (b) with external mass transfer resistance

Effect of external transport on selectivity

For multiple reactions, obtaining high selectivity of the desired products is important. The effect of external transport on selectivity depends on the kinetics of the system. Selectivity at any location in a reactor can be defined as the ratio of the rates of the desirable to the undesirable product. The effect will be discussed at isothermal conditions only.

Case 1 : Isothermal-consecutive reaction:

Consider a first order irreversible consecutive reaction

$$A \xrightarrow{k_1} B \xrightarrow{k_2} C$$

The selectivity of B w.r.t C, S_B can be written as $S_B = \frac{r_B}{r_C} = \frac{k_1 C_{AS} - k_2 C_{BS}}{k_2 C_{BS}}$ (10)

The surface concentration can be expressed in term of bulk values.

For A,

$$(k_m a_m)_A \left(C_A - C_{As}\right) = k_1 C_{As}$$

Or, $C_{As} = \frac{(k_m a_m)_A C_A}{k_1 + \left(k_m a_m\right)_A}$

Similarly for B, (here B is diffused from surface to bulk)

$$\left(k_m a_m\right)_B \left(C_{BS} - C_B\right) = k_1 C_{AS} - k_2 C_{BS}$$

Or, $C_{BS} = \frac{k_1 C_{AS} + \left(k_m a_m\right)_B C_B}{\left(k_m a_m\right)_B + k_2}$

Here C_A and C_B are bulk concentrations of A and B, respectively

Substituting value of C_{AS}

$$C_{BS} = \frac{k_1 \frac{(k_m a_m)_A C_A}{k_1 + (k_m a_m)_A} + \left(k_m a_m\right)_B C_B}{(k_m a_m)_B + k_2}$$

Substituting value of C_{AS} & C_{BS} in S_B (10), selectivity can be obtained in term of bulk concentration

$$S_B = \frac{k_1 C_A}{k_2 C_B}\left[\frac{1 + k_2/(k_m a_m)_B}{\left[k_1/(k_m a_m)_B\right](C_A/C_B) + \left[\frac{1}{(k_m a_m)_A}\right]\left[(k_m a_m)_A + k_1\right]}\right] - 1 \quad (11)$$

In absence of mass transfer resistances $C_s = C_b$ for both A & B

Then, the above equation reduces to

$$S_B = \frac{r_B}{r_C} = \frac{k_1 C_A - k_2 C_b}{k_2 C_B}$$

$$S_B = \frac{k_1 C_A}{k_2 C_B} - 1 \qquad (12)$$

The term in brackets of equation (11) is less than unity hence comparison of (11) & (12) suggests that selectivity is reduced by mass transport effect. As a mass transfer resistance becomes insignificant, the term in bracket in (11) approaches unity and it is in agreement with equation (12).

Qualitatively, the effect of external mass transfer can be explained as follows. The mass transfer limitation will reduce the surface concentration of A below the bulk value. This will reduce rate of formation of B by the first reaction. Again, due to mass transfer resistances in removal of B from the surface, concentration of B will increase near the catalyst surface and thereby result in an increase in the rate of disappearance of B to C by the second reaction. Thus, qualitatively it can be seen that formation of B is reduced while disappearance of B is increased due to external mass transfer effect. Consequently, selectivity of B with respect to C is reduced by external mass transfer limitations.

Case 2 : Parallel reaction (isothermal)

Consider two parallel first-order reactions from the same reactant with B as the desired product.

$A \xrightarrow{k_1} B$ Desired product

$A \xrightarrow{k_2} C$

The selectivity of B w.r.t C is given by :

$$S_b = \frac{r_B}{r_C} = \frac{k_1 C_{AS}}{k_2 C_{AS}} = \frac{k_1}{k_2}$$

Hence selectively is independent of concentration. Hence, external mass transfer does not affect the selectivity in this case. For this type of parallel reaction, the rate is reduced by mass transfer but the selectivity is unchanged.

If the parallel reactions are completely independent

$$A \xrightarrow{k_1} B$$

$$R \xrightarrow{k_2} S$$

Selectivity is then given as

$$S_B = \frac{r_B}{r_S} = \frac{k_1 C_{AS}}{k_2 C_{RS}} = \left[\frac{\frac{1}{(k_m a_m)_R} + \frac{1}{k_2}}{\frac{1}{(k_m a_m)_A} + \frac{1}{k_1}} \right] \frac{C_A}{C_R}$$

In absence of external resistance, selectivity is $S_B^{'} = \frac{k_1}{k_2} \frac{C_A}{C_R}$

Effect of external mass transport on selectivity is given by ratio

$$\frac{S_B}{S_B^{'}} = \left[\frac{(k_m a_m)_R + k_2}{(k_m a_m)_A + k_1} \right] \frac{(k_m a_m)_A}{(k_m a_m)_R}$$

The two mass transfer coefficients are nearly the same for most reaction systems. Hence the ratio becomes

$$\frac{S_B}{S_B^{'}} = \frac{(k_m a_m)_R + k_2}{(k_m a_m)_A + k_1}$$

The selectivity in this case will decrease by external mass transfer only if $k_1 > k_2$

For low mass transfer resistance , no effect on selectivity will be observed as

$k_m a_m >> k_2$ *or* k_1 then $\frac{S_B}{S_B'} = 1$

Book Reference :

- J. M. Smith, Chemical Engineering Kinetics, McGrawHill Book Company, 1981
- H. S. Fogler, Elements of Chemical reaction engineering, Prentice Hall of India., 1999
- J.J. Carberry , Chemical and catalytic reaction Engineering, Dover Publications, 2001
- O. Levenspiel , Chemical reaction engineering, John Wiley & sons, 1995

Lecture 23

Effect of internal mass transport on catalytic reaction rate

Diffusion

Diffusion of reactants within pores is a complex phenomena and results from the contribution of :

1. **Bulk diffusion :** Diffusion due to concentration or pressure gradients. The molecules collide with each other.
2. **Knudsen diffusion :** Diffusion in fine pores governed by molecular velocity and as well as diameter of pore. The diffusing molecule is more likely to collide with a wall rather than another molecule. It is important at low pressures and for pore size below 50 nm.
3. **Surface diffusion:** Transport of adsorbed molecules on a surface by hopping mechanism that is adsorbed molecules tend to migrate to an adjacent empty site if it has sufficient energies to jump or overcome the energy barrier. However, in most cases contribution of surface diffusion to total transport is very small and generally neglected.

For macroporous material with large pore size such as alumina pellets of mean radius of 8000 A^0 , bulk diffusion would prevail in these pores at atmospheric pressure. As the size of the pore decreases, diffusion in the pores is more and more influenced by pore walls and transport is dominated by Knudsen mechanism. Hence in micropores, particularly for gaseous system, transport can be assumed to be entirely by Knudsen diffusion.

The pressure also affects the relative contribution of bulk and Knudsen diffusion for gaseous system. The mean free path is inversely proportional to pressure. Increase in pressure decreases mean free path and probability of collision between molecules increases. Consequently, bulk diffusivity becomes more important as the pressure is increased. On the other hand, as pressure is lowered mean free path is reduced and probability of molecules colliding with the walls is increased. Consequently, transport is dominated by Knudsen diffusion.

The diffusion in binary system is represented by Fick's law which states that molar flux of a species relative to an observer moving with molar average velocity is proportional to the concentration gradient of the species. If A diffuses in a binary mixture of A and B , then according to Fick's law the flux of A is expressed as $\mathbf{J_A = -D_{AB}\frac{dC_A}{dz}}$

Here D_{AB} is the proportionality constant called the diffusion coefficient or diffusivity of A in mixture of A and B.

Different binary diffusion conditions may exists :

1. Equimolar counter diffusion, $N_B = -N_A$
2. Non-equimolar counter diffusion, $N_B \neq -N_A$
3. Diffusion of A through non diffusing B, $N_B = 0$

Here N_A , and N_B are the molar flux of A and B respectively. The negative sign correspond to opposite direction.

Assume that for a gaseous irreversible reaction A → B, the reaction and diffusion in a single cylindrical pore results in equimolal counter diffusion, or $N_B = -N_A$. Then for reactant A, the combined diffusivity in a cylindrical pore is given as

$$\boldsymbol{D = \frac{1}{\frac{1-\alpha y_A}{D_{AB}} + \frac{1}{(D_k)_A}}} \qquad (1)$$

where $\boldsymbol{D_{AB}}$ is the bulk diffusion contribution and $\boldsymbol{(D_k)_A}$ is the Knudsen diffusion contribution.

Here $\boldsymbol{\alpha = 1 + \frac{N_B}{N_A}} = 0$ as $N_B = -N_A$

Or $\boldsymbol{D = \frac{1}{\frac{1}{D_{AB}} + \frac{1}{(D_k)_A}}}$ (2)

When pore radius is large $\left(\boldsymbol{D_k}\right)_A \to \infty$, $\boldsymbol{D = D_{AB}}$ = bulk diffusion. If pore radius is very small, Knudsen diffusivity is controlling and $\boldsymbol{D = D_k}$

Bulk diffusivity at moderate temperature and pressure can be evaluated using Chapman – Enskog equation. For binary gas mixture of A and B

$$\boldsymbol{D_{AB} = 0.0018583 \frac{T^{3/2}\left[\frac{1}{M_A}+\frac{1}{M_B}\right]^{1/2}}{p_t \sigma_{AB}^2 \Omega_{AB}}} \qquad (3)$$

$D_{AB}\left(cm^2/s\right) = bulk\ diffusivity$
$T\left(K\right) = temperature$
$M_A \,\&\, M_B = molecular\ weight\ of\ A\ and\ B,\ respectively$
$p_t\left(atm\right) = total\ pressure\ of\ the\ gas\ mixture$
$\sigma_{AB}\left(A^0\right) =$ constant in Lennard-Jones potential-energy functions for the molecular pair AB
$\varepsilon_{AB} =$ constant in Lennard-Jones potential-energy functions for the molecular pair AB
$\Omega_{AB} =$ collision integral

Knudsen diffusivity can be evaluated by the following equation :

$$\boldsymbol{\left(D_k\right)_A = 9.7\times10^3\ a\left(\frac{T}{M_A}\right)^{1/2}} \qquad (4)$$

$\left(D_k\right)_A \to Knudsen\ diffusivity\ \ cm^2/s$
$T \to temperature\ ,\ K$
$a \to pore\ radius,\ cm$

The diffusivity of A in multicomponent system containing n components is given as

$$\mathbf{D_{A,m} = \frac{N_A - y_A \sum_{i=A}^{n} N_i}{\sum_{i=A}^{n} \frac{1}{D_{Ai}}\left(y_i N_A - y_A N_i\right)}}$$

Here N_i is taken as positive if diffusion is in same direction as that of A and negative if in opposite direction. The D_{Ai} are the binary diffusivities of component A with respect to component 'i'. The y_A is molfraction of A and y_i molfraction of 'i'

Effective diffusivity, D_e

The actual pore network within a catalysts pellet can be quite complex and hence to account for diffusion through the tortuous, random and interconnected arrangement of pores it is essential to develop a pore model that can realistically represent the geometry of void space. The void geometry should also be represented in terms of easily measurable physical properties of catalyst pellets, such as surface area, pore volume, density of solid phase and distribution of void volume according to pore size. Keeping all these factors in consideration, various pore models are developed. The effective diffusivity (D_e) is derived using these pore models from combined diffusivity for a single cylindrical pore.

The steps involved are as follows :

1. Initially combined diffusivity D for a single cylindrical pores is calculated using the equation (2) $\frac{\mathbf{1}}{\boldsymbol{D}} = \frac{\mathbf{1}}{\frac{\mathbf{1}}{\boldsymbol{D_{AB}}} + \frac{\mathbf{1}}{\left(\boldsymbol{D_K}\right)_{\boldsymbol{A}}}}$
2. Then a geometric model of the pore system is used to convert D to D_e for the porous pellet.

Two pore models more commonly used are :

1. parallel pore model
2. random pore model

Parallel pore model

In this model, the effective diffusivity is derived based on assembly of parallel cylindrical pores of uniform radius. The interconnection and non-cylindrical pore shapes for real material is accounted for by introduction of a tortuosity factor δ. Using this model, the effective diffusivity D_e can be expressed as

$$D_e = \frac{\varepsilon D}{\delta} \tag{5}$$

where ε = porosity; D = combined diffusivity ; δ = tortuosity factor

The typical porosity values lies in the range of 0.3- 0.5. The tortuosity factor can varies from less than one to 6. Typically a value of 3 to 4 is used.

Random pore model

This model considers that pellets consist of both macro and micro pores. Pellets consist of assembly of small particles containing micropores and the void space between the particles constitutes the macropores. Transport in the pellet is assumed to occur by combination of diffusion through the macro-regions having void fraction ε_M and the micro regions having void fraction ε_μ. The magnitude of individual contribution is dependent on their effective cross-sectional areas perpendicular to the direction of diffusion.

The resultant expression for effective diffusivity D_e is given as

$$D_e = \overline{D}_M \varepsilon_M^2 + \frac{\varepsilon_\mu^2 \left(1 + 3\varepsilon_M\right)}{1 - \varepsilon_M} \overline{D}_\mu \tag{6}$$

$\overline{D}_M$ and $\overline{D}_\mu$ are combined diffusivity in macropores and micropores, respectively and obtained by applying equation for combined diffusivity D to macro and micro regions as follows.

$$\frac{1}{\overline{D}_M} = \frac{1}{D_{AB}} + \frac{1}{\left(\overline{D_k}\right)_M} \quad \text{and} \quad \frac{1}{\overline{D}_\mu} = \frac{1}{D_{AB}} + \frac{1}{\left(\overline{D_k}\right)_\mu}$$

No tortuosity factor is involved in this model. The actual path length is equal to the distance co-ordinate in the direction of diffusion.

For a pellet containing only macropores, substituting $\varepsilon_\mu = 0$ in equation (6) gives $D_e = \overline{D}_M \varepsilon_M^2$.

Similarly for materials with only micropores, putting $\varepsilon_M = 0$ in equation 18 gives $D_e = \overline{D}_\mu \varepsilon_\mu^2$

Effectiveness factor η

In a porous catalyst, the internal surface area within the pores constitutes the effective surface on which the active metals are deposited. Hence, for reaction to occur, the reactants need to travel through the pores to reach the active sites. If there is any resistance in diffusion of the reactants through the pores, then both the activity and selectivity of the process is affected. In the absence of any internal mass transfer resistance within the pores the concentration of reactants can be assumed to uniform and equal to the surface concentration. Hence, the rate of reaction will also be uniform across the catalyst pellet and equal to the rate evaluated at surface conditions. However, in the presence of diffusional resistance, concentration of reactants gradually decreases from the surface towards the center of the catalyst pellet, resulting in a concentration gradient. When this concentration gradient is large enough, significant variation in reaction rate occurs within the pellet. The average rate within pellet will be less than the rate corresponding to the surface concentration. As pellet size decreases, the effect of intrapellet transport becomes less significant.

Rate of reaction for the whole catalyst pellets at any time is defined with respect to outer surface conditions in term of effectiveness factor η as :

$$\text{Actual rate of whole pellet } (r_p) = \eta \times \text{rate evaluated at outer surface conditions } (r_s)$$

$$\text{or, } \quad \eta = \frac{\text{actual rate of whole pellet}}{\text{rate evaluated at outer surface conditions}} = \frac{r_p}{r_s}$$

Actual rate of whole pellet r_p takes intrapellet mass transfer effects if any into account.

Effectiveness factor at isothermal conditions

For an irreversible first order reaction $A \rightarrow B$, at isothermal condition the rate at surface condition can be written as $r_s = k_1 C_S$. Then the actual global rate at outer surface condition, $r_p = \eta r_s = \eta k_1 C_S$.

For a spherical catalyst pellet of radius 'R_s', mass balance over a spherical shell volume of thickness ΔR at steady state will be :

(Rate of diffusion of reactant into element) – (Rate of diffusion of reactant out of element) = Rate of disappearance of reactant within element due to reaction

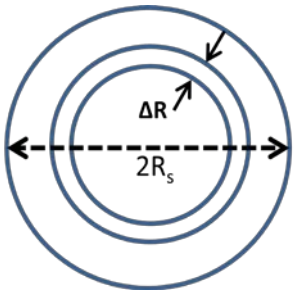

Rate of reaction per unit mass of catalyst = $k_1 C$

Rate of reaction per unit volume of catalyst = $k_1 C \rho_p$.

Where ρ_p is the density of pellet.

Then the mass balance equation over the element of thickness ΔR can be written as

$$\left[-4\pi R^2 D_e \frac{dC}{dR}\right]_R - \left[-4\pi R^2 D_e \frac{dC}{dR}\right]_{R+\Delta R} = \left(4\pi R^2 \Delta R\right)\rho_p k_1 C$$

If limit is taken as $\Delta R \to 0$ and assuming that effective diffusivity is independent of concentration of reactant the above equation can be written as

$$\frac{d^2C}{dR^2} + \frac{2}{R}\frac{dC}{dR} - \frac{k_1\rho_p}{D_e}C = 0 \qquad (7)$$

Boundary conditions :

At the center of the pellet, $\frac{dC}{dR} = 0$ at $R = 0$ (8)

At outer surface $C = C_s$ at $R = R_s$ (9)

Solving the differential equation (7) with boundary conditions (8) and (9) following relation is obtained

$$\frac{C}{C_S} = \frac{R_s}{R}\frac{\sinh\left(3\varphi_s\, R/R_s\right)}{\sinh 3\varphi_s} \qquad (10)$$

Where φ_s is a dimensionless group defined as

$$\varphi_s = \frac{R_s}{3}\sqrt{\frac{k_1\ \rho_p}{D_e}}$$

The φ_s is called Thiele modulus for spherical pellet. Equation (10) gives the concentration profile of A in the pellet.

This concentration profile is used to evaluate the rate of reaction r_p for the whole pellet. Calculating the diffusion rate of reactant into pellet at position R_s per unit mass of catalyst pellet

$$r_p = \frac{1}{m_p} 4\pi R_s^2 D_e \left(\frac{dC}{dR}\right)_{R=R_s} \qquad (12)$$

$$m_P = \frac{4}{3}\pi R_s^2 \rho_p = \text{mass of pellet}$$

Substituting the value of m_p in equation (12)

$$r_p = \frac{3}{R_s \rho_p} D_e \left(\frac{dC}{dR}\right)_{R=R_s}$$

or

$$\eta = \frac{r_p}{r_s} = \frac{3}{R_s \rho_p (r_s)} D_e \left(\frac{dC}{dR}\right)_{R=R_s} = \frac{3}{R_s \rho_p (k_1 C_s)} D_e \left(\frac{dC}{dR}\right)_{R=R_s} \qquad \because r_s = k_1 C_s \qquad (13)$$

Differentiating $\frac{C}{C_S} = \frac{R_s}{R} \frac{\sinh(3\varphi_s R / R_s)}{\sinh 3\varphi_s}$ and evaluating the derivative at $R = R_s$ and substituting in equation (13), following relation for η can be obtained for isothermal conditions.

$$\eta = \frac{1}{\varphi_s}\left(\frac{1}{\tanh 3\varphi_s} - \frac{1}{3\varphi_s}\right)$$

Then substituting the η in the rate for whole pellet in terms of concentration at outer surface $r_p = \eta k_1 C_s$, can be written as

$$r_p = \frac{1}{\varphi_s}\left[\frac{1}{\tanh 3\varphi_s} - \frac{1}{3\varphi_s}\right] k_1 C_s$$

Where for spherical pellets of radius $\mathbf{r_s}$, φ_s for a first-order reaction is given as

$$\varphi_s = \frac{R_s}{3}\sqrt{\frac{k_1 \rho_p}{D_e}}. \qquad (12)$$

k_1 is rate constant, ρ_p is pellet density; D_e is effective diffusivity.

Hence, to calculate Thiele modulus, both effective diffusivity D_e and rate constant k_1 need to be known. Fig 3 shows the typical plot of η vs φ_s.

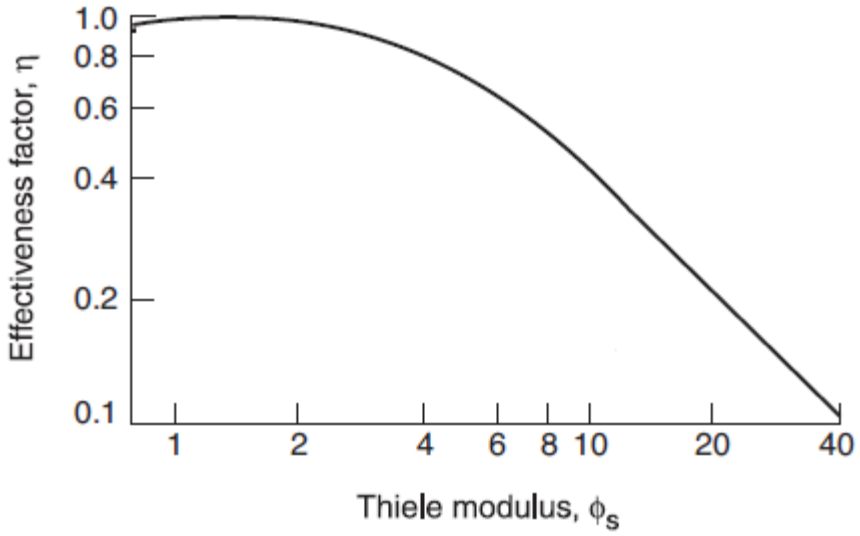

Fig. 3. Typical plot effectiveness factor η as function of Thiele modulus φ_s

As the figure shows, for small values of φ_s, $\eta \to 1$. Equation (13) shows that small values of φ_s are obtained when the :

1. pellets are small
2. diffusivity is large
3. reaction is intrinsically slow (catalysts of low activity).

For $\varphi_s > 5$, η can be approximated as $\eta = \frac{1}{\varphi_s}$. For such large φ_s, intra-particle diffusion has a large effect on the rate. At this condition, diffusion into the pellet is relatively slow and reaction occurs before the reactant has diffused far into the pellet.

When $\eta \to 1$, rate for the whole pellet is the same as the rate at surface concentration C_s and the entire catalyst surface is fully active.

When $\eta << 1$, the concentration within pellets drops from C_s to nearly zero in a narrow region near $\mathbf{r_s}$**.** At this condition, only the surface near the outer periphery of the pellet is

effective and the catalyst surface in the central portion of the pellet is not utilized. This situation can be caused by large particles, low D_e or high $k_{1;}$ that is very active catalysts.

Hence, low effectiveness factors are more likely with very active catalysts. More active the catalyst, the more is the possibility that intrapellet diffusion resistance will reduce global rate. For flat plate or slab of catalysts, opened to reactant only from one side with all other surface being sealed to reactant, the effectiveness factor is given as

$$\eta = \frac{\tanh \varphi_L}{\varphi_L} \qquad \text{where, } \varphi_L = L\sqrt{\frac{k_1 \rho_p}{D_e}} \text{ and } L = thickness\ of\ plate$$

If the slab is open to reactant on both side of the plate, the expression remains similar with L becoming the half of the plate thickness.

Book Reference :

- J. M. Smith, Chemical Engineering Kinetics, McGrawHill Book Company, 1981
- H. S. Fogler, Elements of Chemical reaction engineering, Prentice Hall of India., 1999
- J.J. Carberry , Chemical and catalytic reaction Engineering, Dover Publications, 2001
- O. Levenspiel , Chemical reaction engineering, John Wiley & sons, 1995

Lecture 24

Significance of intrapellet diffusion

P.B. Weis has developed a criterion for detecting whether intrapellet diffusion may be neglected. The basic assumption is that if $\varphi_S \leq \frac{1}{3}$, then $\eta \to 1$.

When $\boldsymbol{\varphi_S \leq \frac{1}{3}}$

Or $\boldsymbol{\frac{R_s}{3}\sqrt{\frac{k_1\rho_p}{D_e}} \leq \frac{1}{3}}$ $\qquad$ $\boldsymbol{\because \varphi_s = \frac{R_s}{3}\sqrt{\frac{k_1\rho_p}{D_e}}}$

Simplifying and squaring , $\boldsymbol{\frac{R_s^2 k_1 \rho_p}{D_e} \leq 1}$

Now $\boldsymbol{k_1 = \frac{r_p}{\eta C_s} = \frac{r_p}{C_s}}$, where r_p is the measured rate and $\boldsymbol{\eta \to 1}$.

Substituting k_1 , $\boldsymbol{\frac{R_s^2 \rho_p r_p}{D_e C_s} \leq 1}$. This is known as the Weisz Criteria.

This criterion can be approximately used for most catalytic kinetics though it is derived for a 1st order reaction. Hence, if criterion $\boldsymbol{\frac{R_s^2 \rho_p r_p}{D_e C_s} \leq 1}$, is fulfilled then $\eta \to 1$ and there is no intrapellet diffusion limitation.

Effect of intrapellet mass transfer on activation energy

Neglecting intrapellet mass transfer can lead to misleading conclusions about reaction activation energies.

At $\varphi_s > 5$, $\eta \cong \frac{1}{\varphi_s}$

For 1st order reaction, $\varphi_s = \frac{R_s}{3}\sqrt{\frac{k_1 \rho_p}{D_e}}$,

Or $\eta = \frac{3}{R_s}\sqrt{\frac{D_e}{k_1 \rho_p}}$

Then the rate of the whole pellet can be written as

$$r_p = \eta k_1 C_s = \frac{3}{R_s}\sqrt{\frac{D_e}{k_1 \rho_p}} \quad k_1 C_s = \frac{3C_s}{R_s}\sqrt{\frac{k_1 D_e}{\rho_p}}$$

Substituting $k_1 = A_1 e^{-E_1/RT}$, where E_1 is the true activation energy.

$$r_p = \frac{3C_s}{R_s}\sqrt{\frac{A_1 e^{-E_1/RT} D_e}{\rho_p}}$$

$$r_p = \frac{3C_s}{R_s}\left[\frac{D_e}{\rho_p}\right]^{1/2} A_1^{1/2} \quad e^{-E_1/2RT} \qquad (1)$$

Now if intrapellet resistance is neglected then the rate of first order reaction is given as

$$r_p = k_1 C_s = A_1^{'} e^{-E_1^{'}/RT} C_s \qquad (2)$$

Here A' and E' are apparent frequency factors and apparent activation energy, respectively. Then comparing (1) and (2)

$$E_1' = \frac{E_1}{2} \qquad (3)$$

Thus apparent activation energy is actually half of true activation energy. When internal mass transfer resistance is not considered than the activation energy obtained will be half of the actual value. These conclusions are same for all reaction orders.

However it should be kept in mind that relation (3) is true only at isothermal condition and effective diffusivity is constant. If temperature varies then effective diffusivity changes and for large φ_s the apparent activation energy is given as

$E_1' = \frac{E_1 + E_{diff}}{2}$. Under this condition, if the activation energy for diffusion (E_{diff}) is much less than the activation energy of the reaction, $E_{diff} << E_1$ then only $E_1' = \frac{E_1}{2}$.

In the plot of ln k vs 1/T , at low temperature the data would give a line with slope equal to –E/R as $\eta \to 1$. At high temperature intrapellet diffusion is important and line with slope –E/2R will be obtained.

Equation 3 shows that rate r_p is inversely proportional to pellet size R_s. If intrapellet diffusion is insignificant, the rate is independent of pellet size.

Effect on order of reaction

For a n^{th} order reaction ,Thiele modulus is given as

$$\varphi_n = \frac{R_s}{3}\sqrt{\frac{k_n \rho_p C_s^{n-1}}{D_e}}$$

For significant intra-pellet diffusion limitations , $\eta = \frac{1}{\varphi_s}$

$$\eta = \frac{3}{R_s}\sqrt{\frac{D_e}{k_n \rho_p C_s^{n-1}}}$$

The rate is given as

$$\left(r_p\right)_n = \eta k_n C_s^n = \frac{3}{R_s}\sqrt{\frac{D_e}{k_n \rho_p C_s^{n-1}}}\;\; k_n C_s^n = \frac{3}{R_s}\sqrt{\frac{D_e}{\rho_p}}\;\; k_n^{1/2}\;\; C_s^{\frac{(n+1)}{2}} \qquad (4)$$

If intrapellet diffusion is not considered the rate can be written as

$$\left(r_p\right)_n = k_n C_s^{n'} \qquad (5)$$

Here n' is called the apparent order. Comparing equation (4) and (5)

$n' = \frac{n+1}{2}$ Here, n is the true order

When n=0 , n′=1/2

n=1 , n′=1

n=2 , n′=3/2

The above relations shows how due to presence of pore diffusion limitations, for zero order and second order reactions, the apparent reaction order appear reduced.

Solved examples:

Dehydrogenation of hydrocarbon (mol.wt = 58) at atmospheric pressure was carried out over chromia-alumina catalysts at 530 ^{0}C. The reaction follows a first order kinetics with rate constant of 0.94 cm^3 /s. g cat. The spherical catalysts are of 30 mm diameter and average pore radius is 11 nm. Pellets have porosity of 0.35 and density of 1 gm/cm^3. Assume Knudsen diffusivity to be dominant. Predict an effectiveness factor for the catalysts. Use parallel pore model with a tortuosity factor of 3.0

Knudsen diffusivity is given as : $\left(D_k\right)_A = 9.7\times10^3\ a\left(\frac{T}{M_A}\right)^{1/2}$

Solutions :

Density of catalysts pellets = 1 gm/cm^3 , T= 530 ^{0}C; D_p= 0.3 cm ; R_s= 0.3/2 = 0.15 cm

k_1= 0.94 cm^3 /s. g cat ; a=pore radius = 11 nm = 11 × 10^{-7} cm

δ = 3 ; ε = 0.35

$\left(D_k\right)_A = 9.7\times10^3\ a\left(\frac{T}{M_A}\right)^{1/2}$

M_A=58 ; a = 11 nm = 11 × 10^{-7} cm ; T= 530 ^{0}C = 530 + 273 = 803 K

$\left(D_k\right)_A = 9.7\times10^3\ \times11\times10^{-7}\left(\frac{803}{58}\right)^{1/2}$ = 0.0397 cm^2/s

$D_e = \frac{\varepsilon D}{\delta}$

D=D_K= 0.0397 cm^2/s ; δ = 3 , ε = 0.35

$D_e = \frac{\varepsilon D}{\delta} = \frac{0.35\times0.0397}{3}$ = 4.63 ×10^{-3} cm^2/s

$\varphi_s = \frac{R_s}{3}\sqrt{\frac{k_1\rho_p}{D_e}} = \frac{0.15}{3}\sqrt{\frac{0.94\times1}{4.63\times10^{-3}}} = 0.712$

$$\eta = \frac{1}{\varphi_s}\left[\frac{1}{\tanh 3\varphi_s} - \frac{1}{3\varphi_s}\right] = \frac{1}{0.712}\left[\frac{1}{\tanh(3\times 0.712)} - \frac{1}{3\times 0.712}\right] = 0.786$$

Effect of internal mass transport on selectivity

Selectivity of a product can be defined as the ratio of global rates for formation of different products at that point. Combined effect of external and internal diffusion resistances on selectivity at isothermal conditions are discussed below.

1. Independent and parallel irreversible first order reactions

   $A \xrightarrow{k_1} B$ B desired product

   $R \xrightarrow{k_2} S$

   It is further assumed that:

   1. $k_1 > k_2$
   2. Isothermal condition
   3. Both external and internal diffusion resistances affect the rate.

At steady state , rate for catalyst pellet can be written as

$$r_p = k_m a_m \left(C_b - C_s\right) \qquad (6)$$

$a_m = external\ area\ for\ masstransfer\ per\ unit\ mass\ of\ catalysts$
$C_b = bulk\ concentration$
$C_s = surface\ concentration$

The rate for catalyst pellet can also be written as $r_p = \eta k_1 C_s$ (7)

Eliminating surface concentration Cs between equations (6) and (7)

$$r_p = \frac{1}{\frac{1}{k_m a_m} + \frac{1}{\eta k_1}}\ C_b$$

Thus external effect can be treated as a separate additive resistance. The reduction in rate due to internal diffusion resistance through η is combined with rate constant k for chemical steps.

If there is only internal mass transfer resistance then $C_s = C_b$

Say $\varphi_s \geq 5$, hence $\eta = \frac{1}{\varphi_s}$

$$r_p = \eta k_1 C_s = \frac{1}{\varphi_s} k_1 C_b \quad \because C_s = C_b$$

Or $$r_p = \frac{3}{R_s}\sqrt{\frac{k_1 D_e}{\rho_p}}\ C_b$$

Then selectivity of B is given as

$$S_B = \frac{r_{p_1}}{r_{p2}} = \sqrt{\frac{k_1 (D_e)_A}{k_2 (D_e)_R}}\ \frac{(C_b)_A}{(C_b)_R}$$

If differences in diffusivities are neglected $(D_e)_A \approx (D_e)_R$

$$S_B = \sqrt{\frac{k_1}{k_2}}\ \frac{(C_b)_A}{(C_b)_R} \qquad (8)$$

In absence of internal mass transfer resistance selectivity of B is given as

$$S_p = \frac{r_{p_1}}{r_{p2}} = \frac{k_1 (C_b)_A}{k_2 (C_b)_R} \qquad (9)$$

Comparison of equations (8) and (9) shows that the intrapellet diffusion resistance reduces the selectivity.

(2) For parallel irreversible first order reaction with same reactant. B is desired.

$$A \xrightarrow{k_1} B$$
$$A \xrightarrow{k_2} C$$

$$S_B = \frac{r_{p_1}}{r_{p2}} = \frac{k_1 (C_b)_A}{k_2 (C_b)_A} = \frac{k_1}{k_2} \quad .$$

Hence at this condition selectivity of B is unaffected by internal transport effect.

(3) For irreversible first order consecutive reaction

$$A \xrightarrow{k_1} B \xrightarrow{k_2} C$$

Here B is the desired product. The selectivity of product B with respect to reactant A is can be expressed as

$$S_B = \frac{\text{net rate of production of B}}{\text{rate of disappearance of A}}$$

or $$S_B = \frac{dC_B}{-dC_A} = \frac{k_1 C_A - k_2 C_B}{k_1 C_A} = 1 - \frac{k_2 C_B}{k_1 C_A} \qquad (10)$$

The C_A and C_B are bulk concentrations of A and B respectively. The equation (10) gives selectivity of B for whole pellet provided that the internal diffusion resistance is negligible. In presence of significant intrapellet diffusion resistance, the concentration of C_A and C_B changes within the pellet and the selectivity will vary with the position within the pellet as C_B/C_A changes. Diffusion resistance causes C_A to decrease from outer surface to the center of pellet. The product B is formed within pellet and has to diffuse out from the pellet into bulk. Hence concentration of B increases toward center of pellet due to resistance. Hence from equation (10) it can be seen that decrease of C_A and increase of C_B toward center of pellet result in reduction of pellet selectivity for B from centre to outer surface. For the given first order reaction in presence of strong diffusion resistance (say $\eta \leq 0.2$) and assuming equal effective diffusivities, the selectivity of B can be obtained as

$$S_B = \frac{(k_1/k_2)^{1/2}}{1+(k_1/k_2)^{1/2}} - \left(\frac{k_2}{k_1}\right)^{1/2} \frac{C_B}{C_A} \qquad (11)$$

Comparison of equations (10) and (11) shows that the selectivity is significantly reduces when internal diffusional resistance is significant.

Book Reference :

- J. M. Smith, Chemical Engineering Kinetics, McGrawHill Book Company, 1981
- H. S. Fogler, Elements of Chemical reaction engineering, Prentice Hall of India, 1999
- J.J. Carberry , Chemical and catalytic reaction Engineering, Dover Publications, 2001
- O. Levenspiel , Chemical reaction engineering, John Wiley & sons, 1995

Lecture 25

Catalyst deactivation

Activity of catalysts normally decreases with time. The life of any catalyst generally depends on type of reactions as well as reaction conditions. For example, catalysts for catalytic cracking lose much of their activity within seconds due to carbon deposition on the surface while promoted iron catalysts used in ammonia synthesis have a lifetime of years. For any catalytic process, the life of catalyst is a major economic factor. To regenerate or replace deactivated catalysts, the process needs to be shutdown and consequently production is disrupted. Subsequent separation and regeneration of catalysts also involve time and cost. Therefore, deactivation of catalysts increases the cost of production significantly. Hence, any catalytic process will be economically viable only if regenerations are required infrequently and can be done inexpensively. A catalyst can be deactivated in three ways

I. Poisoning
II. Fouling
III. Sintering or phase transformation

I. Poisoning

Poisoning basically involve chemisorption of reactants or products or feed impurities on the active sites of the catalyst surface, thereby decreasing the number of active sites available for catalytic reactions. Since poisoning involves chemisorptions, it is known as chemical deactivation. This process can be reversible or irreversible. Compound of sulphur and other materials are frequently chemisorbed on nickel, copper and Pt catalysts. In reversible poisoning, the strength of adsorption bond is not great and activity is regained when the poison is removed from the feed. When the adsorbed material is tightly held on the active sites, poisoning is irreversible and permanent.

II. **Fouling**

Rapid deactivation can be caused by physical deposition of substance on the active sites of catalysts. Carbon deposition on catalysts used in petroleum industry falls in this category. Carbon covers the active site of the catalysts and may also partially plug the pore entrance. This type of deactivation is partially reversible and regeneration can be done by burning in air.

$$C \xrightarrow{air/high\ temperature} CO / CO_2$$

III. **Sintering or phase transformation**

Because of local high temperature, support of catalysts or catalyst itself may undergo structural modification or sintering causing a reduction in specific surface area or change in chemical nature of catalytic agent so that it becomes catalytically inactive. Hence, poisoning and fouling are dependent on concentration of reactant or product or impurities. On the other hand, sintering and phase transformation may be assumed to be independent of fluid phase composition. This is also therefore known as independent deactivation.

Steps to reduce deactivation: Following steps can be taken to reduce the possibility of deactivation of catalysts :

a. Removal of poison material form feed
b. Use of hydrogen which reduces coking
c. Removal of hot spot by proper design of reactor /process control to prevent any thermal deactivation.

Mechanism of catalysts deactivation

The deactivation of catalysts can occur by different mechanism as explained below :

1. Parallel deactivation

Reactant (A) produces a side product (P) which can deposit on the surface thereby deactivating it. Deposition depends on reactant concentration.

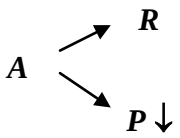

or $A \rightarrow R + P\downarrow$

2. Series deactivation

Reaction product (R) can decompose or react further to produce material (P) that deposits and deactivates the surface. In this case, deposition depends on product concentration.

$$A \rightarrow R \rightarrow P\downarrow$$

3. Side-by-side deactivation

In this mechanism, impurity in feed (P) deposits on the surface deactivating it. Deposition depends on concentration of impurities in the feed.

$$A \rightarrow R$$
$$P \rightarrow P\downarrow$$

4. Independent deactivation

This catalyst decay involves structural modification or sintering of catalyst surface caused by exposure of catalysts to extreme conditions such as high temperature. This decay is dependent on time that the catalyst spends in high temperature conditions and is independent of the materials in the fluid.

Deactivation kinetics

Activity of catalysts pellet at any time is defined as

$$a = \frac{\textbf{rate at which the pellet converts reactant A}}{\textbf{rate of reaction of A with fresh pellet}} = \frac{-r_A'}{-r_{A0}'}$$

Reaction rate can be considered as function of temperature, reactant concentration and present activity of the catalysts pellet. Therefore for n^{th} order reaction, rate can be written as

$$-r_A' = kC_A^n a$$

where a is the present activity of the catalyst.

Similarly, deactivation rate can be considered as function of temperature, concentration of substance that deactivates the catalyst (which can be reactant, product or impurities) and present activity of the catalyst pellet. Hence, deactivation rate can be given as,

$$-\frac{da}{dt} = k_d C_i^{n'} a^d$$

i = A (reactant), R (product) , P(3^{rd} substance)

Here d is called order of deactivation, k_d is deactivation rate constant and **n´** is the concentration dependency.

Deactivation rate for different types.

1. Parallel , $A \rightarrow R + P \downarrow$

Reaction rate is $-r_A' = kC_A^n a$

Deactivation rate is $-\frac{da}{dt} = k_d C_A^{n'} a^d$ d = order of deactivation

2. Series $A \rightarrow R \rightarrow P \downarrow$

Reaction rate is $-r_A^{'} = kC_A^n a$

Deactivation rate is $-\frac{da}{dt} = k_d C_R^{n'} a^d$

3. Side-by-side deactivation , $A \rightarrow R$, $P \rightarrow P \downarrow$

Reaction rate is $-r_A^{'} = kC_A^n a$

Deactivation rate is $-\frac{da}{dt} = k_d C_P^{n'} a^d$

4. Independent deactivation

Reaction rate is $-r_A^{'} = kC_A^n a$

Deactivation rate is $-\frac{da}{dt} = k_d a^d$

Deactivation kinetics for sintering

Most commonly used decay law for sintering is second order with respect to present activity.

$$\mathbf{r_d = -\frac{da}{dt} = k_d\ a^2}$$

The k_d is the sintering decay constant. Integration with a=1 at time t=0 gives

$$\mathbf{a(t) = \frac{1}{1 + k_d t}} \qquad (1)$$

Activity can be measured in terms of amount of sintering. If the total active surface area of the catalyst is S_{ao} at t = 0 and S_a at any time t, then activity can be written as

$$\mathbf{a(t) = \frac{S_a}{S_{ao}}} \qquad (2)$$

From equation (1) and (2)

$$S_a = \frac{S_{ao}}{1 + k_d t}$$

The sintering decay constant k_d is given as

$$k_d = k_d(T_o) \exp\left[\frac{E_d}{R}\left(\frac{1}{T_o} - \frac{1}{T}\right)\right]$$

E_d is the decay activation energy. For reforming of heptanes on Pt /Al_2O_3 value of E_d is in the order of 70 kcal/mol.

Deactivation kinetics for coking or fouling

Various empirical relations are available for calculation of amount of coke deposited on catalyst surface after a time t.

$$C_c = At^n \qquad (3)$$

C_c is the concentration of carbon on the surface in g/m^2. The 'n' and 'A' are fouling parameter functions of feed rate. Representative value of A and n for cracking of light gas oil is 0.47 and 0.5 respectively when 't' is in minute.

The activity can be related to amount of coke deposited on the surface by following relation :

$$a = \frac{1}{1 + k_c C_c^p}$$

Substituting value of C_c from relation (3), in term of process time, activity can be expressed as shown below.

$$a = \frac{1}{1 + k_c \left(At^n\right)^p} = \frac{1}{1 + k_c A^p t^{np}} = \frac{1}{1 + k' t^m}$$

or

$$\mathbf{a = \frac{1}{1 + 7.6t^{1/2}}} \qquad \because \mathbf{t \text{ in seconds}}$$

Other dimensionless fouling correlations are also developed by several groups.

Deactivation kinetics for poisoning

For petroleum feed containing trace impurities such as sulfur, the poisoning reaction can be written as $\mathbf{P + S \rightarrow PS}$

The rate of deactivation is given as

$$\mathbf{r_d = -\frac{da}{dt} = k_d^{'} C_p^m a^q}$$

The C_p is the concentration of poison in feed. The 'm' and 'q' are respective orders.

The rate of removal of poison from the reactant by catalyst sites is proportional to the number of sites that are not poisoned (C_{to} - C_{ps}) and concentration of poisons in the gas phase, C_p. The C_{ps} is the concentration of poisoned sites and C_{to} is the total number of fresh sites initially available. Then rate of removal of poison is equal to rate of formation of poisoned site and is given as

$$\mathbf{\frac{dC_{ps}}{dt} = r_{ps} = k_d \left(C_{to} - C_{ps} \right) C_p} \qquad (4)$$

Dividing throughout by C_{to} and if 'f' is the fraction of the total number of the sites that have been poisoned then equation (4) can be written as

$$\mathbf{\frac{df}{dt} = k_d \left(1 - f \right) C_p} \qquad \because \mathbf{f = \frac{C_{ps}}{C_{to}}} \qquad (5)$$

The fraction of sites available for adsorption (1-f) is essentially the activity a (t). Then equation (5) becomes

$$\mathbf{-\frac{da}{dt} = a_t k_d C_p}$$

Determination of deactivation kinetic parameters

Case 1 : Consider a reaction in a mixed reactor under constant flow condition. Let independent deactivation occur. Assume both the main reaction and deactivation reaction to be first order with respect to activity 'a'.

Then,

Reaction rate $-r_A = kC_A a$ (6)

Deactivation rate $-\frac{da}{dt} = k_d a$ (7)

Integrating equation (7)

$$-\int_{a_0}^{a} \frac{da}{a} = k_d \int_0^t dt$$

Or $\left[\ln a\right]_{a_0}^{a} = -k_d t$ a_o is initial activity

$$\ln \frac{a}{a_0} = -k_d t \quad \text{or} \quad \frac{a}{a_0} = \exp\left(-k_d t\right)$$

or $a = a_0 \exp\left(-k_d t\right)$

or $a = \exp\left(-k_d t\right)$ $\because a_0 = 1$

For mixed reactor , $\frac{W}{F_{A0}} = \frac{X_A}{-r_A}$

Substituting expression for rate from equation (6)

$$\frac{W}{F_{A0}} = \frac{X_A}{kC_A a}$$

Now , $X_A = 1 - \frac{C_A}{C_{A0}} = \frac{C_{A0} - C_A}{C_{A0}}$

Hence, substituting for X_A , $\frac{W}{F_{A0}} = \frac{X_A}{kC_A a} = \frac{C_{A0} - C_A}{kC_{A0}C_A a}$

Or $\frac{WkC_{A0}a}{F_{A0}} = \frac{C_{A0} - C_A}{C_A}$ Or $\frac{WkC_{A0}a}{F_{A0}} = \frac{C_{A0}}{C_A} - 1$

Or $\frac{C_{A0}}{C_A} - 1 = ka\left[\frac{WC_{A0}}{F_{A0}}\right]$

Or $\frac{C_{A0}}{C_A} - 1 = ka\tau_w$ $\because \tau_w = \frac{WC_{A0}}{F_{A0}}$. (8)

τ_w is called the weight time similar to space-time τ . C_A and 'a' vary with time.

Substituting, $a = \exp\left(-k_d t\right)$ in equation (8)

Or $\frac{C_{A0}}{C_A} - 1 = k\tau_w \exp\left(-k_d t\right)$

Or $\ln\left[\frac{C_{A0}}{C_A} - 1\right] = \ln\left(k\tau_w\right) - k_d t$

Plotting $\ln\left[\frac{C_{A0}}{C_A}-1\right]$ versus 't' gives a straight line of slope of $-k_d$ and intercept $\ln(k\tau_w)$

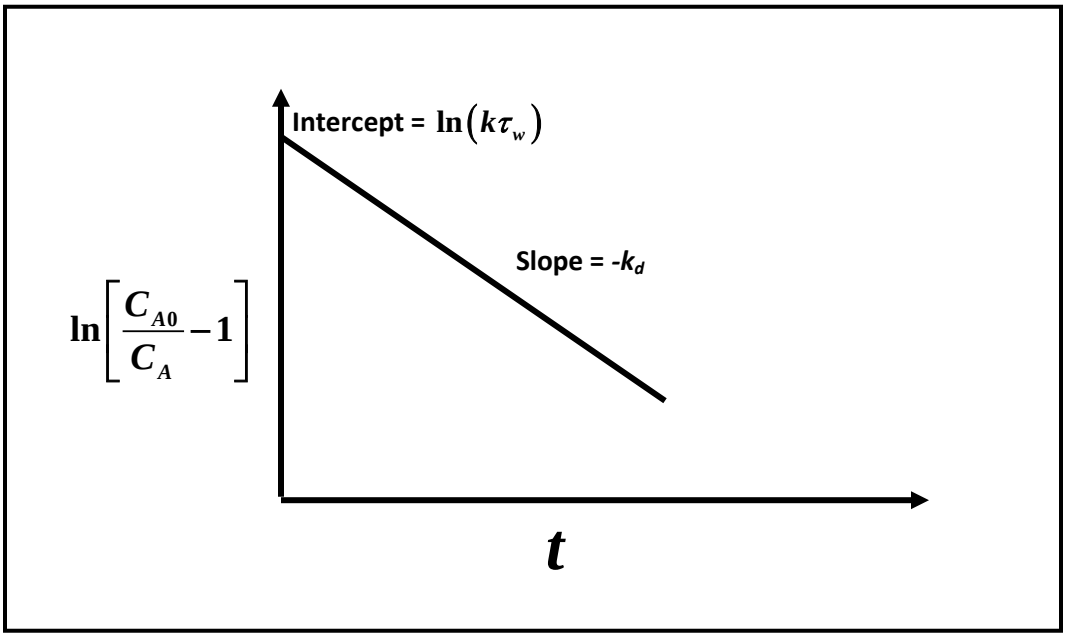

Fig. 1. Plot to determine the rate constant and the deactivation rate constant for a reaction over deactivating catalyst. (For mixed reactor, constant flow and independent deactivation)

Case II : Consider a reaction in a mixed reactor under changing flow condition so that concentration is constant. Let parallel deactivation occur. Assume the main reaction to be n^{th} order and the deactivation reaction to be of first order in activity 'a'.

Parallel deactivation

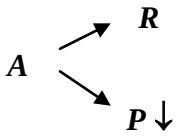

Rate equation $-r_A = kC_A^n a$

Deactivation rate $-\frac{da}{dt} = k_d C_A^m a^d$

Since concentration is constant,

$-r_A = kC_A^n a = k' a \qquad \because k' = kC_A^n$

$$-\frac{da}{dt} = k_d C_A^m a^d = k_d^{'} a^d \qquad \because k_d^{'} = k_d C_A^m$$

For mixed reactor ,

$$\frac{W}{F_{A0}} = \frac{X_A}{-r_A} = \frac{X_A}{k^{'} a} = \frac{C_{A0} - C_A}{k^{'} a C_{A0}}$$

Or $$\frac{W C_{A0}}{F_{A0}} = \frac{C_{A0} - C_A}{k^{'} a}$$

Or $$\tau_w = \frac{C_{A0} - C_A}{k^{'} a} \qquad \because \tau_w = \frac{W C_{A0}}{F_{A0}} \qquad (9)$$

Now , $$-\frac{da}{dt} = k_d^{'} a^d$$

For first order activity , d =1

Again , $$a = \exp\left(-k_d^{'} t\right) \qquad \because a_0 = 1$$

Then substituting ‘ a ’in equation (9)

$$\tau_w = \frac{C_{A0} - C_A}{k^{'} a} = \frac{C_{A0} - C_A}{k^{'} \exp\left(-k_d^{'} t\right)} = \frac{C_{A0} - C_A}{k^{'}} \frac{}{\exp\left(-k_d^{'} t\right)}$$

Or $$\ln \tau_w = \ln\left[\frac{C_{A0} - C_A}{k^{'}}\right] + \ln\left(k_d^{'} t\right)$$

Plotting $\ln \tau_w$ versus 't' gives a straight line of slope of k_d' and intercept $\ln\left[\frac{C_{A0}-C_A}{k'}\right]$.

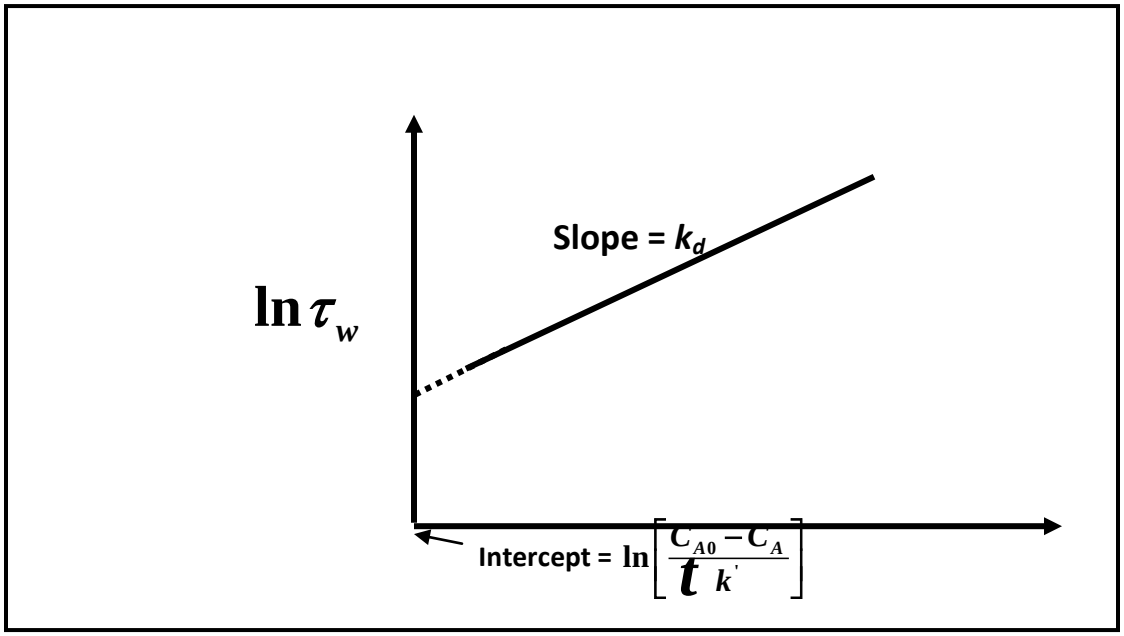

Fig. 2 . Plot to determine rate constant and deactivation rate constant for a reaction over deactivating catalysts for mixed reactor, changing flow condition and parallel deactivation

Book Reference :

- O. Levenspiel , Chemical reaction engineering, John Wiley & sons. 1995
- R. J. Farrauto & C. H. Bartholomew, Fundamentals of Industrial catalytic Processes, Blackie Academic & Professional, 1997
- H. S. Fogler, Elements of Chemical reaction engineering, Prentice Hall of India, 1999
- J. M. Smith, Chemical Engineering Kinetics, McGrawHill Book Company, 1981
- J.J. Carberry , Chemical and catalytic reaction Engineering, Dover Publications, 2001

Lecture 26

Industrial catalytic processes

Industrial catalytic processes can be broadly classified into five major sectors as shown in Fig. 1

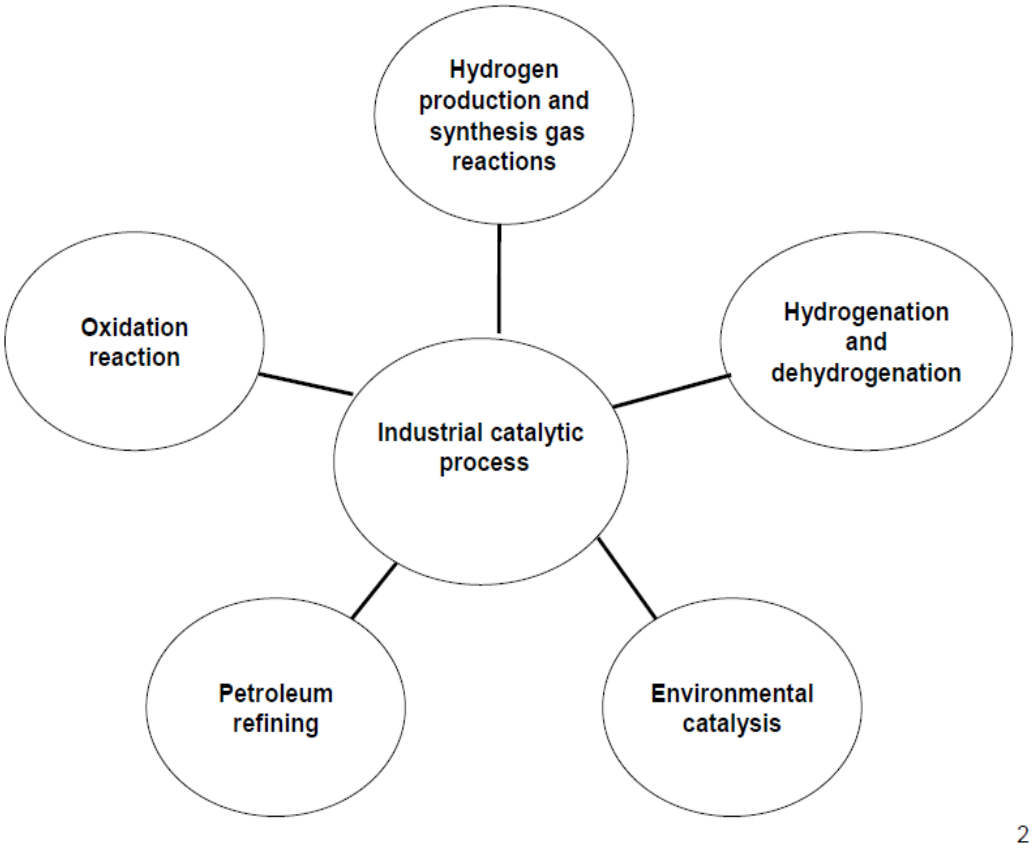

Fig. 1. Classification of industrial catalytic processes

In this section, few representative processes will be discussed emphasizing on the catalyst used, reaction kinetics and catalyst deactivation, if any.

Steam reforming

Synthesis gas or hydrogen is produced most commonly by steam reforming of hydrocarbons. Feed is mostly natural gas or naphtha. Overall process involves mainly six catalytic steps :

1. Purification of hydrocarbons

2. Primary steam reforming

3. Secondary steam reforming

4. High temperature water gas shift reaction

5. Low temperature water gas shift reaction

6. Methanation

Fig 2 shows the schematic flow diagram for hydrogen production by steam reforming of natural gas. The various catalytic steps are discussed below.

Purification of hydrocarbons

Sulfur and chloride compounds in the feed act as catalyst poisons. Therefore, before the reforming process, feed is treated to remove these compounds. Sulfur is removed by desulphurization followed by scrubbing by ZnO adsorbent. By this process, sulfur is reduced to less than 0.01 ppm

$$R\text{-}S + H_2 \xrightarrow{CoMo/Al_2O_3} H_2S + R\text{-}H$$ Hydrodesulfurization

$$H_2S + ZnO \longrightarrow ZnS + H_2O$$ Scrubbing by adsorbent

Chloride is removed by scrubbing using alkali treated alumina to 5 ppb level.

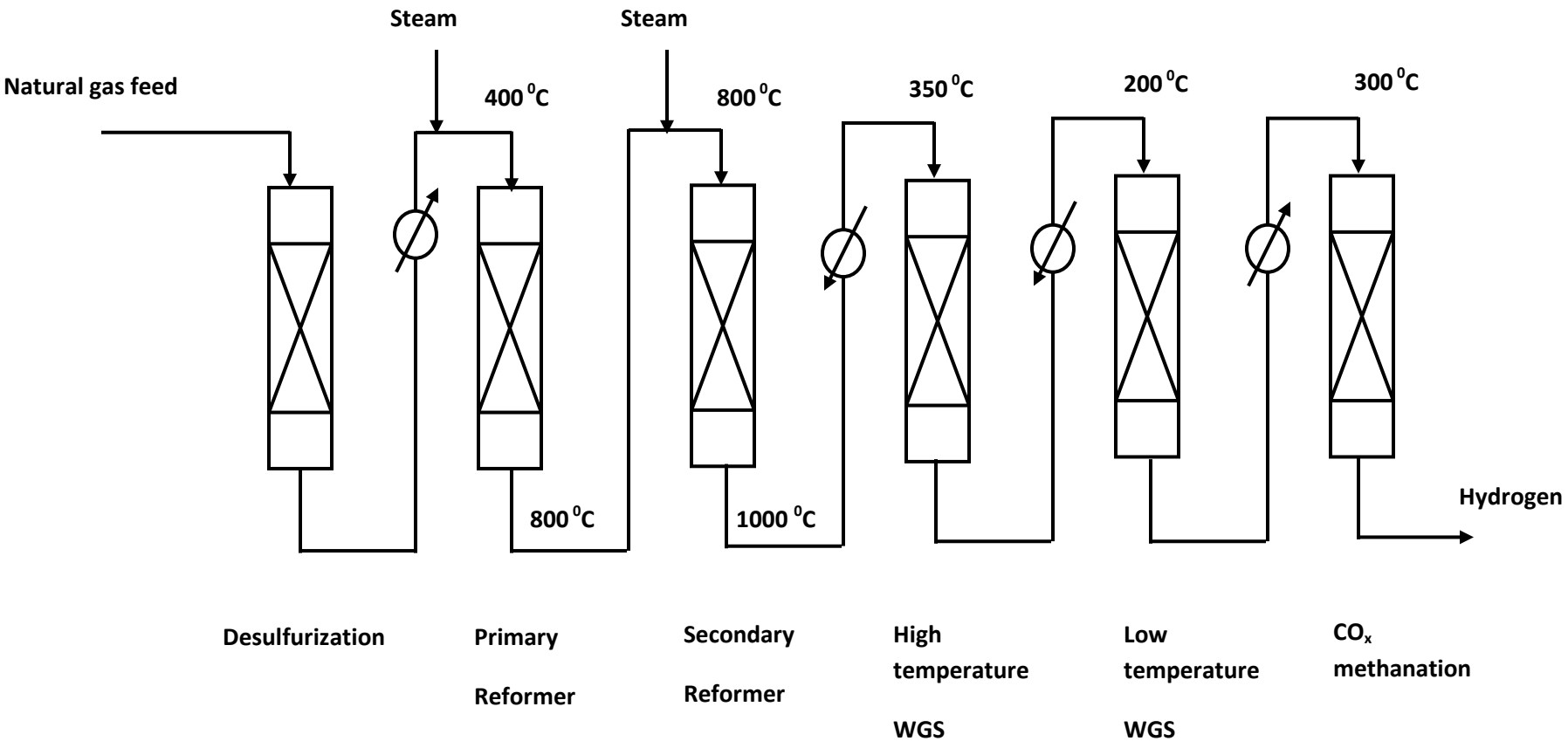

Fig. 2. Schematic flow diagram for hydrogen production from steam reforming of natural gas

Primary steam reforming

For steam reforming of natural gas, which mostly consists of methane, the overall reaction is given as :

$$CH_4 + H_2O = CO + 3H_2 \qquad \Delta H^o_{298K} = +\ 206\ \text{kJ/mol}$$

This reaction is always accompanied with methanation and water gas shift reaction.

$$\textit{Methanation} \quad CO + 3H_2 = CH_4 + H_2O \qquad \Delta H^o_{298K} = -\ 206\ \text{kJ/mol}$$

$$\textit{WGS} \quad CO + H_2O = CO_2 + H_2 \qquad \Delta H^o_{298K} = -\ 41.2\ \text{kJ/mol}$$

The overall process is endothermic and heat is supplied to the reformer. Relative amount of H_2 and CO can be adjusted by process conditions. Since the overall steam reforming reaction is highly endothermic and the product volume is greater than that of the reactants, equilibrium favors the forward reaction at high temperature and low pressure. High steam to methane ratio and high temperature favors conversion of CH_4. As temperature is lowered, the slightly exothermic WGS reaction becomes increasingly more favorable. Higher steam to methane ratios at lower temperature result in lower CO concentration. The H_2 to CO ratio thus depends on operating temperature for steam reforming and water gas shift reactions.

Process

A schematic diagram depicting the typical reaction conditions in primary steam reforming is shown in Fig. 3. For primary steam reforming, the outlet temperature is limited to about 800 ^{0}C to prevent damage to the reactor. Though the reaction is thermodynamically favored at low pressure, a higher pressure is used to increase the reaction rate and throughput, thereby minimizing the reactor volume.

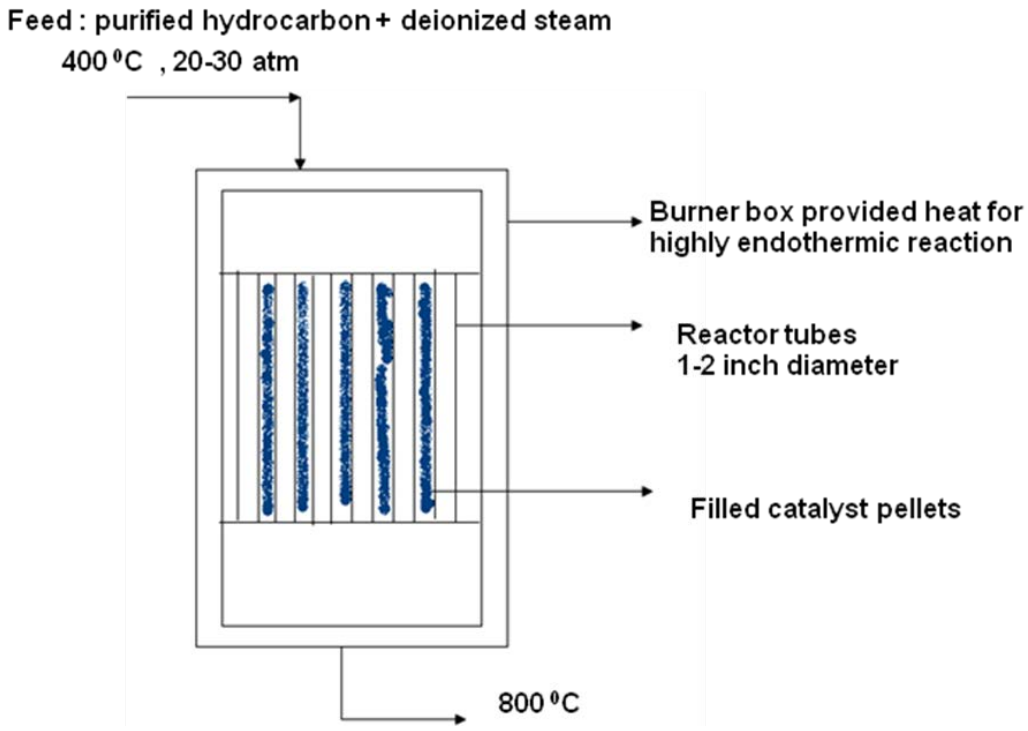

Fig. 3. Schematic diagram showing steam reforming reaction conditions

Operating condition for methane and naphtha steam reforming are very different. For methane steam reforming the reformer exit temperature is typically 800 -900 ^{0}C and

H_2O **:** CH_4 ratio is 1.8 -3. In naphtha steam reforming exit temperature is lower 600-800 ^{0}C and H_2O **:** C ratio is higher 2.5-4.5. In both cases pressure is maintained at 20-30 atm.

Catalysts

Bifunctional catalysts are needed for steam reforming reaction. Two catalytic functions are :

– Metal site for dissociative adsorption of hydrocarbon

– Oxide site for dissociative adsorption of water

Oxide sites are generally located on the surface of the supports. Support also stabilizes the well dispersed metallic phase. Because of the severe high temperature reaction conditions, catalyst must have high thermal stability. The typical decreasing activity order for metals is Rh, Ru > Ni> Pd, Pt >Ni-Cu >Co. This order varies with hydrocarbon.

Pt and Pd are less active than Ni for steam reforming of naphtha, however are more active than Ni for steam reforming of toluene. Noble metals are more resistant to carbon deposition and more tolerant to sulfur poisoning than Ni. However, because of greater availability and lower cost, Ni is the preferred metal catalyst for commercial applications. Thermally stable supports of low acidity are needed to prevent deactivation by sintering and carbon depositions.

The order of decreasing acidity of supports:

SiO_2-Al_2O_3 > SiO_2-MgO> SiO_2>>Al_2O_3>TiO_2>ZrO_2 >CaO, MgO

Thus CaO, MgO are most desirable supports to prevent carbon depositions. These are also among most thermally stable supports. Promoters such as 'potassium alumino - silicate lower the acidity of supports and catalyze carbon gasification with steam.

Typical catalysts for steam reforming consist of NiO / Ca Al_2O_4 or NiO / Al_2O_3. Steam reforming catalysts are chemically and mechanically rugged to maintain physical and chemical integrity in harsh high temperature and high steam environment. Surface area of carrier is low, typically 5-50 m^2/g but adequate for dispersing NiO and maintaining thermal stability. Support is impregnated with nickel nitrate solution a number of times to achieve proper loading. Active catalyst is metallic Ni. Therefore, NiO after calcinations, is reduced by H_2 prior to reaction. Catalysts are formed into relatively large Raschig rings, grooved pellets, wheels etc. for low pressure drop and minimum pore diffusion limitations.

Table 1. Activation energies reported for steam reforming process over various catalysts

Catalyst	Activation energy kJ/mol	Reaction	Reference
$Rh/Ce_{\alpha}\ Zr_{1-\alpha}\ O_2$	84	Methane steam reforming	1
Rh/Ga-Ce	92		1
$Rh/\gamma\text{-}Al_2O_3$	109		1
$Cu/ZnO/Al_2O_3$	101	Methanol steam reforming	2
Ni-based catalyst	96	Methane steam reforming	3

Kinetics and mechanism

Mechanistically, steam reforming involves decomposition of hydrocarbons on metal surface to hydrocarbon fragments. Water undergoes dissociative adsorption to adsorb oxygen atoms and molecular hydrogen. Adsorbed oxygen atom combines with adsorbed hydrocarbon to form CO. The kinetic model proposed by Rostrup and Nielsen [4] is as follows

$$C_nH_m + 2S \xrightarrow{k_A} C_nH_z - S_2 + \frac{m-z}{2}H_2$$

$$C_nH_z - S_2 + nS \xrightarrow{k_H} C_{n-1}H_{z'} - S_2 + CH_x - S_n$$

$$CH_x - S_n + O - S \xrightarrow{k_r} CO + \frac{x}{2}H_2 + (n+1)S$$

$$H_2O + S \underset{}{\overset{K_W}{\rightleftharpoons}} O - S + H_2$$

$$H_2 + 2S \underset{}{\overset{K_H}{\rightleftharpoons}} 2H - S$$

The corresponding rate was derived as

$$r = \frac{k_A p_{c_nH_m}}{\left[1 + \frac{nk_A}{k_r K_W}\frac{p_{H_2}}{p_{H_2O}} p_{c_nH_m} + K_W\left(\frac{p_{H_2O}}{p_{H_2}}\right) + \sqrt{k_H p_{H_2}}\right]^{2n}}$$

Industrial steam reforming reaction is strongly influenced by pore diffusion resistance and therefore apparent activation energies are lower compared to surface reaction controlled system. Activation energy for nickel based catalyst for steam reforming reaction 106 kJ/mol and that for water gas shift reaction 55 kJ/mol [5]. The effectiveness factor is in the range of 0.05- 0.65 [5]

Deactivation

Sulfur and chlorides act as catalyst poisons. As mentioned earlier, the feed is initially pretreated for sulfur and chloride removal. Another major source of deactivation is coke deposition on the catalyst. Formation of carbon occurs by decomposition of hydrocarbon and CO on the surface of catalysts

$$\mathbf{C}_n\mathbf{H}_m \longrightarrow nC + (m/2)H_2$$
$$2CO \longrightarrow C + CO_2$$

Gas phase non catalytic pyrolysis of hydrocarbons also contributes to coke deposition.

All of these processes are favored at high temperature. High temperature also results in sintering, growth of metal crystallites and collapse of catalyst support which can cause decrease in activity.

Carbon can be removed by steam gasification. Carbon deposition can be avoided by operating at sufficiently high H_2O to C ratio.

Secondary steam reforming

The exit gas from the primary reformer contains about 10-13 % CH_4 which is further reformed in secondary reformer. Inlet temperature is 800 ^{0}C and the outlet temperature is 900-1000 ^{0}C. These high temperatures drive the forward reaction and reduce the CH_4 content to less than 1%. Outlet CO concentration is 10-13 %. Reactor is lined with ceramic material to prevent damage.

Catalysts

Catalyst must be able to withstand the severe high temperature. Typical catalysts are Ni supported on alumina or CaO substituted alumina. Potassium is not added due to volatility at this high temperature. Total BET surface area and surface area of active nickel for secondary reforming catalysts are smaller than that of primary reforming catalysts. This is because they are initially calcined at high temperature so that they are thermally stable at process conditions.

Water gas shift reaction

Water gas shift reactions are carried out at conditions of high and low temperature. For the water gas shift reaction, the equilibrium favors the reaction at lower temperature. However, copper based catalyst, active at low temperature, is highly sensitive to residual sulfur or chloride compounds which have passed through the pre-purification steps. Hence, initially the reaction is carried out over catalyst composed of Fe_2O_3 and Cr_2O_3 which is relatively inexpensive, resistant to sintering and tolerant to sulfur and chloride poisoning. However, at low temperature Fe_3O_4 is not sufficiently active hence, the reaction has to be carried out at higher temperature. The high temperature catalyst adsorbs the residual sulfur or chloride compounds thereby, protecting the low temperature copper based shift catalyst from exposure to these compounds. The high temperature process is followed by shift reaction at thermodynamically favorable lower temperature of 200 ^oC over copper based catalyst.

High temperature water gas shift reaction

Gas from the secondary reformer contain 10-13 % CO and is further processed to increase the H_2 concentration. The high temperature water gas shift reaction lowers the CO concentration to about 2-3 % in a fixed bed reactor.

$$CO + H_2O = CO_2 + H_2$$

Process is operated at 350-500 ^0C and 20 -30 atm. Since equilibrium favors the WGS at lower temperature, the feed gas is cooled to 350-400 ^0C before entering the reactor.

Catalysts :

A typical catalyst is composed of 90 % Fe_3O_4 and 10 % Cr_2O_3. Fe_3O_4 acts as the active metal while Cr_2O_3 acts as a stabilizer to minimize sintering of the active iron oxides. The catalysts are prepared by precipitation.

Kinetics

The rate expression from Langmuir Hinshelwood model proposed is given as [4] :

$$r = \frac{kK_{CO}K_{H_2O}\left(P_{CO}P_{H_2O}P_{CO_2}P_{H_2}\right)^2}{\left(1 + K_{CO}P_{CO} + K_{H_2O}P_{H_2O} + K_{CO_2}P_{CO_2} + K_{H_2}P_{H_2}\right)^2}$$

k is the rate constant and K_i's the respective adsorption constants. The 'i' represents the chemical species.

Activation energy for the water gas shift reaction on iron oxide/chromia is in the range of 122 kJ/mol. Reaction over small pellets (5×4 mm) operates with an effectiveness factor of unity below 370 ^{0}C and 31 atm.

Deactivation

The catalyst is deactivated by adsorption of residual S or Cl containing compounds that escape the initial purification steps.

Low temperature water gas shift

The CO concentration of the existing gas from high temperature WGS is 2-3 % and

further reduced to below 0.2 % by low temperature water gas shift reaction. The WGS reaction as favored at low temperature, operating temperature is maintained at 200 ^{0}C, the minimum temperature at which steam is not condensed and operating pressure at 10-30 atm.

Catalysts

A typical catalyst is composed of CuO/ ZnO/Al_2O_3 and prepared by co-precipitation method. The catalyst is highly selective for shift reaction with low activity for methanation reaction. CuO is the catalytically active metal and ZnO minimize sintering of Cu. Cu is highly sensitive to poisoning by S or Cl compounds even at very low level of 1 ppm. ZnO & Al_2O_3 also scavenge the S or Cl compounds protecting Cu which is highly sensitive to poisoning by these compounds. Catalyst is reduced very carefully by H_2 and the bed temperature is never allowed to rise above 230 ^{0}C to avoid sintering of Cu. The high temperature shift catalyst also protects the low temperature catalyst from these poisons.

Kinetics

Kinetic model is based on surface redox mechanism involving dissociation of water to OH radicals which further dissociate to atomic oxygen. The rate expression as proposed by Ovensen et al.[2] is

$$r = A\exp\left(\frac{-E_a}{RT}\right) p_{CO}^m p_{H_2O}^n p_{co_2}^x p_{H_2}^y \left(1-\beta\right) \qquad \beta = \frac{1}{K_{WGS}} \frac{p_{CO_2} p_{H_2}}{p_{CO} p_{H_2O}}$$

A= pre-exponential factor; E_a= activation energies; m, n, x, y = respective reaction orders; β defined as approach to equilibrium and K_{WGS} is equilibrium constant for WGS reaction.

Final CO/CO_2 removal by methanation

After low temperature WGS, the CO content in hydrogen stream is 0.2-0.5 % and must be reduced to 5 ppm level for using the H_2 for ammonia synthesis. The CO is further reacted with hydrogen and converted to methane. The catalyst is typically Ni/Al_2O_3 . MgO is sometimes used as a promoter to minimize sintering of Ni. The process is carried out at 300 -350 ^{0}C and at 30 atm pressure. Care must be taken to avoid formation of poisonous $Ni(CO)_6$ which occurs below 200 ^{0}C at partial pressure of CO greater than ~ 0.2 atm.

Book reference:

- C. H. Bartholomew and R. J. Farrauto, Fundamentals of Industrial catalytic Processes, Wiley, VCH, 2006

Publication reference:

1. M.H Halabi M.H.J.M de Croon, J. van der Schaaf, P.D. Cobden, J.C. Schoulen , Applied catalysis A Gen. 389 (2010) 80-91
2. J. Agrell, H. Birgersson, M. Boutonnet, Journal of Power Sources 106 (2002) 249–257
3. M. Zeppieri, P.L. Villa, N. Verdone, M. Scarsella, P. De Filippis, Applied Catalysis A: General 387 (2010) 147–154
4. J.R . Rostrup –Nielsen , Catalysis Science and technology eds. J.R. Anderson and M. Boudart, Springer –Verlag , Newyork,1984
5. T. Numaguchi and K.Kikuchi, Chemical Engineering Science 43(1988) 2295-2301

Lecture 27

Petroleum refining industry

Petroleum refining industry extensively involves heterogeneous solid catalytic processes. The major catalytic processes are shown in Fig 1.

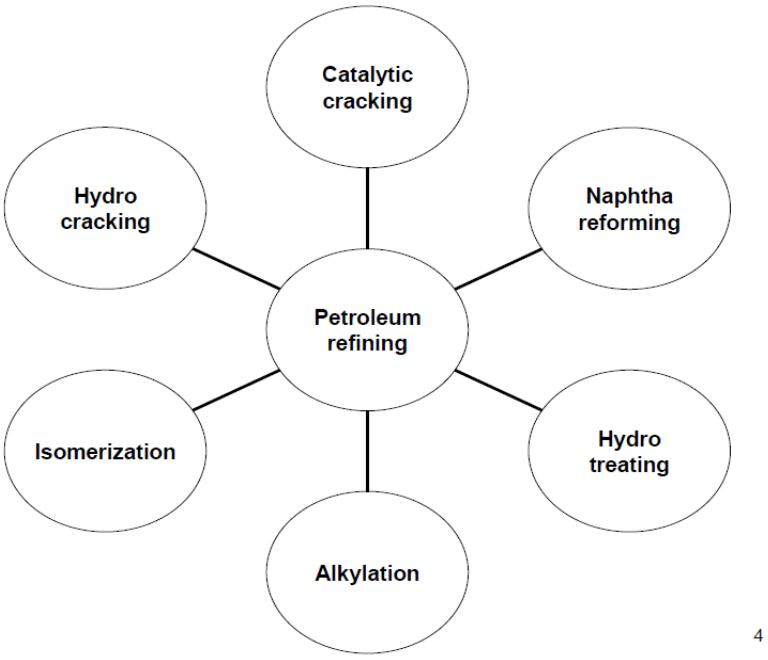

Fig. 1. Various solid catalytic processes in petroleum refining industries

Catalytic cracking

Catalytic cracking of gas oil is among the most important catalytic processes and major source of fuels. This process involves simultaneous occurrence of various reactions. Some typical reactions in catalytic cracking process are shown in Fig. 2.

1. Large alkane cracking
   a. $C_{14}H_{30} \rightarrow C_7H_{16} + C_7H_{14}$
2. Dealkylation of branched aromatics

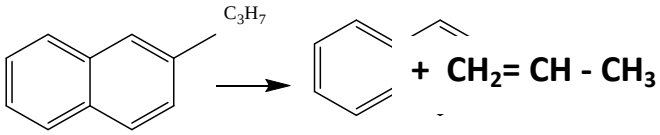

3. Naphthene cracking

4. Hydrogen transfer

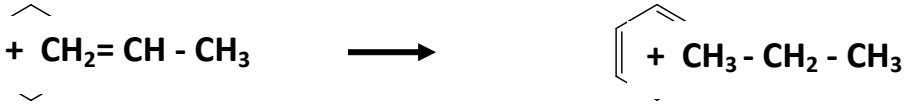

5. Isomerization

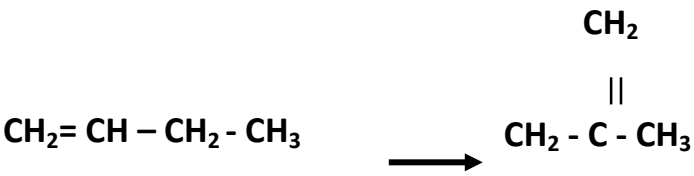

Fig. 2. Some typical reactions in catalytic cracking process

Process

Usually catalytic cracking of gas oil is carried out at 500-550 ^{0}C at 2-3 atm pressure, in a fluidized bed reactor. In the fluidized bed reactor, most of the cracking occurs in the transport-line (riser). Catalyst to oil weight ratio is usually maintained at 4 -6 with residence time of 2-6 seconds in the riser reactor. The gasoil feed stock is usually consist of C_{20}-C_{40} in the boiling range of 350 -550 ^{0}C. Catalyst circulation rate of about 6 ton/m^3 of total feed is maintained for smooth operation. The schematic diagram of a typical fluidized catalytic cracking reactor is shown in Fig. 3.

Catalyst

Common cracking catalysts are amorphous SiO_2-Al_2O_3 and zeolites. Zeolites are alumino-silicates with well- defined crystalline structures having molecular size pores that give rise to its shape selective properties. Zeolites are discussed in detail in later sections. The product distribution in catalytic cracking process also depends on the type of catalyst. The SiO_2-Al_2O_3 catalyst gives higher alkene yield while zeolite catalyst result in higher aromatic yield.

The typical commercial cracking catalyst is a mixture of zeolite and SiO_2 –Al_2O_3. The catalyst can contain 3-25 wt.% zeoliteY. The zeolite is usually ion exchanged with rare earth ions such as La^{+3} or Ce^{+3} to provide additional thermal stability. The balance of mixture is SiO_2-Al_2O_3, similar to the original amorphous cracking catalyst. The function of acidic SiO_2-Al_2O_3 is to crack the large feed molecules to a size which can diffuse into the zeolite channels for further reactions. The alumino-silicate matrix also protects the zeolite from poisons and attrition. The catalyst particles are of 40-100 μm in diameter with pore sizes in the range of 8-10 nm. Surface area of the zeolite ranges from 600-800 m^2/g, whereas, the surface area of the alumino-silicate matrix is in the range of 100-300 m^2/g.

Additives are added to cracking catalyst and constitute about 5 wt. % of catalyst. Commonly used additives include octane boosting additives such as ZSM-5, metal passivators, SO_x reducing agents, and CO oxidation catalyst. Addition of 1-3 wt. % of ZSM-5 increases octane number while decreases gasoline yield. Nickel increases gas and

coke selectivities while vanadium destroys the zeolite lowering the activity. These undesirable effects of Ni can be minimized by adding a passivator such as a compound of antimony and bismuth to the process stream to react selectively with the Ni to form a catalytically inactive Ni-Sb or Ni-Bi species. These are added commonly as organometallic solutions to the process stream.

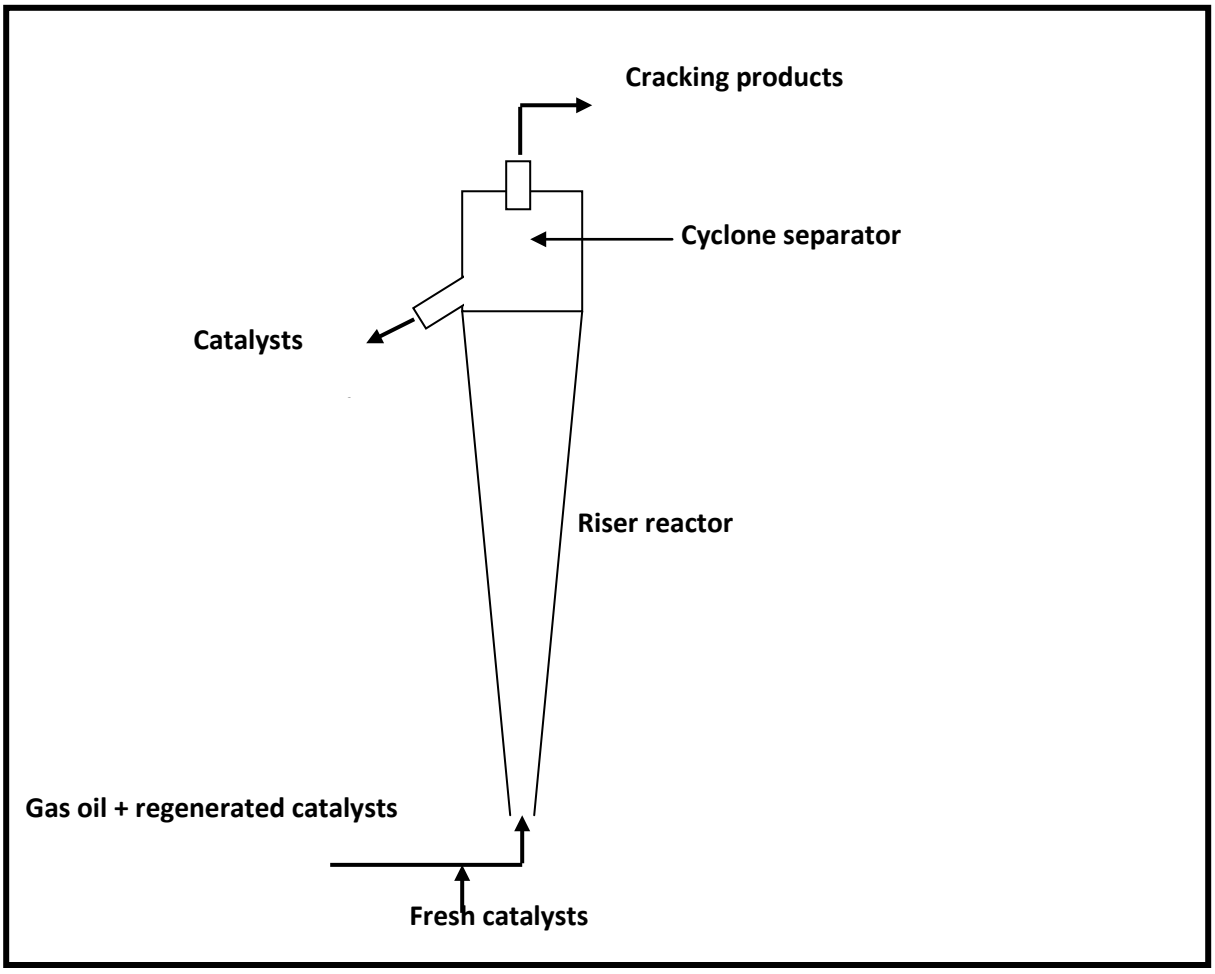

Fig. 3. Schematic diagram for catalytic cracking in Riser reactor.

Mechanism and kinetics

Cracking reactions involve C-C bond rupture via formation of carbocations. Reaction is catalyzed by acid sites on SiO_2-Al_2O_3 and zeolites catalysts. Carbocations are formed on Bronsted and Lewis acid sites of the catalysts. A typical mechanism for catalytic cracking of alkane initiated by protonation is given below:

$$R_1 - CH_2 - CH_2 - R_2 + HZ \rightleftharpoons R_1 - CH_2 - CH_3^+ - R_2 + Z^-$$

$$R_1 - CH_2 - CH_3^+ - R_2 \longrightarrow R_1^+ + CH_3 - CH_2 - R_2$$

$$R_1 - CH_2 - CH_3^+ - R_2 \longrightarrow R_1 - CH_2 - CH^+ - R_2 + H_2$$

$$R_1 - CH_2 - CH^+ - R_2 \longrightarrow R_1^+ + CH_2 = CH - R_2$$

A detailed micro kinetic model for gas oil cracking involve hundreds of elementary reaction steps for which kinetic parameters are to be determined. Due to this complexity of cracking process, the kinetic study of these reactions is extremely difficult. For simplification, the reaction steps and products are combined into groups of species. These groups are called lumps and each lump is considered as an independent entity. This is known as lumped kinetic technique.

A three lumped model proposed by Wojciechowski and Corma [3] for gas oil cracking is shown in Fig. 4. Simple parallel- series kinetic network involves reactions of gas oil to gasoline /diesel (path 1) or to gases/coke (path 2). The gasoline and diesel can further react to give gas and coke.

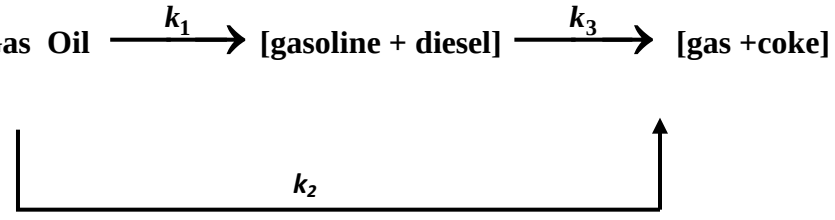

Fig. 4. Three Lumped kinetic model for catalytic cracking of gas oil

The corresponding reaction kinetics was proposed to be first order with respect to each hydrocarbon component of the feed reacting by path 1 or 2.

$$\frac{dC_A}{d\tau} = (k_1 + k_2)C_A = kC_A \text{ ---------(1)}$$

τ = spacetime in a fixed -bed plug flow reactor

C_A =gas oil concentration

k_1 , k_2 = first order rate contants

To account for rapid catalyst decay, each of the rate constants was modified using a time –on-stream functions:

$$k_i = k_{io}(1+Gt)^{-N}(C_A / C_{A_0})^W$$

G= Modified deactivation rate constants [G=(m-1)k_d]

m = true deactivation order

N =modified deactivation order = [1/m + 1]

W= refractory index accounting for difficulty of cracking residue as reaction progress

Upon substituting the modified rate constants for k_1 and k_2 into equations (1) and inserting this expression in equation for plug flow and integrating, an expression was obtained by Wojciechowski and Corma [3] which relates instantaneous conversion $\mathbf{X_A}$ to the time of reaction $\mathbf{t_f}$ while accounting for volume expansion $\boldsymbol{\varepsilon_A}$.

$$(k_{10} + k_{20})(1+Gt)^{-N} Pbt_f = \int_0^{X_A} \left[\frac{1+\varepsilon_A X_A}{1-X_A}\right]^{1+W} dX_A$$

b = constant and P= catalyst to oil ratio

This above model although useful for modeling the kinetics of gas oil cracking, was highly empirical and could not be generalized for kinetics of catalytic cracking.

A five lump kinetic model (Fig 5a) was proposed to describe the gas oil catalytic cracking (FCC) process by Ancheyta-Juárez et al.[4]. The model contained eight kinetic constants, including one for catalyst deactivation. The model included unconverted gas oil, gasoline, LPG, dry gas and coke as lumps. The activation energies of the various steps were in the range of 9-13 kcal/mol. Even seven lump kinetic models for fluid catalytic cracking, as shown in Fig. 5b, are reported in literature. The shown seven-lump model involved residual oil, heavy lump, light lump, gasoline, liquefied petroleum gas, dry gas and coke [5]. The VGO, HFO and LFO in Fig 5b are vacuum gas oil, heavy fuel oil and light fuel oil respectively.

Deactivation

The major sources of catalyst deactivation are

1. Coke formation
2. Deactivation by metals such as Ni, V
3. Sintering

Coke formation on the catalyst surface is the major deactivation source for catalytic cracking catalysts. Very high rate of coke formation results in very low residence time of catalysts in the reactor and high regeneration frequency. The metal residue in the feed can also affect the performance and activity of the catalysts. Nickel increases gas and coke selectivities while vanadium is reported to destroy zeolites and lowers the activity. The effects of metals can be prevented by adding metal passivators. Antimony or bismuth compound can be added which form Ni-Sb or Ni- Bi alloy. Magnesium orthosilicate is also added to form $MgO\text{-}V_2O_5\text{-}SiO_2$. At severe conditions of high temperature and steam, zeolite structure gradually deteriorates.

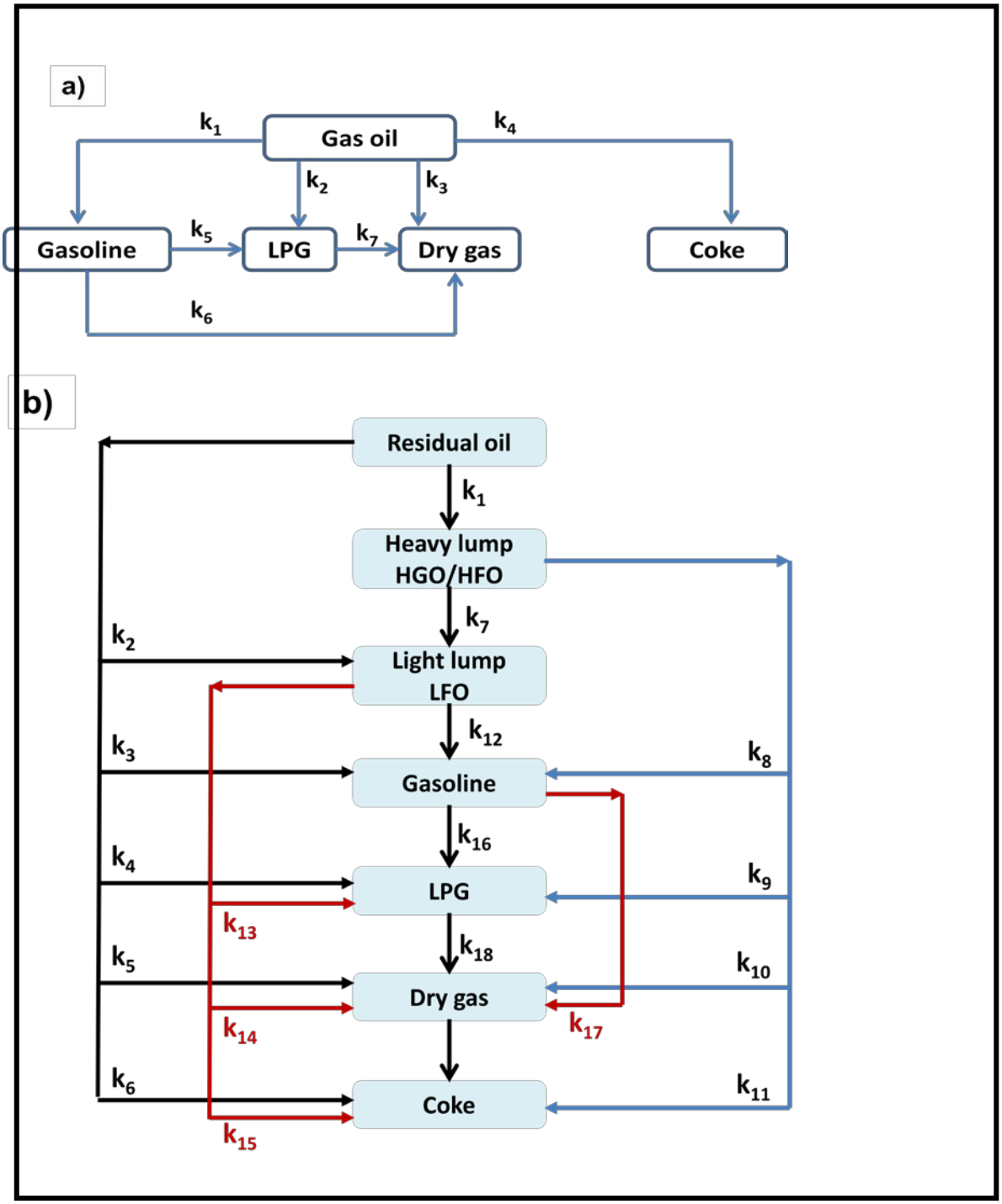

Fig. 5. Lump kinetic models for catalytic cracking (a) Five lump kinetic models [4] (b) seven lump kinetic models [5]

Hydrocracking

This process has wide range of applications including upgradation of petrochemical feedstock, improvement of gasoline octane number, production of high quality lubricants etc. The process upgrades the original feedstock by increasing its overall hydrogen-to-carbon ratio and decreasing the average molecular weight.

Hydrocracking is extensively used for simultaneously cracking and hydrogenating low value gas oil, containing high amount of cyclic polyaromatic and naphthenic compounds, to produce high value products such as gasoline, diesel or jet fuel. Hydrocracking involves multiple reactions such as ring opening, cracking, dealkylation and isomerization with simultaneous saturation due to presence of hydrogen. The major advantage of this process is higher selectivity towards cracking of polyaromatics to desired fuels such as gasoline, diesel or jet fuel and less production of lower hydrocarbons. This is in contrast with catalytic cracking process which gives rise to considerable amount of lower alkene products. Some of the typical reactions are shown in Fig. 6.

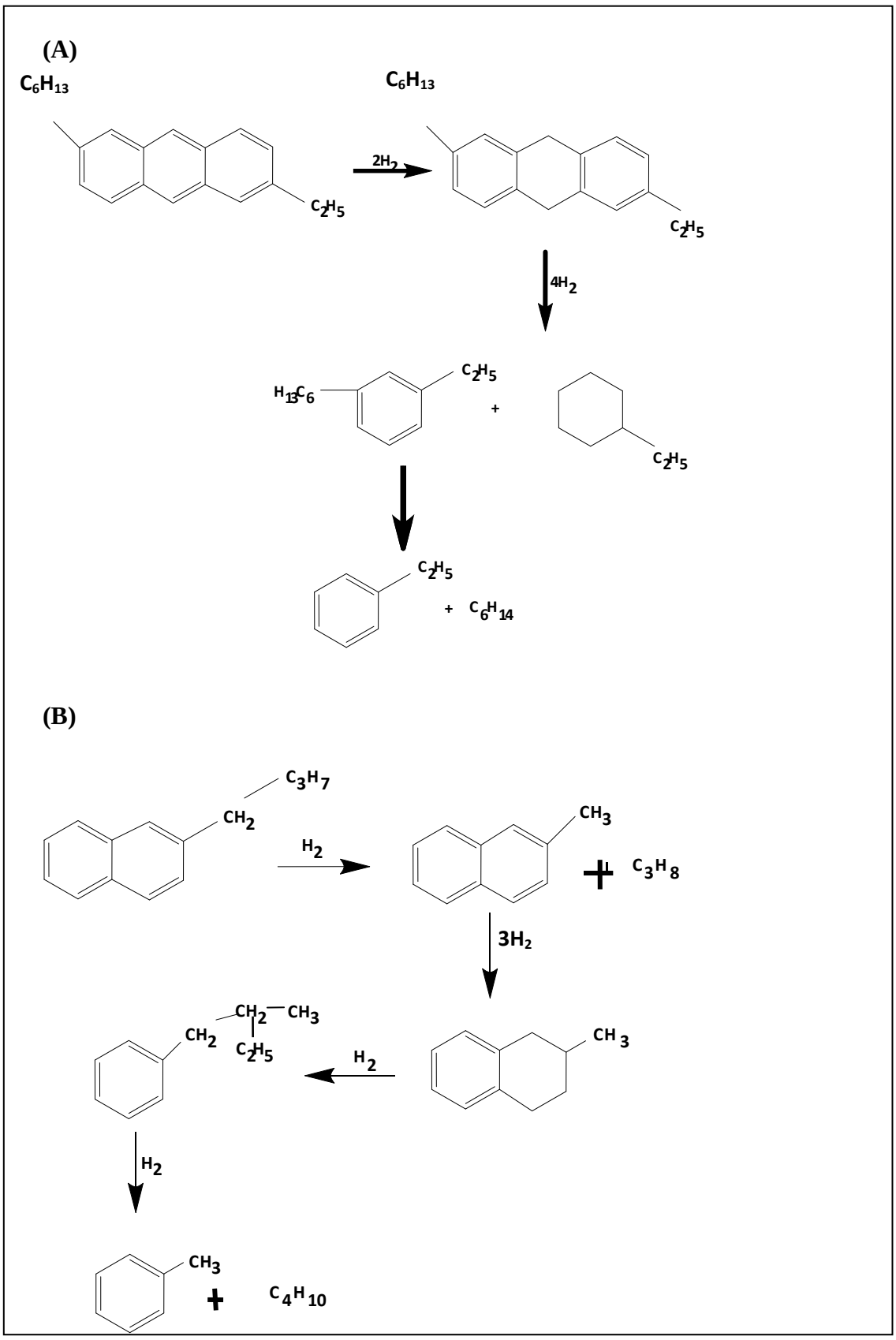

Fig. 6. Typical hydrocracking reactions

Process

The process is typically carried out in a series of fixed bed reactors at 300-450 ^{0}C and 100-200 atm. The process is associated with large heat release due to exothermic hydrogenation reactions which dominate the endothermic cracking reactions. The major disadvantage of the process is the requirement of very high pressure of hydrogen with large energy consumption making the process rather expensive. A typical two-stage hydrocracker is shown in Fig. 7. In first stage 40-50 vol% of the feed is hydrocracked. The first stage also acts as a hydrotreater , where poisonous nitrogen and sulfur compounds are partially hydrogenated. The effluent from the first stage reactor passes through heat exchangers to a high pressure separator where hydrogen-rich gases are separated and recycled. The liquid from the separator is fed to a fractionating tower and the tower bottoms form the feed to the second stage. Usually fixed-bed reactors with liquid down flow are used.

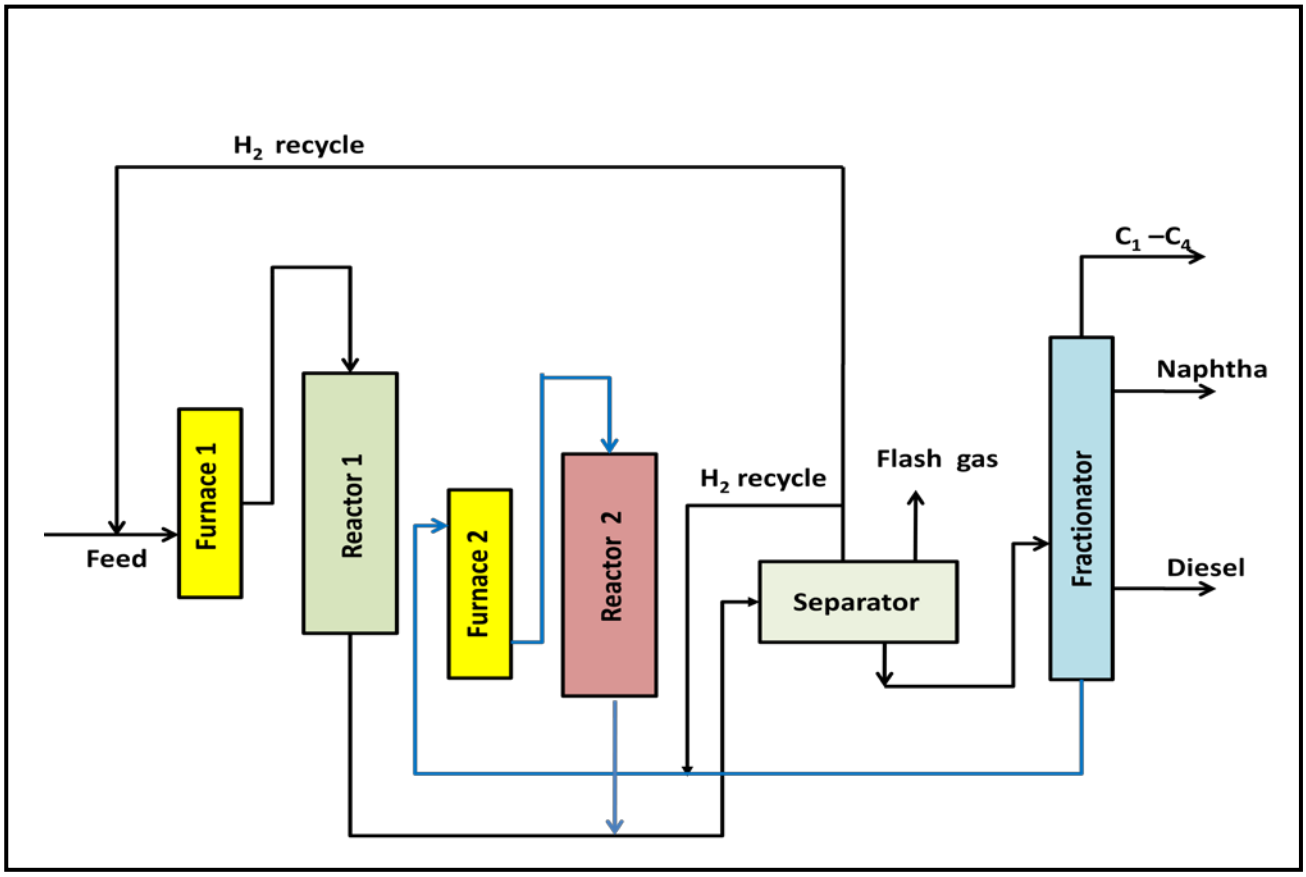

Fig. 7. Schematic diagram of two stage hydrocracking process

Catalysts

The hydrocracking catalyst has to be a bi-functional catalyst :

– Acid sites to catalyze cracking reactions

– Metal sites catalyzing hydrogenation

Catalyst choice depends on the nature of feed and desired product distribution. CoO-MoO_3-Al_2O_3 has been widely used for hydrocracking of heavy feed stocks such as residual raffinate, solvent deasphalted residual oil and vacuum residue. Base metals (Co, Mo, Ni, W) supported on Al_2O_3-SiO_2 and zeolite are used for producing lubricating oils and middle or heavy distillate. Typical catalysts consist of 2% Co 7 % Mo, 6% Ni, 20% W on Al_2O_3-SiO_2 . The Ni/SiO_2-$A1_2O_3$ increased conversion of heavy polynuclear compounds in the feed. Pt or Pd supported on zeolites are used for clean and pretreated feeds and are highly selective towards gasoline, diesel or jet fuel. Typical catalyst is 0.5 wt % Pt or Pd on zeolites prepared by ion exchanges. Ni-Mo-zeolite and Ni-W-zeolite catalysts are used for maximizing gasoline and gas oil production respectively. The Ni-W-impregnated rare earth exchanged X-type zeolite was found to be more resistant to nitrogen and structurally more stable. Catalyst poisoned by deposition of coke and other materials is usually regenerated by burning off the deposits.

Mechanism and kinetics

As discussed earlier hydrocracking of petroleum feedstock also involves a complex network of reactions of large number of components. Reviews [6, 7] on kinetics of hydrocracking of heavy oil fractions include various lumped kinetic models. Callejas and Martinez [8] for hydrocracking of residue over Ni-Mo/γ-Al_2O_3 catalyst in CSTR at 12.5 MPa hydrogen pressure and 375-415 ^oC temperature, used three lumps model (Fig 8a). The three lumps were atmospheric residue (AR), light oils (LO) and gases. The kinetics of hydrocracking of vacuum distillates was studied by Orochko et al. [9] over an alumina–cobalt molybdenum catalyst using a first-order kinetic scheme as shown in Figure 8b. The rate of a first-order heterogeneous catalytic reaction was expressed by the following equation:

$$\alpha\tau = \ln\frac{1}{1-y} - \beta y$$

where α = rate constant, t = reaction time, y = total conversion and b = inhibition factor due to adsorption reaction products on catalysts.

Sanchez et al. [10] proposed a five lump kinetic model (Fig 8c) for moderate hydrocracking of heavy oil in a fixed bed downflow reactor over Ni-Mo/ Al_2O_3 catalyst. The lumps were unconverted residue, vacuum gas oil, distillates, naphtha, and gasses. The model included 10 kinetic parameters. Krishna and Saxena [11] reported a detailed kinetic model with seven lumps (Fig 8d) considering cuts of different temperatures. The lumps were sulfur compounds, heavy and light aromatics, heavy and light naphthenes, heavy and light paraffins. The pseudo components were considered light if they were formed from fractions with boiling points lower than the cut temperature. Sulfur compounds were considered to be a heavy lump.

Deactivation

Catalyst deactivation mainly occurs by deposition of coke on catalysts surface that can be removed by periodic burn-off. The other source of deactivation is presence of sulfur and nitrogen metals in feed. The S and N metals can be removed by feed pretreatment.

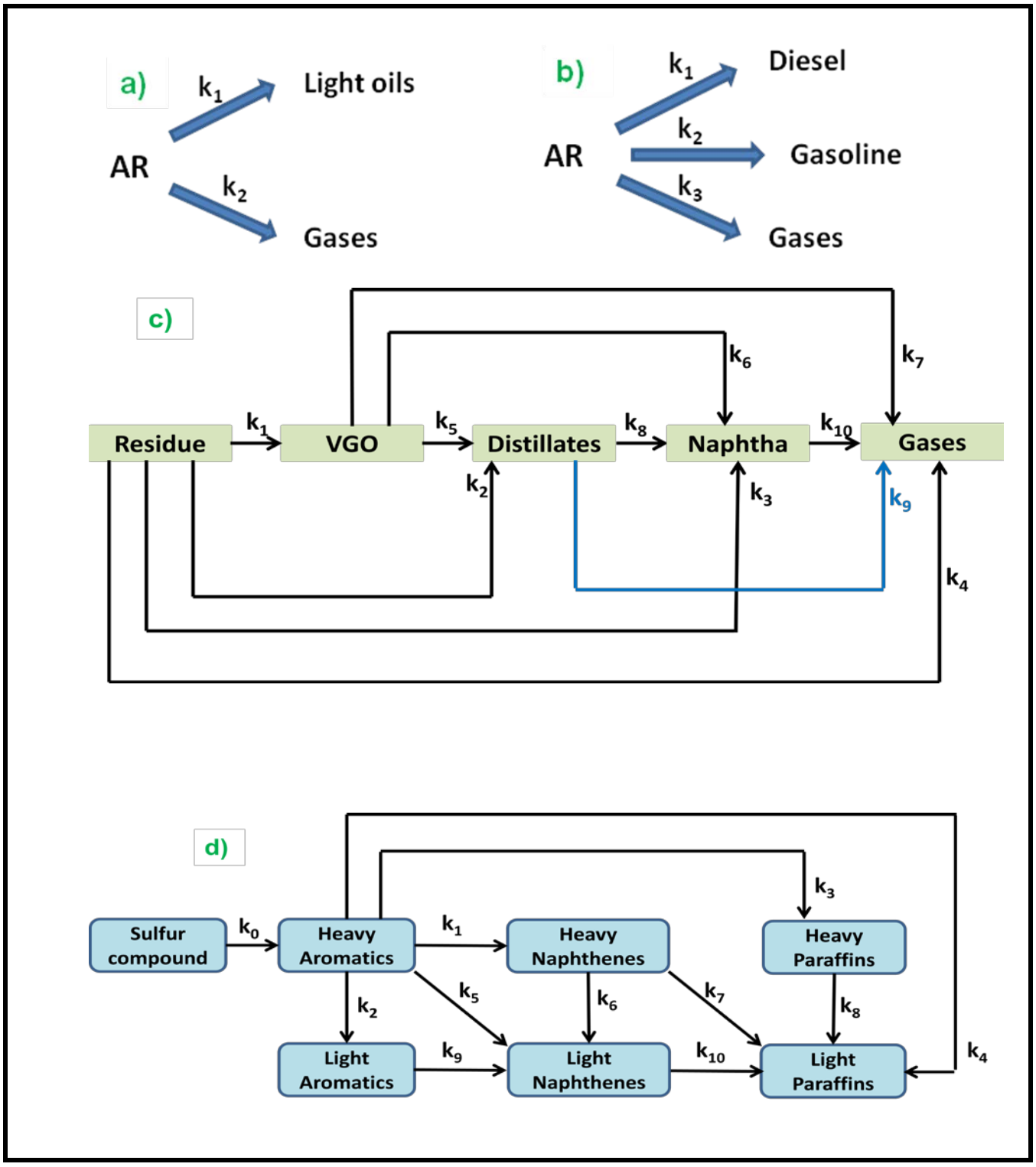

Fig. 8. Various lumped kinetic models for hydrocracking reactions (a) Three lump model [8] (b) Four lump model [9] (c) Five lump model [10] (d) Seven lump model [11]

Book reference:

- C. H. Bartholomew and R. J. Farrauto, Fundamentals of Industrial catalytic Processes, Wiley, VCH, 2006

Publication reference :

1. L. Lloyd, D.E. Ridler, M.V. Twigg, Catalysts Handbook, ed M.V. Twigg Wolfe, Chap6, pp 283-338
2. C.V. Ovensen, B.S. Clausen, B.S. Hammershøi, G. Steffensen, T. Askgaard, I. Chorkendorff, J.K.Nørskow, P.B.Rasmussen, P. Stoltze, P.Taylor J. Catal. 158 (1996) 170-180
3. B.W. Wojciechowski, A. Corma, Catalytic cracking , catalysts chemistry and kinetics , Marcel Dekkar, New York ,1986
4. J. Ancheyta-Juárez , F. López-Isunza ,E. Aguilar-Rodríguez, Appl. Catal. A: General 177 (1999) 227-235
5. M. Heydari, H. AleEbrahim, B. Dabir, Amer. J. of Appl. Sci. 7 (2010) 71-76
6. S. Mohanty, D. Kunzru, D. N. Saraf, Fuel, 69 (1990)1467
7. J. Ancheyta, S. Sánchez, M. A. Rodríguez, Catalysis Today 109 (2005) 76–92
8. M. A. Callejas, M.T. Martínez, Ind. Eng. Chem. Res. 38 (1999) 3285–3289
9. D.I. Orochko, Khimiya I Tekhnologiya Toplivi Masel 8 (1970) 2–6.
10. S. Sánchez, M. A. Rodríguez, J. Ancheyta, Ind. Eng. Chem. Res., 44 (2005) 9409–9413
11. R. Krishna, A. K. Saxena, Chem. Eng. Sci.44 (1989) 703–712.

Lecture 28

Naphtha reforming

Naphtha is a 70-200 ^{0}C petroleum cut containing C_5-C_{10} hydrocarbons. Naphtha feed mainly consist of alkanes and naphthenes or cyclo-alkanes with very low amount of aromatics. Naphtha reforming involves conversion of normal alkanes and cycloalkanes to branched alkanes and aromatics to produce high octane gasoline and aromatic source for chemical production.

The main reactions are dehydrogenation, isomerization and dehydrocyclization. The dehydrocyclization of alkanes needs to be maximized for increase in aromatic production but it is also the most difficult reaction to be accomplished. Typical examples of catalytic hydrocarbon reforming reactions are as follows

1. Dehydrogenation

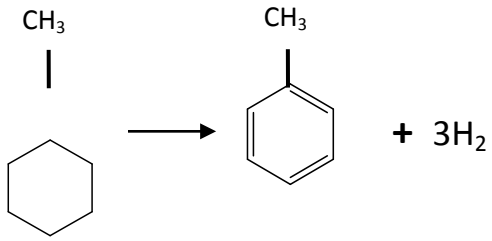

2. Isomerization

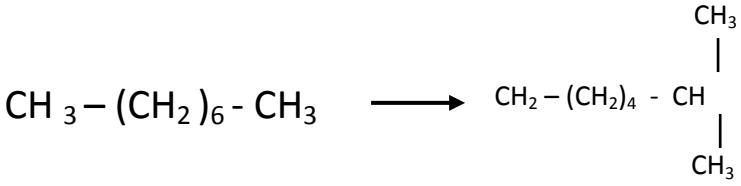

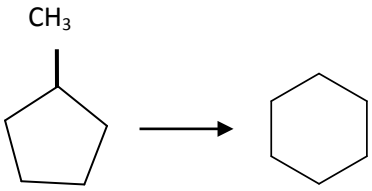

3. Dehydrocyclization

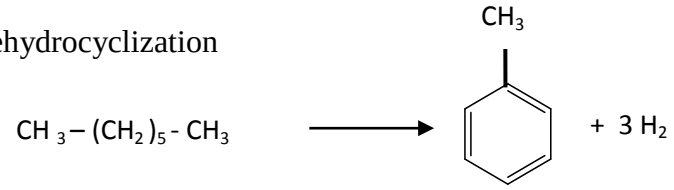

The hydrocracking reactions may also take place. The hydrocracking reactions are usually undesirable as it result in conversion of useful molecules to low molecular weight gasses with consumption of significant amount of hydrogen.

$$CH_3(CH_2)_5CH_3 + H_2 \longrightarrow CH_3CH_2CH_3 + CH_3CH_2CH_2CH_3$$

Process

Naphtha reforming involves different types of reactions which are thermodynamically and kinetically favored at different reaction conditions. For example, dehydrogenations are favored thermodynamically and kinetically at high temperature and low pressure while isomerization is kinetically favored at high temperature and pressure. The high temperature can cause excessive dehydrogenation especially of aromatics in the feed leading to high rates of formation of coke. To minimize the coke formation, the hydrogen is added in large excess to feed. The naphtha feed is initially hydrotreated to remove sulfur and nitrogen compounds as the reforming catalyst are sensitive to these compounds. The naphtha reforming process is therefore carried out in series of different reactors to optimize various reactions. Typically the process involves three reactor setups. The 1st reactor is designed for dehydrogenation of naphthenes to aromatic. The 2nd reactor is designed for additional dehydrogenation with isomerization and the 3rd reactor is for dehydrocyclization reactions which are kinetically least favorable and therefore require large bed volume. The reactors are loaded with increasing amount of catalyst and the last reactor contains the largest amount of catalyst. Depending on feed the commercial reformers are operated at 5-35 atm and 450- 500 ^{o}C Due to endothermic reactions, the exit stream from each adiabatic reactor needs to be reheated to 500 ^{0}C before entering the next reactor.

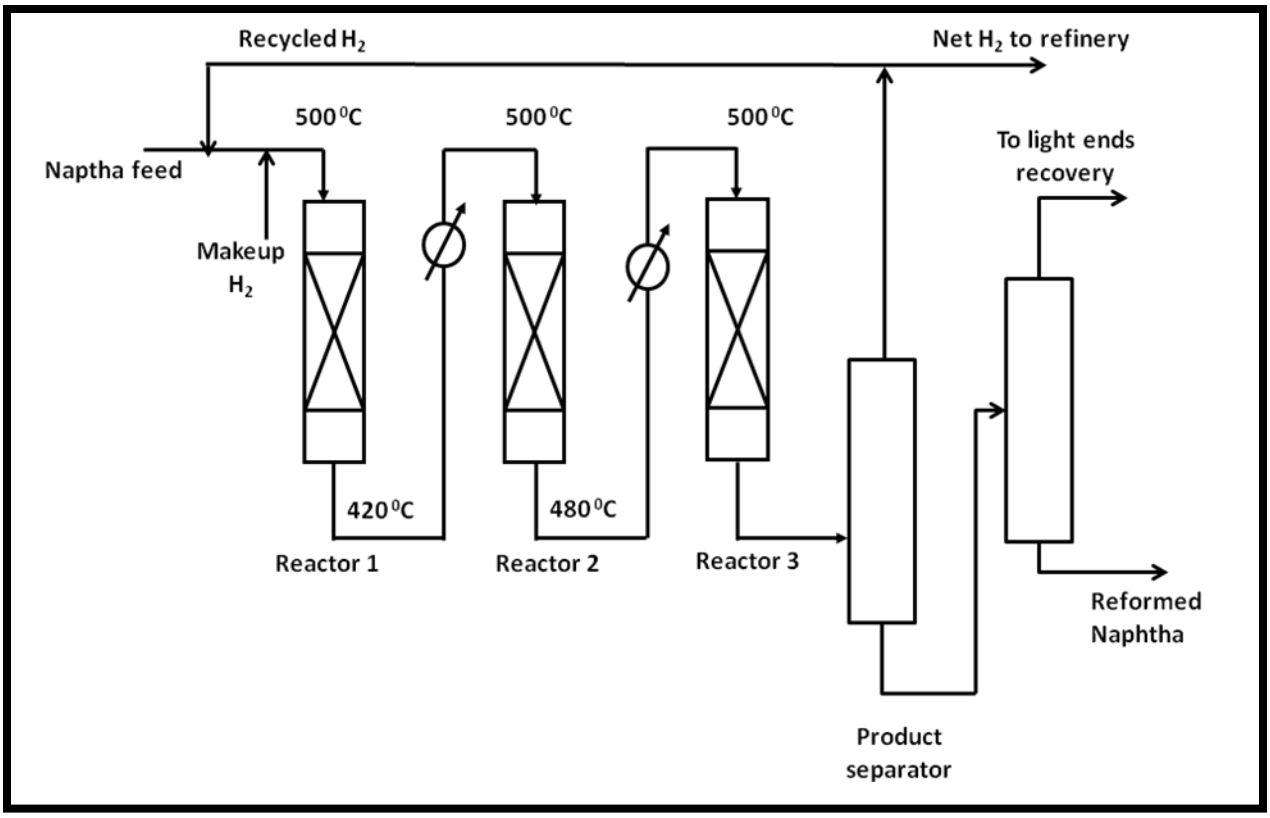

Fig. 1. Schematic diagram for naphtha reforming process

Catalysts

Reforming catalysts involve dual functions; acidity and dehydrogenation function. The acidic center of the catalyst promotes the structural changes involved in isomerization reactions. The dehydrogenation reactions are catalyzed by metal site of the catalyst. Reforming catalyst usually contains Pt as the metal component and modified γ-Al_2O_3 as the source of acidity. The acidity of the Al_2O_3 is further enhanced by incorporation of chloride ions into its structure. Addition of small amount of Re along with pretreatment with H_2S improves the life of the catalyst. Re sulfide breaks up the Pt metal surface into smaller entities and decreases the probability of coke formation. Other promoter such as Ge, Tr and Sn have also been used in place of Re depending upon feed or process condition.

Mechanism and kinetics

Reforming involves simultaneous occurrence of several reactions thereby making mechanism of reforming very complex. Lumped kinetic models are used in which naphtha components are lumped into functional groups i.e. alkanes, naphthenes and aromatics. Some of the reaction scheme used to develop catalytic reforming kinetic model is shown in Fig.2

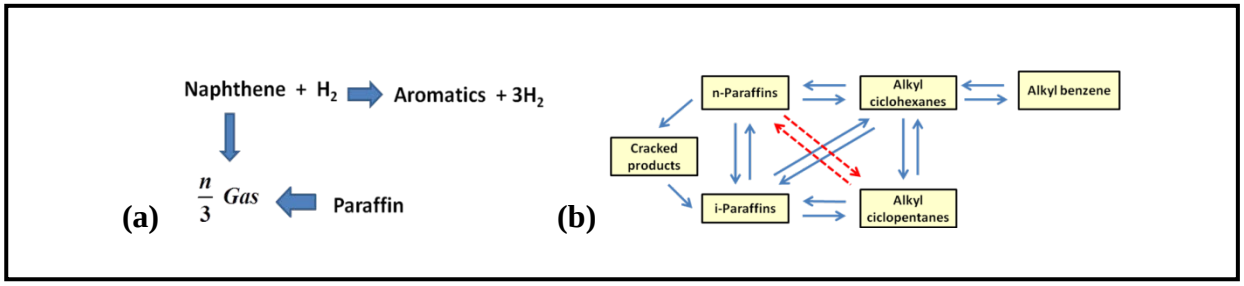

Fig.2. Reaction scheme for catalytic reforming [1]

Deactivation

Major sources of deactivation are:

– Coke formation

– Sintering

– Poisoning by S,N compounds

– Poisoning by Arsenic, Lead, other metals (Cd, Cr, Co, Fe etc.); As< 1ppb; Pb< 20 ppb ; other metals < 600 ppm

Coke formation is highest in the last reactor. The feed is hydrotreated to remove sulfur and nitrogen compounds.

Isomerization

Isomerization involves conversion of less useful hydrocarbons to their corresponding more desirable isomers. For example, normal butane, pentane or hexane can be isomerizd to their branched isomers having higher octane number. Similarly, m-xylene can be isomerized to para-xylene (p-xylene) which is used as feed for production of pure terephthalic acid. Consequently, out of all the xylenes, p-xylene has the largest commercial market.

Reactions & Process conditions

The isomerization reactions of butane, pentane and hexane are as follows.

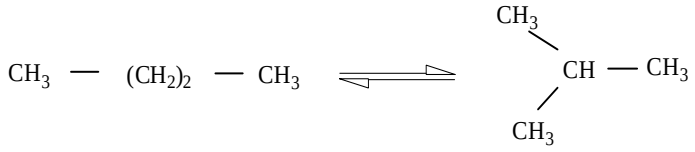

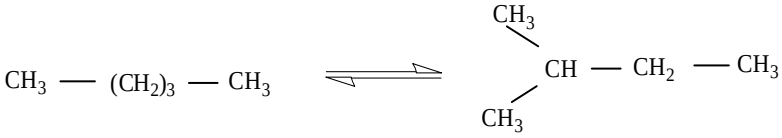

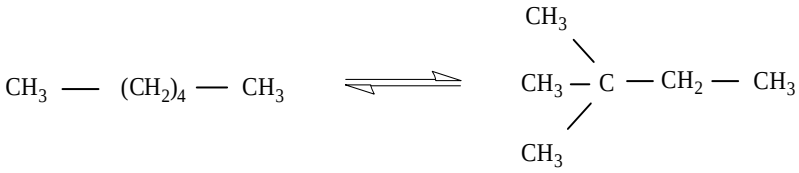

Reaction scheme for xylene isomerization is shown below.

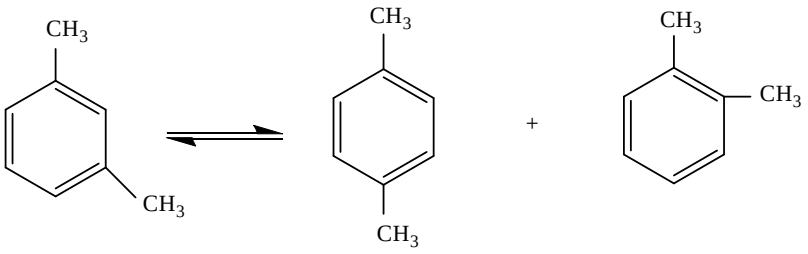

m-Xylene p-Xylene o-Xylene

Isomerization of xylene is carried out at 400-450 ^{0}C and 10-20 H_2 atm over platinum based catalysts and equilibrium distribution of different xylene isomers is obtained. The branched products of the isomerization reactions are thermodynamically more favorable at lower temperature. The most active catalysts are strong acids such as anhydrous $AlCl_3$ which are also corrosive. Solid catalysts such as $Pt/Cl^{-}/Al_2O_3$ are also used although have lower activity at lower temperature.

A typical process flow diagram for isomerization of C_5 and C_6 alkanes to branched products is shown in Fig 2. The process conditions of C_5/C_6 isomerization depend on the activity of the catalyst as well as on the composition of the feed. For example, feed rich in hexane requires high hydrogen pressure (~35-100 atm) to maintain low coke formation where as pentane rich feed can be processed at lower pressure (less than 27 atm) at temperatures between 120- 175 ^{o}C. The feed is mixed with hydrogen to minimize the coke formation and passes through the reactor followed by separator. The hydrogen from separator is recycled. The product is further stabilized by removing lighter gases. The products are separated from the reactants to maintain a favorable equilibrium and the unreacted normal hydrocarbons are recycled. Any isopentane retained in feed or recycle is immediately separated at the front end of the process as shown in the figure.

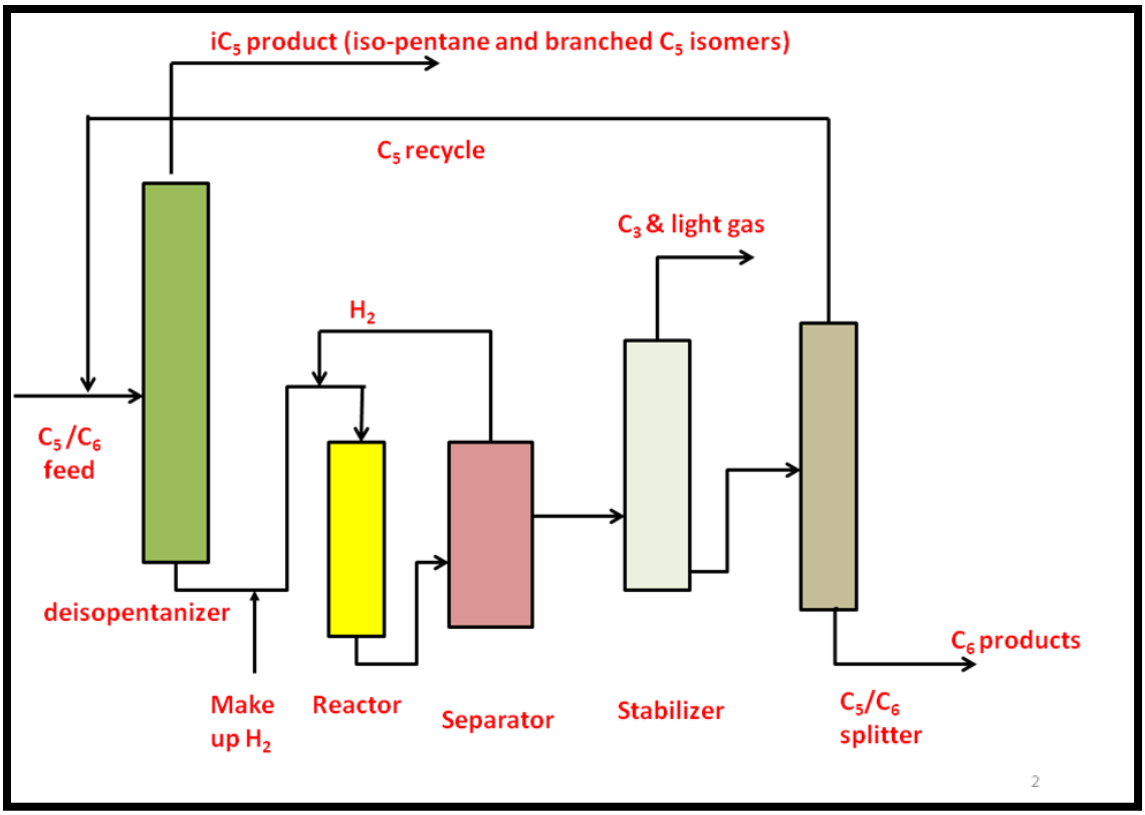

Fig. 2. Process flow diagram for isomerization of C_5 and C_6 alkanes to branched products

Catalysts

Initially, Pt supported on $Al_2O_3 – SiO_2$ was extensively used as the isomerization catalyst. More recently, Pt- ZSM5 zeolite has proved to be a better catalyst. Pt centers dehydrogenate the alkanes while acid sites isomerize the resultant alkenes which are then rehydrogenated by Pt to isomerized alkanes. Pt also serves to moderate the coke formation by hydrogenation of coke precursors.

Mechanism and kinetics

Isomerization of C_4 - C_8 hydrocarbons occurs through carbenium ion intermediate. Both, empirical power rate law and Langmuir–Hinshelwood type of kinetic models have been used to model the kinetics.

Catalysts deactivation

Catalysts are mainly deactivated by coke deposition. Coke deposition can be minimized by increasing H_2 pressure. The catalysts can be regenerated by controlled burning of coke. Other poisons such as sulfur compounds, water and traces of aromatics can also be removed during coke burn off. The adsorbed sulfur and water on the catalyst can also be removed by decreasing their partial pressures in the stream, when they are reversibly adsorbed.

Hydrotreating

Hydrotreating is the process of removal of organic sulfur, nitrogen, oxygen and metals from petroleum crude at high hydrogen pressure. This process is also used for hydrogenation of unsaturates. Examples of sulfur, nitrogen and metal containing compounds as found in pertoleum crude are shown in Fig 10. Importance of hydrotreating is increasing due to decrease in availability of light and sweet crudes. Heavier crudes contain more sulfur, nitrogen and metal compounds requiring increasing treatment for removal of these compounds which act as poison for downstream processes. More and more stringent emission standard for sulfur and nitrogen content in fuels is another reason for higher interest in hydrotreating processes.

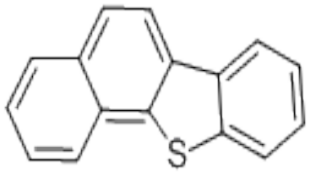

Benzonaphthothiophene

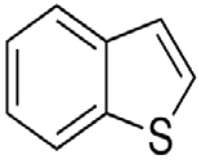

Benzothiophene

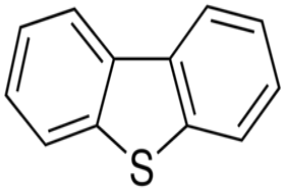

Dibenzothiophene

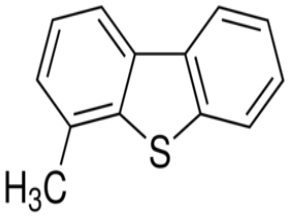

Methyldibenzothiophene

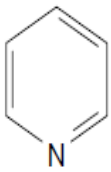

Pyridine

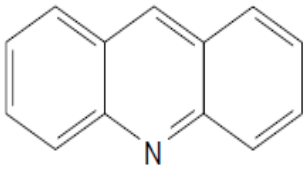

Acridine

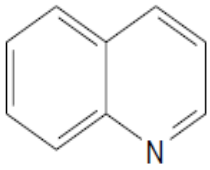

Quinoline

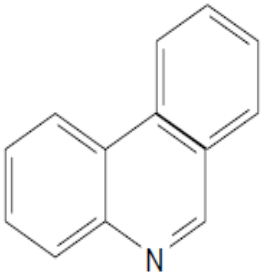

Phenanthridine

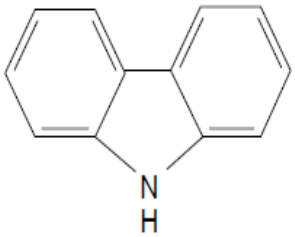

Carbazole

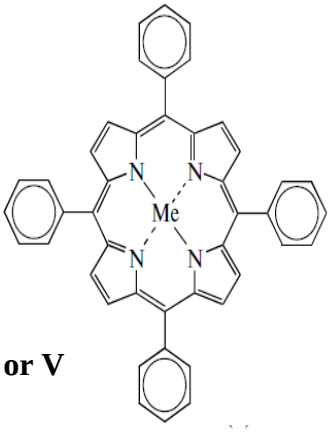

Me= Ni or V

Fig. 10. Examples of sulfur, nitrogen and metal containing compounds in petroleum crude

Reactions involved

The main reactions that are involved during hydrotreating processes are:

1. Hydrodesulphurization (HDS) : HDS can occur by direct removal of sulfur as H_2S or unsaturated complex molecule may initially undergo partial hydrogenation followed by sulfur removal.

$$RSH + H_2 \rightleftharpoons RH + H_2S$$

$$CH_3 - S - C_4H_9 + 2H_2 \rightleftharpoons CH_4 + C_4H_{10} + H_2S$$

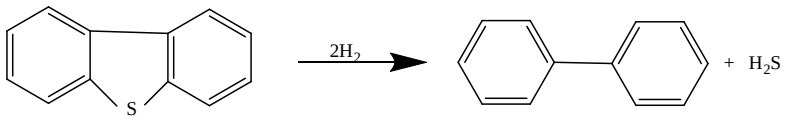

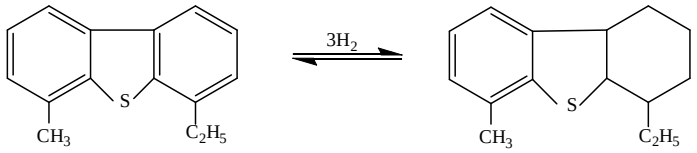

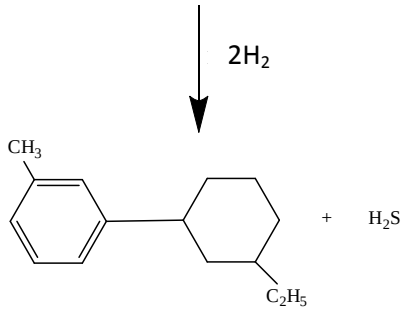

Among the sulfur compounds the approximate order of activity is RSH > R-S-S-R´> R-S-R´ > thiophenes. The reactivity of thiophenes decreases in the order thiophene > benzothiophenoe > dibenzothiophene > alkyl-benzothiophenes. The 4,6 dibenzothiophene is the most refractory of the sulfur compounds hence, most difficult to be removed.

2. Hydrodenitrogenation (HDN) : This involves removal of nitrogen compounds Almost all of the nitrogen in petroleum is present in form of ring compounds. These must be saturated and opened before the nitrogen can be removed.

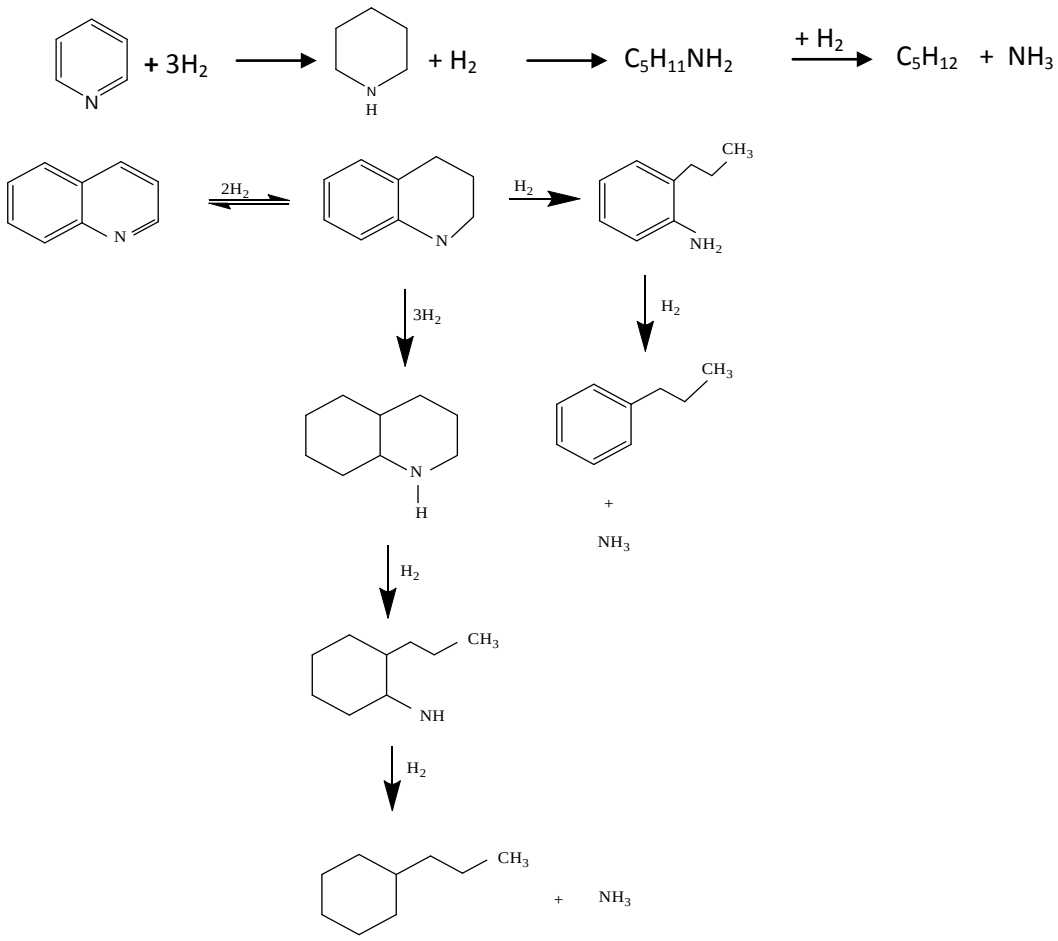

3. Hydrodemetalation (HDM) : Ni, V, Fe removal

$NiEP \rightarrow NiEPH_2 \rightarrow Ni$ NiEP : nickel etioporphyrin

Process conditions

Hydrotreating process condition though depends on feed properties but generally carried out in temperature range of 300-450 ^{0}C at 40-150 atm H_2 pressure. The heavier petroleum feed require more severe conditions and removal is also less efficient compared to light petroleum feed.

Catalysts

For HDS process, sulfided 2-3 % Co -12-15% Mo supported on Al_2O_3 catalysts and for HDN process 2-3 % Ni 12-15% Mo/Al_2O_3 catalysts are reported to be more active. For HDM process MoS supported on large pore Al_2O_3 is suitable. Boron, phosphorus and potassium are frequently used as promoters. Addition of phosphorous increases the activity for HDN.

Deactivation

Deactivation occurs through poisoning and plugging of pores by metal. This can be minimized by stage wise HDM/HDS with moving bed where fresh/regenerated catalyst is added from top and deactivated catalysts are removed from bottom. Formation of coke which is another major source of deactivation can be controlled by periodical burning off.

Book reference:

- C. H. Bartholomew and R. J. Farrauto, Fundamentals of Industrial catalytic Processes, Wiley, VCH, 2006

Journal reference

1. M. A. Rodríguez, J. Ancheyta, Fuel 90 (2011) 3492–3508

Lecture 29

Environmental catalysis

Environmental catalysis involves reduction in emission of SO_x, NO_x, CO_x and volatile organic materials. The sources of these pollutants include mobile sources such as exhaust gases from automobiles and stationary sources such as exhaust gasses from various industries. Removal of these gases is done by catalytic treatment of the exhaust gas. Some of the processes will be discussed here.

Catalytic converter

The pollutants from automobile exhaust gasses are removed by passing the gases through the catalytic converter. Automobile combustion processes generate large quantities of CO_2 and H_2O. However, significant amount of CO and unburned hydrocarbons (HC) are also produced due to inefficiencies of combustion processes. NO_x is produced due to high temperature reaction between N_2 and O_2 of air. The quantity of each pollutant varies with the air to fuel ratio (A/F) used.

CO and HC concentration can be reduced by oxidizing it to CO_2 and H_2O while NO_x is reduced to N_2.

$$CO + 0.5O_2 \rightarrow CO_2$$ **Oxidation**

$$\left(-CH_2-\right)_n + 1.5nO_2 \rightarrow nCO_2 + nH_2O$$ **Oxidation**

$$NO_2 + HC\left(CO\right) \rightarrow N_2 + CO_2 + H_2O$$ **Reduction**

NO_x reduction readily occurs at fuel rich conditions, whereas CO and HC oxidations occur at air rich conditions. However, there exists a narrow window (A/F =14.55 ± 0.1) in which 90% NO_x is reduced to N_2 and 90% CO and 85 % HC are oxidized to CO_2 and

H_2O. Controlling the A/F ratio within this narrow window is critical for efficient conversion and done by using O_2 sensor placed immediately before the exhaust manifold.

Catalysts

At specific stoichiometric value of air- to- fuel ratio using a selective catalyst all the three pollutants, CO, NOx and unburned hydrocarbons, can be removed. The catalyst used for promoting these three reactions simultaneously is known as a three way catalyst. These catalysts consist of cellular monoliths with parallel open channels. Details about auto exhaust catalysts are given by Heck and Farrauto [1]. Ceramic monoliths are shown in Fig 1. These monoliths have large open frontal area (~ 70 %) resulting in low pressure drops and unrestricted flow. The monoliths are usually made of cordierite having composition of $2MgO.5SiO_2.2Al_2O_3$. Typically, the monoliths that are used in automobiles, contains 60-65 cells /cm^2. Monolith catalyst is mounted in a stainless steel container wrapped with matting material. Converters are generally of 10-12 cm diameter and 7-10 cm long.

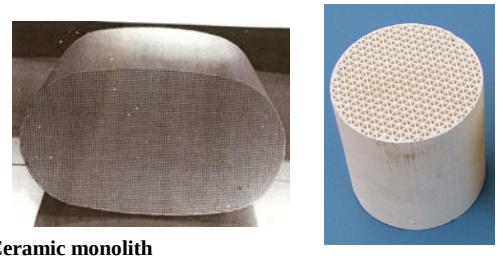

Fig. 1. Ceramic monolith

The typical composition of three way catalysts as defined above is shown in Fig. 2.

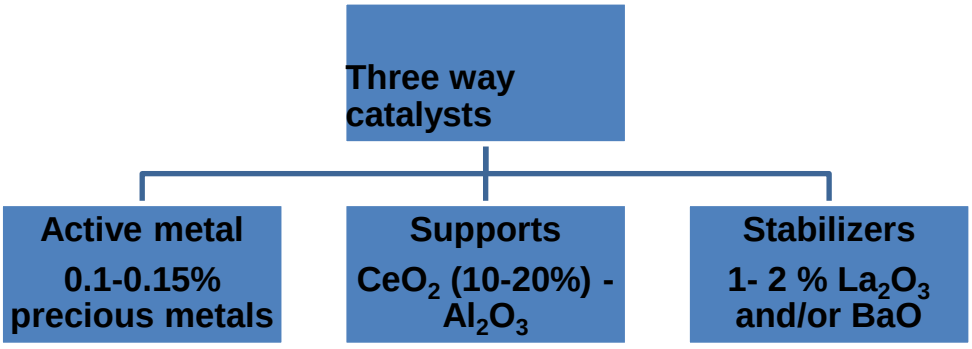

Fig. 2. Typical composition of three way catalysts

The alumina-ceria is deposited on monolith honeycomb by dipping the monolith in the slurry of the components. Alumina washcoat is chemically and physically bonded to the surface. Washcoat is generally about 15 wt% of the finished honeycomb catalysts.

Pt and Rh are used as active metals. Pt is active for oxidation reactions but converts NO_x to NH_3. Rh is highly selective for NO_x to N_2. A bimetallic catalysts with Pt **:** Rh ~ 5**:**1 ratio is generally used. CeO_2 act as O_2 storage component and liberates or absorbs O_2 during air to fuel perturbations according to the following reactions.

$$rich\ conditions: CeO_2 + CO \rightarrow Ce_2O_3 + CO_2$$
$$lean\ conditions: Ce_2O_3 + 0.5O_2 \rightarrow CeO_2$$

CeO_2 also act as steam reforming catalysts.

$$CO\ or\ HC + H_2O \xrightarrow{CeO_2} H_2 + CO_2$$

This H_2 reduces a portion of NO_x to N_2

Kinetics and mechanism

According to Bunluesin et al.[2], mechanism of CO oxidation is significantly affected by CeO_2. In the absence of CeO_2, oxidation of CO over Rh/Al_2O_3 is modeled as

$$CO + M \rightleftharpoons CO - M$$
$$O_2 + M \rightleftharpoons O_2 - M$$
$$O_2 - M + M \rightleftharpoons 2O - M$$
$$CO - M + O - M \rightleftharpoons CO_2 + 2M$$

Here M is the adsorption site. The rate of CO oxidation is given as $r = \frac{k\ P_{O_2}}{P_{CO}}$

P_{O_2} is partial pressure of oxygen and P_{CO} is partial pressure of CO.

While mechanism pathway in presence of Rh/CeO_2 is

$$CO + M \rightleftharpoons CO - M$$
$$O_2 + 2M \rightleftharpoons 2O - M$$
$$O - M + Ce_2O_3 \rightarrow 2CeO_2 + M$$
$$CO - M + 2CeO_2 \rightarrow CO_2 + Ce_2O_3 + M$$

Here M is the adsorption site and rate of CO oxidation is given as $r = k\ P_{O_2}^{1/2}$

Hence, rate is independent of CO partial pressure in the presence of ceria. At high conversion, rate becomes limited by external mass transfer. The rate of CO_2 formation over Pt catalyst has been modeled based on Langmuir-Hinshelwood models. According to Liu et al. [3], CO and O adsorb on adjacent sites on Pt surface. Considering surface reaction between adsorbed CO and O to be the rate-controlling step, the rate expression is obtained as :

$$r = \frac{kP_{CO}P_{O_2}^{1/2}}{\left[1 + K_{O_2}^{1/2}P_{O_2}^{1/2} + K_{CO}P_{CO}\right]^2}$$

where k is forward rate constant for generation of CO_2 . The K_{O2} and K_{CO} are adsorption constants for O_2 and CO, respectively.

Deactivation

At temperatures above 800 ^{0}C in oxidizing atmosphere, Rh can react with Al_2O_3 forming a less active aluminate. Poisoning by SO_2 may also occur to some extent.

Selective catalytic reduction of NO_x

NO and NO_2 are undesirable by-products of combustion of fuels in boilers, engines and turbines as well as in chemical operations such as HNO_3 production. In selective catalytic reduction (SCR) process, ammonia is reacted selectively with NO_x to produce N_2 without consumption of excess oxygen.

$$4NH_3 + 4NO + O_2 \rightarrow 4N_2 + 6H_2O$$
$$4NH_3 + 2NO_2 + O_2 \rightarrow 3N_2 + 6H_2O$$

The process is associated with the following side reactions

1. Oxidation of SO_2 if any present.

$$2SO_2 + O_2 \rightarrow 2SO_3$$

2. Oxidation of ammonia

$$4NH_3 + 5O_2 \rightarrow 4NO + 6H_2O$$
$$4NH_3 + 3O_2 \rightarrow 2N_2 + 6H_2O$$

Selectivity for these different reactions depends on catalyst and operating conditions.

Catalysts

Different types of SCR catalysts are used such as Pt, V_2O_5/TiO_2 and Zeolites. Each of these catalysts has different maximum NO_x conversion temperature and operating window. Pt is active in the temperature range of 100-250 ^{0}C while zeolite is active at temperatures greater than 400 ^{0}C. Most common catalyst is V_2O_5 supported on TiO_2. Its operating temperature is in the range of 300 - 400 ^{0}C. Here vanadia is the active metal and titania stabilizes the vanadia. WO_3 or MoO_3 promoters are added to increase the activity while significantly decreasing SO_2 oxidation activity. SCR of NO_x with ammonia is also carried out with structured monolith based catalysts. For monolith catalyst based process, the pressure drop is lower, resistance to attrition is higher and surface area per volume of catalyst is higher compared to fixed bed. The monolith is usually wash coated with a porous support material such as zeolite or carbon along with incorporation of the active phase. V, Fe or Mn is used as the active phase.

Kinetics and mechanism

Dumesic et al. 1993 [4] proposed following three step mechanism for SCR of NO with ammonia on V_2O_5/TiO_2.

$$NH_3 + M \rightleftharpoons NH_3 - M$$
$$SO + NH_3 - M \rightleftharpoons NH_2M + SOH$$
$$NO + NH_2M \rightarrow N_2 + H_2O + M$$

M = ammonia adsorption site = acidic site

SO = reactive site on which ammonia is activated = H abstraction

The third step that is the reaction between NO and NH_2M is the rate determining step. The derived rate expression is

$$r_{NO} = k_3 P_{NO} \frac{K_1 P_{NH_3} / P_{NO}}{1 + K_1 P_{NH_3} / P_{NO} + K_2 P_{NH_3}} \qquad K_1 = k_2 K_{NH_3} / k_3 \qquad K_2 = k_{-2} / k_3$$

Deactivation

Fouling or solid deposition of side products such as fly ash or ammonium bisulfate on the catalyst surface results in catalyst deactivation. Ammonium bisulphate is formed by the reaction of SO_3 (from SO_2 oxidation) with unconverted ammonia. It is a sticky corrosive compound and causes fouling of heat exchangers and other equipment downstream. Another cause of deactivation is sintering of titania. Abrasion, fouling and/or poisoning by fly-ash can be prevented by installation of an electrostatic precipitator. Fouling by SO_3 can be minimized by keeping the SO_3 concentration low by using lower activity catalyst or by maintaining the temperature lower than 350 ^{0}C or using monolith catalysts which lower the residence time. Sintering can be minimized by addition of promoter.

Book reference:

- C. H. Bartholomew and R. J. Farrauto, Fundamentals of Industrial catalytic Processes, Wiley, VCH, 2006

Journal reference :

1. R. M. Heck, R. J. Farrauto, Applied Catalysis A: General 221 (2001) 443–457
2. T. Bunluesin E. PutnaR. Gorte, Catal Lett,, 41 (1996) 1-5
3. J.Liu, M.Xu, K.Zaera, Catal Lett,, 37 (1996) 9
4. J.A. Dumesic, N.Y. Topsoe, T. Slabiak, P. Morsing, B.S.Clausen, E.Törnqvist, H.Topsøe, Proceedings 10th International catalysis Congress ,1993,Elsvier Vol B 1325-1337

Lecture 30

Hydrogenation and dehydrogenation

Hydrogenation and dehydrogenation are the oldest catalytic processes**.** Catalytic hydrogenation reactions are used for production of fine chemicals, in pharmaceutical industry and polymer industry and for the production of edible and non edible fats and oils. Dehydrogenation reactions are used for production of light alkenes(C_3-C_4) for preparation of acrylonitrile, oxoalcohols or propylene oxides and production of C_4 - C_8 for detergents. The process is also used for preparation of polypropylene, styrene, aldehydes, ketones etc.

Hydrogenation

Some of the hydrogenation processes are :

1. Hydrogenation of alkenes and alkadienes

- Catalysts : Raney Ni, Ni/Al_2O_3, Pt/C, Pt/Al_2O_3
- Temperature : 50-150 ^{0}C
- Pressure : 5-10 atm H_2
- Amount of catalysts: 2-5 by wt %

Example

a. hydrogenation of ethene to ethane

$C_2H_4 + H_2 = C_2H_6$

b. hydrogenation of cyclohexene to cyclohexane

$C_6H_{10} + H_2 = C_6H_{12}$

2. Hydrogenation of aromatics

- Catalyst - Raney nickel
- Temperature – 180-230 ^{0}C
- Pressure – 20- 50 atm H_2

Example : Benzene to cyclohexane which is the precursor for nylon polymer.

$C_6H_6 + 3\ H_2 = C_6H_{12}$

3. Hydrogenation of nitrobenzene

Hydrogenation of nitrobenezene shows how a wide variety of products can be obtained by using different catalysts and reaction conditions.

$$C_6H_5NO_2 + 3H_2 \xrightarrow[50\ ^0C,\ 75psig]{Pd/C} C_6H_5NH_2 + 2H_2O$$

$$C_6H_5NO_2 + 2H_2 \xrightarrow[85\ ^0C,\ 150psig,\ DMSO\ solvent]{Pt/C} C_6H_5NHOH + H_2O$$

$$C_6H_5NO_2 \xrightarrow[150\ ^0C,\ 15\text{-}45\ psig,\ H_2SO_4]{Pt/C} C_6H_4NH_2OH$$

Catalysts

Hydrogenation catalysts can be grouped in two categories as shown in Fig 1. Wide variation in commercial catalysts is available. Surface area, pore structure and presence of surface functional groups in supports greatly influence catalyst properties.

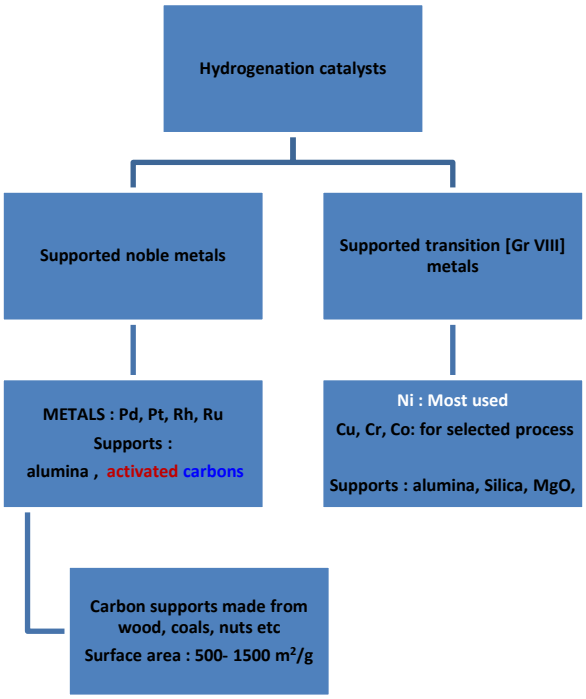

Fig. 1. Catalysts design for hydrogenation catalysts

Raney Ni

Raney Ni is a very important hydrogenation catalyst. Uniqueness of this catalyst is that it is a bulk unsupported catalyst with high surface area. The advantages include absence of support, minimum side reactions and more easy reduction of Ni in absence of interaction with supports. Raney Ni is typically prepared by the following steps:

1. Bulk Ni and Al metals in a 50-50 mixture are melted together.
2. Molten metals are poured into water producing fine grains
3. 20 % NaOH is added to leach Al from alloy leaving a porous matrix rich in Ni 90-95 % with a high surface area ~ 100 m^2/g
4. Raney nickel is stored in an inert atmosphere such as water or fat oil to prevent reoxidation

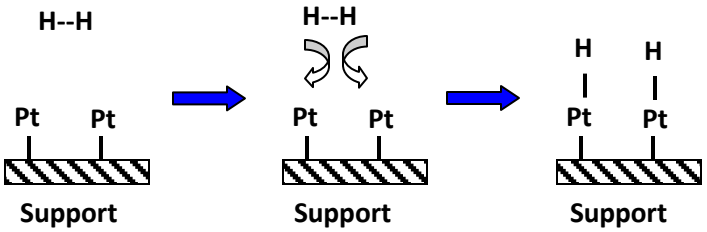

Fig. 2. Dissociative adsorption of hydrogen over Pt active site

Kinetics and mechanism

During hydrogenation of alkene over noble metal based catalysts, at first hydrogen get adsorbed dissociatively on the metal sites (Fig. 2). Dumesic et al. [1] reported that adsorption of hydrogen follows different kinetics at low alkene coverage and at high coverage. For hydrogenation of ethylene two types of site for hydrogen adsorption was proposed. The proposed mechanism is shown below. The two types of site for hydrogen adsorption are represented by 'S' and '*'.The site for adsorption of hydrogen on a surface partially covered with ethene was represented as 'S', whereas hydrogen adsorption site on a clean surface was designated as '*'. At adsorption sites, '*' , both the hydrogen and ethene can get adsorbed but at 'S' site only hydrogen can adsorb.

(1) $H_2 + 2S \rightleftharpoons 2H - S$ occurs on surface covered with ethene

(2) $H - S + S' \rightleftharpoons H - S' + S$

(3) $C_2H_4 + 2* \rightleftharpoons C_2H_4**$

(4) $C_2H_4** + H - S' \rightleftharpoons C_2H_5** + S'$

(5) $C_2H_5** + H - S' \rightleftharpoons C_2H_6 + 2* + S'$

(6) $H_2 + 2* \rightleftharpoons 2H*$ occurs on clean surface

(7) $H* + S' \rightleftharpoons H - S' + *$

Hydrogen adsorbed dissociatively on the Pt surface at 'S' or '*' adsorption sites forming H-S' or 'H*'. The adsorbed hydrogen atom 'H-S' or 'H*' were further assumed to be activated on another site S'as shown by step 2 or 7. The activated hydrogen H-S' then can react with C_2H_4** to give C_2H_5** (step 4) and then with C_2H_5** to give C_2H_6 (step 5). The Step 5 was considered as slowest and rate determining step.

Hydrogenation of organic compounds is usually conducted in liquid phase in a slurry reactor. Most hydrogenation reactions are highly exothermic and hence careful temperature control is required. Solvent is used to affect the product selectivity and to absorb the liberated reaction heat. Hydrogenation reactions in the slurry reactor are typically limited by mass transfer of H_2 from gas bubbles through liquid to each suspended catalyst particle. For hydrogenation reaction to occur, the hydrogen has to be transported from bulk phase to liquid phase through gas – liquid interface and then from bulk liquid to surface of solid catalyst for final reaction. The Fig. 3 schematically shows the various concentrations of hydrogen at different positions for a single bubble and particle combination. The C_g, C_L and C_s shown in the figure represent concentration of hydrogen in gas bubble, liquid and catalyst surface respectively.

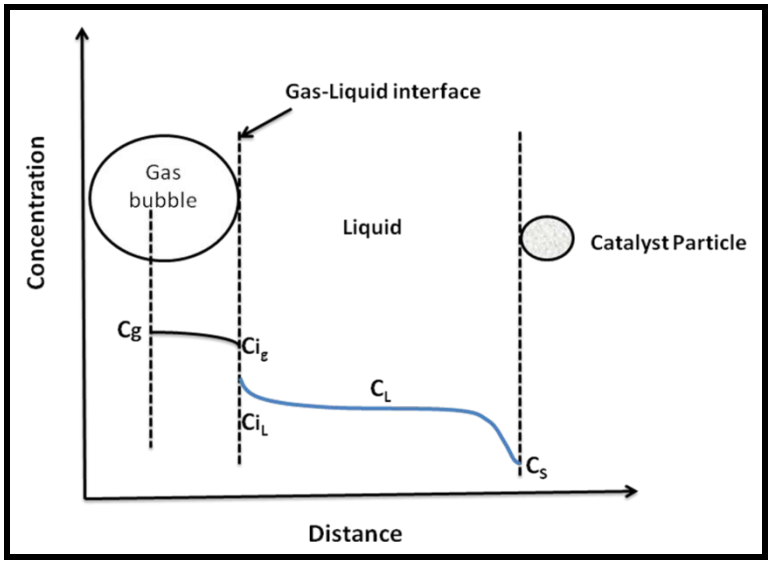

Fig. 3. Concentration profile of gaseous reactant in slurry reactor

For first order irreversible catalytic reaction, the surface reaction rate per unit volume of bubble free slurry may be written as

$$r_v = k\ a_c C_s \tag{1}$$

Where,

a_c = external area of catalyst particles per unit volume of liquid (bubble free)
k = first order rate constant
C_s = concentration of reactant (hydrogen) at the outer surface of catalyst particle

The rates of three mass transfer processes for hydrogen may be expressed as

$$r_v = k_g a_g \left[C_g - C_{ig} \right] \quad \text{for transport from bulk gas to gas – liquid interface} \tag{2}$$

$$r_v = k_L a_g \left[C_{iL} - C_L \right] \quad \text{for transport from gas – liquid interface to bulk liquid} \tag{3}$$

$$r_v = k_c a_c \left[C_L - C_S \right] \quad \text{for transport from bulk liquid to catalyst surface} \tag{4}$$

where, a_g is the gas bubble – liquid interface area per unit volume of bubble free liquid and k_g, k_L and k_c are the appropriate mass transfer coefficient.

H_2 pressure decreases across the gas film due to film diffusional resistance. At the gas liquid interface, a concentration of hydrogen in the liquid is determined in accordance with Henrys law. If equilibrium exists at the bubble-liquid interface C_{ig} and C_{iL} are related as $C_{ig} = H\ C_{iL}$ (5)

Where, H is known as Henry´s constant. From equations 1,2,3,4 and 5 the C_{ig}, C_{iL}, C_L and C_s can be eliminated and the rate can be expressed in terms of reactant in gas as

$$r_v = k_o\, a_c\, C_g$$

Where k_o is given as

$$\frac{1}{k_o} = \frac{a_c}{a_g}\frac{1}{k_g} + \frac{a_c}{a_g}\frac{H}{k_L} + H\left(\frac{1}{k_c} + \frac{1}{k}\right)$$

The k_o is the function of three mass transfer coefficients, the reaction rate constant and area ratio of catalyst and gas bubble in contact with liquid. The values of mass transfer coefficients can be obtained from several correlations available in literature.

Deactivation

Deactivation of catalysts mainly occurs by poisoning of metal surface with sulfur, halogens, phosphorus and nitrogen compounds. As the hydrogenation reactions occur in slurry condition, mechanical attrition is another major source of loss of catalysts. In addition, pore blockage may occur due to coke deposition.

Dehydrogenation

Catalysts

Important catalysts include chromic oxide/alumina and zirconia, Mo/alumina, Pt-Sn/alumina depending on the type of dehydrogenation reaction. Examples of important dehydrogenation reactions & catalysts are given below :

1. $\text{alkanes} \xrightarrow[400-600\ ^0\text{C},1-3\text{atm}]{Cr/Al_2O_3} \text{alkenes}$

2. $\text{n-Butane} \xrightarrow[500-600\ ^0\text{C},1-3\text{atm}]{Pt-Sn/Al_2O_3} \text{isobutene}$

3. $\text{ethylbenzene} \xrightarrow[600-650\ ^0\text{C, steam}]{Fe_2O_3-K_2O/Cr_2O_3} \text{styrene}$

4. $\text{alcohols} \xrightarrow[250-400\ ^0\text{C}]{Cu-K/SiO_2} \text{aldehyde, ketones}$

Kinetics and Mechanism

Dehydrogenation reaction can be modeled based on Langmuir-Hinshelwood kinetics. The Langmuir-Hinshelwood model of isobutane dehydrogenation proposed by Cortright et al. [2] for Pt-SnO_2 based catalysts is given as

(1) $C_4H_{10} + 2* \rightleftharpoons C_4H_9* + H*$

(2) $C_4H_9* + 2* \rightleftharpoons C_4H_8** + H*$

(3) $C_4H_8** \rightleftharpoons C_4H_8 + 2*$

(4) $H_2 + 2* \rightleftharpoons 2H*$

Where '*' is the active site. The second step of dissociative adsorption of isobutane is the slow and rate determining step. The corresponding rate expression is given as

$$r_{DH} = k\theta_*^2 \left[P_{iC_4H_{10}} - \frac{P_{iC_4H_8} P_{H_2}}{K_{eq}} \right]$$

where r_{DH} is the net dehydrogenation rate, k is the rate constant for the dissociative adsorption of isobutane, K_{eq} is the overall equilibrium constant for isobutene dehydrogenation, and θ_* is the fraction of sites that is free of adsorbed species.

Deactivation

Main problem for dehydrogenation reaction is rapid deactivation by coke deposition requiring very frequent regeneration.

Oxidation reaction

Oxidation processes consist of oxidation of inorganic compounds and partial oxidation of organic compounds. Oxidation of inorganic compounds is used to produce chemical feed stocks and is among the oldest and largest processes. Production of sulphuric acid by SO_2 oxidation and nitric acid by ammonia oxidation are amongst the major basic chemical industry. Oxidation processes will be illustrated by few examples.

Oxidation of inorganics

SO_3 production

SO_2 is oxidized to SO_3 which is further converted to sulphuric acid. This process is one of the highest tonnage processes in the world.

$SO_2 + ½\ O_2 = SO_3$

Catalyst for this process is vanadium potassium sulfate supported on silica rich carrier such as natural clay. Minimum inlet temperature required for vanadium based catalysts is 400 ^{0}C. For single pass operation at 400 ^{0}C, the temperature rises to 600 ^{0}C and the conversion is limited to 60% by equilibrium. Therefore, multiple pass reactors, with intermittent heat exchange, is used to achieve near 100 % conversion.

Mars and Maessen [3] proposed a two step redox mechanism as shown below. Second step is the rate determining.

$$SO_2 + 2V^{5+} + O^{2-} \rightleftharpoons SO_3 + 2V^{4+}$$
$$2V^{4+} + 0.5O_2 \rightarrow 2V^{5+} + O^{2-}$$

Using Langmuir-Hinshelwood model, rate is given as

$$r = \frac{k\ P_{SO_2}^{l} P_{O_2}^{m} P_{SO_3}^{n}}{\left(1 + AP_{SO_2} + BP_{O_2} + CP_{SO_3}\right)}$$

Where l and m lie between 0.5 to 1 and n lies between -1 to 0.

Partial oxidation of organics

Methanol to formaldehyde

Methanol is partially oxidized to produce formaldehyde. Formaldehyde is used for production of urea, disinfectant, preservative etc.

$CH_3OH + 0.5\ O_2 = HCHO + H_2O$

The process is carried out at 600-700 ^{0}C temperature at near atmospheric pressure using silver needles or gauges catalysts. As a result of high process temperature, the unsupported silver catalyst tends to sinter resulting in increased pressure drop and reduced activity. To minimize these adverse effects without compromising adequate contact of reactants with the catalyst, a shallow (4 to 5 cm thickness) but wide bed (~ 3m) of Ag needles or gauge is used. The unsupported silver catalyst is sensitive to S, N, halide compounds. Methanol oxidation process at dilute condition is carried out over Fe_2O_3-Co_2O_3-MoO_3 catalyst at lower temperature of 300 – 400 ^{0}C at atm pressure.

Ethylene to ethylene oxide

Ethylene oxide is used to produce ethylene glycol. Polyethylene glycols are important monomers for liquid plasticizers, lubricants. Ethylene oxide is produced by partial oxidation of ethylene and is a highly exothermic process. Process is carried out at 200 – 250 ^{0}C temperature over silver supported on alumina catalysts. The process is always associated with secondary oxidations of ethylene oxide (equation 6) or total oxidation of feed to carbon oxides and water (equation 7) as shown below. This can be minimized by controlling process conditions and proper catalyst selection.

$$CH_2 = CH_2 + 0.5\,O_2 \xrightarrow{Ag} CH_2OCH_2 \longrightarrow \underset{\text{undesired secondary oxidation}}{CO_2 + H_2O} \quad (6)$$

$$CH_2 = CH_2 + 3O_2 \xrightarrow{Ag} 2\,CO_2 + 2H_2O \text{ undesired total oxidation} \quad (7)$$

Kinetics and mechanism

Ethylene oxide formation over silver catalysts is proposed to occur through dissociative chemisorption of oxygen. The proposed mechanism by Haul and Neubauer [4] is as follows :

Ethylene oxide formation pathway :

$$O_2 + S \rightleftharpoons S - O_2$$
$$S - O_2 + S \rightleftharpoons 2S - O$$
$$C_2H_4 + S - O \rightarrow S - O - C_2H_4$$
$$S - O - C_2H_4 \rightarrow S + C_2H_4O$$

Total oxidation pathway :

$$S - O - C_2H_4 \rightarrow S - O - CHCH_3$$
$$S - O - CHCH_3 + 5O - S \rightarrow 6S + 2CO_2 + 2H_2O$$

Park and Gau [5] proposed a Langmuir –Hinshelwood rate expression for supported silver over barium doped silica as $r = \dfrac{k_1 K_E K_O P_E P_O}{\left(1 + K_E P_E + K_O P_O\right)^2}$

Here E = ethylene and O = oxygen

Deactivation

Unsupported silver catalysts are very sensitive to poisoning by S, N and halide compounds. Very high temperature also results in fusion of silver catalysts. Catalysts life for of silver catalysts is only 6 months. Fe_2O_3-Co_2O_3-MoO_3 is more rugged and lasts for about 1-2 years.

Book reference:

- C. H. Bartholomew and R. J. Farrauto, Fundamentals of Industrial catalytic Processes, Wiley, VCH, 2006

Journal reference :

1. J.A . Dumesic, D.F Rudd, L.M Aparicio , J.E. Rekoski and A.A. Trevino , The microkinetics of heterogeneous catalysis, ACS ,1993
2. R.D. Cortright, Per E. Levin, J. A. Dumesic, Ind. Eng. Chem. Res. 1998, 37, 1717-1723
3. P. Mars and J.G. Maessen , J. Catal. 10 (1968) 1257
4. R. Haul and G. Neubauer J. Catal. 105 (1987) 39
5. D.W. Park and G. Gau, J. Catal. 105(1987) 81